UNIVERSITY OF SOUTHAMPTON

Regulation of the hepatic and pancreatic stellate cell by Interferon alpha

Fiona Mairi Joyce Walker

School of Medicine

August, 2003

UNIVERSITY OF SOUTHAMPTON

ABSTRACT

FACULTY OF MEDICINE, HEALTH AND BIOLOGICAL SCIENCES

MEDICINE

Doctor of Philosophy

Regulation of the Hepatic and Pancreatic stellate cell

By Fiona Mairi Joyce Walker

Interferon alpha, used as an antiviral in the treatment of Hepatitis C viral infections, has been shown to reduce fibrosis. Despite previous studies, the mechanism by which this is achieved is as yet unknown, and to date the results have been conflicting.

The hepatic stellate cell (HSC) has been shown to be pivotal in the progression and perpetuation of liver fibrosis. During development of liver fibrosis the HSC becomes activated, losing its retinoid droplets, expressing alpha smooth muscle actin and increasing synthesis of matrix metalloproteinases and their inhibitors, tissue inhibitors of matrix metalloproteinases.

Interferon alpha has been shown to have both antiproliferative and pro-apoptotic effects in cancer cell lines. Therefore, I hypothesized that Interferon alpha ameliorates liver fibrosis by the downregulating central aspects of the activated HSC. In addition, stellate cells isolated from the pancreas were studied to compare their activated phenotype with that of the HSC. Hepatic and pancreatic stellate cells were also treated with Interferon alpha to study whether a common response to Interferon alpha could be demonstrated.

At 72hrs, Interferon alpha downregulated the production of alpha smooth muscle actin in cultured HSC. However, no effect was observed on the expression of MMP-2, MMP-9 and collagen-I. As analysed by Acridine Orange, apoptosis was unaffected, but by ^{3}H Thymidine incorporation treatment of hepatic stellate cells with Interferon alpha significantly reduced proliferation and was statistically significant. This was confirmed with assessment of total DNA and activation of ERK1 and ERK2 by western blotting.

To further determine the effects of Interferon alpha, an *in vivo* model was studied to evaluate the effect of therapy on an established liver fibrosis following carbon tetrachloride treatment. A statistically significant decrease in fibrosis was observed in rats treated with Interferon alpha relative to control treated with carbon tetrachloride treatment alone. In addition there was a reduction in alpha smooth muscle actin staining in sections of treated liver. Treated animals also demonstrated a reduction in ascites. Other parameters assessed demonstrated no significant changes between the untreated and treated groups.

Therefore the antifibrotic effects of Interferon alpha may be due to antiproliferative properties. Interferon alpha may only modestly regulate the phenotype of the activated stellate cell but may enhance the reduction in fibrosis possibly through decreasing stellate cell proliferation. Furthermore, I have demonstrated a common mechanism between two stellate cells when activated, adding to work in this area.

Contents

Figures

Acknowledgements

"'"Well, this is the end, Sam Gamgee," said a voice by his side. And there was Frodo, pale and worn, and yet himself again; and in his eyes there was peace now, neither strain of will, nor madness, nor any fear. His burden was taken away."

Return of the King, Part 3, Lord of the Rings. J.R.R. Tolkien

Many thanks go to many people for getting me all the way to Mordor! Most importantly, I would like to thank my very own Sam who stood by my side unfailingly every step of the way. He was always there to encourage me and most importantly pour me a Gin and Tonic on those very worst of days when I ran my RNA gel backwards!

Secondly, I would like to thank my three supervisors, Prof. J.P. Iredale, Dr. R.C. Benyon and Dr. D. Mann for all their help. My thanks to John for all the encouragement and his entertainment of song and dance in the lab. My thanks to Chris for bringing me down to earth and pointing out all my scientific errors – which were many! And my thanks to Derek for doing the boring stuff like forms and stepping in when John and Chris were away.

And last of all I would like to thank my colleagues from the laboratory, Dr. F. Shek who was so much fun to work with for 3 years, Dr. M. Gaca, Dr. J. Maltby, Dr. C. Brooks, Dr. E. Williams and Dr. P.R. McCrudden who taught me everything I know and always called me for coffee.

And last but not least,, thanks to my mother for all her support and encouragement.

Abbreviations

Abbreviation	Name
αSMA	Alpha smooth muscle actin
2'5'OAS	2'-5'-Oligoadenylate Synthetase
ADAR	Adenosine deaminase RNA-specific
ALT	Alanine aminotransferase
AP-1	Activation Protein 1
AST	Aspartate aminotransferase
BDL	Bile duct ligation
BSA	Bovine serum albumin
BTEB1	basic transcription element binding protein
CRBP1	Cellular retinol binding protein 1
DEPC	diethylpyrocarbonate
DISC	Death inducing signalling complex
DMN	Dimethylnitrosamine
ECM	Extracellular matrix
eIF-2	Endoribonuclease Initiation Factor 2
ERK1	extracellular signal-regulated kinase 1
ERK2	extracellular signal-regulated kinase 2
ESB	Electrophoresis Sample Buffer
EST	expressed sequence tag
FADD	Fas associated death domain protein
FCS	Fetal calf serum
GDP	Guanosine Diphosphate
GFAP	Glial Fibrillary Acidic Protein
GIT	Guanidium isothiocyanate
GMA	Glycol Methracrylate
HCV	Hepatitis C virus
HSC	Hepatic stellate cell
ICAM-1	Intercellular adhesion molecule 1
IFN-α	Interferon alpha
IFN-β	Interferon beta
IFN-γ	Interferon gamma
IFN-ω	Interferon omega
IFN-τ	Interferon trophoblast
IFR9	interferon regulatory factor 9
IL-1β	Interleukin 1 beta
IL-6	Interleukin 6
IMPDH	inosine 5'-monophosphate dehydrogenase
ISGF3	interferon-stimulated gene factor 3
$I_{\kappa}B$	Inhibitor of Nuclear factor kappa B
JAK 1	Janus kinase 1
KLF6	Kruppel-like factor 6
MAP kinase	Mitogen activated protein kinase
MAP kinase 1	Mitogen activating protein kinase 1
MAP kinase 2	Mitogen activating protein kinase 2

MIP-2	Macrophage inflammatory protein 2
MMP	Matrix metalloproteinase
MOPS	3-(N-morpholino) propanesulfonic acid
MTS	3-(4,5-dimethylthiazol-2-yl)-5-(3-carboxymethoxyphenyl)-2-(4-sulfophenyl)-2H- tetrazolium
$NF_{\kappa}B$	Nuclear Factor kappa B
NK	Natural Killer cells
PAF-1	Platelet activating factor
PAI-1	Plasminogen activator inhibitor 1
PBMC	peripheral blood mononuclear cells
PDGF	Platelet derived growth factor
PEA-3	polyomavirus enhancer activator 3
PIIIP	type III procollagen propeptide
PKR	Protein Kinase 1
PSC	Pancreatic stellate cell
PSG	Penicillin, Streptomycin, Gentamycin
RBP	Retinol binding protein
REH	Retinyl ester hydrolase
ROI	Reactive oxygen intermediates
SMAD	SMA and MAD retaed protein
SP-1	Specificity protein 1
SSC	Sodium chloride-Sodium Citrate solution
STAT 1	signal transductor and activator of transcription 1
STAT 2	signal transductor and activator of transcription 1
TGF-β	Transforming growth factor-beta
TIMP	Tissue inhibitor of matrix metalloproteinase
TNF-α	Tumour necrosis factor alpha
TYK 2	tyrosine kinase 2
VCAM-1	Vascular adhesion molecule 1
VEGF	Vascular endothelial growth factor

1. GENERAL INTRODUCTION

1.1 INTRODUCTION TO LIVER FIBROSIS

Liver fibrosis occurs after injury to the liver from a variety of insults, such as: alcohol abuse; autoimmune disorders e.g. primary biliary cirrhosis; gene defects; haemachromatosis; parasitic infestation, e.g. Schistosomiasis, and Chronic viral hepatitis. Regardless of the type of initial injury, the fibrotic mechanism, a wound healing response remains the same and in the chronically injured liver, tissue becomes distorted by progressive deposition of interstitial collagens. In chronic cases the end-stage is liver cirrhosis where the liver architecture becomes irreversibly disrupted. Within the UK, liver fibrosis and the complications surrounding it accounts for 6000 deaths annually, and is currently one of the major reasons for admission to hospital (Benyon 1998).

Following injury, the wound healing responses of hepatic regeneration and fibrosis are initiated. Hepatic regeneration enables the liver to recover any loss of hepatic mass due to injury, such as necrosis of the hepatocytes (LaBrecque 1994). Hepatocyte necrosis also stimulates the wound healing response of fibrosis, an increase and alteration in the synthesis of the extracellular matrix (ECM). The increased synthesis of ECM also allows for the regeneration of the liver lobules following injury. Both of these responses are tightly controlled and their balance is crucial to recovery of the liver (Knittel 1995). In the case of acute injuries the liver is able to regenerate and repair, restoring not only its original cell mass but also the structure necessary for liver function (LaBrecque 1994).

However, with chronic injury the balance is lost and the healing responses cause functional problems as a result of architectural distortion. Pockets of highly

regenerative hepatocytes are thought to provide the necessary conditions for the development of Hepatocellular Carcinoma (HCC), one of the potential risks of liver cirrhosis (Neuberger 1994). Due to the high level of hepatocyte necrosis the synthesis of matrix turnover is strongly stimulated. The now unbalanced synthesis of matrix turnover builds distorted structures and eventually fibrotic bands are formed throughout the liver, causing scarring of the liver (Friedman 1999). The increase in altered matrix synthesis can itself cause perpetuation of fibrosis (Alcolado 1997). The resulting distortion to the liver macrostructure causes loss of liver function. Individual constituents of the ECM are known to effect cell phenotype (Friedman 1989).

1.2 INTRODUCTION TO PANCREATIC FIBROSIS

Fibrosis also occurs within the pancreas, again in response to injury, and is characteristic of Chronic Pancreatitis (CP). In addition to fibrosis, inflammatory lesions are formed within the pancreas and destruction of the exocrine parenchyma and endocrine tissue occurs. Atrophy of the acinar cells occurs and strictures form (Sarles 1990). As in the liver, the fibrosis alters the structural architecture of the pancreas, altering in turn the morphology and function of the pancreas. Until recently little had been known about the pathology of the fibrotic pancreas.

Chronic pancreatitis is only found in 3/100,000 of the Western population (Riela 1990), but remains an expensive disease to treat, due mainly to the high level of pain suffered by the patient. The leading cause of Chronic Pancreatitis is alcoholism, responsible for two thirds of all cases (Muench 1992). In the remaining third the cause has not yet been identified, although several factors have been implicated such as hereditary genes, viral infections and gallstones.

1.3 FUNCTION OF THE LIVER

The Liver performs many essential functions: secretion of bile; metabolising carbohydrates, proteins and lipids; storage of Glycogen, iron and vitamins; the degradation of hormones and inactivation of drugs.

When blood glucose is high, the liver provides the principle place of storage for glycogen and likewise, following intracellular glycogenolysis, releases glucose when blood sugar levels are low. Additionally, it is also the principle place of storage for the vitamins A, D and $B_{12,}$ and also Iron.

Synthesis of the plasma proteins such as fibrinogen, albumin, α and β globulins and prothrombin also occurs in the liver. The liver can also metabolize both lipids and proteins: the latter results in the by-product of ammonia which within the liver can only be metabolized further to urea which is excreted by the kidneys.

Degradation and excretion of hormones and drugs occurs in the liver. Hormones such as Adrenaline and Noradrenaline are inactivated by oxidation and methylation reactions. Once inactivated or rendered water soluble i.e. steroid hormones, they can be excreted.

The secretion of bile by the liver is also an important part of the digestive process. Bile contains mainly bile acids, but also pigments, lecithin, cholesterol and other substances. The Bile acid emulsifies lipids aiding lipid-digesting enzymes, and also forms micelles with the lipids. These micelles are small and can be absorbed across the membrane of the intestinal microvilli.

1.4 STRUCTURE OF THE LIVER

The liver is divided into four lobes, left, right, quadrate and caudate; this is an anatomical divide not symmetrical. Histologically the lobes divide further into lobules, a division not readily found in sections of human liver, but it is a functional division. These lobules have in their centre the central vein, which takes all the blood out of the liver. On the outside of the lobule are several portal triads, these consist of the portal vein, the hepatic artery and the accompanying bile duct (Figure 1-1).

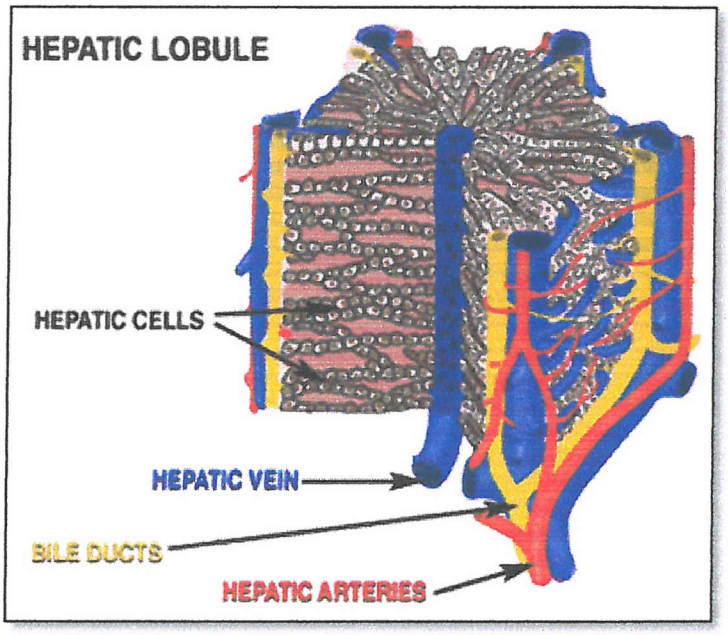

Figure 1-1 Diagrammatic representation of the liver sinusoids.
A central vein is found in the middle of the lobe from which cords of hepatocytes radiate out. Between these cords are the hepatic sinusoids. The blood flows into the liver through the hepatic artery and portal vein, flows through the sinusoid and then leaves the liver via the central vein. Picture reproduced from http://www.livercancer.com

Blood enters the liver from two sources: the hepatic artery and the portal vein. Blood from the portal vein provides 75% of the blood flow, it contains many nutrients as it has passed along the gastrointestinal capillary bed, but due to this it has a low oxygen content. Blood in the hepatic artery provides only 25% of the blood flow, but in

comparison to that of the portal vein is well oxygenated as it flows from the celiac trunk. Blood from both sources is drained into the sinusoids, a highly branched network, which ensures that the plates of hepatocytes are never far from the sinusoidal blood. The highly fenestrated sinusoidal endothelial cells give the hepatocytes almost direct contact with the sinusoidal blood. This close but unusual contact between parenchymal cells and the blood enhances absorption of the blood filtrates (Figure 1-2 and Figure 1-3).

1.5 CELLS OF THE HEPATIC SINUSOID

The cells of the liver are arranged structurally to allow the hepatocytes - the cells that functionally support the liver - close access to the sinusoidal blood. The blood supply, as described earlier, brings to the liver blood rich in both oxygen and filtrates. The cells can be divided into two: the parenchymal cells, the hepatocytes and the non-parenchymal cells, the sinusoidal endothelial cells, the HSCs and the Kupffer cells (Figure 1-2 and Figure 1-3).

1.5.1 Hepatocytes

These cells, forming 80% of the total liver cells, are the major working force of the liver. These cells form palisades radiating out from the central vein, with the bile canaliculi running between them. The microvilli which project from the hepatocytes aid absorption of particles from the blood, and through these cells the blood filtrates are collected, synthesized and secreted out in the bile. Hepatocytes have many functions, in addition to the formation and secretion of bile they metabolize drugs, degrade hormones, collect chylomicrons from the blood and secrete cholesterol for the rest of the body.

Figure 1-2 Schematic diagram of hepatic sinusoid in cross section – not to scale.

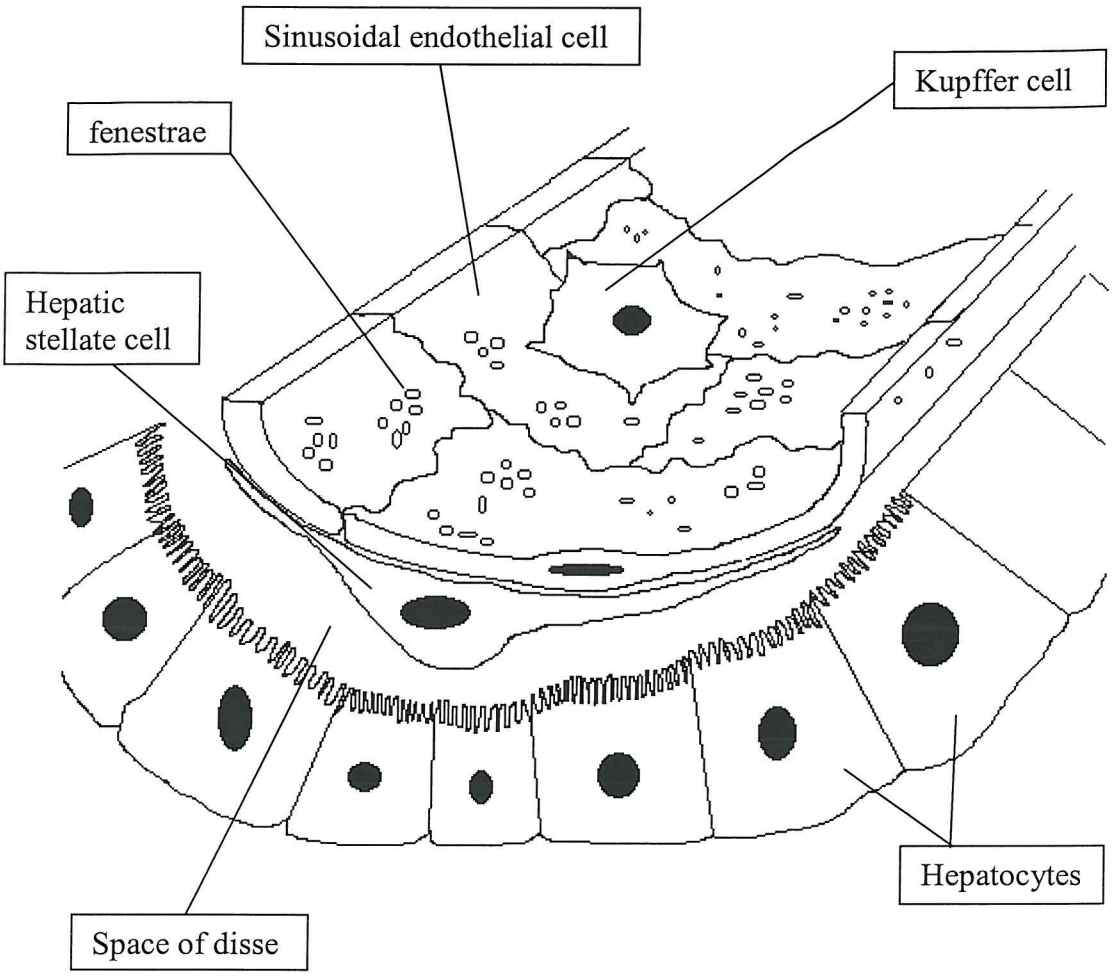

Hepatocytes absorb cholesterol from the blood which is converted to primary bile acids. These are excreted into the blood stream and back through the liver once again where they are finally converted into a tertiary bile acid conjugated with glycine or taurine. Finally these tertiary bile acids are then secreted out into the bile canaliculi as micelles, where they mix with other bile components and the aqueous secretion of the bile duct epithelial cells. Hepatocytes also secrete into the bile cholesterol phospholipids, which are secreted as vesicles that mix with the bile acid micelles. If too much cholesterol is present and the micelle is unable to contain any more, the cholesterol forms crystals which go on to form gallstones.

Figure 1-3 Picture taken with Electron microscope of a cross-section of an hepatic sinusoid.

1. Lumen of sinusoid. 2. Nucleus of sinusoidal endothelial cell. 3. Squamous endothelium. 4. Endothelial gaps. 5. Perisinusoidal space of Disse. 6. Bundles of collagenous fibrils. 7. Bases of hepatic cells with microvilli projecting into the space of Disse. 8. Mitochondria. 9. Lipid droplets. 10. Lysosomes. 11. Chylomicron.
The distance between the asterisks is 10 microns. Reproduced from the Rhodin Atlas of Histology.
(http://webcampus.med.mcphu.edu/EMAtlas/toc.htm)

Bilirubin, an end product of red blood cell break down is bound to albumin in the plasma; this is also removed by the hepatocytes. This is conjugated to glucuronic acid molecules and also secreted into the bile, giving the bile its characteristic yellow colour.

The hepatocytes are responsible for the breakdown of hormones such as epinephrine and norepinephrine, which are both broken down by the monoamine oxidase and catachol-O-methyltransferase enzymes found in the hepatocytes. Steroid hormones, such as cortisol, are also degraded to an inactive product and secreted back out for secretion via the urine.

1.5.2 Sinusoidal endothelial cells

The sinusoidal endothelial cells which line the sinusoids are highly fenestrated, a feature which makes them especially permeable (Wisse 1985). These fenestrae are about 100nm in diameter and can occur either alone, or in clusters that are then referred to as sieve plates. Fenestrae of this size can allow large proteins to pass out of the sinusoidal lumen to the hepatocytes, but prevent any of the cells of the blood passing through. Chylomicrons are also able to pass through, even those up to 300nm are thought to squeeze through, but larger chylomicrons are unable to pass.

The matrix in the Space of Disse controls fenestrae within the endothelial cells (McGuire 1992). Changes in this matrix in fibrotic liver have been shown to decrease the numbers of fenestrae, as have alcohol and hypoxia (Clark 1988). In addition to their ability to sieve the blood, endothelial cells of the sinusoid are also able to scavenge unwanted filtrates such as denatured proteins.

1.5.3 Kupffer cells

Kupffer cells are macrophages found only in the liver, and constitute the largest pool

of macrophages within the body (Toth 1992). They are found within the sinusoids, particularly in the periportal zones, lying either in the sinusoid, between the endothelial cells or occasionally within the Space of Disse (Wisse 1970).

Like all macrophages, Kupffer cells have many lamellipodia, microvilli and filopodia with cytoplasmic processes extending out to enable close contact between the sinusoidal cells. As the sinusoidal blood has come directly from the gastrointestinal capillary wall Kupffer cells have first contact with any antigens and bacteria from the gut. Their role within the liver is therefore of vital importance, and they have been shown to remove up to 95% of bacteria entering the liver (Beeson 1985). Unlike most macrophages, Kupffer cells do not seem to process and present antigens, although MHC class II antigen expression has been found in liver injury (Rogoff 1981). Primarily Kupffer cells phagocytose any unwanted particles within the blood. However, their immuno-responsive actions also include the secretion of chemokines and cytokines, and as well as secreting some matrix metalloproteinases (Smedsrod 1994).

1.5.4 Hepatic Stellate cells

The hepatic stellate cell was previously known as the Ito cell or the fat-storing cell, and its discovery was linked with that of the Kupffer cell. Kupffer first discovered these lipocytes in 1876, although he then named them sternzellen and proposed they had phagocytic properties. The definition of these cells was not clear until 1951 when Ito, using studies with electron microscopy, proposed that there were two individual populations of cells (Ito 1952). This was later confirmed, and the phagocytic cells are now named the Kupffer cells, and the fat-storing cells are the Ito cells or Stellate cells (Wake 1971).

Stellate cells, which comprise 5-8% of the total cells of the liver (Ramadori 1991), lie within the Space of Disse. The stellate cells surround the endothelial cells with their extensive processes (Wake 1980), through which it has been proposed they may have a contractile role, modulating blood flow at a local level through the sinusoid. HSCs are rich in lipid droplets, which contain vitamin A stored as retinyl palmitate which provides 90% of the body's vitamin A (Kawada 1997). This provides one of their most distinctive features; these vitamin A droplets fluoresce in the presence of 328nm wavelength light.

Quiescent HSCs, i.e. those found in the normal undiseased liver, have been shown to express proteins used as markers of several different cell types. They express desmin, a muscle cell-specific intermediate filament protein (Yokoi 1986), but also they contain vimentin which is found in fibroblasts (Rockey 1992) and additionally glial fibrillary acidic protein (GFAP) a marker of astrocytes in the central nervous system (Gard 1985). There is some evidence, such as the expression of GFAP, to suggest that the HSC is derived from the neural crest, (Niki 1999). Rat neural crest stem cells are also capable of altering to a myofibroblastic phenotype which expresses alpha smooth muscle actin (α-SMA) (Morrison 1999). Although α-SMA expression has been found at a negligible level in quiescent cells, it becomes highly expressed following HSC activation through injury.

One of the primary function of HSCs in the liver is the uptake and storage of dietary retinol. Retinyl esters are transported in chylomicrons; these are absorbed by the hepatocyte via remnant receptors. Once in the hepatocyte the retinyl esters are hydrolyzed to retinol by retinyl ester hydrolase (REH). The retinol is then bound to either retinol binding protein (RBP), cellular retinol binding protein 1 (CRBP1). If bound to RBP then the retinol is secreted into the blood stream for dispersion

throughout the body. However, if the retinol is bound to CRBP1 then it is either degraded by cytochrome P450 dependant enzymes or is oxidised to retinal and retinoic acid. But if bound to CRBP1 it can also be transferred to the HSC through a currently unknown pathway. In the HSC the retinol is re-esterified for storage purposes to retinyl esters, and from this it can be released through the same pathway as in the hepatocyte; REH alters the retinyl esters to retinol, which is then released from the HSC through binding to RBP (Geerts 2001).

1.6 THE LIVER EXTRACELLULAR MATRIX

The extracellular matrix (ECM) of the liver is formed from a wide range of the typical ECM proteins, such as collagens, glycoproteins and proteoglycans. Within the sinusoids, the liver ECM has a distinct structure when compared to typical epithelial tissue structure. Characteristically epithelial cells sit on a basement membrane matrix underneath which is the stroma, and then the endothelial cells. However, the liver epithelial cells (the hepatocytes) sit on a low-density matrix, not even visible by electron microscopy. However, immunohistochemistry (Schuppan 1990) has shown this matrix contains small amounts of fibrillar collagens, collagen VI, collagen IV (human only), laminin, fibronectin, heparan sulphate proteoglycans and hyaluronic acid. This low-density highly permeable matrix is critical for the hepatic cells to function correctly, e.g. the ability of the hepatocytes to absorb particles from the blood stream. However, attenuated basement membrane is not found throughout the liver; the ECM of the central vein and the liver capsule have a typical basement membrane.

1.6.1 Collagen

Collagen is a fibrous protein and is the most abundant protein found in mammals (25%) (Alberts 1989). They have a left-handed triple helical structure, with the

repeating sequence (Gly-X-Y) of which every third X is a proline and every third Y a hydroxyproline. The amino acids glycine and proline enable the triple helix to

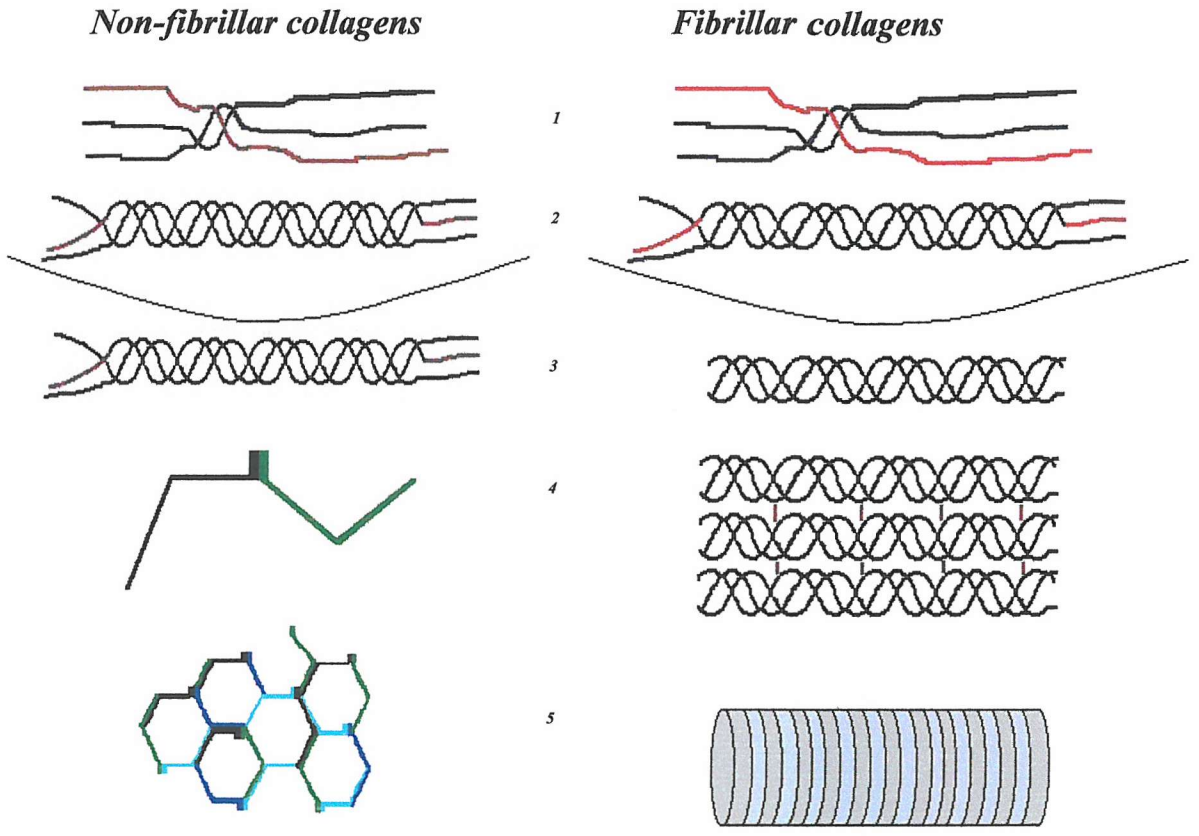

Figure 1-4 Diagram showing the production of collagens, both fibrillar and non-fibrillar.
1) Collagens are produced as procollagens in the cell with propepetides on both the C- and N-terminus. 2) The C-terminal aids the formation of the triple helix. 3) The helices are secreted from the cell. The fibrillar collagens have the propepetides cleaved by proteolytic enzymes. The non-fibrillar collagens do not lose their propeptides. 4) The fibrillar collagens lie in a staggered fashion side by side with crosslinks between them, forming collagen fibrils. The non-fibrillar collagens bind C-terminus to C-terminus. 5) The fibrillar collagens viewed through an electron microscope show a striated pattern due to the staggered pattern of the collagen helices. The non-fibrillar collagens form a lattice-like structure, due to their C-terminus binding and their distortion in their helices.

form: glycine is small and allows the close packing of the helix; proline has a ring structure that stabilizes the helical turns. There are currently 20 known collagens which can be divided into fibrillar and non-fibrillar. Interstitial collagens or fibrillar collagens, e.g. Collagen I, II, III V and XI, are so named due the fibrils formed. The

fibrillar collagens are commonly found in connective tissue, and can form even larger bundles within the ECM called collagen fibres. These fibres, several micrometers wide, can be observed with a light microscope.

The non-fibrillar collagens include collagens IV, VI, VII, VIII and X, of these collagens IV and VI are found within the liver. These non-fibrillar collagens do not form fibrils, but rather a mesh or sheet-like structure.

When the triple helical collagen is secreted from the cell it has a propeptide at both its carboxy- and amino- terminal ends. It is this propeptide which allows the different structures of the fibrillar collagens compared to the non-fibrillar. The propeptides enable the triple helix of individual collagen chains to form correctly. When fibrillar collagens leave the cell, enzymes cleave the propeptides leaving the collagen helices free to form fibrils. However, with non-fibrillar collagens, the propeptide is not cleaved off and the strands interact via these propeptides to form the mesh-like structure. Additionally, their regular amino acid sequence is occasionally interrupted thus disrupting their triple helix.

Within the liver, 40% of healthy total liver collagen is collagen I which is found in surrounding the portal tracts and central veins and also in the liver capsule. Collagen III makes up another 40%, surrounding the periportal and centrolobular areas. Collagen IV and VI are less abundant and are present around larger vessels. The matrix of the peri-sinusoidal space contains a low density matrix, which has been shown to contain fibrillar collagens I, III, V and VI, and basement membrane collagens IV and XVIII. However, ECM in the Space of Disse is typically a type IV collagen rich (Kaplowitz 1992).

1.6.2 Proteoglycans

Proteoglycans are also a key component of the ECM. These are formed from

glycosaminoglycans (GAGs) covalently bonded to protein cores. The glycosaminoglycans are long unbranched polysaccharide chains, which are inflexible (i.e. not globular) and due to this occupy a large amount of space for their mass. This enables them to form gels - fundamental to the formation of ECM – which allows them to organize the matrix structure by giving stability and regulating its assembly. Additionally they are hydrophilic and thus the matrix binds much water. Hyaluronic acid is the only GAG that is not found attached to a protein. It is smaller and simpler than the rest of the family and has been implicated as having a particular role in injury and repair. It is especially found around migrating cells but is degraded when the cell migration has ceased (Alberts 1989).

1.6.3 Glycoproteins

Glycoproteins are also found within the ECM. In particular, fibronectin and laminin are of importance. Fibronectin, known as an adhesive glycoprotein, forms fibrils, and has several roles within the matrix. It has been found to have binding sites for cells, collagen and heparin, thus it plays a major role in organisation of the matrix. The domain for cellular binding has been identified, a tripeptide sequence R-G-D which if blocked will prevent cells binding to fibronectin (Alberts 1989).

Laminin found in the basal lamina also has particular binding sites for collagen IV, heparan sulfate and receptor proteins on the cell surface. Both fibronectin and laminin have been found in the portal tracts, but they are also found within the lobules in the basement membrane-like matrix.

1.7 DEGRADATION OF THE ECM

1.7.1 Matrix metalloproteinases

Matrix metalloproteinases (MMPs) are a family of zinc and calcium dependent matrix degrading enzymes, currently numbering 25 (Table 1-1), which are capable of degrading ECM (Benyon 2001). All MMPs have similar structural domains and conserved sequences, are synthesized in a prepropeptide form, and secreted in a propeptide form. Both HSC and Kupffer cells secrete MMPs (Knittel 1999).

Each MMP has a N-terminal propeptide domain (approx. 80 amino acids) which contains a conserved amino acid sequence PRCGVPDV. Binding of the cysteine residue (the cysteine switch) in this sequence to the zinc within the catalytic domain holds latency. The catalytic domain (approx. 170 amino acids) also contains a conserved sequence, HEXGH a zinc-binding motif, which binds the zinc ion to the cysteine residue during enzyme latency.

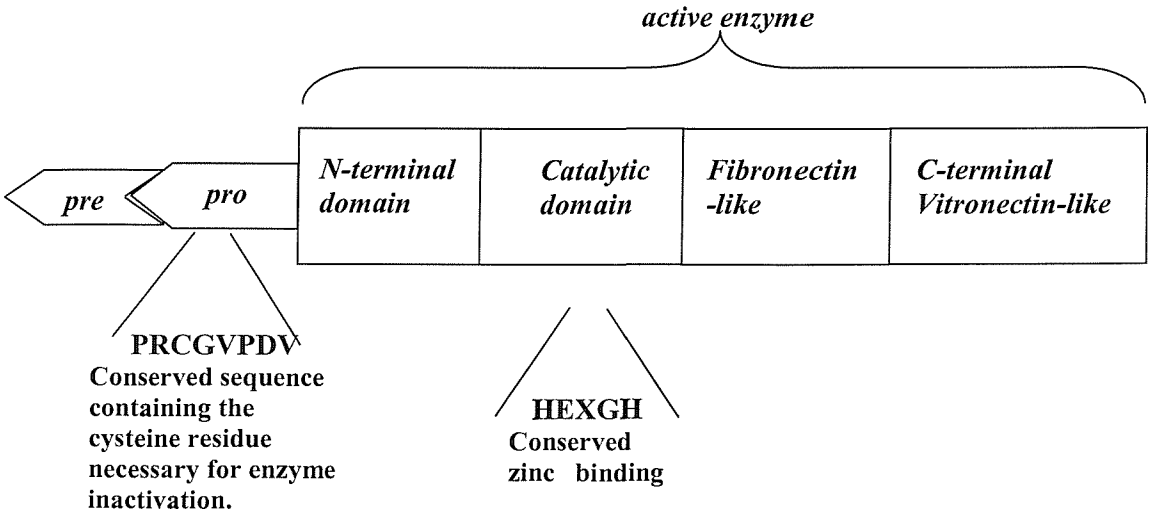

Figure 1-5 Structure of the MMP Gelatinase A
All MMPs contain the pre-, pro-, N-terminal and catalytic regions, but only MMP-7 (Matrilysin) has these regions alone. Most also contain C-terminal regions with various domains, and some have domains inserted into the catalytic region as found in Gelatinase A which has a fibronectin-like domain as shown above.

Some of the enzymes contain C-terminal domains which enable substrate specificity. Collagenase has a C-terminal vitronectin-like domain (approximately 200 amino acids) which is necessary for the degradation of collagen triple helixes. This initial degradation then causes the collagen to become susceptible to the other MMPs such as Gelatinases (Goldberg 1992).

Some MMPs are bound to the cell membrane and are called membrane-type MMPs (MT-MMP). These MMPs have a transmembrane and intracytoplasmic domain that anchors them to the cell surface. MT-MMPs, like MMP-23 and MMP-11 do not have the conserved cysteine switch, but have a propeptide processing sequence in the C-terminal domain (Sato 1996). These MMPs are thought to be activated intracellularly by furins (intracellular proteases).

MMPs were originally thought to have individual substrates and properties, and were thus divided into three groups: Collagenases, Gelatinases and Stromelysins. Whilst there is a certain degree of substrate specificity, their functions do overlap, and so they are now also classified by their numbers.

At the gene level these enzymes are controlled by growth factors and cytokines such as IL-1, PDGF, TNF-α, b-FGF and TGF-β. For the most part these growth factors upregulate expression of the MMPs, however, the effects can be very variable between the growth factor and the MMP involved.

MMP-1 and MMP-8 are both interstitial collagenases, together with MMP-2, MMP-8 and MT1-MMP remain the only MMPs capable of degrading native or non-denatured interstitial collagen. Despite having similar degradative properties, they respond differently to growth factors found in the liver: IL-1, which induces MMP-1, has little effect on MMP-13 (Benyon 2001).

Table 1-1 List of known MMPs and their substrates

MMP classification	Referred name	Substrates
MMP-1	Interstitial collagenase	Collagens I,II,III,VII,VIII,X; gelatin; proteoglycans; casein; aggrecan; tenascin
MMP-2	Gelatinase A	Gelatin; denatured collagens; collagens I,IV,V,VII,X,XI; type IV collagenase; fibronectin, elastin, laminin
MMP-3	Stromelysin-1	Procollagens; proteoglycan; gelatin; collagens I,II,IV,V,VIII,IX,X,XI; laminin; activates procollagenase; gelatinase B; aggrecan; vitronectin
MMP-7	Matrilysin or PUMP	Gelatin; elastin; aggrecan; fibronectin; activates procollagenase; vitronectin; laminin
MMP-8	Neutrophil collagenase	Collagens I,II,III,VII,X; gelatin; proteoglycan; aggrecan
MMP-9	Gelatinase B	Denatured collagens; collagens I,IV,V,VII,X,XI; type V collagenase; vitronectin; elastin; aggrecan
MMP-10	Stromelysin-2	Gelatin I,III,IV,V; collagen I,III,IV,V,VIII,IX; activates procollagenase; fibronectin; laminin; elastin; aggrecan
MMP-11	Stromelysin-3	N-terminal domain cleaves casein
MMP-12	Macrophage elastase	Elastin; gelatin; collagen IV; fibronectin; laminin; vitronectin; proteoglycan
MMP-13	Collagenase-3	Collagens I,II,III,VII,X; gelatin; aggrecan
MMP-14	MT1-MMP	Activates progelatinase-A, possibly other MMPs; collagen I,II,III; fibronectin; gelatin; vitronectin
MMP-15	MT2-MMP	Fibronectin; tenascin; laminin; aggrecan; perlecan; activates MMP-2
MMP-16	MT3-MMP	Collagen III; fibronectin
MMP-17	MT4-MMP	Fibrinogen; fibrin; activates TNF-α
MMP-24	MT5-MMP	Activates MMP-2; proteoglycans
MMP-25	MT6-MMP	Collagen IV; gelatin; fibronectin; fibrin

In contrast, TGF-β1 inhibits MMP-1, but upregulates MMP-13, whereas Retinoic acid downregulates only MMP-1(Kaplowitz N 1996). Platelet derived growth factor (PDGF), tumour necrosis factor-alpha (TNF-α) and basic fibroblast growth factor can all upregulate MMP-1, but not MMP-13. An important point relating to these two particular MMPs lies in the fact that no rodent MMP-1 has been found, in rodents the primary interstitial collagenase is MMP-13 (Henriet 1992).

Activation of nearly all MMPs occurs extracellularly, involving cleavage of the propiece and release of the cysteine switch inhibition at the catalytic site. In vitro this can be induced with proteases and detergents, and likewise *in vivo* proteases also activate the MMPs, but additionally some MMPs can activate others (Murphy 1999). MMP-1, MMP-8, MMP-9 and the stromelysins are activated through plasmin, a serine

Figure 1-6 Diagram of the activation of MMP-1 and MMP-3 by plasmin.

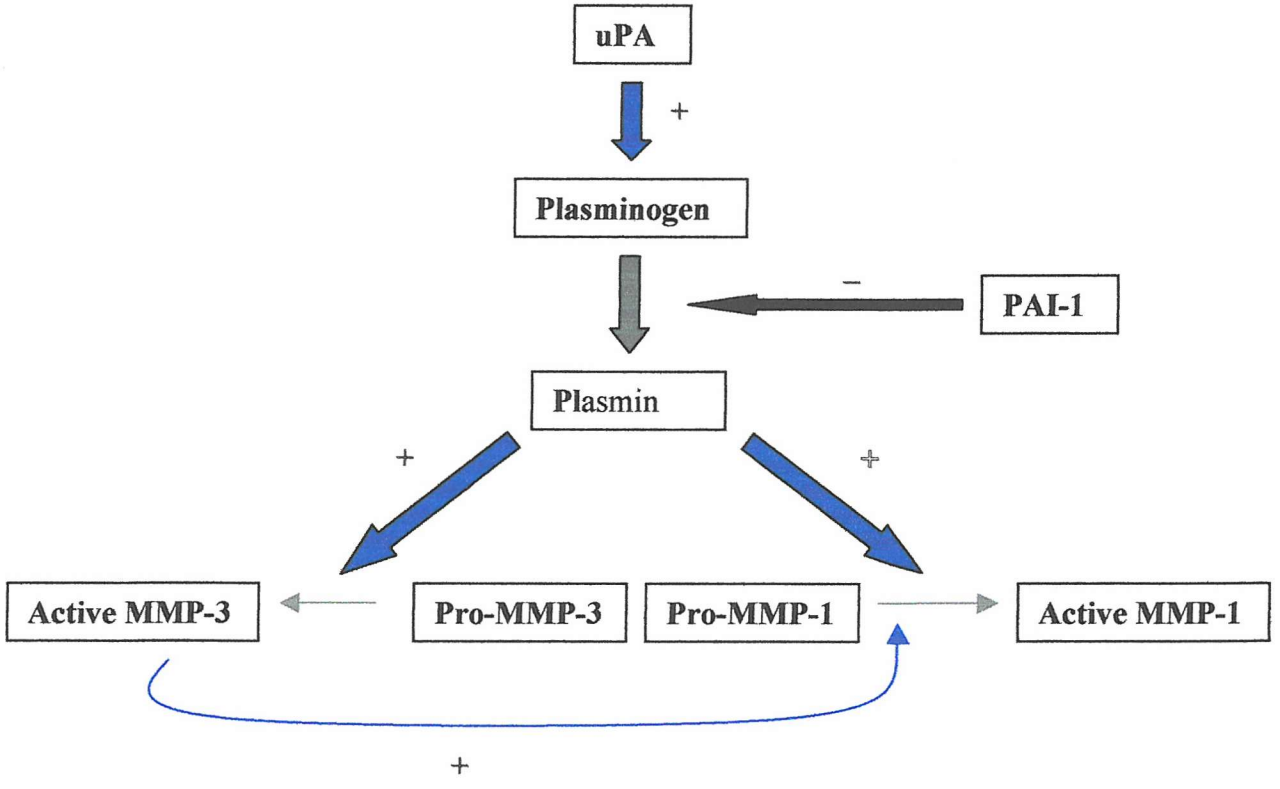

protease derived from plasminogen by urokinase plasminogen activator (uPA) (He 1989). Full activation of MMP-1 requires a further step after cleavage by plasmin, cleavage by stromelysin is also required (Suzuki K 1990). Plasmin synthesis is in turn inhibited by plasminogen activator inhibitor (PAI-1). TGF-β inhibits the synthesis of plasmin, but upregulates PAI-1 synthesis (Edwards 1987). Activation of MMP-2 requires TIMP-2 and MT1-MMP (MMP-14), whilst MMP14 is activated by the intracellular furins (Sato 1996). TIMP-2 acts as a linker to both MMP-14 via its N-terminal and to MMP-2 via its C-terminal allowing a separate MMP-14 molecule to remove the propiece of MMP-2 (Butler 1998). MMP-2 itself is able to activate MMP-13 (Knauper 1996). However, MMP-13 is also cleaved by MMP-14, but requires further cleavage to activate. It is not yet known if this is through forming a similar complex with TIMP-2 as found in the activation of MMP-2.

These enzymes are a normal part of tissue remodelling, of ECM turnover and regrowth, however, if uncontrolled these enzymes could cause great damage, and are thus tightly controlled at three levels: gene expression, activation and inhibition.

The net effect of this process in the presence of TGF-β (found in liver fibrosis) is the increase in deposition of matrix and the decrease of matrix degradation.

1.7.2 Tissue inhibitors of matrix metalloproteinases

Tissue inhibitors of matrix metalloproteinases (TIMPs) which bind stochiometrically (but reversibly) to the MMPs are the major form of MMP inhibition. There are four TIMPs so far identified which all bind and inhibit MMPs, although TIMP-2 is also necessary in the activation of MMP-2.

Although each TIMP is a separate gene product they share certain structural similarities, in particular, TIMP-1 and TIMP-2 have 40% amino acid homology. The protein core of the TIMPs is typically about 21kDa, and have a large number of

disulphide bonds involving 12 cysteine residues, linking three looped structures. The N-terminal is crucial to the inactivation of the MMPs. Cysteine ^{1} and cysteine^{70} of the TIMP molecule bind in a chelate fashion to the active zinc in the MMP and additionally CTCVP amino acid sequence binds to the active site of the MMP (Murphy 1992). TIMP-1, which has been truncated leaving the N-terminus, still has inhibitory activity (Edwards 1992). The C-terminus allows for inhibition of the propeptide MMPs; TIMP-1 binds to proMMP-9 inhibiting its activation by stromelysin and TIMP-2 to proMMP-2, where it is required for its activation by MMP-14. TIMP-1 and TIMP-2 are diffusible molecules but TIMP-3 is able to bind to the ECM with C-terminus (Leco 1994).

Table 1-2 Properties of the TIMPs

Tissue inhibitors of matrix metalloproteinases	Form	Properties
TIMP-1	*Soluble*	*Inhibits active MMPs* *Binds to pro-Gel A & pro-Gel B*
TIMP-2	*Soluble*	*Inhibits active MMPs* *Activates Gel A through binding in TIMP-2/MT1-MMP/pro-Gel A complex*
TIMP-3	*Bound to ECM*	*Inhibits MMPs* *Binds to MT1-MMP*
TIMP-4	*soluble*	*Inhibits MMPs* *Binds to pro- Gel B*

The TIMPs bind to all MMPs although they have different affinities to them. One deviation from this is that TIMP-1 cannot inhibit MMP-14, MMP-15 and MT5-MMP (Will H 1996).

TIMP-1 may have a role in the regulation of cell growth as it has been shown to accumulate in nuclei of fibroblasts in a cell cycle dependant manner (at S-phase) (Li 1995). Furthermore, TIMP-1 has been implicated in the reduction of apoptosis in activated HSC, through MMP inhibition (Murphy 2002). TIMP-3 conversely induces apoptosis in vascular smooth muscle cells and also in tumour cells (Baker 1998).

Another inhibitor of MMPs is Alpha-2-macroglobulin, a plasma globulin that inhibits coagulation and fibrinolytic cascades. It is able to bind to and inactivate the MMPs. However, α2-macroglobulin is also able to bind and inactivate plasmin, thus α2-macroglobulin not only inhibits the activated MMPs but also their activation process (Nagase 1994). The regulation of the TIMPs is, like the MMPs, controlled at different levels: at the level of gene transcription and via inhibition and stimulation of their activity at the extracellular level. Like the MMPs, the TIMPs are also affected differentially by soluble growth factors such as TNF-α and TGF-β. TNF-α induces TIMP-1, but not TIMP-2: TGF-β however, induces TIMP-1 but inhibits TIMP-2 synthesis (Zafarullah 1996). Both TIMP-1 and TIMP-3 are inducible by phorbol esters, but TIMP-2 is not effected.

The promoter sequences of both MMPs and TIMPs share some similarities between the regulatory motifs of their promoter sequences. It is thought that the varied distribution of these sequences accounts for the different consequences of growth factors on the TIMPs. For instance in the mouse, TIMP-1 and MMP-1 have AP-1 and PEA-3 binding sites but in different configurations (Edwards 1992). AP-1 is also found within the MMP-9 promoter but not within the MMP-2 promoter (both members

of the gelatinase family). In humans, TIMP-1 and TIMP-2 also both have AP-1 consensus sequences, but in TIMP-1 it is associated with a PEA-3 motif whereas in TIMP-2 it is further upstream, and associated with AP-1 and AP-2, several SP-1 sites and a TATA box (McCrudden 2000). TIMP-3 also has several SP-1 sites.

1.8 FIBROSIS IN THE LIVER

Chronic liver injury, regardless of its initial cause, results in the same wound healing response. One of the major factors of liver injury however, is the increase in ECM; six times as much ECM is found following chronic injury to the liver. The balance of components within the ECM is altered, especially the collagen content (Seyer 1977; Hahn 1980). In the healthy liver the ECM within the Space of Disse predominantly consists of collagen IV, but in injury, although all collagen production is increased, collagens I and III are found to be particularly high within the new matrix (Hahn 1980; Schuppan 1990). Collagen III accumulates early on in the injury but collagen I and IV increase over time. In long term chronic injury, bands of collagen I can be seen throughout the liver, these bands eventually link around the portal triads, but in so doing, form nodules within the liver as found in the cirrhotic liver. Other components of the normal matrix such as laminin, fibronectin, hyaluronan, chondroitin sulphate and heparan sulphate glycans also increase (Schuppan 1990).

This increase and alteration of ECM has a number of effects on the surrounding cells. Experiments in vitro growing hepatocytes on a commercially made normal basement membrane-like matrix have shown that they retain their cuboidal, and polarized phenotype, but when grown on collagen I matrix or plastic (which imitates the ECM

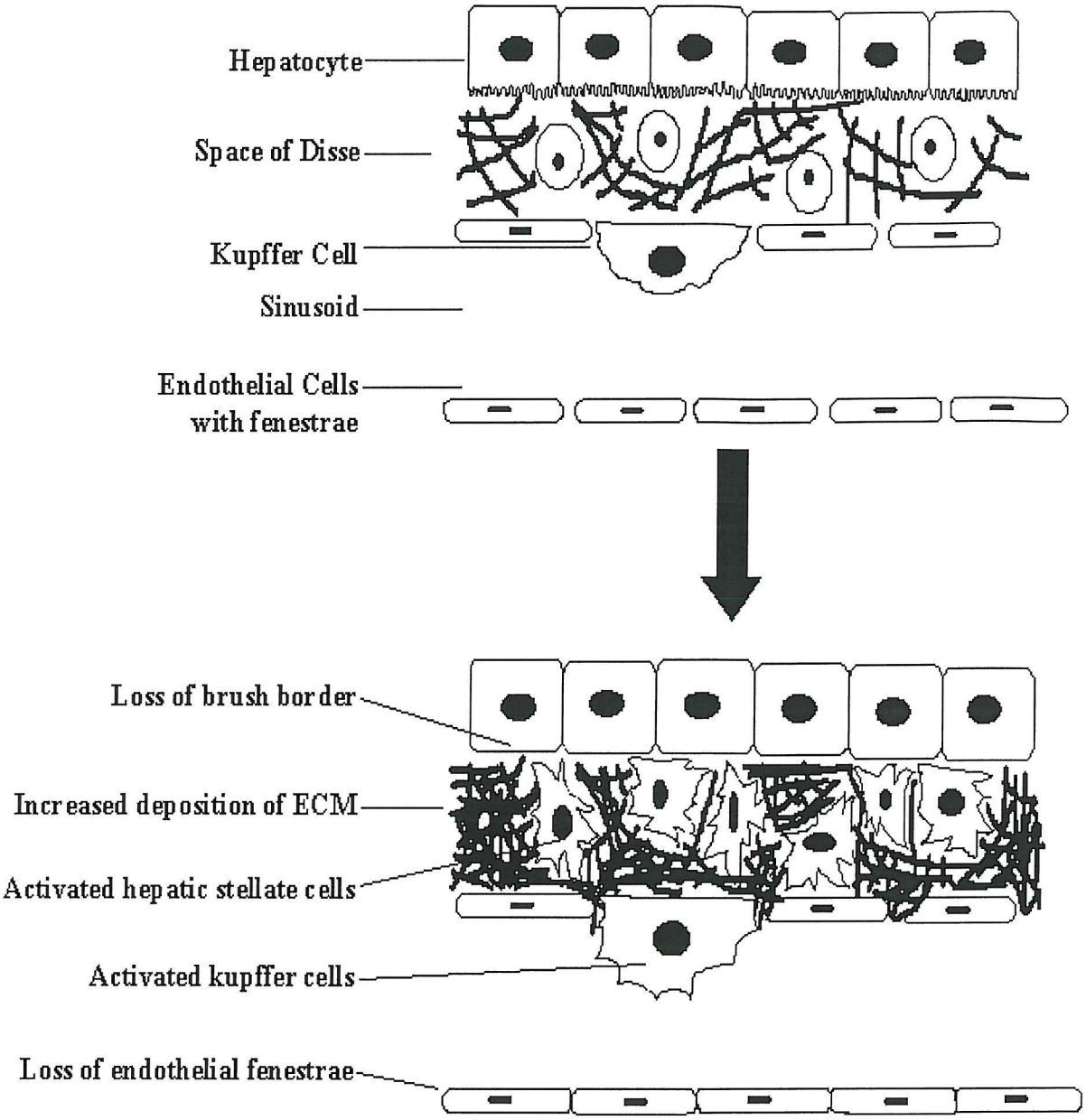

Figure 1-7 Transition to injury within the sinusoid.
Following injury to the liver, the HSCs activate and increase their secretion of MMPs and TIMPs. The ECM within the Space of Disse becomes electron dense due to the high fibrillar collagen content and large increase in other basement membrane components. The hepatocytes lose their microvilli and there is a loss in endothelial fenestrations and the kupffer cells activate.

found in injury) the hepatocytes become flattened(Schuetz 1988). Likewise, hepatic stellate cells are greatly influenced by their surrounding ECM. Whilst on normal basement-membrane-like matrices they retain their retinyl palmitate containing lipid

droplets, but when transferred to collagen I or plastic they too flatten out to their myofibroblastic phenotype (Friedman 1989).

The sinusoidal endothelial cells in a healthy liver are highly porous due to their fenestrae, however, in the fibrotic liver capillarization of the sinusoid occurs, whereby the fenestrae within the sinusoidal endothelial cells are lost. It has been shown that the ECM can alter the porosity of the endothelial cells in culture (via their fenestrae) (Clark 1988). Endothelial cells grown on any one component of the ECM have reduced porosity when compared to endothelial cells grown on normal basement membrane-like matrices (McGuire 1992). Additionally, alcohol and nicotine can both effect the number and size of the endothelial cell fenestrae (Clark 1988; Fraser 1988). These factors may explain why capillarization occurs during injury to the liver. Capillarization, which compromises macromolecular transfer through to the hepatocytes, is associated with the loss of the hepatocyte brush border that is necessary for the uptake of blood filtrates. The injured hepatocytes necrose and release reactive oxygen intermediates (ROI) which can activate the HSC (Nieto 2002). This effect is amplified by the lack of antioxidants that are normally found within the healthy liver. Media from hepatocytes undergoing oxidative stress has been shown to activate the HSCs, causing in particular an increase in proliferation and collagen I synthesis (Nieto 2002).

Kupffer cells activated by the hepatocyte necrosis are known to secrete many cytokines and regulatory factors. Culture of HSC in Kupffer cell-conditioned medium upregulates proliferation and synthesis of collagen. Proliferation is induced through the upregulation of PDGF receptor which could be inhibited with neutralizing antibodies, whilst the increase in collagen synthesis is due to Kupffer cell secretion of TGFβ (Friedman 1989; Roth 1998). In addition, the use of Gadolinium chloride to

deplete the Kupffer cell population in a liver fibrosis model has shown a reduction in TGFβ and activated HSC (Rivera 2001).

Lymphocytes also contribute to the development of liver fibrosis. Lymphocytes divide into two subsets, Th1 and Th2, cell-mediated immunity and humoral immunity respectively. This division is based on the cytokines produced and the resulting immune reaction. Using different mice strains exhibiting a Th1 and Th2 biased profile, liver fibrosis was shown to be most severe in the Th2 response, whilst the in the Th1 mediated immune response only a minimal fibrosis developed (Shi 1997).

Although neutrophil influx into liver is a feature of CCl4 and bile-duct ligation induced injury, recent studies using neutrophil depleted rats have shown that these cells make little contribution to development of fibrosis (Saito 2003). Mast cells, which proliferate in response to liver injury in humans and animal models can produce a variety of pro-fibrotic mediators such as tryptase and heparin but studies using mast cell deficient mice suggest that mast cells are not required for fibrogenesis (Sugihara 1999).

HSC have been shown to secrete the chemokines MCP-1 and MIP-2, both of which induce leukocytes chemotaxis (Marra 1993; Sprenger 1997). Furthermore, the cell adhesion molecules ICAM-1, V-CAM-1 and PAF-1 are known to be expressed in the HSC which would all aid the extravasation of leukocytes into the parenchyma (Pinzani 1994; Knittel 1999).

1.8.1 The Hepatic stellate cell in liver fibrosis

Activation of the HSC has been shown to be pivotal in the onset and perpetuation of hepatic fibrosis: HSC are the main source of the newly synthesized matrix components, MMPs and TIMPs in the fibrotic liver. The activated HSC develops a myofibroblast-like phenotype and starts to express α-SMA, a marker of smooth muscle

cells. Although this is only a true marker in activated rat HSCs, some human HSCs in normal liver can express α-SMA. When the HSCs activate the many retinoid droplets are gradually lost, and the morphology alters as the cell becomes highly fibrogenic and contractile (Friedman 1993).

This activation occurs through the release of mediators and cytokines from activated Kupffer cells, necrotizing hepatocytes and a change in the surrounding ECM all factors in the fibrotic liver (Friedman 1999). In this activated state the cell is very proliferative and secretes a range of mitogenic growth factors, many of which act in an autocrine manner such as PDGF (Pinzani 1998). Deposition of collagens I, II, IV, V and VI is increased within the fibrotic liver, and the HSC has been shown to be the predominate point of synthesis for these collagens (Maher 1990).

Cultured HSCs provide an *in vitro* model for studying their alteration of phenotype in injury. HSCs spontaneously become activated by culture on plastic in serum containing medium. Studies of these cells show that in the first three days the HSCs express MMP-3, MMP-1 (in humans) or MMP-13 (in rats) and urokinase plasminogen activator (uPA) but do not express TIMP-1 or TIMP-2. Thus they display a matrix-degrading phenotype (Benyon 2001). However, this is only transient and with the continuance of culture on plastic downregulation of MMP-1/-13 and MMP-3 is observed. The expression of MMP-2, MMP-14, PAI-1, TIMP-1 and TIMP-2 is upregulated, as is the expression of matrix proteins, collagens I and III. Overall, the HSC has changed to a cell which promotes matrix deposition and inhibits matrix degradation. In addition, perpetuation of HSC activation through the autocrine pathways of the cytokines leads to continual proliferation and their survival against apoptosis (Friedman 2000).

These factors are also found upregulated in models of liver fibrosis such as carbon tetrachloride (CCl_4) induced-liver fibrosis in rats. Our group have found an increase in TIMP-1 and TIMP-2 levels of 260-526% in human fibrotic livers as compared to control livers. In addition, MMP-2 also increased by 324-430% as compared to control, however, MMP-1 did not significantly alter (Benyon 1996). Expression of TIMP-1 and MMP-1 have also been studied within our group in rat models of liver fibrosis. An increase in TIMP-1 was shown both with cells cultured on plastic and with extracts from non-parenchymal cells from fibrotic rat livers. As found before, no change in MMP-1 was found (Iredale 1996).

One study by Knittel showed the expression of MMP-2, MMP-3, MMP-9, MMP-14, TIMP-1 and TIMP-2 to be upregulated after a single dose of CCl_4 (Knittel 2000). After repeated CCl_4 administration, fibrosis develops and increases with the duration of the liver injury and also TIMP-1 and TIMP-2 becomes persistently raised. Yoshiji (2000) showed in a model of CCl_4 induced liver fibrosis using mice transgenically over-expressing TIMP-1 gene, that whilst there was increase in the amount of fibrosis development there was no increase in alpha-SMA, pro-(alpha1)-collagen I and pro-(alpha2)-collagen IV. Therefore it appears that TIMP-1 itself does not activate the HSCs (Yoshiji 2000). However, due to the seven-fold increase in fibrosis within the TIMP-1 transgenic mice following 4-weeks CCl_4 treatment the role of TIMP-1 has been shown to promote the course of fibrosis. The expression of MMP-1 and MMP-13 however does not change in this model.

This supports data found in our group showing that in liver fibrosis TIMP-1 expression increases following which the expression of procollagen 1 also then increases. Therefore when collagen is deposited collagen degradation is already inhibited (Iredale 1996).

This fibrotic process has been shown within our group to be reversible (Iredale 1998). Following injury to the liver, a 28-day recovery period was allowed. During this recovery the levels of TIMP-1 and TIMP-2 were found to decrease whilst at the same time there was an increase in collagenolytic activity from levels observed at peak fibrosis. However, there was no change in the mRNA levels of MMP-13. This again suggests that the degradative properties of MMP-13 (MMP-1 in humans) is inhibited by TIMPs 1 and 2. However, in recovery the levels of these TIMPs decrease and the collagen-rich matrix can be degraded (Iredale 1998).

In contrast to the above data, in a rat model of CCl_4 induced liver fibrosis, Watanabe (2000) found that MMP-13 mRNA was not upregulated throughout the course of liver fibrosis. However, when the livers were allowed to recover, at the 5 day timepoint there was a significant but transient upregulation of MMP-13 (Watanabe 2000).

Kupffer cells, also activated in liver injury, respond by the secretion of growth factors and cytokines which can activate the HSC, i.e. platelet derived growth factor (PDGF), transforming growth factor beta 1 (TGF-β1) and also reactive oxygen intermediates (ROI) (Friedman 1989). These cells also contribute to liver fibrosis as their depletion using galadium chloride ablates CCl_4 induced liver fibrosis. Hepatocytes, when damaged also release cytokines such as Insulin-like growth factor-1 (IGF-1), fibroblast growth factor (FGF) and also transforming growth factor (TGF-α) (Gressner 1995). All of these are able to activate the HSC, thus causing the HSC population to proliferate, increase their secretion of fibrillar collagens, upregulate synthesis of MMPs and upregulate the TIMPs.

Figure 1-8 Activation of the Hepatic Stellate Cell
The activated hepatic stellate cell loses its retinoid droplets, becomes highly proliferative, has increased secretion of ECM components, MMPs and TIMPs.

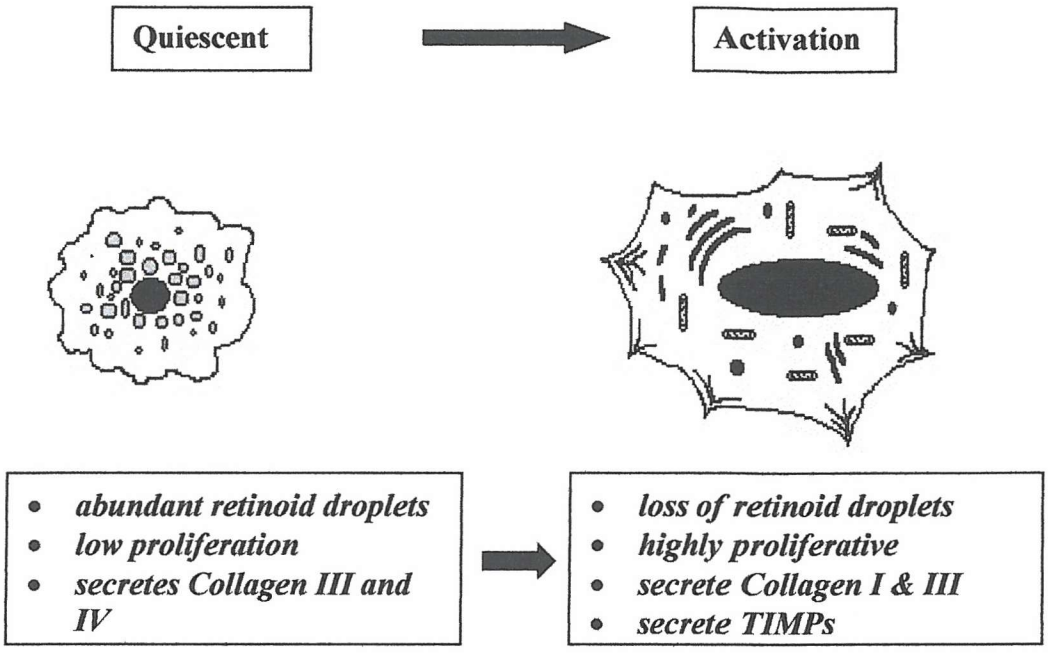

Figure 1-9 Graph displaying the changes in expression of regulators of the ECM during activation of the hepatic stellate cell in vitro.

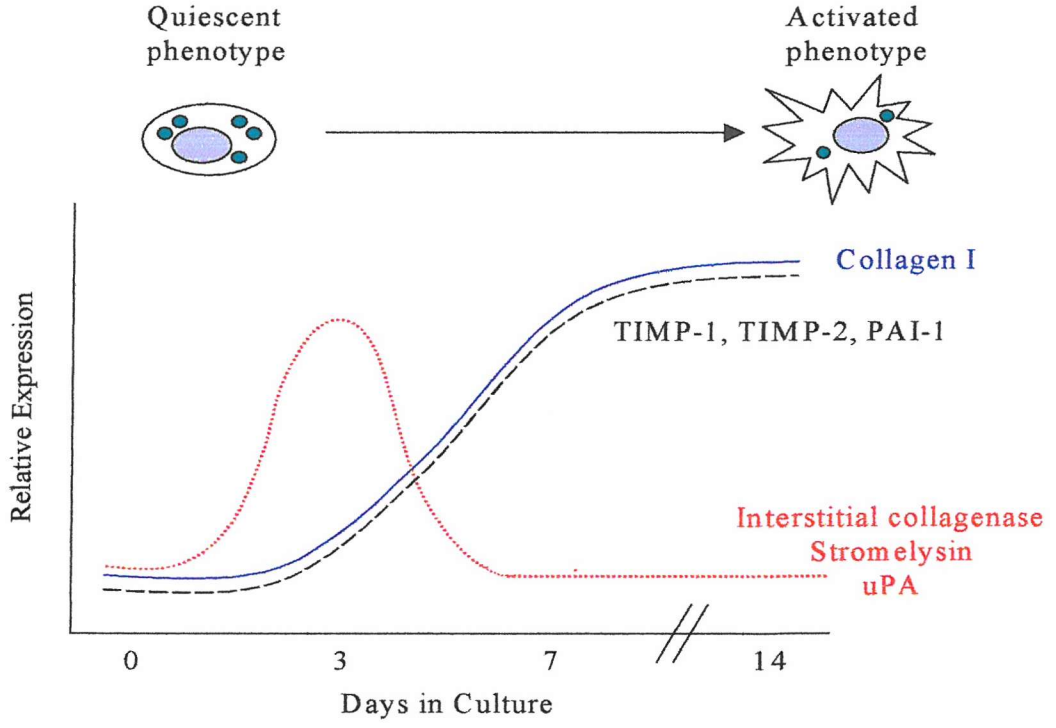

The most potent cytokine to cause proliferation in the HSC is PDGF, which acts in an autocrine manner, there being upregulation of the cytokine and its receptors. Of the three forms of PDGF (-AA,-BB,-AB), the most potent is PDGF-BB (Liu 2000). FGF-2 or basic-FGF (b-FGF) is also a powerful mitogen to the HSCs, and additionally acts as a chemoattractant (Fibbi 1999). Both PDGF and FGF-2 have been found to be upregulate the production of urokinase-plasminogen activator (u-PA) by the HSC (Fibbi 1999). u-PA activates plasminogen to plasmin which can activate the MMPs. Further to the upregulation by PDGF and FGF-2, Fibbi 1999 found that the addition of exogenous uPA could stimulate HSC proliferation, chemotaxis and chemoinvasion, and antibodies to u-PA and u-PA receptor inhibited this effect. Another cytokine with an autocrine pathway is vascular endothelial growth factor (VEGF); like PDGF the expression of both the cytokine and its receptors are upregulated in the activated HSC. VEGF is able to stimulate growth, and can be upregulated by soluble factors found in situations of oxidative stress and hypoxic conditions. However, in late liver injury, activation of VEGF decreases α-SMA expression and the contractile properties of the HSC (Corpechot 2002). Endothelin-1 (ET-1), which is secreted by the endothelial cells as well as the HSCs themselves, stimulates contractility in the HSCs. In quiescent cells ET-1 causes proliferation, but this action is inhibited in the activated HSC by agonists to the ET receptor A (ETA). Conversely, in the activated HSC ET-1 inhibits growth, this action is via the ET receptor B (ETB) (Rockey 1995).

One the most important cytokines found in liver fibrosis is transforming growth factor beta (TGF-β). The isoform most commonly found within the liver and used in previous studies, has been TGF-β1, although TGF-β2 and TGF-β3 appear to have similar properties. TGF-β is secreted by many of the cells in the liver, the endothelial cells, hepatocytes, Kupffer cells and HSCs (Roth 1998; Roth 1998). Kupffer cells

secrete most of the TGF-β found in normal liver. However, in models of liver fibrosis, whilst TGF-β is found within the Kupffer cells, it is mainly localized in the HSCs (Roth 1998; Breitkopf 2001). Levels of hepatic TGF-β mRNA increases through time correlating with the increase in the Kupffer cell and HSC populations (Czaja 1989). This cytokine if neutralized *in vivo* prevents liver fibrosis, and likewise, the overexpression of TGF-β increases the deposition of matrix within the liver. Increase in TGF-β levels also correlates with the increase in procollagen type I levels (Milani 1991).

Transforming growth factor-beta induces apoptosis of the HSC, a major mechanism in resolution of liver fibrosis (Issa 2001). There are conflicting reports on the actions of TGF-β on growth of HSC, some have found no effect, some reports have found inhibition and others still have found it can induce growth. However, TGF-β does accelerate the transformation of the quiescent HSC to its activated state, and prolonged exposure can cause an increase in DNA synthesis via PDGF (Bachem 1993). The overall effect on an HSC population may be to cause a net increase in the numbers and activation status.

The most important effect of TGF-β is its ability to alter the balance of ECM constituents. This change is mediated by upregulation of collagen synthesis in the HSC (both that of fibrillar and non-fibrillar collagens), and inhibition of MMPs and by upregulation of the TIMPs (Bedossa 1995). TGF-β can upregulate collagens I, III and IV, fibronectin and laminin, all of which are upregulated constituents of the matrix found in liver injury (Czaja 1989). Additionally, TGF-β inhibits the MMPs, which would otherwise degrade the new matrix. The production of MMP-1 and MMP-3 have both been shown to be inhibited by TGF-β in fibroblasts, whereas TIMP-1 is induced (Edwards 1987).

The regulation of transcription factors has also been studied during the activation of the HSC. One transcription factor, Nuclear Factor kappa B ($NF_\kappa B$) has been shown to protect against apoptosis of the activated HSC (Lang 2000). NGF which has recently been demonstrated to induce a dose-dependent increase in apoptosis in HSC, also caused inhibition of $NF_\kappa B$ activity (Oakley 2003). $NF_\kappa B$ is activated by the cytokines TNF-α and IL-1β in activated HSC which induce expression of MIP-2 and IL-6, both of which are pro-inflammatory factors (Hellerbrand 1998). The MAP kinases, ERK-1 and ERK-2 have been shown to activate rapidly following injury to the liver, despite the method of insult (Marra 1999; Svegliati-Baroni 2003). Furthermore, a specific inhibitor of ERK was associated with a dose-dependant inhibition of PDGF induced HSC proliferation which also inhibited binding of AP-1 and STAT-1 to their regulatory elements (Marra 1999).

TGF-β differentially regulates the SMAD family of transcription factors. SMADs 2,3,4 and 7 have all been localized in the cirrhotic liver whilst only weak expression was found in non-cirrhotic livers (Kitamura 2003). A CCl_4 induced model of liver fibrosis using SMAD 3 knockout mice found a reduction in collagen alpha I (I) mRNA levels by nearly 60% (Schnabl 2001).

Transcription factors have also been studied in the context of matrix, MMP and TIMP regulation. The consensus sequence for AP-1, as mentioned in 1.7.2. is found in the TIMP-1 promoter sequence, and the AP-1 protein JunD is required for TIMP-1 transcription in the activated HSC (Smart 2001). The activated HSC also expresses three Kruppel-like transcription factors, SP1, BTEB1 and KLF6, which all regulate α1 (I) collagen (Rippe 1995; Ratziu 1998; Chen 2000). However, $NF_\kappa B$ which inhibits α1 (I) collagen transcription operates through an interaction with SP1 (Chen 2000).

1.8.2 The fate of HSC in resolution of liver fibrosis

Liver fibrosis is known to resolve sometimes following elimination of the underlying insult, i.e. use of anti-viral agents in HCV, venesection in haemachromatosis. Although resolution of fibrosis has not been well studied in human liver, emerging studies with rodent models have shown that resolution is associated with the apoptosis of HSC. Following a 4 week CCl_4 liver fibrosis model, resolution of the liver morphology to close to control parameters was achieved over a 28 day period (Iredale 1997). Resolution of liver fibrosis has also been shown in a bile duct ligation model following 3 weeks of injury demonstrating also decrease in HSC numbers and an increase the rate of HSC apoptosis (Issa 2001). Additional evidence that recovery of liver fibrosis is associated with HSC apoptosis is a CCl_4 model concurrently administering gliotoxin. This fungal metabolite induces apoptosis in the HSC, demonstrated a reduction in fibrosis correlating with a reduction in activated HSC (Wright 2001).

HSC are known to express Fas, and in the presence of FasL will undergo apoptosis (Saile 1997). Within the injured liver, cytokines and growth factors are able to induce or protect the HSC from apoptosis. For example, IGF-1 and TIMP-1 have the ability to protect HSC from apoptosis in vitro (Issa 2001; Murphy 2002). The effects of TIMP-1 were shown to be due to its MMP inhibitory capacity. TIMP-1 might protect HSC from apoptosis by stabilising ECM from degradation. This is suggested by studies using r/r mutant mice which produce type I collagen which is resistant to MMPs. Unlike their normal littermates, in these mice, cessation of CCl4 dosing after 8 weeks did not allow resolution of fibrosis or apoptosis of HSC (Issa 2003). These studies suggest that intact type I collagen is a survival factor for HSC. This underlines the role of ECM in dictating cell fate, as described in various other cells such as

mammary gland epithelial cells (Sympson 1994). In contrast, TGF-β and NGF both induce apoptosis of the activated HSC in vitro (Issa 2001; Oakley 2003). The NGF receptor, like Fas, is a member of the Tumour Necrosis Factor superfamily. Following ligand binding, the receptors trimerize, forming a death inducing signalling complex (DISC). Fas-associated death domain protein (FADD) is recruited to the complex, in turn recruiting many pro-caspase 8 molecules which through close proximity to each other activate the enzyme. Caspase 8 then initiates a caspase cascade resulting finally in apoptosis of the cell (Figure 1.10).

Figure 1-10 Diagram of the Fas/FasL receptor.
FasL binds to the Fas receptor, this induces trimerization of the receptors. FADD is then recruited, which in turn recruits pro-caspase 8. Pro-caspase 8 is then activated through close proximity to other pro-caspase 8 molecules.

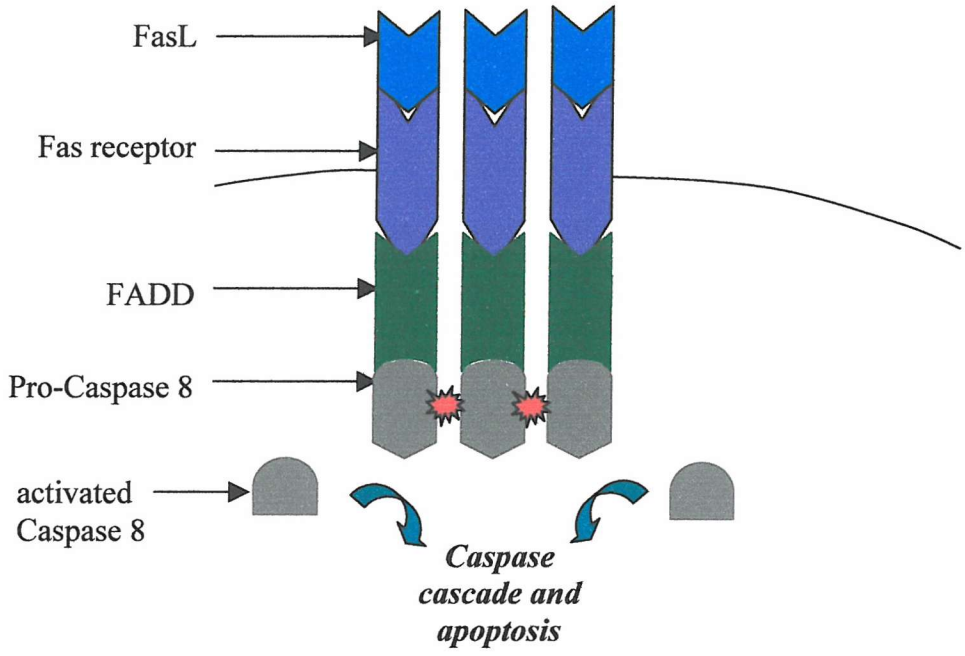

1.9 THE PANCREAS

The fibrotic wound healing response occurs in several organs throughout the body. Evidence for myofibroblasts playing a central role in this process has been found in the lung, the kidney, the liver and lately the pancreas.

The Pancreas is a glandular organ that lies transversely behind the stomach, and is divided anatomically into a head, neck and tail. The exocrine section is important in the digestive process as it is responsible for the secretion of enzymes essential in the digestion of carbohydrates, protein and fat. The acini form the exocrine section and account for 98% of the pancreas. The pancreas is divided into lobules which are separated by areolar tissue. Each lobule contains many clusters of acini which are blind-ended tubules.

Figure 1-11 Diagram of an acinus within the Pancreas
Schematic representation of the pancreatic acinus – not to scale.

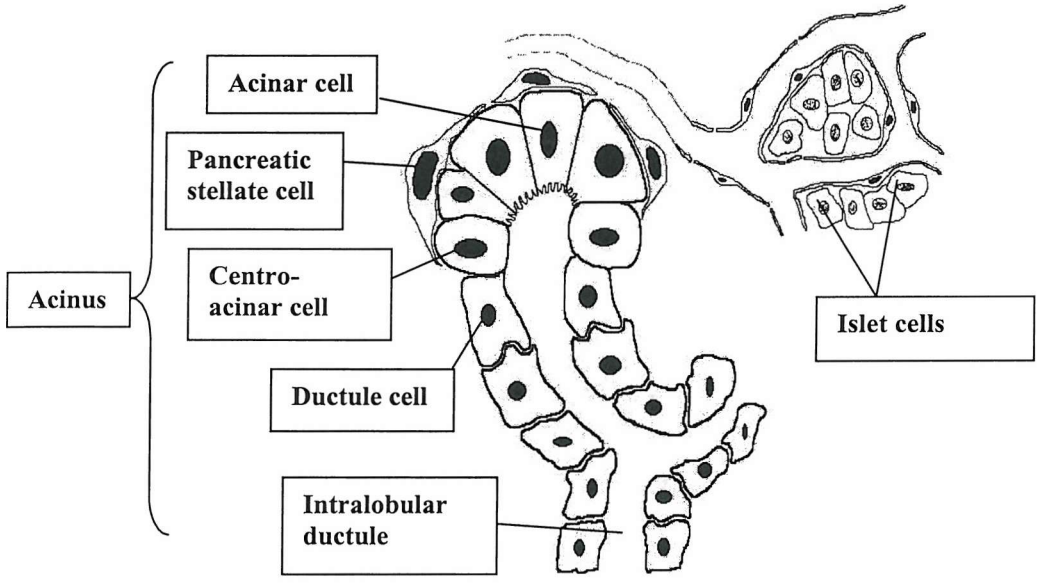

Figure 1-12 Representation of the acinus compared with a histological section
Figure reproduced from Physiology 510, Pancreatic Physiology, University of Michigan, http://www.med.umich.edu/phys/510/handouts/Pancreas.pdf

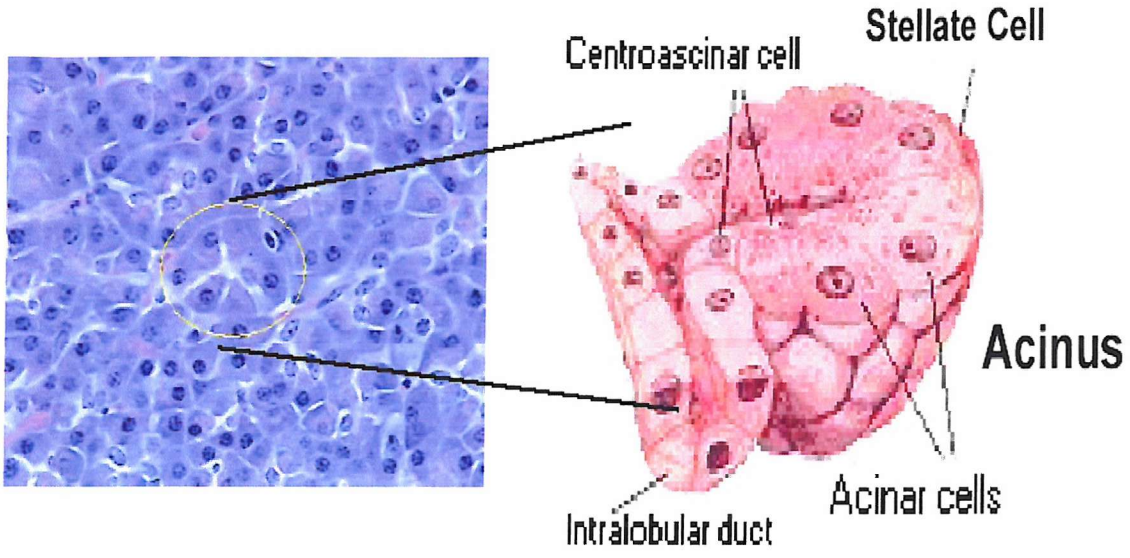

Each individual acinus drains into an intercalated duct, which then drains into an interlobular duct. The interlobular ducts leave the lobules, and converge with an extralobular duct which again converges, with the main pancreatic duct. This joins with the main bile duct as it empties into the duodenum.

The acinar cells are polarized cells, and contain many zymogen granules in their apical cytoplasm which are released after a meal through exocytosis. The number of these granules increase between meals, ready for later release. Enzymes secreted by the acinar cells include proteases, lipases and ribonucleases. Proteases such as trypsin, chymotrypsin and carboxypeptidase cleave polypepetides to peptides, whilst carboxypeptidase removes amino acids from C-terminals. Amylase is also secreted, and reduces starch to maltose and other dextrins. Likewise, Lipases are secreted, these include triacylglycerol hydrolase and phospholipase A_2, both of which cleave ester bonds to release free fatty acids. Cholesterol ester hydrolase, also secreted acts on

cholesterol esters and releases cholesterol and free fatty acids. In addition, biocarbonate ions are secreted to neutralize acid chyme from the stomach. Though only weighing approximately 10g, 1litre of pancreatic juice is released every day. The endocrine section of the pancreas is represented by the Islets of Langerhans and accounts for only 2% of the pancreas. It regulates endogenous glucose and ensures the energy requirements of the body are met at all times.

1.9.1 Fibrosis within the Pancreas

Pancreatic fibrosis is found in Pancreatitis, a disease as mentioned before found in 3 in 100,000 of the Western population (Riela 1990). Whilst relatively rare, pancreatic disease is extremely painful and requires a large amount health management. Pancreatitis itself can be divided into two classifications: acute and chronic. It is matter of some dispute as to whether repeated bouts of acute pancreatitis lead to the onset of chronic pancreatitis, or whether the two diseases are in fact separate. However, in the context of scarring in the pancreas and the continuation and irreversibility of fibrosis, it is chronic pancreatitis which will be discussed.

Chronic pancreatitis has two mains forms of the disease. Chronic calcifying pancreatitis, which accounts for 95%, results in the formation of calculi or protein plugs which cause obstruction. Obstructive pancreatitis is due to a scar or obstruction (such as a tumour) in the pancreatic duct, but this obstruction occurs before the disease, and is not formed due to the disease (Sarles 1992). The resulting chronic pancreatitis is the result of a continuing inflammation, regardless of the primary insults.

Alcohol abuse is by far the most common cause of pancreatitis, and results in the chronic calcifying pancreatitis. However nicotine, and high protein and fat diets are also causes of chronic pancreatitis. Hereditary pancreatitis allows the formation of

calcifying plugs thus causing blockage within the ducts and pancreatic duct hypertension (Sarner 1995).

From all of these insults arises the same sequelae from which acute episodes may occur before the onset of the chronic disease and its symptoms. There is severe destruction and loss of exocrine parenchyma, and much fibrosis, particularly periductular fibrosis. The fibrotic lesions are rich in collagens I and III, and this ECM gradually replaces the exocrine parenchyma (Kennedy 1987) (Haber 1999). Many protein plugs form which cause blockages throughout the pancreatic ducts, causing obstruction of the pancreatic juices. With the loss of these juices malabsorption in the patient occurs due to their increasing inability to efficiently digest their food. The obstructions throughout the pancreas cause a histologically patchy look due to the areas of necrosis. New ducts form in a chaotic fashion and, later in the course of the disease there is also loss of endocrine tissue, resulting also in loss of function. Many patients of chronic pancreatitis develop diabetes later on in the disease progression (Sarles 1992).

1.9.2 The Pancreatic stellate cell

In recent years a PSC has been identified, which may mediate fibrosis and inflammation within Pancreatic Fibrosis in a similar fashion to the HSC. Stellate-type cells were first identified in 1982 by Watari (1982) by the presence of fluorescence (when subjected to 328nm wavelength) within the pancreata from vitamin A-loaded mice (Watari N 1982). These cells were also found by Ikejiri 1990 in sections of normal rat and human pancreas. Sections of human chronic pancreatitis were also examined and these displayed stellate-type cells in association with collagen I bands (Ikejiri 1990).

The PSC was finally identified by Apte (1998) and Bachem (1998) (Apte 1998; Bachem 1998). These cells are found to have a periacinar distribution and comprise 4% of the total cells of the pancreas (Apte 1998). Like the HSCs, the PSCs also have long cytoplasmic processes, which encompass the base of adjacent acinar cells. When cultured on plastic, like the HSC the PSC phenotype becomes activated to an α–SMA expressing myofibroblast-like phenotype (Apte 1998; Bachem 1998). The PSCs were retinoid rich, and autofluoresced when primarily isolated, but following activation on plastic tissue culture plates these retinoids were lost. Within the normal pancreas, or on isolation these cells expressed GFAP and desmin but following 48hrs activation these cells expressed α–SMA (Apte 1998). Immunostaining has shown that the cultured or activated PSCs produce ECM proteins such as procollagen III, collagen I, laminin and fibronectin (Apte 1999). These PSCs were also shown to be responsive to the mitogenic cytokines PDGF and TGF-β, which both increased proliferation and collagen synthesis in vitro. Transforming growth factor-beta can also upregulate expression of the PDGF receptor (Apte 1999). Our group has shown the expression of several activation markers, collagen-1, TIMP-1, TIMP-2, MMP-2 and MT1-MMP and found regulation by TGF-β. Collagen was found to increase and MMP-3 and MMP-9 to increase following treatment with TGF-β1. Furthermore, PSC proliferation also decreased but with the addition of pan-TGF-β neutralising antibody proliferation was increased (Shek 2002).

Thus there are many similarities between the fibrotic process within the pancreas and the liver. In both organs the fibrotic process deposits large quantities of collagen –rich matrix, which in turn disrupts the architecture of the organ. This disruption to structure aids the end failure of the organs. In both cases, the PSC and HSC activate from quiescent vitamin-A rich cells to highly proliferative activated stellate shaped

cells. In the activated state, both the HSC and the PSC have been shown to synthesize large quantities of the ECM proteins. In addition both these cells have also been shown to synthesize the MMPs and TIMPs, an increase of the latter is found in with activation.

1.10 INTERFERON ALPHA

Interferon alpha (IFN-α), a cytokine with antiviral properties, was first discovered in 1957 by Isaacs and Lindenmann. The Interferons (IFNs) themselves divide into two groups, type I and type II IFNs. There are four known type I IFNs; IFN-α, IFN-β, IFN-ω, and IFN-τ (trophoblast IFN, only found in sheep and cattle) and IFN-γ is the only described type II Interferon.

The type I IFN genes are found on chromosome 9, where more than thirteen genes encode for IFN-α, as compared to the one gene that codes for IFN-β. Unlike other cytokines, the IFN-α gene has no introns. IFN-α proteins and glycoproteins (of which it is estimated there are at least 23) typically contain 166 amino acids with molecular weights of between 16,000-28,000 daltons (Medscape 2000). These proteins have been shown to have different activities in cells, although how this is achieved is not yet understood (Foster 1996; Yanai 2001).

Although IFN-α is an antiviral, it cannot prevent a viral infection of the cells unless those cells have been exposed to IFN-α prior to their exposure to the viral infection (Medscape 2000). In the presence of a virus IFN-α acts by inducing the production of anti-viral proteins. These have a variety of mechanisms inducing effects such as modulation of cell transcription and translation (to hinder viral replication) and reduction of cell proliferation (again hindering viral replication). It is thought that most cells can secrete IFN-α, in contrast to type II IFN-γ which is only secreted from

T-cells and Natural killer cells (Maeyer-Guignard 1994). However, those cells found to be principally responsible for IFN-α secretion are also the macrophages, monocytes, non-B, non-T lymphocytes and Natural killer cells. IFN-α proteins are principally secreted in response to viral stimuli but also to other growth factors and cytokines .

1.10.1 Interferon alpha receptors

Interferon alpha exerts its effects through specific binding to cell surface receptors, which are also utilized by IFN-β (IFN-γ has its own receptor). The Type I Interferon receptor is a member of the class II cytokine receptor family, a heterodimer, and consists of two subunits IFNAR1 and IFNAR2, also referred to as IFNARα and IFNRβ. The IFNRβ is found in three forms, the active $IFNR\beta_L$ (long), the $IFNR\beta_S$ (short) is a truncated 55kDa inactive version (Domanski 1995) and also smaller soluble form (40kDa) has been identified (Novick 1994). The IFNAR1 subunit is a 63kDa transmembranal protein of 557 amino acids: an extracytoplasmic domain of 409 amino acids (which divides into two distinct domains each approximately 200 amino acids each); a transmembrane domain of 21 amino acids and an intracytoplasmic domain of 100 amino acids which contains four tyrosines. IFNAR2 is a type-I IFN high-affinity 115kDA protein of 315 amino acids, also with an extracytoplasmic domain of 217 amino acids, a transmembranal domain of 20 amino acids and an intracytoplasmic domain of 80 amino acids (Stark 1998).

IRNAR1 is associated with tyrosine kinase 2 (Tyk2) and INFAR2 is associated with Janus kinase 1 (JAK1) and signal transductor and activator of transcription 1 (STAT1), to which signal transductor and activator of transcription 2 (STAT2) is associated.

When binding of IFN-α/-β occurs the two subunits dimerize; this dimerisation allows for the cross-phosphorylation and activation of Tyk1 and JAK1. In turn Tyk1 and

JAK1 phosphorylate IFNAR1 to create a docking site for STAT2. With STAT2 now bound to IFNAR1, IFNAR1 becomes phosphorylated creating a different docking site for STAT1. STAT1 and STAT2 form a heterodimer, which is released from the IFN receptor complex. The heterodimer associates with interferon regulatory factor 9 (IRF-9) and is then referred to as interferon-stimulated gene factor 3 (ISGF3). Binding to IRF-9 is necessary, as studies where the IRF-9 gene was disrupted have shown a lack of response by IFN-α to viral stimulation (Harada 1996; Kimura 1996). The ISGF3 complex translocates to the nucleus where it binds to specific DNA sequences. These sequences contain a common motif, an interferon-stimulated regulatory element (ISRE). Promoters containing this motif are activated allowing transcription of interferon stimulated genes encoding the interferon proteins (Garcia-Sastre 2002).

Figure 1-13 The IFN-α receptor pathway

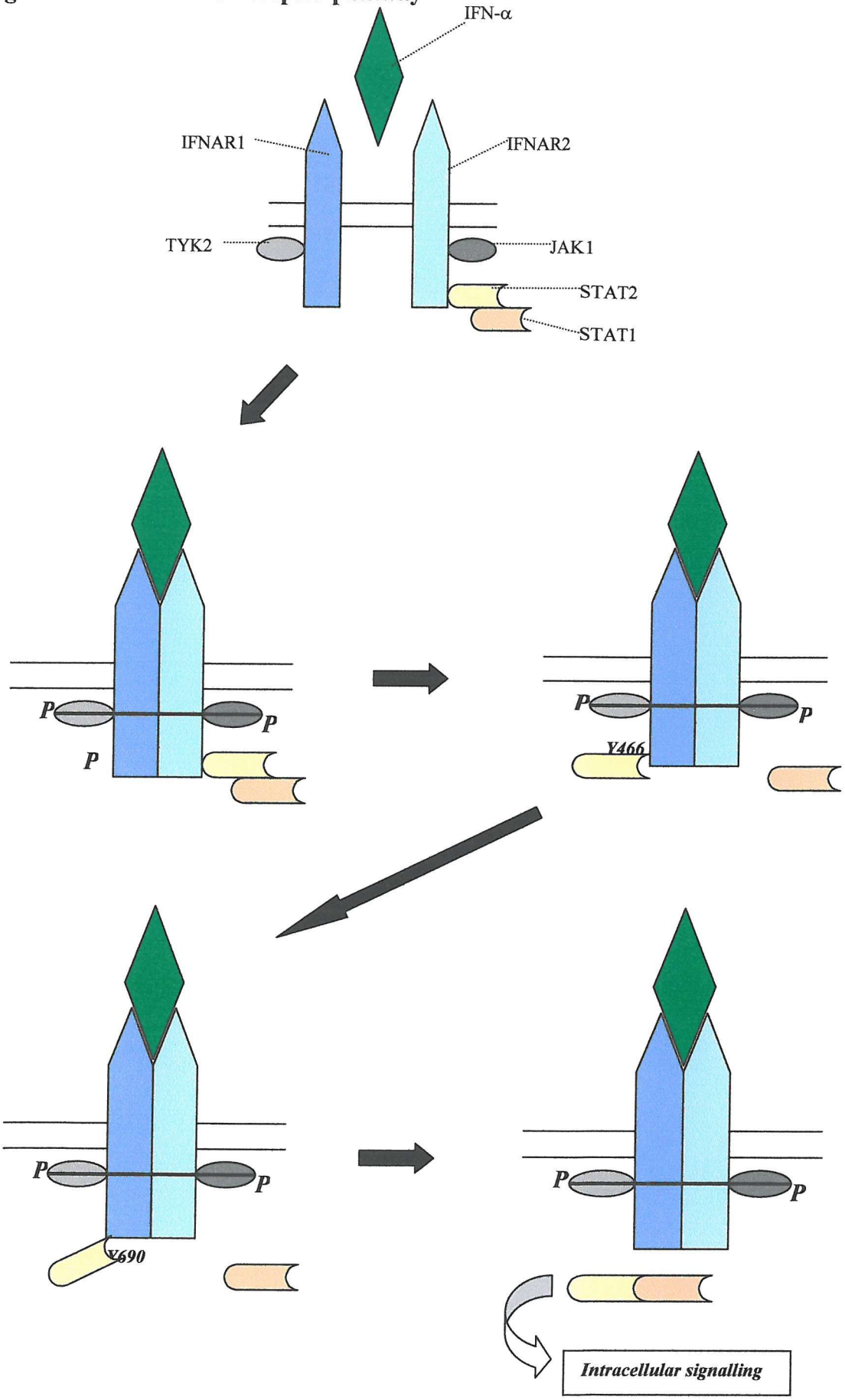

1.10.2 Interferon alpha induced proteins

IFN-α exerts its antiviral effects through the production of IFN-induced proteins. The induction of these proteins result in the effects which cause the anti-viral state of the cell. The proteins aim to inhibit or prevent viral replication; as viral replication uses the cells' own replicative system the proteins are designed to either focus on the particular difference of viral RNA, or to inhibit functions such as protein synthesis. They are also thought to induce a pro-apoptotic state and IFN-α itself can effect the cells and cytokines of the immune system. Additionally, some proteins induced by IFN-α are proteins from the IRF and the STAT family, used in type I and type II IFN signalling (Garcia-Sastre 2002). The most predominant proteins produced are: 2'-5'-oligoadenylate synthetase (2'5'OAS); Protein kinase P1 (PKR) and the Mx proteins.

1.10.2.1 2'-5'-oligoadenylate synthetase

2'-5'-oligoadenylate synthetases (2'5'OAS) are a family of nucleotide polymerases, all are induced by IFN, all require dsRNA and all polymerize ATP to 2'-5'-linked oligonucleotides (although other nucleotide triphosphates can be used). The enzymes are found in three sizes: small, medium and large (Sen 2000). The small group form homotetrameric complexes, the medium family dimers and the large family monomers. All share a homologous region of protein, found once in the small group, twice in the medium and three times in the large family. The proteins, found in humans on chromosome 12, are encoded by alternatively spliced mRNA, which gives them the same amino-terminal sequence, but distinct carboxy-terminal sequences (Sen 2000). The 2'5'OAS enzymes are part of an endonuclease enzyme system able to cleave single-stranded RNA (ssRNA) both from the virus and the cell itself (Stark 1998). Following induction by type 1 IFNs, 2'5'OAS converts ATP to 2'-5'-linked

oligonucleotides. These 2'-5'-linked oligonucleotides can inhibit mRNA-dependant protein synthesis and increase the rate of mRNA degradation. Most importantly, 2'-5'-linked oligonucleotides can, in the presence of double stranded RNA (dsRNA) and single stranded RNA (ssRNA) activate an enzyme, endoribonuclease RNase L (Hartmann 1998). (As dsRNA is normally only found in viral replication, and is not found in the normal processing of a cell this provides a reliable induction mechanism.) It is this RNase L which cleaves viral and host ssRNA (Ghosh A 2000). The function of RNase L consists of a N-terminal region which acts as a repressor, and contains a P-loop motif, the C-terminal contains a region homologous with protein kinase, a cysteine-rich domain and the ribonuclease domain. RNase can be reversed through its C-terminal end region by binding to 2',5'-oligonucleotides (Sen 2000).

Although IFN treatment increases the level of the 2'5'OAS enzymes within the cell, they remain inactive until in the presence of dsRNA. The different enzymes are found associated in different locations throughout the cell, for instance the p100 (large) is associated with ribosomes. There is also evidence for the role of 2'5'OAS in inducing apoptosis as RNase L -/- mice not only had an impaired antiviral function, but also developed severe enlargement of the thymus due to a suppression of apoptosis. In addition, fibroblasts from these mice exhibited suppression of apoptosis when treated with different apoptotic agents (Zhou 1997).

Figure 1-14 The 2'5' oligoadenylate synthetase system
IFN-α induces 2'5'oligoadenylate synthetase, which in the presence of dsRNA converts ATP to 2'5'oligoadenylates. These activate endoribonuclease RNase L which cleaves ssRNA.

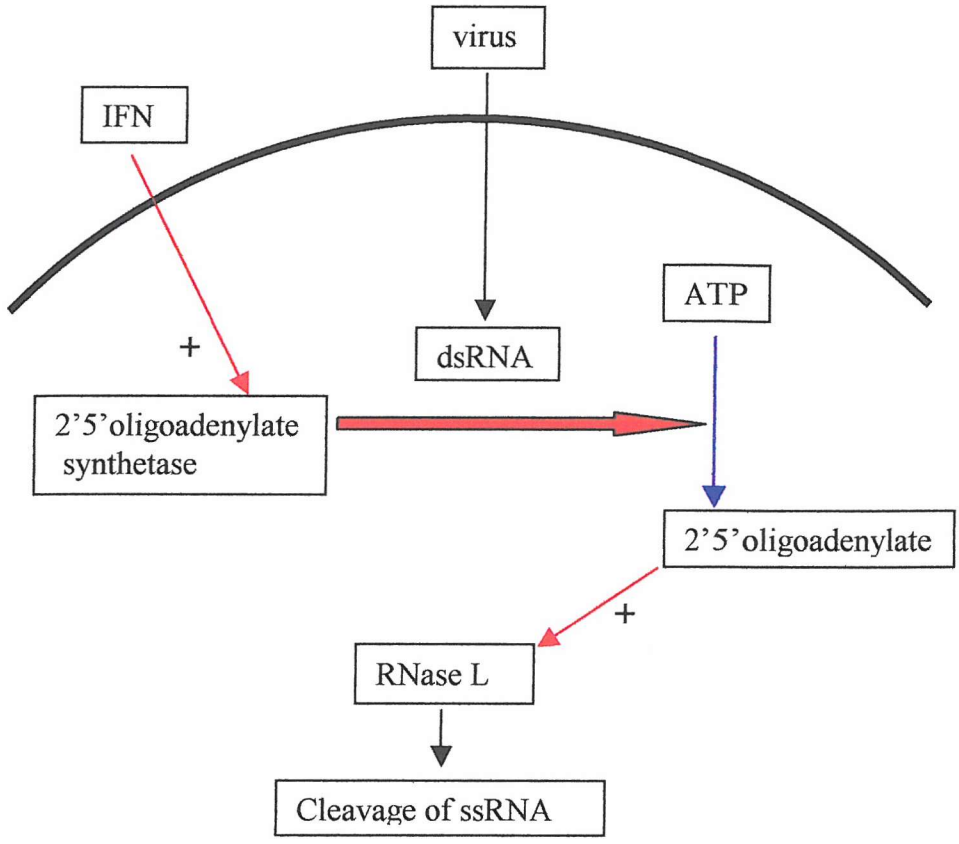

1.10.2.2 Protein kinase P1

Protein kinase P1 (PKR) is a serine-threonine kinase also induced by the presence of dsRNA, and likewise, requires the presence of ATP. Normally inactive in the cell, in the presence of dsRNA it autophosphorylates. PKR binds via motifs in its N-terminal region to the minor grooves of dsRNA (Sen 2000). This binding causes a conformational change which exposes an ATP-binding site on the PKR protein allowing autophosphorylation. PKR is then able to phosphorylate the alpha subunit of eukaryotic initiation factor-2 (eIF-2). This binding inactivates eIF-2 by forming an eIF2-GDP, an inactive enzyme complex. The eIF-2 enzyme is essential in the

initiation of protein translation, and therefore activation of PKR results in inhibition of translation (Sen 2000).

PKR has also been shown to bind to and phosphorylate other proteins such as histones, I_kB, and the HIV protein Tat, although there is no evidence to shown these are true substrates (Williams 1999). Further evidence for this role lies in the induction of tumours when only a mutant PKR is expressed, suggesting a role in proliferative regulation. There is also evidence to suggest that the PKR pathway may induce apoptosis

Figure 1-15 The activation of PKR by Interferon alpha
IFN-α induces PKR, which in the presence of dsRNA autophosphorylates, PKR then phosphorylates eIF-2. When eIF-2 is phosphorylated it is unable to initiate translation within the cell.

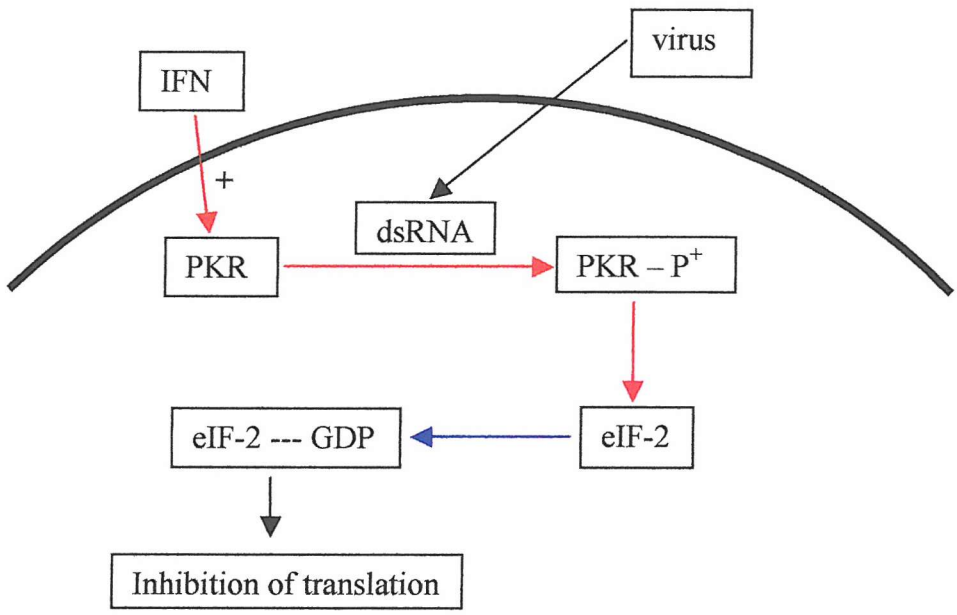

Overexpression of PKR has inhibited growth in both yeast cells (Dever 1992). Balachandran (1998) found that in the presence of dsRNA mouse cells expressing mutant PKR became malignant whilst those overexpressing PKR underwent apoptosis. They also showed that members of the Tumour Necrosis Factor (TNF) receptor family, such as Fas and Bax, were upregulated. Furthermore, mouse fibroblasts which lack

Fas-associated death domain (FADD) did not undergo apoptosis induced by dsRNA (Balachandran 1998). However, it has been shown that whilst PKR induces apoptosis, despite the additional upregulation of Fas, evidence indicates that the FADD-caspase 8 pathway is the pathway used, but that the Fas-FasL interaction is not required for apoptosis to occur (Gil 2000). PKR mediated apoptosis can be blocked by expression of bcl-2 (Lee 1997).

1.10.2.3 Other Interferon-inducible proteins

The Mx proteins are GTPases which are members of the dynamin superfamily – a family of proteins which assemble into horseshoe and ring shaped helices. Little is know about the precise mechanism of the Mx proteins. However, it is known that these proteins bind and hydrolyse GTP to GDP, and that it is the binding of the GTP which is crucial to there antiviral effect, not the hydrolysis (Maeyer-Guignard 1994). The Mx proteins are thought to inhibit growth of the viruses although, this often occurs at different points. The human MxA protein exerts its effect in the cytoplasm late in the viral replication, however, the murine Mx1 protein acts in the early stage of protein translation. This is also virus specific, e.g. human cytoplasmic MxA protein inhibits the growth of influenza, measles and hanta viruses, but not the Dhori viruses (Stark 1998).

Another IFN-stimulated protein is ADAR, a adenosine deaminase also specifically induced by dsRNA. ADAR catalyzes the C-6 deamination of adenosine to yield inosine. Changes of adenosine to inosine are found throughout viral RNA, especially in persistent infections (Samuel 1998). P56 is a strongly induced by IFN, and is thought to inhibit protein synthesis by competing with eIF-3. It has been found to inhibit synthesis in a dose-related fashion, a effect which could be ameliorated by the addition of eIF-3 (Guo J 1998).

The P200 family also appear to inhibit cellular transcription, and may possibly have a role outside of IFN induction. P202, a member of the family has been shown to bind to proteins such as Retinoblastoma protein (RB) (Choubey 1995), NF_kB subunits P65 and P50 and also c-jun and c-fos (Min W 1996).

1.10.3 Effects of Interferon alpha

1.10.3.1 Cellular growth and apoptosis

Interferons have been shown to have a growth inhibitory effect throughout many cell lines. Interferon alpha is able to lengthen each phase of the cell cycle, and halts cells in the G0 phase, the resting phase (Oberg 1992; Matsuoka 1998; Thomas 1998; Sangfelt 1999). This inhibition of proliferation is a dose-dependant effect, seen in many cell types such as colon carcinoma cells, malignant breast tissue cells, megakaryocytes and fibroblasts.

There is much evidence to demonstrate the role of IFN-α in inducing apoptosis. Kaser (1999) found that IFN-α upregulated mRNA for FAS and FAS-L in peripheral blood mononuclear cells (PBMC) (Kaser 1999). As mentioned previously, Zhou found that in RNase L -/- mice, apoptosis was prevented (Zhou 1997). Balachandran (1998) found also that activation of the IFN-α induced protein PKR increases expression of Fas and Bax in murine cell lines (Balachandran 1998). In glioma cells IFN-α sensitizes them to FasL induced apoptosis, and increases activation of caspase-3 (Roth 1998). Renal cell carcinoma patients treated with IFN-α displayed higher apoptotic indices and increased labelling for Fas and FasL in the carcinoma tissue. However, when three hematopoietic cell lines were compared, IFN-α had a different effect in each line. In Daudi cells (derived from B-cell lymphoma), cell cycle arrest occurred, but no apoptosis followed. This antiproliferative effect has been linked to

the downregulation of the nuclear transcription factor NF-kappaB. Suppression of NF-kappaB was found to correlate in a dose-dependant fashion with IFN-α. In U-266 cells (derived from myeloma cells) and in H9 cells (derived from T-cell lymphoma) apoptosis was induced rapidly (Sangfelt 1997). In Jurkat cells (derived from T-cell leukaemia), IFN-α decreased cell growth rate, but again did not induce apoptosis (Petricoin 1997). In T-lymphocytes from healthy donors, IFN-α was found to inhibit their proliferation by blocking entry on the cells into S-phase.

Due to its antiproliferative capacity much work has centred around malignant cells and IFN-α has been used as a treatment for some forms of cancer. IFN-α can decrease the transcription of oncogenes such as c-myc, c-mos, c-abl and c-src (Harvey 1994; Martinelli 2000). In some cell lines continual exposure to IFN has not only decreased their level of transcription of these oncogenes, but has partially reverted to a normal phenotype (Samid 1984). In contrast to much of the work above, IFN-α has been found in increase proliferation in bone marrow fibroblasts (Wickenhauser 2000).

1.10.3.2 The Immune response

IFN-α has a variety of effects on the immune response. It is an innate cytokine and therefore is able to respond immediately to a viral infection. Within the peripheral blood mononuclear cells (PBMCs) a sub-population has been identified as natural interferon producing cells, which compromise approximately 1% of the total PBMCs (Ferbas 1994). IFN-α is found continually expressed at low levels in the spleen, liver, kidney and peripheral blood mononuclear cells (Maeyer-Guignard 1994).

IFN-α induces the activity, cytotoxicity and proliferative ability of Natural Killer cells (NK cells). However, at high concentrations IFN-α inhibits the NK cell activity (Biron 1984; Jewett 1995). It has been shown lately, that IFN-α stimulates NK cell proliferation through upregulation of IL-15, also a potent inducer of proliferation and

survival (Nguyen 2002). Pre-NK cells can also be recruited by IFN-α (Biron 1984), whilst not mature they are able to bind target cells although unable to lyse them.

Indeed, it has previously been observed that in patients with chronic liver disease, NK cell activity was increased using IFN-α treatment (Hirai 1986). This was later confirmed using rats with liver fibrosis induced with thioacetamide. NK cell activity was shown to be reduced with administration of thioacetamide, but this activity level was recovered following IFN-α treatment (Shirachi 1998).

There is also evidence to show that IFN-α can induce expression of the IgG receptors by B-cells (Medscape 2000). IFN-α has been shown to induce the interferon producing cells to differentiate into dendritic cells in addition to inducing dendritic cell maturation. This increases the opportunity for antigen presentation to T-cells and also initiates their secretion of IFN-α (Kadowaki 2000) (Montoya 2002).

A further response to IFN-α is the upregulation of MHC class I proteins. This aids the immune response as presentation of antigen to the T-cells is such a major factor of the cell-mediated response (Erusalimsky 1987). Some species of IFN-α are also capable of upregulating MHC class II, although this is far more strongly induced by IFN-γ (Stark 1998).

1.10.3.3 Effect on fibrosis related-proteins

IFN-α has been shown to antagonize TGF-β1 protein production in both normal fibroblasts and those from dermal wounds. In addition, TGF-β stimulated collagen production is also inhibited by treatment with IFN-α in both types of fibroblast (Tredget 2000). However, IFN-α induces secretion of TGF-β1 in macrophages (Wickenhauser 2000). Collagenase also increases two-fold in the presence of IFN-α in

ermal fibroblasts (Ghahary 2001). However, a study in glioma cells shows a decrease in MMP-2 following three day IFN-α treatment.

1.10.4 IFN-α and Liver Fibrosis

1.10.4.1 Clinical evidence of the effect of IFN-α

As my project studied the effects of IFN-α on liver fibrosis in a rat CCl_4 model, it is formative to outline previous studies. Two groups, Isaacs and Lindenmann and Nagano and Kojima first discovered Interferon alpha as an antiviral agent in 1957 and 1954 respectively (Nagano 1954; Isaacs 1957). Following this Interferon alpha was introduced as an antiviral treatment for patients with Hepatitis B virus (HBV) in the early 80's. This was then extended to the treatment of Hepatitis C virus (HCV) where monotherapy achieved a 20% response within patients. This was later developed to include concurrent treatment with Ribavirin (an IMP inhibitor), together the drugs can achieve a 40% sustained response rate.

Recently a new form of IFN-α therapy has been introduced, Pegylated IFN-α2b™ (PEG-Intron™) Roche. This is a conjugate of recombinant IFN-α with monomethoxy polyethylene glycol (PEG), the addition of which stabilises the IFN-α in the patient. This then allows for a once weekly injection instead of the current regime of three times a week, the latter injections peaking and subsiding within 24hrs. The sustained levels of IFN-α are thought to aid recovery, and is still given with Ribavarin.

However, it was quickly noticed that patients treated with IFN-α had improved histology of the liver. Immunohistochemistry of fibrotic livers showed a significant reduction in α-SMA in the acinar regions of liver biopsies (Sobesky 1999) and a decrease in collagen after IFN-α therapy (Sakaida 1999). An assessment comparing viral clearance together with liver histology following IFN-α therapy showed that 67%

of cirrhotics who demonstrated a sustained decrease in viral load, also demonstrated normalized serum alanine aminotransferase (ALT) (Everson 1999). ALT is an enzyme released when hepatocytes are damaged (which occurs in the process of liver fibrosis), thus it provides a measure of the disease progression. A long term study by Guerret (1999) compared biopsies of non-responders to IFN-α therapy . These patients were retreated with IFN-α therapy and the biopsies studied one and five years later. Five years following IFN-α therapy 43% of patients had maintained a constant reduction in collagen content. However, a significant decrease was found in all patients following prolonged therapy (Guerret 1999).

Sakaida (1999) also showed a correlation between the number of α-SMA positive cells and the degree of histological fibrosis, complete responders showing a correlation between reduction in α-SMA and a reduction in the ALT levels (Sakaida 1999).

Further evidence followed in clinical studies where specific markers of fibrosis were studied. One such study measured the level of serum N-terminal propeptide of procollagen type I (PIIIP). In patients with improved fibrosis their PIIIP levels had normalized, becoming significantly lower in sustained responders compared to relapsed- and non-responders (Serejo 2001). Serum levels of PIIIP were also compared with serum TIMP-1 in a study by Mitsuda (2000). This showed a significant decrease in PIIIP in all groups of patients, responders, relapsed-responders and non-responders. However, TIMP-1 only decreased significantly in the sustained responders group (Mitsuda 2000). Additionally, two groups have found that IFN-α treated patients increases the MMP1:TIMP-1 ratio, thereby tipping the balance towards healing .

In addition, TGF-β has also been found to be reduced following IFN-α treatment. Evidence for this is shown with a decrease in TGF-β found in liver biopsies, and also,

a decrease was found in plasma TGF-β1 levels in IFN-α treated HCV patients (Bedossa 1993; Tsushima 1999).

Together, such evidence suggests that IFN-α is able to inhibit the fibrotic process, potentially by the downregulation of the HSC. This is supported by the decrease in α-SMA staining in post-treatment biopsies, and the corresponding decrease in alpha procollagen and TIMP-1, both known to be primarily secreted by the HSCs. Based on the evidence found in other cell lines, it seems likely that this is due to the specific inhibition of stellate cell proliferation or the induction of stellate cell apoptosis.

Interestingly, studies looking at the effect of IFN-β on HCV patients found similar but not identical results, despite IFN-β being a type I Interferon, using the same receptors as IFN-α. This group found that serum levels of TIMP-1 and MMP-2 correlated with fibrosis, being significantly higher in sustained responders and lower in non-responders. No change was found in MMP-1 between the groups of patients. They state that the MMP-2:TIMP-1 ratio is higher in non-responders than in sustained responders. Treatment with IFN-α to dermal fibroblasts has been shown to reduce the production of glycosaminoglycans, whilst having no effect on fibronectin, it upregulates collagenase production (Duncan 1989).

1.10.4.2 Effects in IFN-α on HSC

Only three groups have looked at the HSC in vitro (Mallat A 1995; Shen 2002) (Saile 2003). However, the results from the former two groups have been contradictory.

The first study showed that proliferation of the human HSC can be inhibited in a dose-dependant manner, and additionally that DNA synthesis is reduced by 69%. IFN-α decreased DNA synthesis in HSCs by 69%, correlating with a 65% decrease in cell growth (assessed by cell numbers). A reduction in α-SMA expression was also

confirmed with both northern analysis and western blotting. Finally, the human HSC were shown to reduce their secretion of total collagen (Mallat A 1995).

The second study looked at IFN-α, IFN-β and IFN-γ and found that whilst IFN-β and IFN-γ reduced HSC proliferation, IFN-α did not. They found similar results with regulation of α-SMA protein following 6 days treatment (Shen 2002).

The third group studied only the antiapoptotic effects of IFN-α in both freshly isolated and day 7 activated HSC. Using DNA synthesis, IFN-α was found to inhibit apoptosis by 50% in both day 2 quiescent HSC and day 7 activated HSC. This was confirmed by flow cytometry which again showed a significant reduction in apoptosis in the IFN-α treated HSC. By use of Brd-U and TUNEL staining 90% untreated HSC demonstrated signs of apoptosis as compared to 30% in IFN treated HSC (Saile 2003).

One further study, related to this area, treated a fibrosarcoma cell line with IFN-α and gene chip technology to analyse the expression of 6,800 human genes. Of these a list of 100 genes were found to be upregulated following treatment with IFN-α. These genes included 2'5'-oligoadenylate synthetase, MxA, MxB, pro-apoptotic genes such as phospholipid scramblase and also anti-apoptotic genes such as bcl-2 (Der 1998).

1.10.4.3 Effect of IFN-α on liver fibrosis

Muriel (1995) found treatment with recombinant leukocyte IFN-α did ameliorate the amount of fibrosis. The levels of collagen deposition and of serum alkaline phosphatase were both reduced to near control levels. Liver structure was preserved in the IFN-α treated group with only a slight increase in the level fibrosis. This study allowed fibrosis to be established, IFN-α treatment was started 15 days following bile duct ligation (BDL) (Muriel 1996).

Following this, Fort (1998) ran a study inducing liver fibrosis in rats using both bile duct ligation (BDL) and carbon tetrachloride (CCl_4) (Fort 1998). The rats were treated

with CCl_4 every five days for eight weeks, and controls were given the CCl_4 vehicle and analgesic only. The BDL group were operated under anaesthetic, and sham controls were also operated on, being opened but the ducts were not tied. Rats from each group were then given 100,000UI/day IFN-α_{2a} either for the total four weeks of the BDL study or the nine weeks of the CCl_4 study, and again controls were given the IFN-α_{2a} vehicle only.

Both groups of rats had a high mortality rate, 20% of the BDL group with and without IFN-α_{2a} and 31% of the CCl_4 group and 35% of the IFN-α_{2a} treated rats.

This study demonstrated that there was no difference between groups in body weight gain and liver function tests. However, the level of fibrosis was decreased significantly in the CCl_4 group treated with IFN-α_{2a}, but this was not found in the BDL group treated with IFN-α_{2a}. Correspondingly, decreases in the levels of serum hyaluronate and hydroxyproline content were also found in the IFN-α_{2a} treated CCl_4 group. In addition, these rats showed a significant decrease in alpha 2 procollagen I mRNA levels although not fibronectin (Fort 1998).

In 2000, Bueno et al also looked at the effect of IFN-α_{2a} treatment with bile duct ligated rats, again left for 4 weeks following BDL and given daily IFN-α_{2a} treatment. Mortalilty was 25% in each group, but they also found a resolution of fibrosis. In homogenates of non-parenchymal cells of the liver from the IFN-α_{2a} treated group, the gelatinases demonstrated a high level of activity. Comparatively, in homogenates of whole liver and hepatocytes only, the activity was minimal. They further assessed the mRNA levels of procollagen and TIMP-1 and found that only procollagen levels were downregulated. In addition, the levels of active PAI-1 in whole liver homogenates were found to have a significant decrease compared to the treated groups, whereas the

BDL only rats demonstrated a clear increase compared with sham operated rats (Bueno 2000).

Based on the activation of HSCs by oxidative stress, Vendemiale (2001) induced liver fibrosis using dimethylnitrosamine (DMN) (Vendemiale 2001). Two types of IFN-α (leukocyte alpha and recombinant alpha 2b) were used as therapeutics comparing their effects against the antioxidant N-acetylcysteine (NAC).

This study used the presence of fibronectin staining as a marker of fibrosis, and found that the group treated with leukocyte alpha IFN-α (leIFN-α) had a significant decrease (80% had no fibronectin deposition). In comparison the groups treated with recombinant alpha IFN-α (r IFN-α) and NAC did not show any decrease in deposition compared to the DMN only group. Likewise, both the ALT levels and the hydroxyproline concentrations were significantly reduced in the leIFN-α group but not the rIFN-α. Both levels were also reduced in the NAC group.

Of particular interest in these results is the dramatic difference between the two types of IFN-α. It also proposes that IFN-α has antioxidant properties and perhaps through its regulation of nitric oxide is able to reduce fibrosis within the liver (Vendemiale 2001).

1.10.5 Hypothesis and Aims

The hypothesis studied in this thesis is that IFN-α is able to reduce the development of fibrosis through modulation of the HSCs. This is achieved through either the induction of apoptosis or inhibition of proliferation or activation. Furthermore, this action is generic in all cells involved in the fibrotic processes throughout the body.

Aims

1. To study the consequence of IFN-α treatment on hepatic stellate cell apoptosis, proliferation and activation, using a recombinant IFN-α known to be active on rat derived cells.
2. To examine the potential antifibrotic effect of IFN-α on liver fibrosis in a rat CCL_4 model.
3. To extend the relevance of the findings beyond liver fibrosis, i.e. to show that IFN-α might have a generic anti-fibrotic effect, using in vitro studies of effects of IFN on pancreatic stellate cells.

To achieve aim 3, to develop a method for efficient extraction of the PSC, resulting in optimum numbers and cell viability.

2 MATERIALS AND METHODS

Reagents with an asterisk are defined in Appendix I, otherwise they are stated when required.

2.1 LIVER PERFUSION AND EXTRACTION OF HSCS

Materials
Sagatal (Rhone Merieus Ltd)
Collagenase (Roche Diagnostics, Lewes, UK)
Pronase (Roche Diagnostics, Lewes, UK)
Deoxyribonuclease (DNase), (Roche Diagnostics, Lewes, UK)
Hanks buffered salt solution (HBSS) with and without calcium, (Roche Diagnostics, Lewes, UK) *
Optiprep, (Life Technologies, Paisley, UK)
Dulbeccos Modified Essential Medium (DMEM), (Life Technologies, Paisley, UK) *
Foetal calf serum (FCS), (Life Technologies, Paisley, UK) *
Penicillin/streptomycin/gentamycin (PSG) *
Trypan Blue

Primary rat HSCs were obtained by perfusion of the rat liver. The rat liver is cannulated via the portal vein and heparin 250U/ml in calcium-free HBSS is perfused through to prevent any blood clots forming. The liver is then digested in situ with Pronase 2mg/ml in HBSS containing calcium, followed by Collagenase 0.2mg/ml HBSS containing calcium, all of which was perfused through at 10ml/min. Following this the liver digest was resuspended in DNase (3mg/ml) and HBSS with calcium, and strained through a sterile nylon gauze to remove any undigested areas. The suspension was then spun for 7 mins at 400g, resuspended with DNase and HBSS with calcium three times. The HSCs were then crudely obtained from the cell suspension by separation on an 11.35% Optiprep salt gradient spun at 1400g for 20mins. The HSC band was then removed and resuspended in HBSS with calcium, where it is further purified by centrifugal elutriation using a rotor speed of 1500rpm against a flow rate of 18 ml/min in HBSS with calcium.

2.1.1 Cell viability

Cell preps were studied for viability on a regular basis, using 0.05% weight/volume Trypan Blue. Viable cells are small and round, and do not stain blue, whereas unviable cells will take up the blue dye.

The HSCs were then plated out at a density of $1x10^6$ per ml in DMEM containing 16% FCS and 4% PSG.

2.2 EXTRACTION OF HUMAN HSCS

Materials
As above for rat HSCs

Human liver sections were obtained from liver resections carried out to remove liver tumours. In the removal of liver tumours, excess healthy tissue is removed to give the highest assurance that no cancerous tissue remains. The resection is examined by a pathologist, and any healthy tissue not required for diagnostic purposes was removed by the pathologist and given to our department for research purposes. Consent was always obtained from the patient by a Research Fellow. All procedures were performed with the local ethics committee approval.

Tissue was always declared by the pathologist to be normal, however, when abnormal cells were subsequently discerned within extracted cell populations, these populations were not used.

Liver tissue was washed in HBSS without calcium two or three times to remove any remaining blood. The tissue was then cut into small strips of <1cm width, and these sections were then homogenised briefly in HBSS without calcium. The fragmented liver was then incubated in HBSS with calcium, with 12.5mg/ml Pronase and 25mg/ml Collagenase in a shaking incubator at 37°C. The liver digest was left for approximately 10mins, or until any liver fragments had softened.

The liver digest was then strained through a nylon gauze and the procedure followed the same protocol as with rat HSCs.

2.3 CARBON TETRACHLORIDE MODEL OF HEPATIC FIBROSIS

Carbon tetrachloride (CCl_4) induced liver fibrosis in rodents is a commonly used hepatotoxic agent. CCl_4 is reduced to CCl_3 through cytochromes such as cytochrome P450. The presence of this radical initiates the generation of reactive oxygen species and lipid peroxidation in turn causing hepatocytic necrosis. As mentioned previously, the damaged hepatocytes induce both inflammatory infiltrates and the release of ROIs which activate the HSCs (Teschke 1983; Geerts 1991; Castillo 1992).

All animals used had free access to standard chow and water and were monitored daily for general health. The studies complied with UK Home Office guidelines. Male Sprague-Dawley rats were injected intra-peritoneal with 0.05ml/100g of sterile CCl_4 in a 1:1 ratio with olive oil, twice weekly for 2 weeks, following which they were injected with 0.1ml/100g for the remainder of the trial. On completion of the trial, animals were sacrificed using a Schedule 1 method, blood collected and the liver, spleen and pancreas removed. Each animal had one lobe of liver snap-frozen in liquid nitrogen RNA extraction and one lobe sliced and placed in formaldehyde and GMA for immunohistochemistry. Blood samples were immediately placed on ice, and later centrifuged to separate the serum for biochemical analysis.

2.4 EXTRACTION OF RNA

All RNA work was done using gloves as hands provide a rich source of natural RNases. Glassware was baked at 200 ^{0}C for 5 hours, and microfuge tubes and pipette tips were all autoclaved. All plastic-ware and gel apparatus was washed with Sodium hydroxide and rinsed with DEPC treated water.

2.4.1 Extraction from cell culture

Materials
Guanidium isothiocyanate (GIT) 4M *
β-mercaptoethanol
Qiagen RN-Easy kit (Qiagen)

RNA was extracted from cultured cells using GIT lysate: media was poured out of the flask, and 900µl of 4M GIT was added to one 75cm^2 tissue culture flask. The flask was left on a shaker for 20 mins following which the cell lysates were removed. The 1ml lysate was then stored in an autoclaved microfuge at -40^{0}C or was immediately processed to remove the mRNA. The lysates were processed using a Qiagen RNeasy kit to extract mRNA.

2.4.2 Extraction from whole liver

Materials
Guanidium isothiocyanate (GIT) 4M *
β-mercaptoethanol
Qiagen RN-Easy kit (Qiagen)

RNA was extracted from whole liver also using GIT lysate. Approximately 500mg of snap frozen whole liver was placed into 2mls of ice cold GIT lysate and immediately homogenized using a mechanical homogenizer for 30secs. The liver homogenates were then processed using the Qiagen RNeasy kit to extract mRNA.

2.4.3 Analysis of RNA integrity

Materials
Sodium hydroxide
DEPC water (1ml DEPC (Sigma) per 1 litre of water)
Agarose
3-(N-morpholino)propanesulphonic acid (MOPS) 10x *
37% formaldehyde
Ethidium Bromide 1mg/ml
Loading buffer (ESB) *

Spectrophotometry was used to assess the total quantity of mRNA. 2µl of RNA sample was added to 80µl DEPC'd H_2O. RNA is quantified at a wavelength of 260nm using the equation: when $\lambda 260 = 1$ then total mRNA = 40mg/ml. RNA integrity was checked by electrophoresis through a 1% denaturing agarose gel. The addition of formaldehyde disrupts the secondary structure of RNA improving the resolution of the RNA through the gel. From each sample 2µg of RNA was mixed with 3µl of RNA loading buffer and which was vortexed, centrifuged and heated at 65^0C for 10mins to denature the RNA. Finally 1µl of ethidium bromide was added to each of the samples which were vortexed and centrifuged again before loading into the gel. Addition of the ethidium bromide allows the 18S and 28S bands to be visualized in the gel with UV light. If two clear bands were present the RNA is not degraded, but if smearing was found this indicates RNase degradation due to contamination.

2.5 NORTHERN BLOTTING

This method allows the identification of specific mRNA from total cellular RNA. Equal loading of 5µg mRNA per sample was loaded onto a 1% SDS-PAGE gel, and run through to separate the different sized RNA bands. The RNA was stained with ethidium bromide and visualized under UV light.

Materials
DEPC'd H_20

50mM Sodium hydroxide
10x Salt Sodium Citrate (SSC) *
Chromatography 3 mm filter paper, (Whatman, Maidstone, UK)
Nylon membrane, Hybond N, (Amersham, Little Chalfont, UK)

2.5.1 Transfer of mRNA

Once the integrity and concentration of the mRNA has been assessed, the mRNA samples were loaded equally (typically 5μg) onto an agarose gel. Once the mRNA has been separated through the gel, the gel is washed in DEPC'd H_2O for 10 mins to remove formaldehyde. This is followed by washing in 50mM Sodium hydroxide for 20 mins, which partially hydrolyses the RNA, and then a further wash in DEPC'd H_2O for another 10 mins. Finally, the gel is washed in 10x SSC for 10 mins.

The RNA is then transferred to a nylon membrane via elution with 10x SSC. The 10x SSC is drawn through the gel, eluting the RNA and depositing it onto the nylon membrane. The membrane is then air dried, and exposed to low level UV light which immobilises the nucleic acids due to crosslinking between the RNA bases and the amide groups.

2.5.2 Prehybridisation of the membrane

Materials
Membrane with transferred mRNA
Hybridisation buffer (Ambion)

The mmbrane is then prehybridised for 3-4 hours in a hybridisation buffer at 42^0C. This buffer blocks non-specific sites across the membrane due to the inclusion of herring sperm DNA and Denhardt's reagent within the buffer. In addition, the buffer has a high ionic strength of the buffer due to 5x SSC which also aids the probe in annealing to its target RNA on the membrane.

2.5.3 Random primed radiolabelled probes

Materials
Hybridisation buffer (Ambion)
[α-^{32}P] deoxyadenosine triphosphate (α^{32} dATP), (Amersham, Little Chalfont, UK)
Glass wool
dTTP, dCTP, dGTP
cDNA probe
Random hexamers
Reaction buffer
Klenow fragment
Sephadex G-50 (Sigma)

Radiolabelled probes were made using random hexamer oligonucleotides which act as primers for DNA synthesis. 100-200ng of the template cDNA was added to 5µl of random hexamers. This mixture was heated for 5mins at 95^{0}C causing the cDNA to disanneal to allow the random hexamers to initiate DNA synthesis. Subsequent to this, 4µl of deoxycytosine triphosphate (dCTP), deoxythymidine triphosphate (dTTP), deoxyguanosine triphosphate (dGTP), 5µl α^{32}P-ATP (Amersham International, Amersham, Bucks) 5µl reaction buffer and 2µl Klenow fragment were added to the mixture and incubated at 37^{0}C for 60 mins allowing the transcription of radiolabelled dsDNA. All reagents were from a megaprime DNA labelling kit (Amersham International, Amersham, Bucks). To purify the probe by removing uncorporated dNTPs the radiolabelled probe is centrifuged through a Sephadex G-50 column. The particles in Sephadex contain fine pores which allow trap free dNTPs whilst the radiolabelled probe passes through the column and is collected. The purified probe is then heated for 5 mins at 95°C before being added to fresh hybridisation buffer. The membrane is incubated in this buffer overnight at 42^{0}C.

2.5.4 Hybridisation and stringency washing of the membrane

Materials

Radioactively labelled probe
Hybridisation buffer (Ambion)
Prehybridised membrane
Stringency buffer *

Following this the membrane undergoes stringency washes to remove any probe which is not bound to the membrane. Three stringency washes were done for 15 min in 0.2% x SSC/0.2% SDS at 42^0C. Hybrids weakly bound with few hydrogen bonds are thus removed. To increase the stringency the washes are altered to have low salt conditions and higher temperatures. Finally, the membrane is wrapped in clingfilm, and was visualised using either autoradiography or a Storm phosphorscreen (Kodak).

2.6 RT-PCR

Materials
5x Buffer (Promega)
10mM dNTPs (Promega)
0.5mg/ml Random Hexamers (Promega)
200U/µl M-Mu LV Tase (Promega)
40U/µl RNasin (Promega)
DEPC'd H_20
mRNA (1µg)

RT-PCR envolves the production of double stranded cDNA in a 5' to 3' prime direction catalysed by RNA dependent DNA polymerase. Hexamers (or Random primers) bind to the mRNA template and, acting as primers so generate random oligonucleotides. As the random hexamers are randomly generated oligodeoxynucleotides they bind throughout the mRNA template and result in an equal frequency of cDNA from all parts of the template.

A stock solution is made from 4µl of reaction buffer (Promega), 2µl of 10mM deoxyribonucleotides (dNTPs), 2µl).5mg/ml random hexamers, 200U/µl Moloney Murine Leukaemia Virus Reverse Transcriptase (M-Mu LV Tase) and 0.5µl 40U/µl RNase inhibitor (RNasin). Added to this solution was 1µg sample RNA and the total volume made up to 20µl with DEPC'd water.

The samples were then heated at 37^0C for 60 mins, followed by 95^0C for 10 mins to inhibit the reaction. The solution was made to a total of 100µl by the addition of 80µl of DEPC'd water, therefore assuming a final concentration of 10ng/µl.

2.7 TAQMAN® REALTIME PCR

TaqMan® Realtime PCR is a quantative method of PCR. In addition to the specific primers of the candidate sequence TaqMan® Realtime PCR also uses a probe. This probe is designed to anneal on the cDNA sequence between the start points of the two primers. The probe has at one end a fluorophore and at the other a quencher - this quencher prevents the fluorophore from fluorescing whilst the probe anneals to the single stranded DNA sequence. However, as DNA synthesis begins the quencher is removed from the probe, and the fluorophore gives off light. This light signal is then detected by the TaqMan® machine. Several fluorophores have been designed at different wavelengths, this allows for two individual DNA sequences to be examined in one sample in one well.

2.7.1 Probe and primer design

TaqMan® primers and probes were all designed using the PE Biosystems Primer Express® software. All TaqMan® primers and probes were designed within the following guidelines:

Primer

- *The Tm of the primer should be within 58-60^{0}C.*
- *The GC content of the primer should be within 20-80%.*
- *The length should be between 9-40 bases.*
- *There should be no more than 2 G/Cs at the 3' end.*

Probe

- *The Tm should be 10^{0}C higher than the primer Tm.*
- *The GC content of the probe should be within 20-80%.*
- *The length should be between 9-40 bases.*
- *There should be no more than four contiguous Gs.*
- *Must not contain more G's and than C's.*
- *Amplicon should be between 50-150bp in length*

The housekeeping gene used is L37a ribosomal protein. Whilst GAPDH and β-actin are typically used, Affymetrix work by Roche showed that these genes increased by three- or four- fold in the activation of an HSC. However, it was found that this gene did not increase or decrease by HSC activation (Dr. E. Murray, Roche, personal communication) and therefore was used as the housekeeping gene in the TaqMan® PCR work.

L37a ribosomal protein (rat)

Probe: TTC CGG CGA CAT GGC TAA ACG C

Forward primer: TCT TCG GGC TTG GGC TTC

Reverse primer: ACGATCCCGACCTTCTTGG

2',5', oligoadenylate synthetase (rat)

Probe: CCG GCC TCG AAG CTC GAT CAG TTT A

Forward primer: GGA GCA GGA ACT CAG GAG CAT

Reverse primer: TGA TGT CGG GAA GAT GAA CCT

TIMP-1 (rat) designed by Dr. J Lora

Probe: AGA GGC TCT CCA TGG CTG GGG TGT A

Forward primer: AGCCTGTAGCTGTGCCCCAA

Reverse primer: AAC TCC TCG CTG CGG TTC TG

Collagen 1 alpha 1 (rat)

Probe: CCT CCC TCT AAC AGT CAC

Forward primer: GGC CCA CAC CAT GAG GTA TT

Reverse primer: AAG AAC CAG GCA GCT AAG CAG AT

MMP-13 (rat

Probe: AGG TGA AAA GGC TCA GTG CTG CGG T

Forward primer: AAT ATC TGA CCT GGG ATT TCC AAA

Reverse primer: TCT TCC CCG TGT CCT CAA AG

2.8 EXTRACTION OF PROTEIN

2.8.1 Protein from cell cultures

Materials
PBS x1 (autoclaved)

Protein was extracted from cultured cells using PBS. Media was removed from the cell culture flasks, which were then washed three times with 10x PBS, and after each wash tapped dry. Finally, 400µl of PBS was added to one 75cm^2 tissue culture flask and left in a 4^{0}C fridge overnight. The following day the flask was scraped and the lysate removed and placed in an microfuge at -40^{0}C until use.

2.8.2 Protein from whole liver

Materials
Homogenizing buffer *

Protein was extracted from snap frozen whole liver using a homogenizing buffer which contains serine- and thiol- protease inhibitors. Approximately 500mg of snap frozen liver was placed into 2mls of ice-cold buffer and immediately homogenized mechanically for 30secs. The samples were then centrifuged at 14,000g at 4C for 20mins to remove cell debris.

2.8.3 Analysis of protein content

Materials
Working reagent
Bovine Albumin standards
Nunc maxisorb 96-well plate

Protein was measured using the Bicinchoninic Acid Protein analysis method. Briefly, 10µl of each standard and of each sample was loaded in triplicate into a 96-well plate.

Following this, into each well 200µl of working reagent was added, and the plate then incubated at 37^{0}C for 30mins, in the presence of water to prevent the plate drying out. The plate was then analysed with spectrophotometry at 540nm. The standards were used to create a calibration line, from which the concentration of the samples could be read.

2.9 WESTERN BLOTTING

2.9.1 Separation of the proteins

Materials
Ammonium persulphate (APS) 10% w/v (Sigma)
Distilled water
N, N, N', N'-Tetramethylenediamine (TEMED) (Sigma)
Sodium dodecyl sulphate (SDS) 10% w/v
Acrylamide solution with acrylamide monomer and bis-acrylamide (40%) (Sigma)
Tris-HCl (0.5 M, pH 6.8)
Tris-HCl (1.5 M, pH 8.8)
Ethanol
β-Mercaptoethanol
Sample buffer *
SDS-PAGE broad range prestained molecular weight (MW) markers (New England BioLabs, Hitchin, UK)
Running buffer (1x) *

Proteins can be separated by size by running them through a sodium dodecyl sulphate polyacrylamide gel (SDS-PAGE). Samples are boiled for 10 mins in a SDS containing buffer with the addition of a reducing agent, β-mercaptoethanol to denature the protein. The SDS binds to the denatured protein, giving it a negative charge which is in proportion to the length of the protein. With the application of an electrical charge, the samples run through the gel, separating according to their charge and therefore size.

The minigel apparatus was assembled, having been cleaned with ethanol and water, and allowed to dry. The resolving gel (10%) is cast first and covered with a layer of ethanol to ensure that the upper edge is flat and to prevent any evaporation occurring.

This is left for 30 mins to allow polymerization to occur. Following this, the stacking gel, is cast on top and the combs inserted into this to form wells for the sample loading. Samples were loaded equally for protein content, typically 5μg was used.

2.9.2 Transfer of the proteins

Materials
Transfer buffer *
PVDF membrane

The protein samples are then transferred to a polyvinyl-difluoride (PVDF) membrane. The PVDF membrane pre-soaked in methanol was sandwiched with the SDS-PAGE gel for 1 hour at 60V. This transferred the protein from the gel to the membrane.

2.9.3 Immunological detection

Materials
Tween-Tris buffer solution (TTBS) *
Antibody diluent
Primary and secondary antibodies
Enhanced chemiluminescent kit (ECL) (Amersham, UK)
Autoradiography films

Following transfer of the proteins, the membranes were blocked with Marvel in Tween-Tris Buffer Solution (TTBS), washed again in TTBS and incubated overnight with the primary antibody in 0.01% Marvel in TTBS. Individual conditions for the antibodies can be found in Table 2-1.

The membranes were then washed three times in TTBS, before incubating with a peroxidase-conjugated secondary antibody in 0.01% Marvel in TTBS for 1-4hrs before developing using a commercial enhanced chemiluminescent kit (ECL, Amersham). ECL detection solution contains a substrate for the peroxidase-conjugated secondary antibody. The reduction of hydrogen peroxide is coupled to luminol which when oxidised produces blue light. This blue light is detected by blue light sensitive film,

autoradiography film. In all Western blots a rainbow marker was included to ensure that the proteins detected were of the correct weight.

Table 2-1 Table of conditions

Primary Antibody	Concentration	Secondary antibody	Concentration	% blocking/ time used
α-SMA (Sigma)	1:500	Goat anti-mouse HRP (Sigma)	1:2000	5% 30 mins
MT1-MMP (Chemicon)	1:2000	Goat anti-Rabbit HRP (Dako)	1:3000	1% 30 mins
ERK1/ERK2 (Sigma)	1:1000	Goat anti-Rabbit HRP (Dako)	1:3000	5% 30 mins
Albumin (ICN Biomedicals)	1:1000	Goat anti-Rabbit HRP (Dako)	1:3000	5% 30 mins
PAI-1 (Santa Cruz)	1:400	Goat anti-Rabbit HRP (Dako)	1:3000	5% 30 mins

2.10 ZYMOGRAPHY

Materials
Conditioned media (serum free)
Sample buffer (2 x) *
SDS-polyacrylamide gel
Distilled water
Gelatin (10 mg/ml)
Triton X-100 2.5% v/v Sigma
Incubation buffer *
Coomassie blue stain *
Destain *

This technique allows the detection of gelatin degrading enzymes, separating them by size. As with Western blotting, the samples are run through an SDS-PAGE gel to separate them by size according to the surrounding charge. The samples are run through the gel in a loading buffer containing no reducing agent, this allows the enzymes to contain their shape and activity. In addition, gelatin is added to the SDS-PAGE gel as a substrate for the enzymes. Finally, any pro- forms of the enzymes are activated by the presence of SDS which disrupts the inhibitory cysteine switch leaving the enzyme in the active form.

Media samples were collected from treated and untreated cells cultured in serum free media due to the large amount of gelatinases found in FCS. Samples were mixed with an equal volume of loading buffer (containing no β-mercaptoethanol), loaded onto 8% polyacrylamide gel with 20mg/ml gelatin and run at 100V for approximately 60mins. Following this, the gel is washed twice in 2.5% Triton X-100 to remove the SDS in the gel and is then left in proteolysis buffer overnight at 37^0C. The gel is then washed in Coomasie blue stain, which stains the gelatin containing areas of the gel. Thus any areas without stain show the presence of a gelatinase enzyme, as the gelatinase will be degraded away. Gels were then destained to give clear bands. Two identical gels

would be run together, with one gel incubated in proteolysis buffer containing no calcium. This ensured that any degradation was due to metalloproteinases which are calcium dependant.

Cultured rat HSC were also treated for 24 hours with concanavalin A (30 μg/ml) in media containing 0.5% FCS and 4% PSG to stimulate gelatinase synthesis and thereby aid identification of gelatinolytic bands in the zymogram (Benyon 1999).

2.11 ^{3}H THYMIDINE INCORPORATION PROLIFERATION ASSAY

Materials
Ethanol
HBSS (containing calcium) (Roche Diagnostics, Lewes, UK) *
Methanol:acetic acid (95:5 volume/volume)
Sodium hydroxide 0.25 M/Sodium dodecyl sulphate 0.2%
[Methyl-^{3}H] Thymidine (Amersham, Little Chalfont, UK)

Cell proliferation can be measured using the incorporation of ^{3}H Thymidine into cellular DNA during its synthesis in S phase of the cell cycle.

Cells were plated out in 24-well plates and cultured until sub-confluent. The cells were then cultured in 0.01% BSA, FCS-free media to quiesce the cells at G0, before treatment.

Cells were exposed to the IFN-α for 24hrs in 5% FCS containing serum, for the last 16hrs (overnight) cells were pulsed with ^{3}H Thymidine 1μCi/ml. The cells were then washed twice with Hanks buffered saline solution (HBSS) to remove any unincorporated radioactivity, before the cells are fixed in 95% methanol/5% acetic acid at –20^{0}C for 60mins.

The cells were then washed three times with HBSS before being lysed with cell dissociation solution, which after 15mins incubation is neutralized with 5M HCl. With the addition of 3mls scintillant, the samples are measured by scintillation counting (Wallac 1257 Rack-beta liquid scintillation counter). Proliferation as assessed by counts per minute per sample, each sample being run in quadruplicates and then averaged. Each assay contained a positive control in the form of cells cultured in 16% FCS containing media to show a positive increase in proliferation.

2.12 CELLTITER 96 AQUEOUS ONE SOLUTION CELL PROLIFERATION ASSAY

Materials
CellTiter 96 Aqueous One Solution Reagent (Promega)

The CellTiter 96 Aqueous One Solution kit uses a Tetrazolium salt, which is absorbed into the active cell. Following reduction in the mitochondria, the water-soluble, colourless compounds form uncharged coloured but nonfluorescent formazans allowing for quantitation by standard spectrophotometric techniques. Cells were plated out based on a titration of cell numbers per well as advised by Promega. Cells were treated with IFN-α for 24hrs, and for the last 2hrs incubated with 20μl of CellTiter 96 Aqueous One Solution Reagent to 100μl of cell media. Absorbance was assessed using spectrophotometry at 490nm.

2.13 IMMUNOCYTOCHEMISTRY

2.13.1 Indirect Immunoperoxidase (for αSMA and Desmin staining)

All materials for immunostaining were obtained from BDH unless stated otherwise

Materials
Acetone Analar grade
Tris buffered saline (TBS) x1 *
DAB substrate (Menarini, Wokingham)
15% azide solution
Mayers Haemalum *
Alcohols, 100% & 70%
Xylene
DPX
Primary antibody αSMA (Sigma) 1:40,000
Primary antibody Desmin (Dako) 1:50
Mouse IgG HRP conjugated (Dako)

Method

Cells were grown on glass slides (Lab-Tech, Life Technologies) and maintained until semi-confluent. Media was removed from the cells, and the cells were allowed to dry. The cells were fixed with water-free acetone for 15mins at room temperature. The acetone was then allowed to evaporate, following which the slides were incubated with the primary antibody at room temperature for 30mins. The slides were washed three times for 2mins each with TBSx1 before incubation with the secondary antibody for 30mins. The slides were washed as above and then the DAB substrate was added for 10mins at room temperature. DAB substrate is 3,3'-diaminobenzidine which when oxidized by HRP (on the secondary antibody) produces a brown end product insoluble in alcohol. 100μl of 15% azide solution was added per 5mls of DAB to block any endogenous peroxidase which would also oxidize the DAB giving non-specific staining. The slides were washed again in TBSx1 before rinsing in water, and counterstaining in Mayers haemalum. The slides were then dehydrated through a

series of increasing percentage alcohols, before being placed in xylene and finally mounted in DPX.

2.13.2 Haematoxylin and Eosin staining

Materials
Harris' haematoxylin *
Eosin stain *
Acid-alcohol solution (1% HCl in 70% alcohol)

Method

Serial sections were cut, deparaffinized by immersion in xylene (2 x 5 minutes) and passed through decreasing graded alcohol (2 x 5 mins each wash) to rehydrate and finally washed twice (5 mins) in dI H_2O. The slides were treated in Harris' haematoxylin for 20mins and then washed in running water for 5 mins plus until the sections turn blue. Wash in acid-alcohol solution briefly and rinse again in running water until sections turn blue again. Treat with Eosin for 5mins, rinse in running water, dehydrated by immersion in increasing graded alcohol, and mounted in DPX.

2.13.3 Diastase PAS

Materials
Periodic acid solution
Schiff's reagent
Diastase

Method

Serial sections were cut, deparaffinized by immersion in xylene (2 x 5 minutes) and passed through decreasing graded alcohol (2 x 5 mins each wash) to rehydrate and finally washed twice (5 mins) in dI H_2O. The slides were then treated with Diastase for 30mins, washed in dI H_2O and then treated with periodic acid for 5 mins. Following three 5 min washed in dI H_2O the sections were covered with Schiff's solution for 15mins. Finally, the sections were washed in water, counterstained with

Harris' hematoxylin, dehydrated by immersion in increasing graded alcohol, and mounted in DPX.

2.13.4 Immunostaining of CD3, PCNA and αSMA in liver sections

Materials
Distilled water
0.01M Citric acid (pH 6.0)
Diaminobenzidine (DAB)
Streptavidin biotin peroxidase complex (DAKO)
Harris Haematoxylin *
Alcohols, 100% & 70%
Xylene
DPX
Primary antibody CD3 (Dako) 1:150
Primary antibody PCNA (Sigma) 1:3000
Primary antibody αSMA (Sigma) 1:3000
Mouse IgG HRP conjugated (Dako)
Dako ARK™ kit (Dako)
Method

Sections were de-paraffinised by two 5 minute incubations in xylene. The sections were then rehydrated through a series of graded alcohols and then placed into distilled water at 5 minute intervals. Endogenous peroxidase within the sections was inhibited (as its presence can cause high background staining) in using 0.1% sodium azide and 0.3% hydrogen peroxide for 10 mins, followed by two 5 minute washes in distilled water. It was then necessary to further unmask the antigen by microwaving the slides in a citric buffer for 30 minutes. The primary antibody was then applied at the appropriate dilution in TBS and the sections incubated overnight at 4°C. Slides were treated with biotinylated secondary antibody at the appropriate dilution in TBS for 30 minutes, after which the streptavadin biotin peroxidase complex was added for a further 30 minutes at room temperature. The slides were then incubated for 10 minutes in diaminobenzidine hydrogen peroxidase substrate. Finally, the sections were washed in water, counterstained with Harris' haematoxylin, dehydrated by immersion in graded alcohol, and mounted in DPX.

αSMA staining was achieved using the Dako ARK™ (Animal Research Kit), Peroxidase. Sections were de-paraffinised by two 5 minute incubations in xylene. The sections were then rehydrated through a series of graded alcohols and then placed into distilled water at 5 minute intervals. After this the ARK kit was used according to the manufacturer's instructions. This kit allows immunohistochemical staining with mouse antibodies on formalin-fixed, paraffin-embedded tissues from the rat and mouse species.

2.13.5 Sirius Red staining of paraffin sections

Materials
Distilled water
0.2% phospho molybdic acid
Picro Sirius Red *
0.01% HCl
Mayers Haemalum *
Alcohols, 100% & 70%
Xylene
DPX

Method

The paraffin sections are first washed in distilled water two times for 5mins each before being treated with 0.2% phospho molybdic acid for 5 mins. (The phospho molybdic acid acts as a mordant to the Picro Sirius Red.) The sections are then stained with Picro Sirius Red for 2hrs following which they are rinsed in 0.01% HCl and washed again in distilled water. The Sirius Red is an anionic dye with sulphonic acid groups which produces a stain by reacting with the basic groups in the collagen molecules. The sections are counterstained with Mayers Haematoxylin for 2 minutes and washed finally in distilled water for 5mins. The sections were dehydrated through a series of increasing percentage alcohols, before being placed in xylene and finally mounted in DPX.

2.13.6 Staining procedure for Glycol Methacylate (GMA) embedded tissue

Materials
0.1% sodium azide
0.3% hydrogen peroxide
TBS x1 *
StreptABComplex/HRP (Dako)
Culture medium blocking solution *
DAB (Menarini Diagnostics, Wokingham)
Mayers Haemalum *
Distilled water
Crystal Mount (Biogenesis)
DPX
Primary antibody αSMA FITC conjugated (Sigma) 1:3000
Rabbit anti-FITC (Dako)
Swine anti-rabbit biotinylated (Dako)
StretABComplex/HRP (Dako)
Avidin Biotin block (Vector Laboratories)

Method

This method was developed to allow staining of rat tissue with mouse antibodies. Mouse antibodies give strong non-specific staining in rat tissue due to species cross-reactivity. Therefore, this method includes an extra antibody stage to eliminate this reactivity. The primary antibody used, αSMA, is FITC conjugated. The second antibody is a rabbit anti-fluorescein isothiocyanate (FITC) so secondary binding only occurs to the primary antibodies. To this second antibody a third is added, an anti-rabbit antibody, which is biotinylated. This biotinylation allows for the binding of the avidin conjugated HRP complex. Finally, the HRP oxidizes DAB causing the brown end product, thus resulting in specific staining of rat αSMA.

Initially, the endogenous peroxidase is inhibited using 0.1% sodium azide and 0.3% hydrogen peroxide for 30 mins. The sections are washed with TBSx1 three times for 5mins following which an avidin biotin block was applied. This blocks the endogenous avidin and biotin within the liver sections. A further block is applied of culture medium blocking solution as a blanket block in the section. Each block was

applied for 20mins at room temperature. The culture medium was drained from the sections and the primary antibody αSMA added at room temperature and left overnight (16hrs) in the dark. The sections were washed again three times with TBSx1 and then the second stage antibody (rabbit anti-FITC) added for 90mins. After washing as above the final antibody was added, biotinylated swine anti-rabbit added for a further 90mins. The StreptABComplex/HRP was then added for 90mins followed by a further TBSx1 wash before application of the DAB substrate for 10mins at room temperature. Finally the sections were washed in TBSx1 followed by distilled water. Sections were counterstained with Mayers Haematoxylin, dehydrated through a series of increasing percentage alcohols, before being placed in xylene and finally mounted in DPX.

2.14 ACRIDINE ORANGE

Materials
Acridine Orange 1mg/ml Sigma

Method

Acridine orange staining was used to assess cell death (Baker 1994) following treatment with IFN-α.

Cells were cultured until sub-confluent before treatment with IFN-α for 24hrs. Acridine orange was then added at a final concentration of 1μg/ml, and left for 10mins before examination under the inverted microscope (Leitz). For each well three random views were taken from the centre and the apoptotic cells counted. Each condition was done in triplicate wells, and each plate contained a positive and negative control, namely cells cultured in 16% FCS containing media and 0.01% BSA, FCS free media. All treated cells were cultured in 5% media and results normalized to the 5% control.

2.15 COLLAGEN ASSAY

Materials
conditioned media
0.01% BSA
25μg/ml Ascorbic acid
NEM *
Tris/$CaCl_2$ *
Collagenase (Lorne Laboratories)
Collagenase buffer with *
Collagenase buffer without *
Trichloroacetic acid (TCA) 50% Sigma
Trichloroacetic acid (TCA) 10%
^{3}H Proline (Amersham)
Method

Collagen synthesis was measured by assessing the incorporation of ^{3}H Proline into newly synthesized collagen. The total amount is assessed by digesting the newly synthesized collagen with collagenase and then subtracting collagen count samples digested incubated with collagenase from the collagen counts of identical samples incubated without collagenase.

Cells were grown until confluence in a 12-well plate. The cells were washed in DMEM only, before being treated with the relevant conditions in 0.01% BSA, FCS free media also containing 25μg/ml Ascorbic acid. The cells were incubated for 24hrs, after which the treatment is repeated with the addition of 1μCi/ml ^{3}H Proline. Those cells treated only for 24hrs had only the second treatment containing ^{3}H Proline. The supernatants were then collected and 100μl of each placed into four wells of a 96-well plate. Of these two of the wells were used for incubating with collagenase and two for incubation without. 50μl of collagenase (125U) was then added to the wells for incubation with collagenase and the plate incubated for 90 mins at 37^{0}C.

50% Trichloroacetic acid (TCA) was added and the plate incubated on ice for 60mins to precipitate the collagen. The plate was then washed with 10% TCA before vacuum drying. 40μl of scintillant was added to each well and the ^{3}H Proline was to

determined by scintillation counting (Wallac 1257 Rack-beta liquid scintillation counter).

2.16 PICOGREEN DNA ASSAY

Materials
Herring sperm DNA, Promega, Southampton, UK
PicoGreen reagent, Molecular Probes, Europe
TE buffer (1 x)

Whole cell lysates were scraped in 500µl of TE buffer, the samples removed and placed into individual microfuges to be sonicated (Branson 2210, 60 sonications/minute) for 15 minutes. The samples were plated out in triplicate in a 96-well plate, and a series of Herring sperm DNA standards was also plated out in triplicate. 100µl of Picogreen (1:200) was added to each well, and the plate immediately placed in a cytofluor II microwell florescence spectrophotometer (Persephic Biosystems) for reading at an excitation of 480 nm and emission of 530 nm.

2.17 COLLAGENOLYTIC ASSAY

Materials
^{3}H acetic anhydride labelled acid-soluble type I collagen
10% TCA
Gelatin
Scintillation fluid

Method

In the fibrotic liver the fibrillar collagens which are composed of three intertwined helical polypeptide chains predominate. The collagenases are the only proteinases known to specifically cleave native triple helical collagens. This collagenase assay is based on the principle that ^{14}C radiolabelled collagen is digested by the collagenase in the liver homogenates. The proteins are precipitated, the samples centrifuged so that

undigested collagens form a pellet. The supernatant containing the digested collagen fragments is removed and read in the scintillation counter.

Purified acid-soluble type I collagen was extracted from rat tails, labelled with ^{3}H acetic anhydride was kindly donated by Dr. X. Zhou. Protein extracted from whole liver homogenates was mixed with acetylated collagen (0.5μCi) and incubated at 30°C for 16hrs. The samples were then chilled on ice for 20mins before adding 10% TCA and gelatin (20mg/ml) which precipitated any remaining intact collagen. The samples were then centrifuged at 10,000g for 15mins at 4°C. 500μl of supernatant was then added to 1.5ml scintillation fluid and mixed. Degradation of collagen was assessed by scintillation counting (Wallac 1257 Rack-beta liquid scintillation counter); a high count demonstrating high collagenolytic activity.

2.18 HYDROXYPROLINE ASSAY

Materials
Citrate buffer *
Chloramine T reagent *
Erlich's Reagent *

Approximately 15% of the amino acids within collagen are hydroxyproline which is found almost entirely in collagen (Tougaard 1973). This hydroxyproline can be used as a marker to quantify the collagen content of a tissue. This assay, to measure hydroxyproline, is based on a previously described method (Bergman 1963). The hydroxyproline is liberated by hydrolysis of the tissue with HCl, then oxidized (by the chloramine T reagent) to a compound similar to pyrrole, which is then condensated with Erlich's reagent to give a red solution. The intensity of the red colour achieved has been shown to be proportional to the hydroxyproline concentration of the samples (Bergman 1963).

400mg of snap-frozen whole liver was weighed out. The liver fragment was added to 2mls of 6N HCl and heated at 105°C for 16hrs to hydrolyse and dry the sample. Using hydroxyproline a standard curve was prepared also in 6N HCl from 0–1mM. 200µl of dI H_20 was added to 200µl of each sample and of each standard. (Both standards and samples were assayed in duplicate.) The samples were then dried by heating at 105°C and the caps were removed. 1ml of citrate buffer was then added and the samples were placed on a multi-vortexer for 20mins. 250µl of chloramine T reagent was added and the samples incubated for 15mins only before the reaction was stopped by placing all samples on ice. 2mls of Erlich's reagent was added and the samples left for 16hrs gently shaking. Absorbance was measured by reading all standards and samples at 560nm.

2.19 IN VITRO TRANSCRIPTION AND AFFYMETRIX ANALYSIS

see Appendix II, Ch.8.

2.20 AFFYMETRIX DATA

Gene chips are silicon wafers which contain synthetic DNA sequences representing thousands of human genes. The genes on the GeneChip® are reconstituted from up to 20 short stretches of genetic information which are obtained from public databases. The GeneChip® used in this work was U95A Affymetrix chip, which contains almost 63,000 probe sets, each gene or expressed sequence tag (EST) interrogated by a GeneChip® array is analyzed with 11-20 pairs of specific 25-mer oligonucleotide probes. The U95A chip represents nearly 10,000 full-length genes.

Figure 2-1 Illustration of a GeneChip®
Different colours represent different genes. For simplicity, only 3 arrayed genes are shown. A Genechip® may represent up to 11,000 different genes.

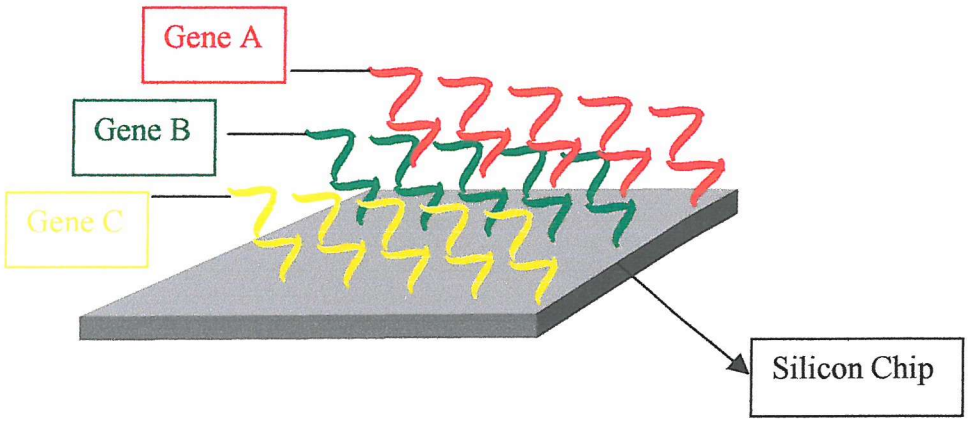

To analyze gene expression mRNA is extracted and purified from both diseased and normal tissue, is modified by the addition of a fluorescent label, phycoerythrin. This label emits light under a laser which is detected by a scanning device in the event that hybridisation occurs. In this work, healthy human resected liver was used to isolate fresh ("quiescent") hepatic stellate cells (HSCs). Freshly isolated HSC are defined as quiescent due to the lack of expression of α-SMA as compared to the activated HSC which expresses α-SMA when grown on plastic or in the diseased liver. Some of these were lysed immediately and the rest were activated by 14 day culture on plastic in the presence of 16% serum at which stage cells were harvested. Total RNA was extracted and used to generate biotinylated complementary RNA to use as probes for subsequent micro-array analysis. This procedure is entailed a double in vitro transcription step developed by Dr. E. Murray, Roche, described in appendix II. A minimum of 4 probes were made from each total RNA extract. Three independent matched "quiescent" and *in vitro* activated HSC were sampled with four independent gene chips. The replicate data sets were combined using proprietal software and normalised using the total sum of signal intensities. To ensure uniform experimental conditions, the hybridisation efficiency for each micro-array was monitored by introducing four "spikes" into each

probe. These defined amounts which act as standard controls between chips. In addition, host control gene levels were closely followed using two control binding sequences; 3' end host GAPDH gene and 3' end ribosomal protein L37A gene. All the controls demonstrated internal consistency within the database. Oligonucleotides with critically altered sequences are also present to control for non-specific hybridisation. The numbers of expressed genes in each dataset was calculated and a threshold of 20 was assigned to any genes with <20 intensity of hybridisation signal. This avoids arithmetic error when calculating increases in expression. Fold changes are only considered significant when the magnitude of change was at least greater than 2.5 fold and with a statistical quality score of >1 (meaning that the sum of the two standard deviations is less than the difference between the two mean quiescent and activated expression values).

2.21 INTERFERON ALPHA A/D

IFN-α was obtained from PBL Biomedical Laboratories. It is an Interferon hybrid constructed from recombinant Hu-IFN-αA and Hu-IFN-αD thus forming human interferon alpha A/D [*Bgl*II]. IFN-α A/D is described as being active on many mammalian cells, such as human, monkey, mouse, rat, rabbit, sheep, pig and hamster.

2.22 STATISTICAL ANALYSIS

All data was evaluated using Microsoft Excel with results normalized to the control. Statistical significance was analyzed using the Student's T-Test, with significance taken to be $p<0.05$. The results are shown with error bars which reflect standard error of the mean (SEM).

Results

3 RESULTS - ISOLATION AND CHARACTERISATION OF THE PANCREATIC STELLATE CELL

3.1 INTRODUCTION

To investigate the biology of the PSC and the apparent similarities between the HSC and the PSC, it was necessary to develop a technique that could reproducibly isolate supply of PSCs. Recently groups had developed methods to extract these cells, however, the main method of extraction envolved growing explants from sections of pancreatic tissue. To date, our group had only ever achieved two populations of poorly growing cells.

3.2 EXTRACTION AND IDENTIFICATION OF PANCREATIC STELLATE CELLS

Several problems were encountered with obtaining cells from the rat pancreas. The first of which was the length of time between the death of the animal and the point at which the pancreas became available for the isolation procedure. The second problem was establishing the amount of enzymatic digestion required to free the PSCs from the surrounding tissue, and the final problem was the purification of the PSCs from the resulting cellular suspension.

The first problem, that of the delay before the Pancreas was available, was a problem unfortunately not controllable. The rats from which the pancreata were taken were used for liver perfusions to obtain HSCs. Following the perfusion, the liver was extracted and removed into a petri dish for the final part of the perfusion. Until the

liver had been safely removed from the rat, the pancreas could not be extracted and placed in the enzymatic solution. The time taken varied between 10mins and 30mins. This situation meant that the cells of the pancreas were subjected to a decrease in temperature, hypoxia, and also blood clotting occurred within the ductules of the pancreas: the cells would have been exposed to necrotic stimuli.

Table 3-1 Flowchart to show the process of isolating the PSC.

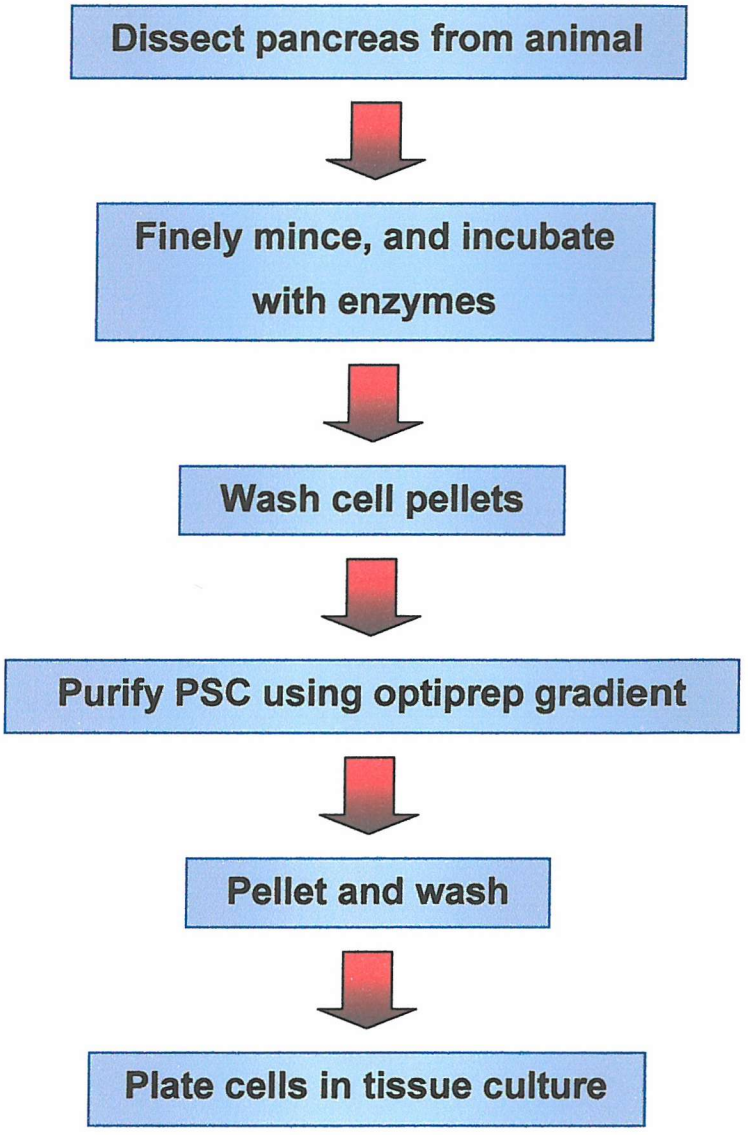

This situation could not be changed, so conclusions were drawn from observations. In brief, the shorter the time before the pancreas was placed in the enzymatic solution the better the cell isolation in terms of both viability and numbers of cells obtained. However, to obtain the optimum cell isolation, a rat would have to be sacrificed for the sole purpose of a pancreatic digest. This would allow the pancreas to be perfused with heparin to prevent blood clots, with HBSS-Ca to wash through, and finally with the appropriate enzymes, which would be delivered more efficiently through the ductules.

3.2.1 The Enzymes

The second area that needed to be optimised was the enzymatic solution used to degrade the pancreas. The correct enzyme concentrations would degrade away the connective tissues thus allowing the PSCs to be released into solution.

The recommended protocol used an enzymatic solution comprised of 2.4% Collagenase and 6IU Dispase shaken for 40mins in a 37°C incubator. Following two cell spins and washes the pellet was then centrifuged on an Optiprep salt gradient for 20 mins at 500g.

At this high concentration of enzymes the final cellular pellet consisted of much debris and very few cells of low viability (Table 3-2). Previous papers by Apte (Apte 1998) used lower concentrations of 0.05% Collagenase and, after comparison with the procedure for the extraction of HSC, the levels of both enzymes, collagenase and dispase were both lowered to 0.08% and 2.4IU respectively. The original protocol included 4.8IU Dispase II, however Apte (1998) had used a different protease, Pronase, to digest away proteins (Apte 1998). Dispase, an amino-endopeptidase, is known for it's milder proteolytic action which maintains membrane integrity during dispersal of the cells. Dispase dissociates fibroblast-like cells more efficiently than epithelial cells and therefore the use of Dispase was continued due to it's milder action

than Pronase (Worthington Biochemical Corporation 2003). Pronase has been shown to be able to detach fibroblasts from both their basement membrane and also from each other without damaging the cell itself unlike other proteases (Roche 2002) (Roberts 1985).

At this concentration there was noticeably less debris. To investigate if the level of debris could be further reduced, the time given for the digestion of the pancreas in the enzymatic solution was reduced to 30 mins.

At this point the yield numbers had dramatically risen and were now consistent between preps (*1*,Table 3-2). Despite this it was felt that the debris could be further reduced. To this end, the concentration of collagenase was further reduced to see if this would still degrade the cell substratum to free the PSC. However, at this point the cell count reduced and suggesting that this was not a high enough concentration to free the stellate cells, regardless of the diminished debris (*2*,Table 3-2).

One notable difference between the protocols for the extraction of PSC and HSC was the use of 0.1% DNase in resuspending the cell pellets after each spin cycle. This was then introduced, as it had been found that with the increasing numbers of cells, clumping of the cells had been observed. Additionally, the length of time given for the enzymatic digestion was again increased. It was hoped that maintaining the lower level of collagenase but increasing the length of time would achieve a balance between allowing more tissue degradation (thus freeing the stellate cells), whilst being sufficiently low enough in concentration so as not to damage the cells.

This immediately increased the cell numbers (*3*,Table 3-2); it is thought that this increase was due to the cells now sufficiently dissociated settling at the correct point within the Optiprep salt gradient, as if the cells were in clumps they would settle out at a different level (3.2.2). Following this, DNase was then included in the enzymatic

solution. It was added to ensure that, even at this point, any cells that had been detached did not adhere to each other or to DNA from cell lysis. Additionally it would then enable the collagenase and the dispase to carry on digesting throughout the remaining tissue: this addition did seem to improve the counts (*4*,Table 3-2). However, once again it was felt that the debris could be further reduced.

To this end, the length of time allowed for the enzymatic digestion was first reduced, to further limit the degradation by the enzymes. The longer time period that the cells are incubated with the enzymes increases the likelihood that the cells themselves will not only be released from the tissue, but that they are also damaged. However, this gave less than half the number of cells than previously. Therefore, the amount of dispase alone was reduced, and this resulted in even lower cell counts. The concentration of DNase was reduced to 0.5mg/ml which had no effect on cell counts. However, with the exception of the reduction in DNase concentration, these final alterations did not improve the cell numbers, and it was determined that the best protocol was as follows: **Enzymatic solution of 0.045 collagenase, 4.8IU dispase II and 4mls of 1mg/ml DNase to be incubated for 45mins at 37°C.**

Table 3-2 Examples of the development of the pancreatic stellate cell extraction.

Collagenase concentration	Dispase concentration	DNase concentration and use	Time given for enzymatic digest	No: of g for Optiprep spin	Final cell count
0.12%	12IU	Not used	40mins	500g	Few, much debris
0.08%	4.8IU	Not used	40mins	500g	400,000
0.08%	4.8IU	Not used	30mins	500g	[1] 798,000
0.04%	4.8IU	Not used	30mins	500g	[2] 500,000
0.04%	4.8IU	0.2% – in cell pellet spins	45mins	500g	[3] 1,330,000
0.04%	4.8IU	0.008% added to enzymatic solution	45mins	500g	[4] 1,489,600
0.04%	4.8IU	0.008% added to enzymatic solution	30mins	500g	638,400
0.04%	2.4IU	0.008% added to enzymatic solution	45mins	400g	30,756
0.04%	2.4IU	0.008% added to enzymatic solution	30mins	400g	Few
0.04%	***4.8IU***	***0.008% added to enzymatic solution***	***45mins***	***500g***	

3.2.2 The Optiprep gradient

The Optiprep gradient step is used to purify the PSCs from the cell suspension gained from the digestion. This suspension contains not only the PSCs but also contaminants such as acinar cells and many blood cells. Contaminating cells are removed by spinning the cells through an Optiprep gradient, which suspends the cells according to their density; unlike other cells types including fibroblasts PSCs are buoyant due to their high content of retinoids.

The density of the gradient used was 13.3% and was centrifuged for 20 mins: both Schaffer 1987. and Apte 1998 used a 13.12% gradient centrifuged for 20 mins (Schafer 1987; Apte 1998). Whilst both these groups centrifuged the gradient at 400g, it was found that the best band was achieved by spinning at 500g.

3.2.3 Contamination within the prep

One frequent problem encountered were populations of contaminant cells which appeared (Figure 3-1 and Figure 3-2). There were a couple of possible reasons for their presence. In the first case, the pancreas was attached to much connective tissue and in preliminary preps some of this tissue was not cleanly dissected away. Populations of cells were then found to grow within the PSC population (Figure 3-1) where they were able to proliferate at such a rate they quickly occupied the entire cell culture flask. To confirm this observation cell isolations from carefully dissected pancreas were compared with cell isolations from the surrounding connective tissue. The cell isolations resulted in two separate populations of cells, as described above. From the connective tissue the cells were highly proliferative, epithelia-like in morphology but two-thirds the size of an activated PSC. It is of interest that this cell was also isolated from within the same band in the density gradient. Future removal of

pancreata have been quite precise, although occasional contaminating populations have still appeared: no attempt was made to identify them.

The second reason was found within the isolation procedure itself. It was found that the band formed in the gradient needed to be removed precisely and taking any solution above or below this band would lead to an increase of contaminants in the final cell count. Additionally, the concentration of enzymes also affected the number of contaminant cells. These cells seemed to be more resistant to the digestive effects of the enzymes: when using higher concentrations of enzymes more contaminants were present despite all other conditions being identical.

Figure 3-1 One of the contaminant populations found in PSC isolations.
Small arrow pointing to one individual cell.

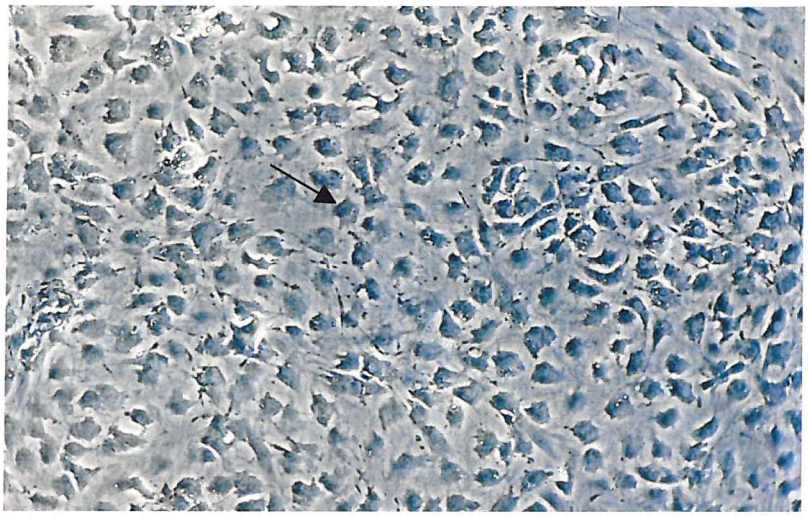

Figure 3-2 Slide showing two different populations of contaminant cells
The population shown above (small arrow), this time growing with a second contaminant population (large arrow).

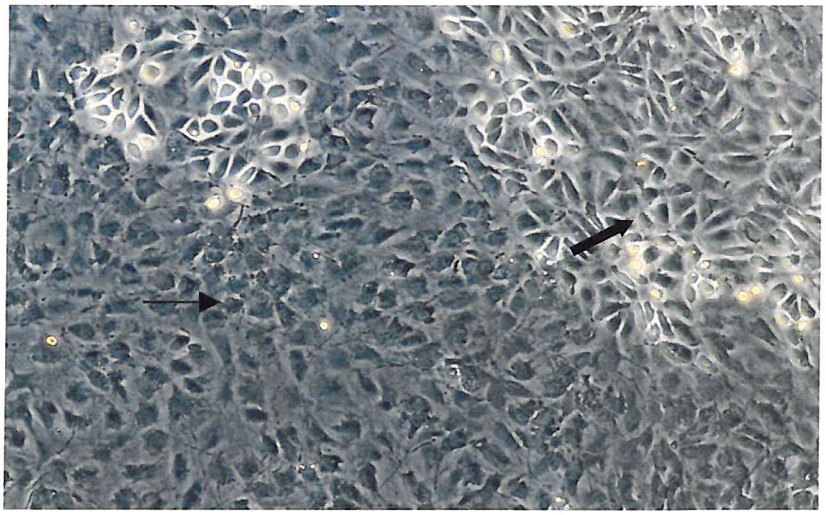

Figure 3-3 Some contaminant cells growing amongst the PSCs – this culture was later overgrown by the former. (Small arrow shows a contaminant cell, large arrows show activated PSC).

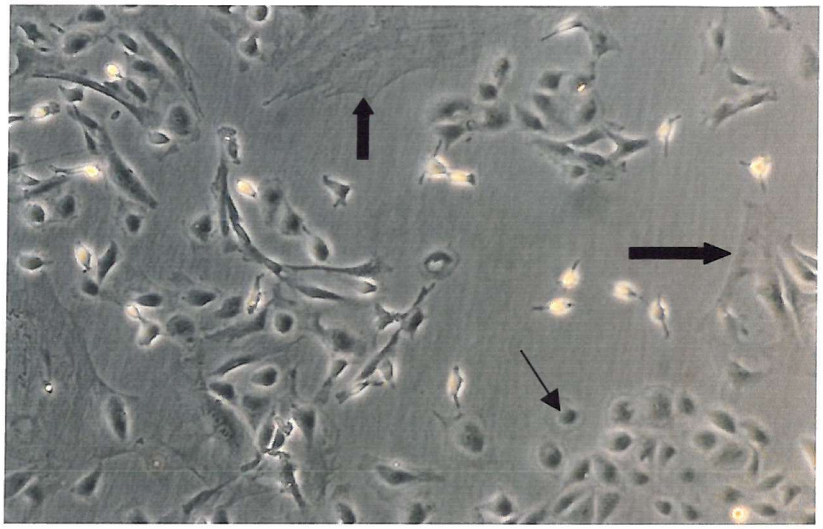

Figure 3-4 A culture of activated PSCs.

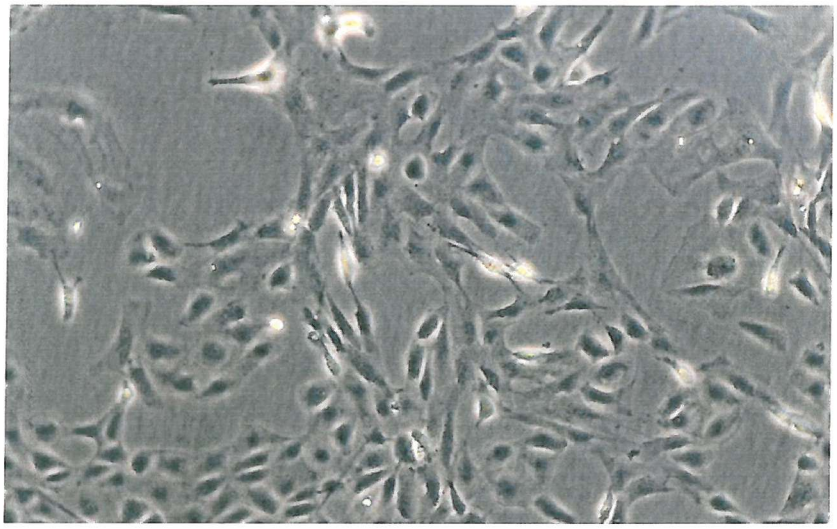

3.3 IDENTIFICATION OF THE PANCREATIC STELLATE CELL - MARKERS OF STELLATE CELL ACTIVATION

HSCs express certain proteins which enable them to be differentiated from normal fibroblasts. Two proteins in particular are used to identify the HSC, Glial fibrillary acidic protein (GFAP) and Desmin. Both Desmin and GFAP are each expressed in an 70-80% fraction of a rat HSC population. These fractions are not necessarily the same but do overlap, together covering 90% of the population. Thus immunocytochemistry for both these protein markers is the most secure identification of the quiescent HSC (Niki 1996). However, this is only a clear definition in the rat HSCs as human HSCs do not express Desmin or GFAP at a high level even when activated (Kawada 1997) (Levy MT 1999).

The activated HSCs display a myofibroblastic phenotype which, in addition to a change in morphology, is typically characterised by the expression of activation markers. The classical activation marker, or marker of the myofibroblastic phenotype, is α-SMA, a cytoskeletal protein which is not found in the quiescent HSCs. Again, α-SMA is only found in 90% of rat HSCs but is generally accepted as a reliable marker of HSC activation (Ramadori 1990).

The expression of these proteins has also been shown in PSCs thus demonstrating their homology with the HSC. Therefore, both Desmin and α-SMA were identified within our populations of PSCs.

Activated PSCs were plated out in immunocytochemistry wells and grown until semi-confluent; these cells were then immuno-stained for α-SMA and Desmin . PSCs were grown in tissue culture plates to activate them in the same way HSCs are activated.

These were also grown until confluent and then lysed for the extraction of protein.

Western blotting was used to look for the presence of α-SMA protein.

Figure 3-5 Immunocytochemistry demonstrating the presence of alpha smooth muscle actin (by P. Johnson).
PSC were cultured for 14 days on plastic. α-SMA shown in brown, can be seen in the cytoplasm of the cell. The typical stellate morphology is clearly seen in this picture, analogous to the HSC.

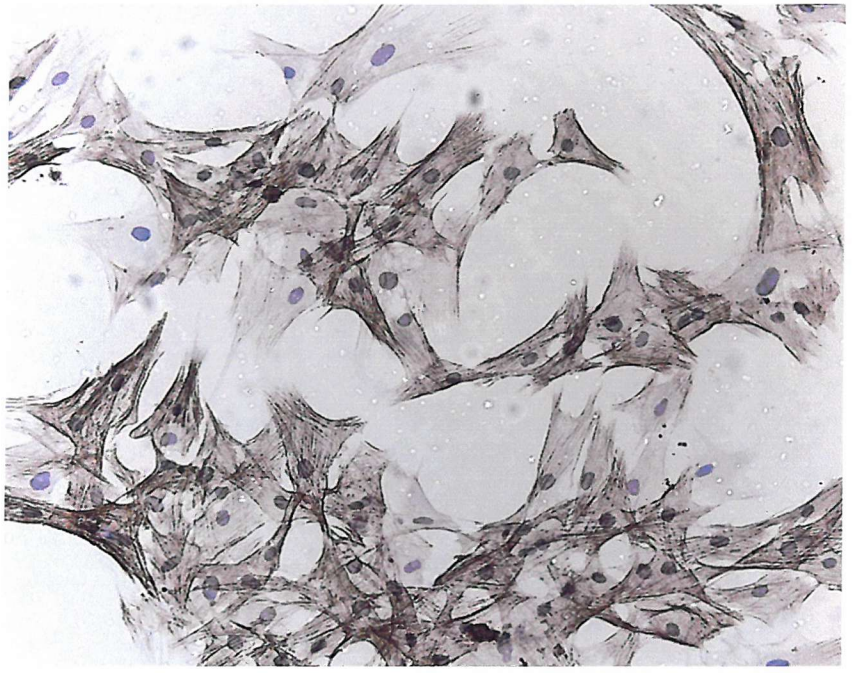

Figure 3-6 Western blotting demonstrating the presence of alpha smooth muscle actin protein in PSCs (n=4)
Two representative populations of activated PSCs cultured on plastic, 2μg of protein was loaded for each sample, populations were of passage 2/3.

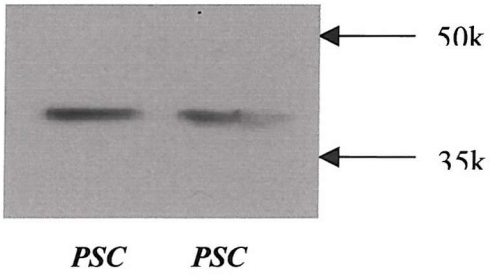

Figure 3-7 Immunocytochemistry demonstrating the presence of Desmin (by P. Johnson).
PSC cultured for 14 days on plastic. The Desmin, shown in brown, can be seen in the cytoplasm of the cell.

3.3.1 Markers of stellate cell activation

Given the apparent homology between the hepatic and PSC, characteristic markers found in the HSC were examined during PSC activation in vitro. Markers examined were those typically found upregulated in HSCs in the activated or diseased state.

PSCs were grown in 16% FCS containing media and used at passages up to and including passage 3. Cells were grown until confluence, and then lysed for mRNA extraction or protein extraction. For the identification of secreted Gelatinase A and B from the PSCs, previously activated cells growing in the above conditions were given serum free media containing 0.1% BSA, and the media was collected after 24hrs. Gelatinases were identified by gelatin zymography.

Markers of collagen degradation and inhibitors of degradation, the MMPs and TIMPs, were also analysed: MMP-2, MMP-14, TIMP-1 and TIMP-2. Having previously determined the presence of α-SMA protein, this was confirmed again with northern blotting for the presence of α-SMA mRNA (Figure 3-9). The expression of TIMP-1 and TIMP-2 mRNAs were also shown using northern blotting (the TIMP-2 studies were done by Dr.P.R. McCrudden) (Figure 3-8 and Figure 3-9).

Figure 3-8 Northern blot analysis to detect TIMP-1 and α1PC1 mRNA in activated PSCs.
TIMP-1 was found at 0.9kb and alpha1 procollagen 1 at 4.1kb.

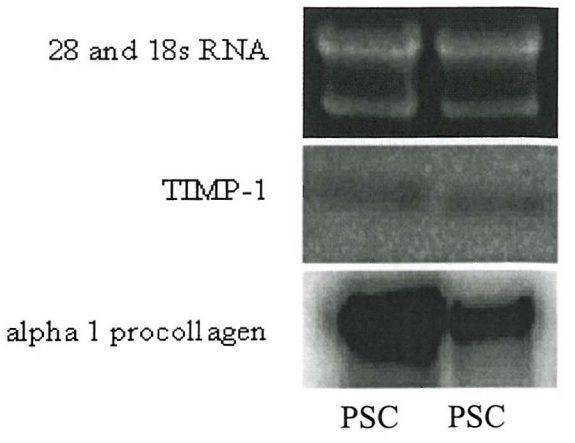

Figure 3-9 Northern blot analysis to detect αSMA and TIMP-2 mRNA in activated PSCs (work by Dr. R McCrudden).
αSMA was found at 1.8kb and TIMP-2 at 1kb and 3.4kb which is in accord with the splice variants of this transcript.

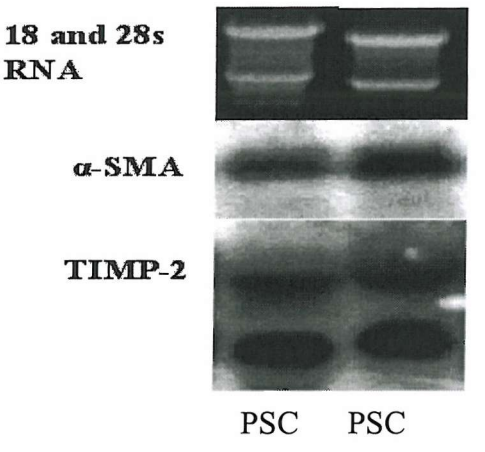

In addition, the presence of alpha 1 procollagen 1 (α1PC1) mRNA was shown with northern blotting (Figure 3-8). The presence of MMP-2, a gelatinase, was shown using zymography (Figure 3-10). Gelatinase A was present as the proenzyme of 72kDa with little evidence of conversion to the active form (62kDa). MMP-14, or MT1-MMP, was shown using Western blotting (Figure 3-11).

Figure 3-10 Zymography showing the presence of MMP-2(Gelatinase A).
Lysates from activated PSCs were used with Con-A treated HSC as a positive control.

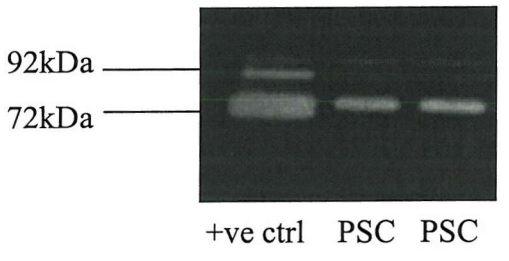

Figure 3-11 Western blot showing MMP-14 (MT1-MMP) protein in activated PSCs.
A signal of 45kDa, the correct weight was found in each sample, n=3.

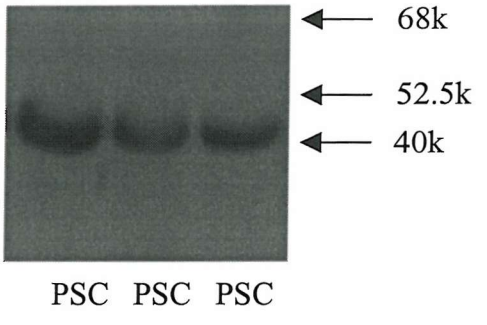

These markers, found to be upregulated in the HSC during liver fibrosis, were used to establish the potential of these PSCs to be pivotal in the onset and perpetuation of pancreatic fibrosis. Therefore it can be concluded that the PSC may be activated in the same way as the HSC and probably plays a similar role in pancreatic fibrosis as the HSC in hepatic fibrosis.

3.4 REGULATION OF PANCREATIC STELLATE CELL ACTIVATION

Data from the Southampton Liver Group suggests that liver fibrosis is a reversible process (Iredale 1998) and recovery from CCL_4 induced liver fibrosis in rats was associated with apoptosis of the HSCs. However, recent studies of our group have shown that under conditions of matrix remodelling, or in recovery an alternative fate exists for activated HSCs. During recovery from liver fibrosis, collagen I surrounding HSCs becomes degraded and there is a return to the normal basement membrane-like matrix. The full implications of this change in pericellular matrix for HSC survival, proliferation and activation are uncertain. Gaca (2000) have noted that activated HSC can be deactivated by plating on matrigel (Gaca 2000). (Matrigel is a soluble basement membrane extract from the Engelbreth-Holm-Swarm tumour, the major components of which are laminin, collagen IV and entactin.) Therefore, HSC deactivation is possible and might occur during recovery from liver fibrosis. This reversal of phenotype has been shown in the HSC in vitro, therefore as a continuation of the homology between the HSC and PSC, and the possibility for a common antifibrotic mechanism this was investigated in the PSC.

We hypothesized that the PSC, like the HSC, would alter its phenotype in response to changes in its pericellular matrix, thus raising the potential for the reversibility of pancreatic fibrosis.

Activated PSC (passage 2/3) were removed from their plastic plates by trypsinization. The populations were then divided in two and replated onto matrigel-coated plates or plastic. These were then left for 24hrs, 72hrs, 5 days and 7 days. The cells were maintained in 16% FCS containing media, and the media was changed every 2/3 days.

During this time, the cells maintained a compact, spherical shape. These cells did not flatten and exhibit the morphology normally found in the parallel stellate cell cultures on plastic. However, cells lying in near proximity to each other were able to extend towards each other, and those cells left for longer timepoints occasionally made contact. If plated at too high a density, the PSCs also showed a high affinity for each other, forming 3-D clusters on the matrigel, again showing a preference for cell to cell binding rather than binding to the matrigel (Figure 3-12).

Figure 3-12 Morphology of PSCs on matrigel compared to plastic.
The pictures show PSC after 24hrs, with cells grown on matrigel on the left, and cells grown on plastic on the right. The cells on matrigel display the typical rounded morphology, whereas the cells grown on plastic are flattening and showing a "stellate" shape.

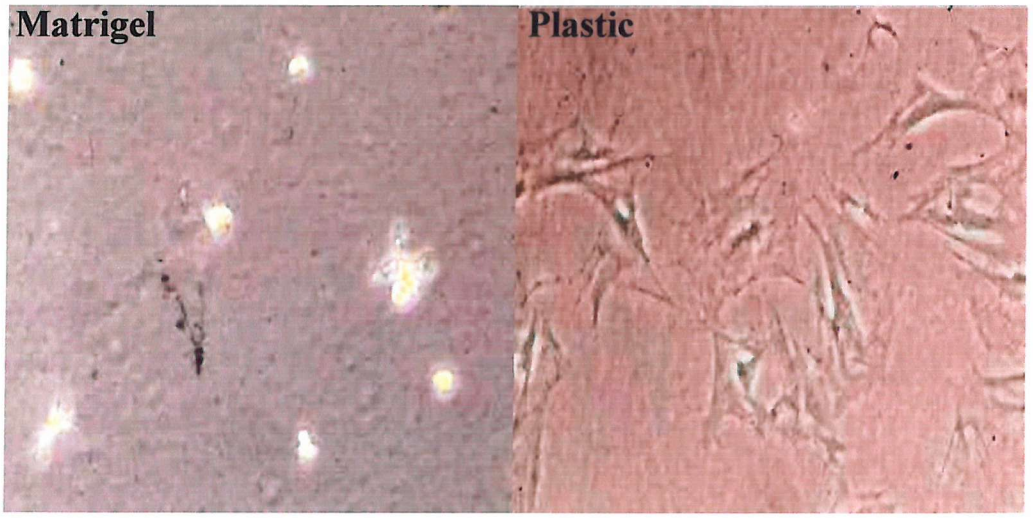

To assess whether the PSCs had become deactivated on the matrigel-coated plastic or whether the change was purely morphological, northern blotting was used to study two markers of stellate cell activation, TIMP-1 and alpha 1 procollagen 1. TIMP-1 was analyzed at all four timepoints, 24hrs, 72hrs and 5 days, where it was found to decrease (Figure 3-13). At 5 days TIMP-1 expression was minimal. As can be seen at 7 days both TIMP-1 and alpha 1 procollagen 1 expression appears to be completely inhibited (Figure 3-14).

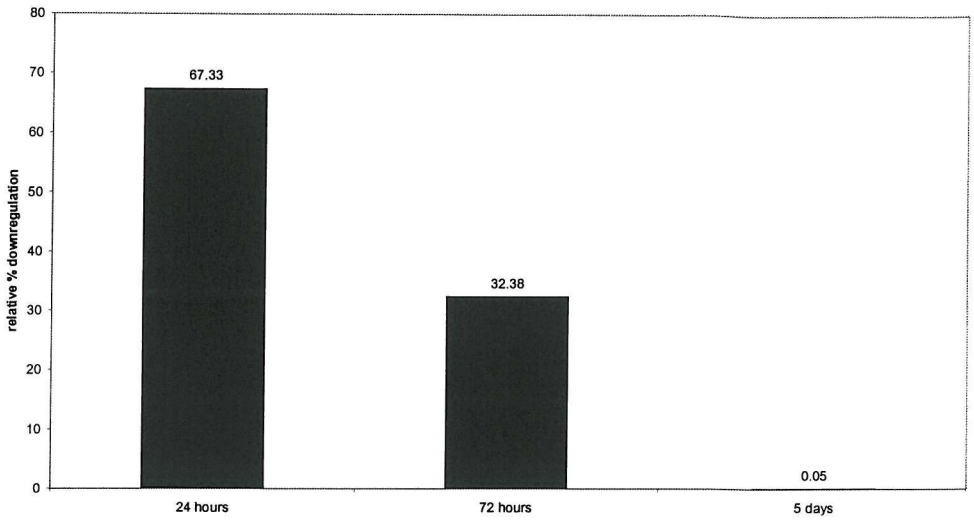

Figure 3-13 Densitometry showing comparative downregulation of TIMP-1 in PSCs at three timepoints, all normalized to the ribosomal bands.
Cells of passage 2 were plated on matrigel for 24hrs, 72hrs and 5 days respectively. Cells were then harvested and the mRNA extracted. Note: data is representative of n=2, except for 24 hours were n=1

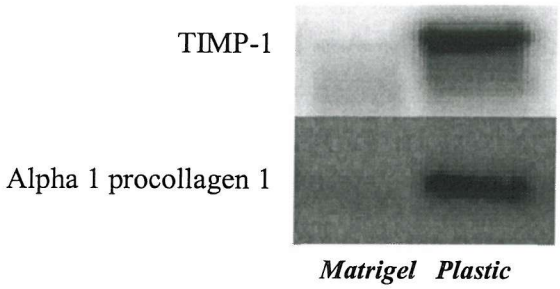

Figure 3-14 Northern blotting showing TIMP-1 and alpha 1 procollagen 1.
Representative northern blots showing the comparative downregulation of TIMP-1 and alpha 1 procollagen 1 at 7 days of replating on matrigel and plastic. (n=3)

3.5 CONCLUSION

Chronic pancreatitis is a progressive inflammatory disease which induces fibrosis throughout the pancreas, resulting in loss of pancreatic functions both endocrine and exocrine. This loss of pancreatic function is the result of morphological changes within the architecture of the pancreas due to a massive deposition of collagen-rich scar tissue.

A cell seemingly analogous to the hepatic stellate cell was isolated from the pancreas (Watari N 1982). This cell was also localized to areas of fibrosis within the pancreas (Ikejiri 1990). Previous studies have also studied the synthesis of ECM proteins by this PSC (Apte 1998).

Primarily I developed the method for extraction of these cells to enable a reliable and reproducible method for regular isolation of the maximum number of cells. Following this I analyzed the expression of some fibrotic markers in the activated PSC. The PSCs were activated by culture on plastic and the markers compared with those found synthesized by HSCs cultured on plastic. The PSC were found to express α-SMA, which is accepted as a reliable marker for stellate cells. However, as smooth muscle cells also express this marker and to further confirm that the cells were stellate cells, they were also analyzed, and found to be positive for, desmin.

The PSC were then studied for the presence of TIMP-1, TIMP-2, alpha 1 procollagen, MMP-2 and MMP-14, all markers found to increase with activation of the hepatic stellate cell. The PSC were used passaged and grown in serum containing media. In the activated state, the PSC were found to express all of the markers. TIMP-1, TIMP-2 and alpha 1 procollagen 1 were analyzed using northern blotting. MMP-14 was analyzed with western blotting, and the presence of α-SMA was further confirmed

using both western and northern blotting. MMP-2 expression was studied by zymography.

This data demonstrates that these PSC have the full compliment of matrix degrading apparatus. As previously revealed in the HSC, the activated PSC has developed a phenotype promoting matrix deposition, expressing TIMP-1 and TIMP-2, collagen and MMP-2. Activation of MMP-2 can occur when TIMP-2 binds to both a MMP-2 and MT-MMP14 molecule, allowing a further MT-MMP14 molecule to remove the propiece of MMP-2. However, although all these were expressed no active MMP-2 was found by zymography possibly due to excess TIMP-2 blocking MMP-14.

Following this, I analyzed whether the cells phenotype was responsive to changes in the ECM, as has previously been found within our group using HSC. Cells were removed from their plastic flasks with trypsin, divided into two, with one half replated on plastic and the other plated on matrigel, a basement membrane-like matrix. The mRNA was extracted from these populations and TIMP-1 and alpha 1 procollagen were studied using northern blotting. It was found that synthesis of both TIMP-1 and alpha 1 procollagen 1 decreased in those cells plated on matrigel as compared to those cells replated on plastic. However, it must be appreciated that n numbers were low. This suggests though that the phenotype of the PSC is reversible, and can be altered by its surrounding ECM. This was proposed by Iredale et al 1998 in reference to the HSC, and has also been found in our group with the HSC cultured on matrigel.

Therefore, the PSC is analogous to the HSC in both its synthesis of fibrotic markers when activated and its response to the surrounding ECM. It is therefore a valid comparison with the HSC for its response to IFN-α, and further work in this area will either confirm a common fibrotic response or bring to light differences between these stellate cells.

4 RESULTS - REGULATION OF STELLATE CELL SURVIVAL, PROLIFERATION AND ACTIVATION BY IFN ALPHA

4.1 INTRODUCTION

Interferon alpha (IFN-α) has been shown to reduce the collagen content of the liver in clinical studies of chronic viral hepatitis (HCV) (Duchatelle 1998). However, these studies have only been carried out in patients with virally induced liver fibrosis, e.g. HCV. As IFN-α is given as an anti-viral, any improvement in fibrosis may potentially result from the decrease in viral load that is frequently observed in these patients and indeed is a goal of therapy. It has been proposed that IFN-α may ameliorate fibrosis through an alternate mechanism to its antiviral properties (Yagura 2000). One such study looked at non-responder patients with HCV induced liver fibrosis at all stages of fibrotic development. Non responder are patients with chronic viral hepatitis in which IFN-α treatment fails to eradicate the virus. Biopsies were collected from these patients before IFN-α treatment, following short term treatment (<1yr mean =7.5mths) and long term treatment (>1yr mean =21.8mths). Following long term treatment an improvement in fibrosis occurred throughout the entire group of patients. The level of fibrosis, as scored by histological scoring and morphometry, showed a significant decrease in fibrosis. However, within the cirrhotic group specifically, only 43% patients demonstrated a constant regression in collagen content (Guerret 1999).

Clearly because of its central role in fibrogenesis the HSC is a candidate cell to mediate any fibrotic effects of IFN-α. To date, there have been two in vitro studies using the HSC; Mallat 1995 and Shen 2002. The first study used human IFN-α 2c to treat cultured human HSC and found a decrease in proliferation, collagen synthesis and αSMA synthesis following IFN-α treatment (Mallat A 1995). The second, using a rat IFN-α found no effect on proliferation of rat HSCs or on the synthesis of αSMA (Shen 2002).

These two studies demonstrate contradictory data on the effect of IFN-α. Whilst human IFN-α was used on the human HSCs, these cells were from outgrowths, a method which can give mixed populations of cells. Both the previous studies used 10% FCS containing media which may have provided the cells with many growth factors, thus masking any effects of IFN-α.

The mechanism and action by which IFN-α is able to ameliorate the fibrosis is as yet unknown. The cells that synthesize the greatest proportion of collagen during the fibrotic process are the HSCs. These cells also play a crucial part in the perpetuation of fibrosis. Previous studies in literature demonstrated that IFN-α has the potential to regulate both proliferative and apoptotic properties (Elias 1987; Sangfelt 1997; Thyrell 2002). IFN-α is a species specific cytokine (personal communication Roche) (Medscape 2000) and therefore, using a rat specific IFN-α I investigated the effect of IFN-α on the activated HSC, examining activation markers, proliferation and apoptosis.

4.2 AFFYMETRIX DATA.

The affymetrix work gave much data on gene regulation differences between the quiescent and activated HSC. One critical early observation from this work was that

GAPDH expression increases during HSC activation which suggests that this gene is inappropriate for normalising between quiescent and activated HSC gene expression. However, one gene was found to be an appropriate control between the quiescent and activated HSC. Ribosomal protein L32a did not alter expression levels (personal communication, Roche).

The data demonstrated:

- 4000-5000 active genes were identified in quiescent and activated
- 900 gene modulations are common to all three HSC samples.
- 400 genes are consistently and significantly upregulated during HSC activation.

Interrogation of this database was used to ascertain all affymetrix results.

4.2.1 Analysis of activation markers in human HSC.

Affymetrix work was done in collaboration with Dr. E Murray, Roche Discovery. Human HSCs were separated and mRNA from quiescent (freshly isolated) and activated (day 14) cells generated. Passaged cells were maintained in 16% FCS containing media, which was changed every two or three days until the flasks were confluent. The cells were lysed with a GIT lysate and the mRNA extracted. This was then assessed for purity using an integrity gel and the quantity was assessed using a spectrophotometer. The mRNA was transcribed to form cDNA, which was incubated on the U95A affymetrix chip. The difference in binding between the two data sets, quiescent and activated, was used to derive a change factor or value of difference. Initially we assessed markers of activation which have previously been studied within our group. This was to confirm the viability of the data produced from the Affymetrix chips.

The activated human HSC demonstrated the upregulation of all the expected genes as compared to the quiescent human HSC, a selection of these proteins are shown in Table 4-1. (A positive change factor demonstrates an upregulation of a gene in an activated HSC as compared to a quiescent HSC).

Table 4-1 Table of activation markers found in the human HSC

Gene	Change factor
Collagen, type I, alpha 2	78.24
Collagen, type I, alpha 2	63.22
procollagen alpha 2(I) chain	60.62
Collagen, type V, alpha 2	45.89
Collagen, type VI, alpha 1	32.05
Collagen, type III, alpha 1	19.5
Collagen, type V, alpha 1	303.4
Collagen, type IV, alpha 1	8.51
Collagen, type IV, alpha 2	7.69
Collagen, type VI, alpha 3	8.67
matrix metalloproteinase 1 (interstitial collagenase)	2.9
92kD type IV collagenase (MMP-9)	10.16
tissue inhibitor of metalloproteinase 1 (TIMP-1)	1.43
Human platelet-derived growth factor receptor alpha	15.52
platelet-derived growth factor PDGF-A	5.75
Smooth muscle actin	4.32
TGF-beta 1	10.75
TGF-beta 2	4.63

4.2.2 Expression of IFN-α regulated receptor and genes in the quiescent and activated human HSC

Having established the data correlated with our previous work, Interferon receptors and regulated genes were examined. It was necessary to confirm the presence of these to justify the planned treatment with IFN-α.

As can be seen in the table, the expression of receptors of IFN-α was not affected by activation of the stellate cell. This suggests that any difference in response to IFN-α due to activation or quiescence of the cells is due to intracellular mechanisms.

As shown in Table 4-2, the IFN-α induced genes also little affected by the activation of the HSC. However, the contribution of these genes to HSC activation is unknown.

Table 4-2 Table displaying the expression of the IFN-α receptor in quiescent and activated cells.

Gene	Change factor
interferon (alpha, beta and omega) receptor 1	1
interferon (alpha, beta and omega) receptor 2	-0.26
interferon (alpha, beta and omega) receptor 2	-0.26
interferon (alpha, beta and omega) receptor 2	-0.34
interferon (alpha, beta and omega) receptor 2	-1.04
interferon (alpha, beta and omega) receptor 2	0

Table 4-3 Table showing the expression of IFN-α regulated genes.

Description	Change factor
2',5'-oligoadenylate synthetase 1	-2.29
2',5'-oligoadenylate synthetase 1	-5.13
2'-5'-oligoadenylate synthetase 2	-1.74
interferon, alpha-inducible protein (clone IFI-6-16)	-0.5
interferon, alpha-inducible protein (clone IFI-6-16)	0.09
myxovirus (influenza) resistance 1, (interferon-inducible protein p78)	-1.58
myxovirus (influenza) resistance 2,	-1.55
protein kinase, interferon-inducible double stranded RNA dependent activator	0.84
protein kinase, interferon-inducible double stranded RNA dependent	-0.29

4.2.3 Regulation of an interferon-regulated gene, 2'-5'-oligoadenylate synthetase, by Interferon α A/D in the HSC.

The Affymetrix data confirmed that the IFN-α regulated genes were expressed by the HSC, and in addition, that the IFN-α receptor was expressed in both quiescent and activated HSCs. I then assessed regulation of an IFN-α regulated protein, 2'-5'-oligoadenylate synthetase, in HSCs following IFN-α treatment. The regulation of 2'-5'-oligoadenylate synthetase was performed to establish that the HSCs were responding to IFN-α treatment.

HSCs were treated with IFN-α A/D for 24hrs in DMEM with 5% FCS. The mRNA was removed and RT-PCR was performed to gain cDNA. The PCR was run in an Applied Biosystems 7700 and assessed using a TaqMan® Realtime Quantitative PCR reaction. Probes and primers were designed according to the Applied Biosystems guidelines. The results were normalized using a housekeeping gene L37a ribosomal protein (as advised by Roche, personnel communication).

As shown in Figure 4-1 and Figure 4-2, whilst there appears to be a dose response in the HSC this is not significant due to the error bars. However, in the PSC population (Figure 4-3) this increase is much larger, nevertheless this is only one population.

Figure 4-1 Graph showing the response of 2'-5'-oligoadenylate synthetase following 24hrs IFN-α treatment in HSCs.

HSC were incubated in 5% FCS containing media for 24hrs in the presence of three doses of IFN-α. Relative expression was determined by normalizing data first to the housekeeping gene ribosomal protein L37a and secondly to the control group. Data is then logarithmically assessed. No significant difference was found between groups (n=3).

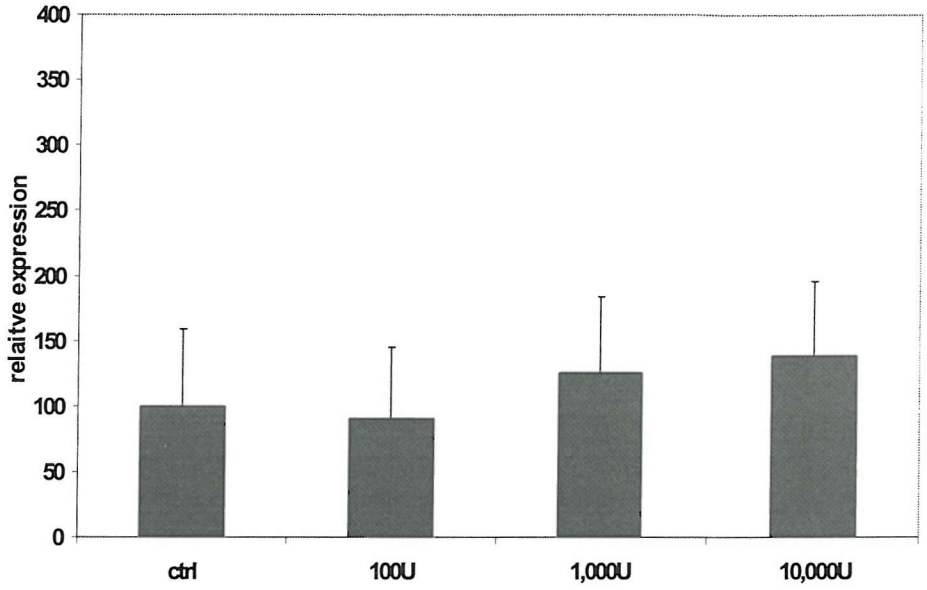

Figure 4-2 Graph showing the response of 2'-5'-oligoadenylate synthetase following 72hrs IFN-α treatment in HSCs.

HSC were incubated in 5% FCS containing media for 72hrs in the presence of three doses of IFN-α. Relative expression was determined by normalizing data first to the housekeeping gene ribosomal protein L37a and secondly to the control group. Data is then logarithmically assessed. No significant difference was found between groups (n=3).

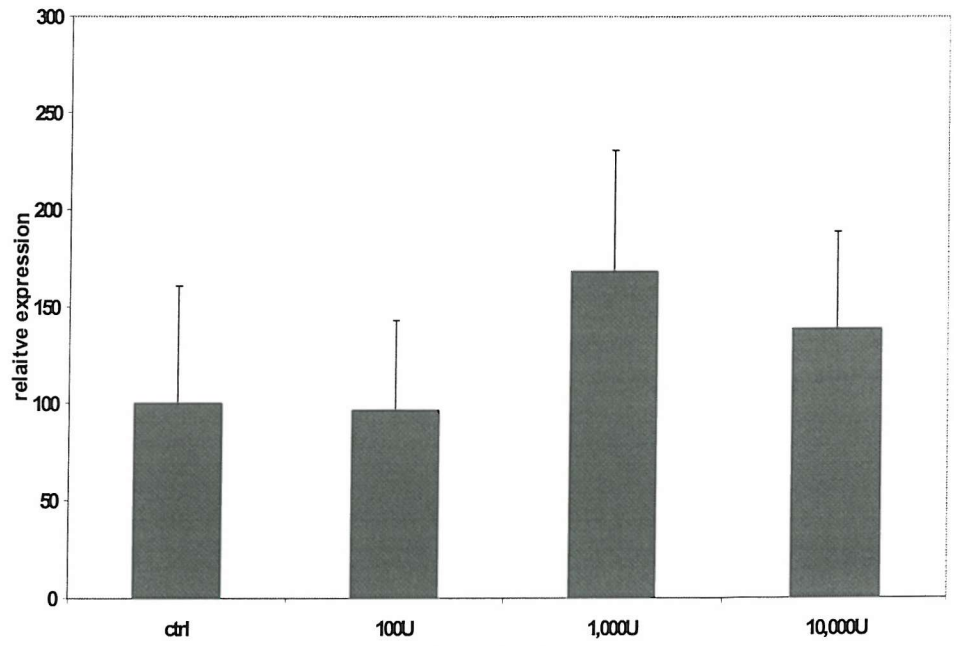

Figure 4-3 Graph showing the response of 2'-5'-oligoadenylate synthetase following IFN-α treatment in PSCs.

PSC were incubated in 5% FCS containing serum for 24hrs (n=1) with IFN-α A/D at 100U/ml, 1000U/ml and 10,000U/ml and without (as control). Cells were then lysed and cDNA prepared for analysis using TaqMan® Realtime Quantitative PCR.

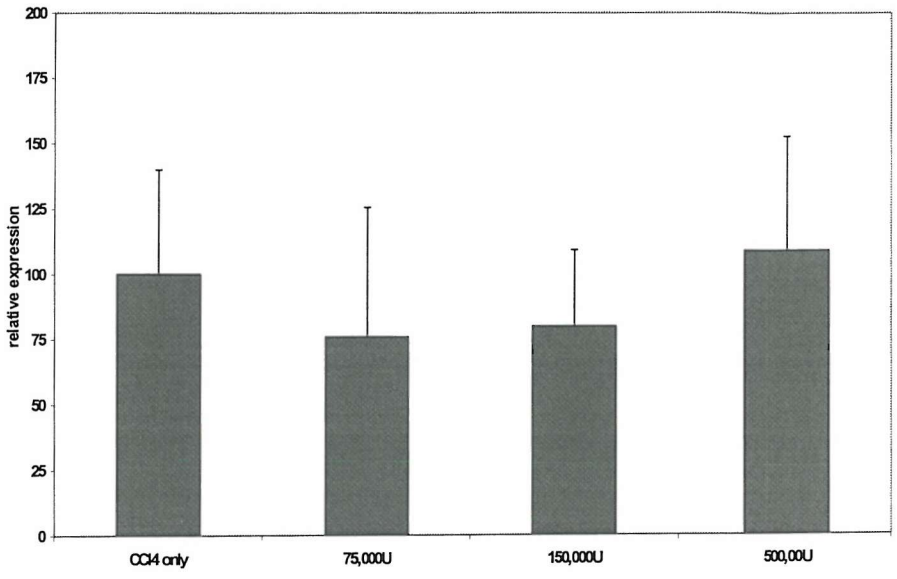

4.3 THE EFFECT OF IFN-α ON PROLIFERATION AND APOPTOSIS

4.3.1 Effect of IFN-α on apoptosis

Many studies report the ability of IFN-α to increase the rate of apoptosis in a variety of different cultured cells including Daudi cells and T-cells (Kaser A 1999; Gisslinger 2001). If IFN-α had such effects on HSC, then it might limit the development of fibrosis within the patient or facilitate resolution of fibrosis by critically altering the HSC population dynamics. To assess this cells were plated in DMEM with 5% FCS, and treated with IFN-α for 24hrs at 100U/ml, 1000U/ml and 10,000U/ml. Cells were also plated in serum free media which enhances the rate of apoptosis of stellate cells and acts as a positive control. Cells were also plated in 16% FCS containing media to provide conditions where apoptosis is suppressed due to increased provision of survival factors. Acridine orange staining was used to count apoptotic cells. IFN-α did not induce apoptosis in the HSCs, neither did it confer any protection (Figure 4-5). A small increase, as compared to control, was found in the lowest doses, 100U and 1,000U IFN-α, however these were not statistically significant. The highest dose of 10,000U IFN-α was equivalent of that of the control group. However, in the PSC population studied IFN-α did decrease the apoptotic rate and appeared to have a protective effect in the PSC. Only one population of PSCs were studied, and therefore statistics were not applied (Figure 4-6).

Figure 4-4 Picture showing HSC stained with Acridine orange.
Within the picture one apoptotic HSC can be seen – this is shown with an arrow and the inset picture shows this same cell at a higher magnification. (Picture taken by Dr. C. Constandinou).

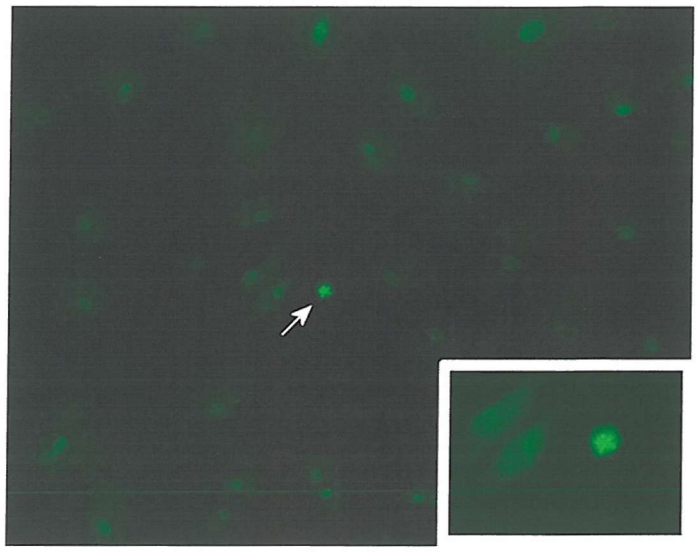

Figure 4-5 Graph displaying the apoptotic response to IFN-α by the HSCs (n=3).
Counts from both FCS free and 16% FCS containing media were included to demonstrate positive and negative controls. No significant difference was found between groups.

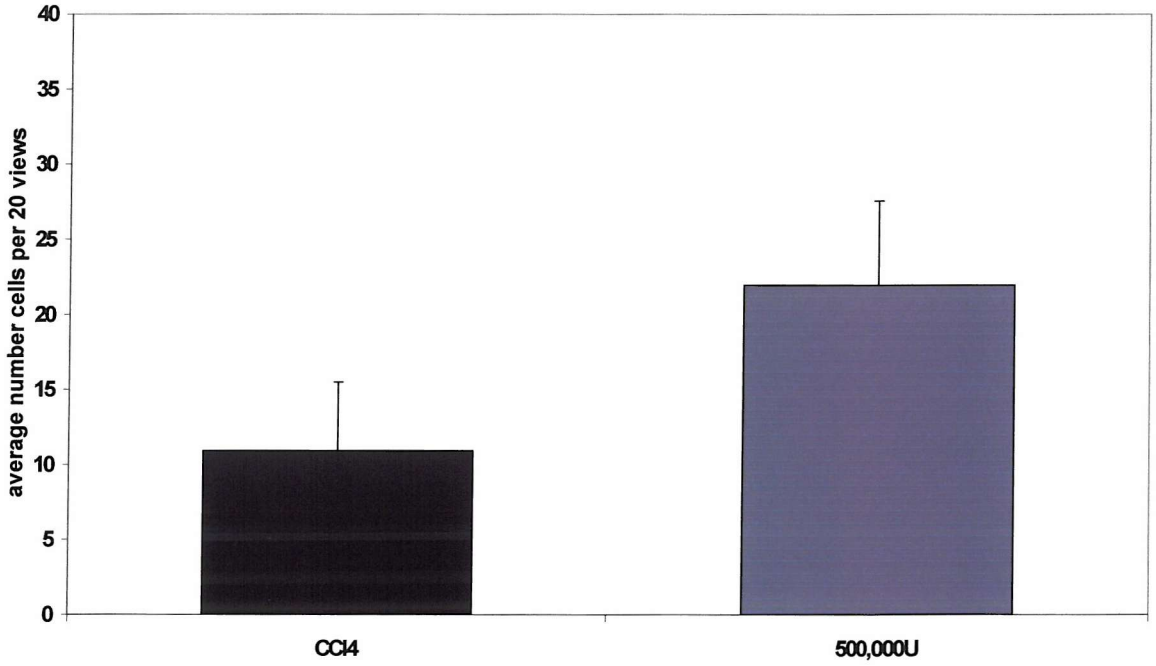

Figure 4-6 Graph displaying the apoptotic response to IFN-α by the PSCs (n=1). *Counts from both FCS free and 16% FCS containing media were included to demonstrate positive and negative controls. No significant difference was found between groups.*

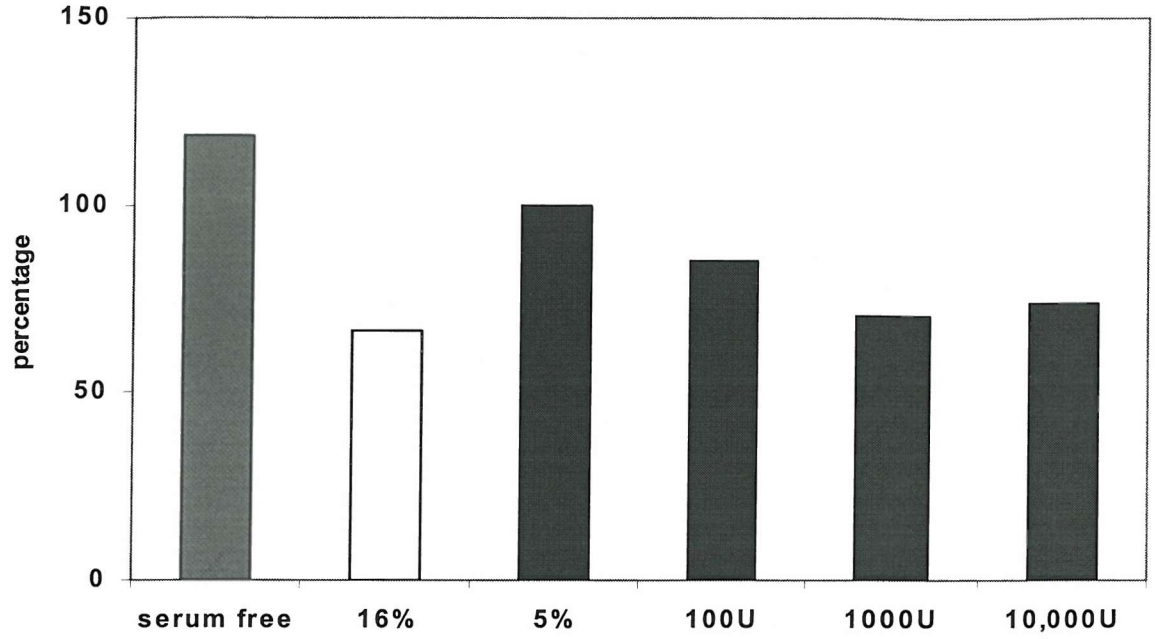

4.3.2 Effect of IFN-α A/D on cell proliferation

Several studies have demonstrated the antiproliferative effects of IFN-α, and in particular, the work of Mallat 1995 showed an inhibition of proliferation in human HSC cells. However, using IFN-α known to be active on rat cells, I also corroborated this same effect in the rat hepatic and PSCs. For this purpose the incorporation of ^{3}H Thymidine was assessed as means of calculating cellular proliferation. The cells were given IFN-α A/D in DMEM with 5% FCS for 24hrs and for the last 16hrs of this were additionally given H^{3} Thymidine. At the end of this timepoint, the amount of ^{3}H Thymidine incorporated into the newly synthesized DNA within the cells was measured. Each experiment incorporated a positive control where the cells had no IFN-α A/D but plated in DMEM with 16% FCS. The increased contents of FCS in the medium should show a marked rise in proliferation against the control group with 5%

FCS containing media. In the HSC (Figure 4-7) a reduction in proliferation found to be statistically significant using the student's T-test statistical was found at 1,000U ($p=0.007$) and 10,000U ($p=0.002$). In the PSC (Figure 4-8) no statistically significant difference was found at any dose despite the large decrease at 10,000U where $p=0.12$. Curiously, an increase was seen in both HSC and PSC in the lowest two doses of IFN-α. These were not significantly different at either dose in either population.

Figure 4-7 Effect on IFN-alpha on the proliferation of HSC after 24hrs treatment (n=5) using ^{3}H Thymidine incorporation.

HSC exposed to varying concentrations of IFN-α A/D in the presence of 5% FCS were analysed for proliferation. A positive control of 16% FCS, no IFN-α A/D, was included. A statistically significant decrease in proliferation was determined using the Student's t-test at 1,000U (p=0.007) and 10,000U (p=0.002) (✦) of IFN-α relative to control.

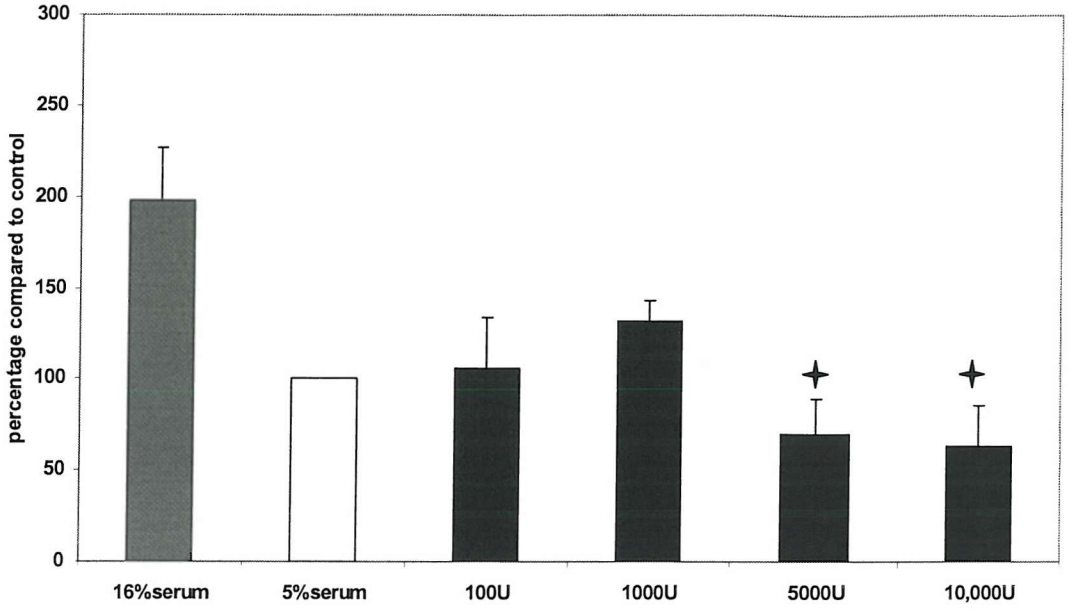

Figure 4-8 Effect of IFN-alpha on the proliferation of PSC (n=3) after 24hrs treatment.

HSC exposed to varying concentrations of IFN-α A/D in the presence of 5% FCS were analysed for proliferation. A positive control of 16% FCS, no IFN-α A/D, was included. Although a decrease was found at 10,000U it was not statistically significant (p=0.122).

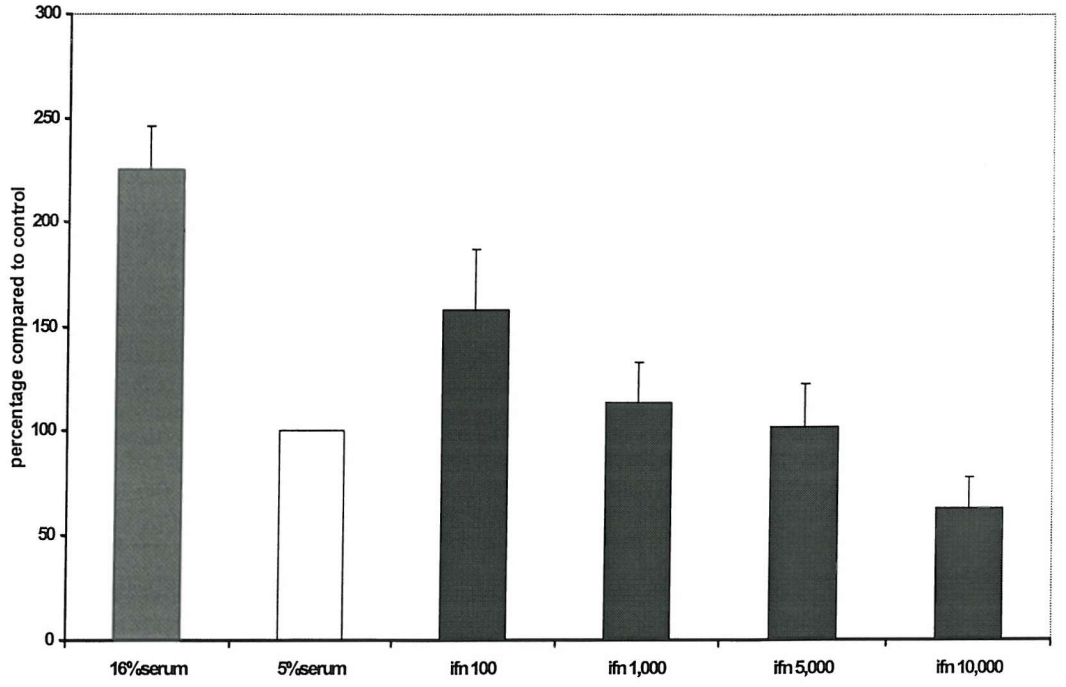

4.3.3 CellTiter 96® Aqueous ONE Solution cell Proliferation Assays

To further substantiate the proliferation data found with the incorporation of ^{3}H Thymidine, a second assay was used. The CellTiter 96® Aqueous ONE Solution cell proliferation assay (Promega) was chosen whereby a tetrazolium salt, 3-(4,5-dimethylthiazol-2-yl)-5-(3-carboxymethoxyphenyl)-2-(4-sulfophenyl)-2H- tetrazolium (MTS), is added to the cell media. Dehydrogenase enzymes within the cell's mitochondria reduce the tetrazolium salt to a soluble coloured formazan product. Therefore, strictly the assay measures mitochondrial activity, but is a commonly used as an extra method of measuring cell proliferation. The final colour is assayed by a spectrophotometer at 490nm.

To assess the cell numbers required for this assay per well of a 96-well plate, an assay was carried out using a sequentially increasing number of cell numbers well. Cells were plated out in a 96-well plate and then left to proliferate for 4hrs, 24hrs and 48hrs, the Aqueous One Solution added for the last 2hrs of the assay. Data from this experiment gave a linear correlation with the HSCs with each time point (Figure 4-9), but little response was found from the PSCs at any time point (Figure 4-10).

Based on this data, HSCs were plated out at 100,000 cells per well of a 96-well plate, thus allowing for an increase or decrease in proliferation. Cells were treated with IFN-α for 24hrs in 5% FCS containing media. Compared to the 5% media control the IFN-α treated samples showed some decrease, however the data was not validated by the positive and negative controls (Figure 4-11), 16% FCS containing media and FCS free, 0.01% BSA media respectively. The data from the assay showed an apparent increase in FCS free media with 0.01% BSA as compared to both 5% and 16% FCS containing media controls. As it is known that FCS media quiesces and eventually induces

apoptosis of the cells the data was not used. Further repetitions of this experiment also gave questionable results.

Figure 4-9 Effect of cell number on absorbance reading at 490nm (HSC).
HSC were plated in the presence of 5% FCS at a range of increasing cell densities and left for 4hrs, 24hrs and 48hrs. The absorbance is plotted and the data correlates well with cell number.

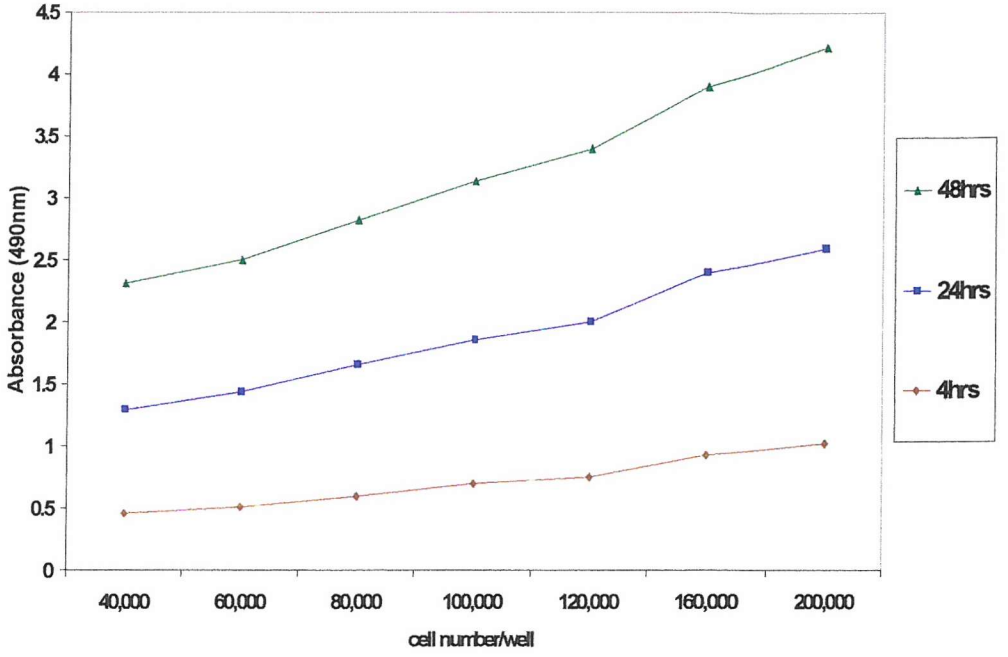

Figure 4-10 Effect of cell number on absorbance reading at 490nm (PSC).
PSC were plated in the presence of 5% FCS at a range of increasing cell densities and left for 4hrs, 24hrs and 48hrs. The absorbance is plotted but the data shows little change with cell number.

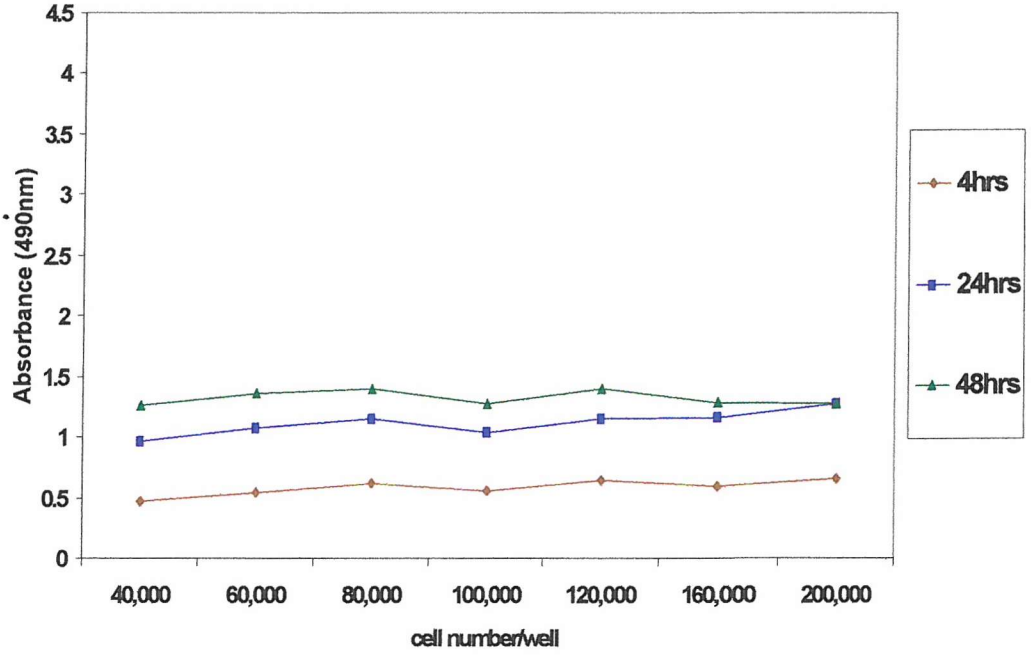

Figure 4-11 Proliferation of HSCs and PSCs after 24hrs treatment.
HSC and PSC were exposed to three concentrations of IFN-α A/D in the presence of 5% FCS, and proliferation was assessed using MTS reduction. This data was disregarded as the positive control demonstrated only a negligible increase and the negative control demonstrated a large increase. The controls established the invalidity of this method and the data provided by it.

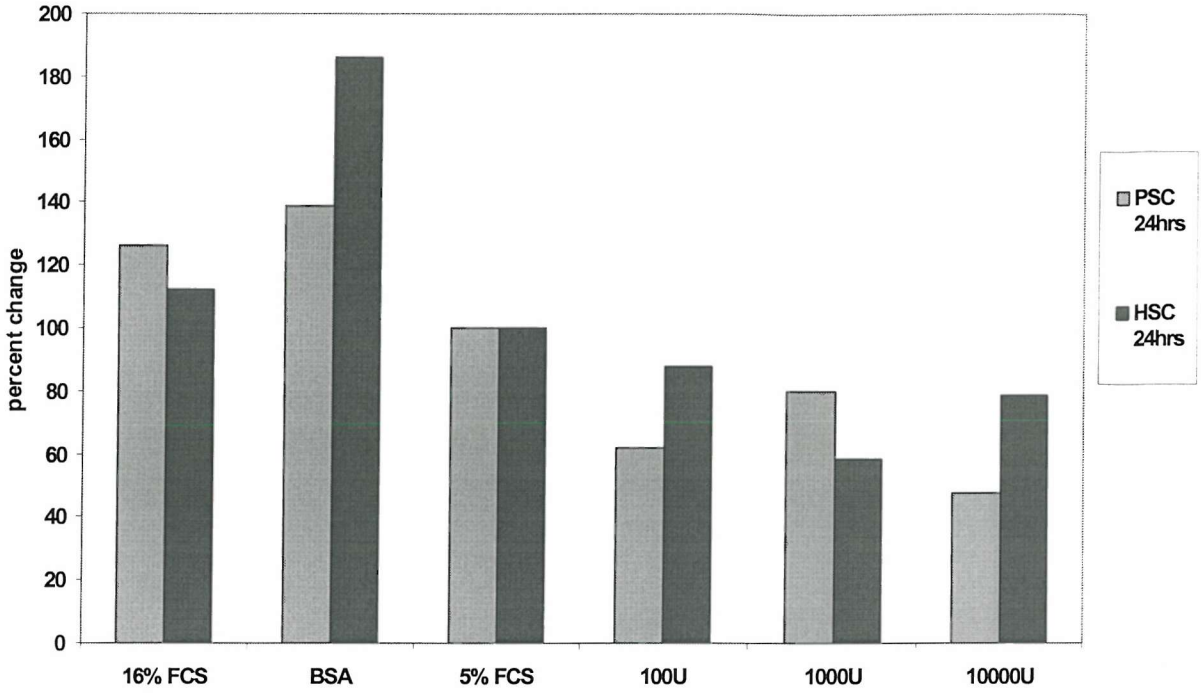

To ascertain whether the media was the cause of the different absorbance readings, the three types of media were plated out, with no cells present, and left in the plate within the incubator for 24hrs. As can be seen, no substantial change between media types was found (Figure 4-12).

Figure 4-12 Media background levels with no cells in each well.

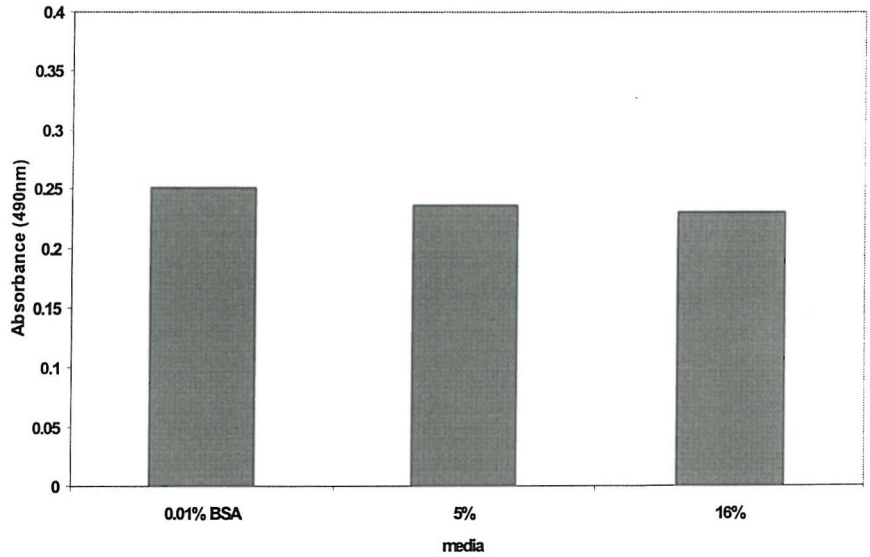

4.3.4 Analysis of changes in cell number after IFN-α A/D treatment

As the CellTiter 96® Aqueous ONE Solution cell proliferation assay had not worked consistently or satisfactorily other methods were used to further the ^{3}H Thymidine data demonstrating regulation by IFN-α. Therefore, as the ^{3}H Thymidine technique does not measure absolute changes in cell number, the Pico Green DNA assay was used to assess actual changes in the quantity of DNA following IFN-α A/D treatment.

Cells were divided into two and plated out, one half was treated for 24hrs and the other for 72hrs. The quantity of DNA was measured at both time-points and the difference in DNA amounts subtracted; the first timepoint from the latter, thus giving an analysis on the amount of cell proliferation and growth.

Figure 4-13 Graph showing the increase in quantity of DNA over 48hrs.
DNA was analyzed at 24hrs and 72hrs following plating. The difference between the two timepoints was calculated. Data is represented as percentage of control. A clear dose dependant decrease can be seen but was not statistically significant (n=3). This supports the ^{3}H Thymidine data.

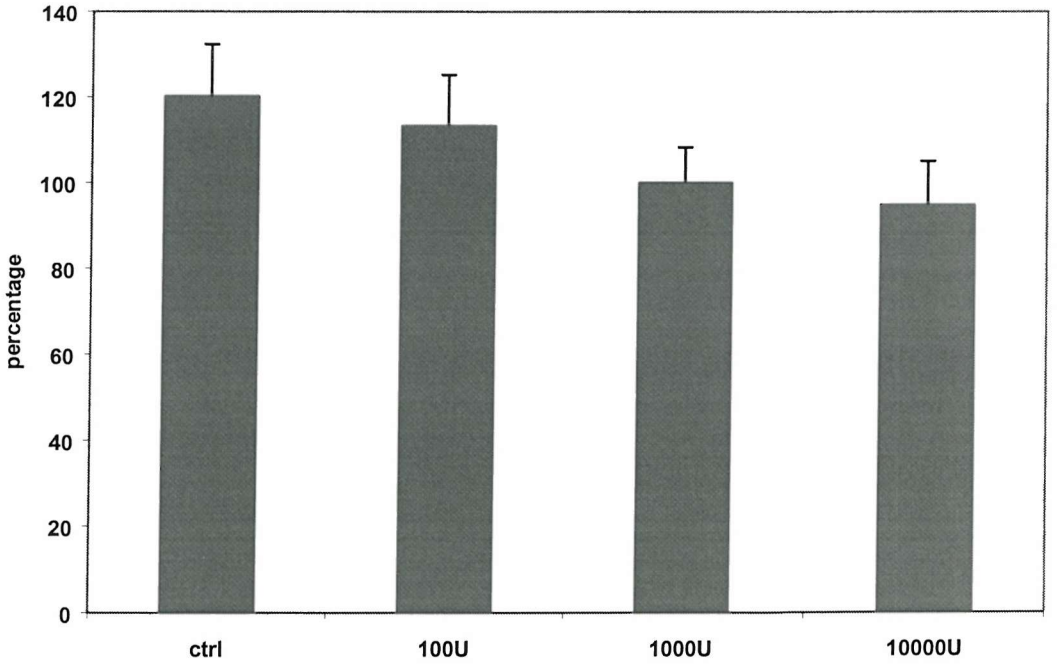

Figure 4-14 Graph showing the increase in quantity of DNA during 48hrs.
DNA was analyzed at 24hrs and 72hrs following plating. The difference between the two timepoints was calculated. Data is represented as percentage of control. No dose dependant response was found with the PSC (n=1) as seen with the ^{3}H Thymidine data.

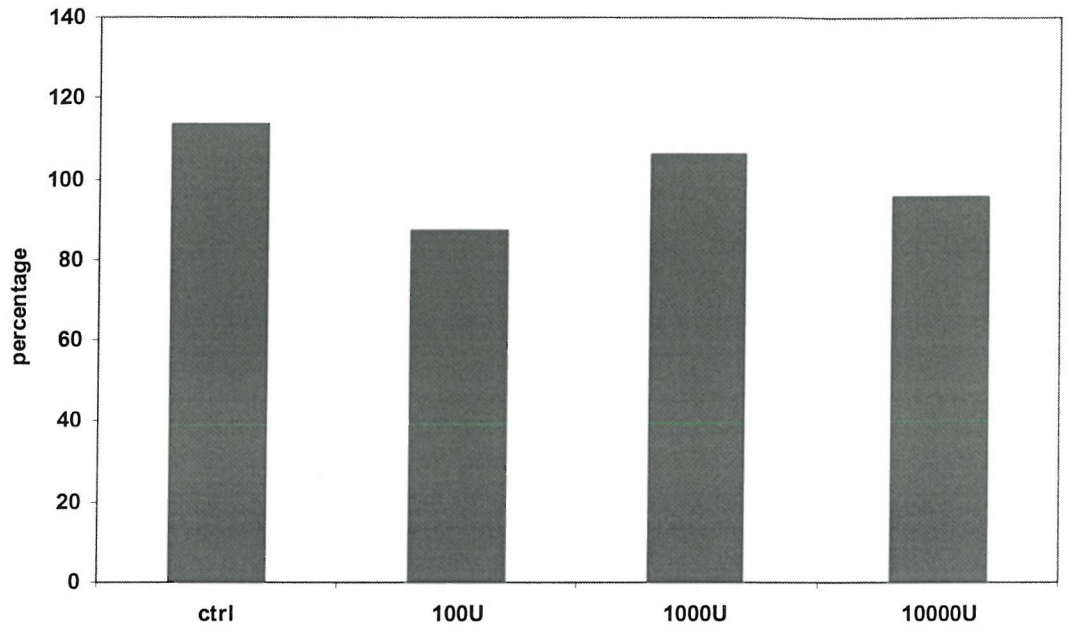

Overall, a decrease in DNA quantity was found in the IFN-α treated cells and this appears to show a dose response. However, this data demonstrated a trend comparable with the ^{3}H Thymidine. Nonetheless, there was not a statistically significant difference between any of the groups. The IFN-α treated PSCs also had less DNA than control, but due to the lack of population numbers this is not clearly seen and is therefore not statistically different.

4.3.5 Downregulation of ERK1 and ERK2 by Interferon alpha.

Our group has previously shown the rapid upregulation of the MAP kinases ERK1 and ERK2 corresponding with the upregulation of proliferation in the HSC (Gaca 2002). Upregulation of ERK1 and ERK2 has also been shown with the onset of PSC proliferation (Jaster 2002). Therefore the levels of ERK1 and ERK2 were assessed by treatment with IFN-α for 24hrs in 0.1% FCS containing media. To stimulate the cells, and thus ERK1 and ERK2, the IFN-α containing media was removed and replaced with 16% FCS containing media. Previous work within our groups demonstrates that when HSC are stimulated, following cell-cycle arrest, ERK1 and ERK2 are rapidly switched on. As demonstrated in expression of ERK1 and ERK2 were found to be decreased as compared to control (untreated with IFN-α). This decrease was most clearly seen at 30 mins and 1hr following stimulation with 16% FCS containing media (Figure 4-15). Thus, this corresponds with previous work within our group. No difference was seen at any timepoint when treating the PSCs as shown in Figure 4-16.

Figure 4-15 Western blot showing the effect of IFN on the stimulation of ERK1 and ERK2 in rat HSCs (n=3).
HSCs were incubated in 0.1% FCS containing media with and without IFN for 24hrs before stimulation with 16% FCS containing media. The cells were washed with ice-cold PBS at the given timepoints and the lysates then extracted. At the early timepoints of 30mins and 1hr downregulation of ERK1 and ERK2 can be seen in response to IFN-α relative to control. This disappears at 3hrs and is maintained through to 6hrs.

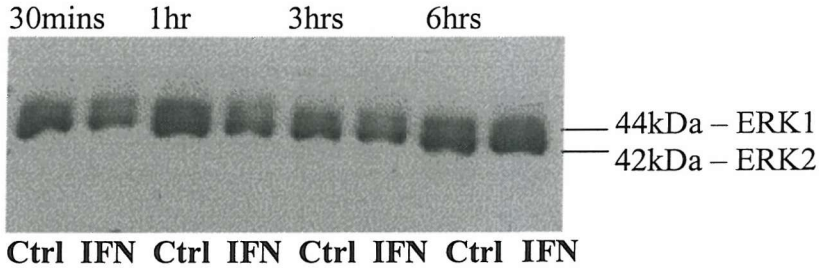

Figure 4-16 Western blot showing the effect of IFN on the stimulation of ERK1 and ERK2 in the rat PSC (n=1).

PSCs were incubated in 0.1% FCS containing media with and without IFN for 24hrs before stimulation with 16% FCS containing media. The cells were washed with ice-cold PBS at the given timepoints and the lysates then extracted. Downregulation of either ERK1 or ERK2in response to IFN-α is not clearly seen in this population.

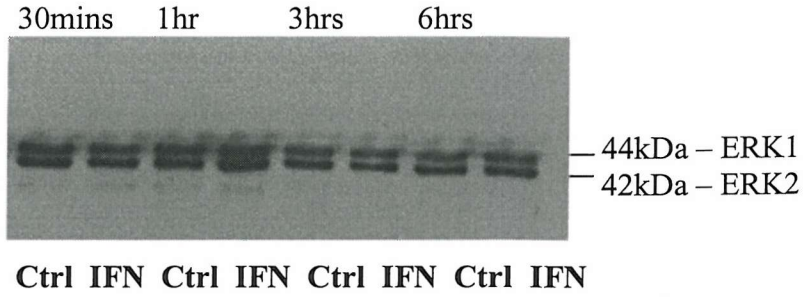

4.4 EXPRESSION OF ACTIVATION MARKERS IN HSC AND PSC FOLLOWING IFN-α A/D TREATMENT

4.4.1 α-SMA expression

Mallat 1995 showed a downregulation in the expression of α-SMA mRNA after 48hrs and in α-SMA protein after 3 days in HSC. Initially, to confirm this protein lysates from IFN-α treated cells were examined after 24hrs and 72hrs for α-SMA expression. HSCs and PSCs were grown and activated on plastic, used between passage 1 and 3 and were grown in 5% FCS containing media. The cells were cultured for 24hrs in the presence of IFN-α at a range of concentrations. At 24hrs no downregulation of the α-SMA protein expression was observed (Figure 4-17). Furthermore, the response to IFN-α did not alter when cultured in serum free media (Figure 4-18).

Figure 4-17 Western blot for α-SMA after 24hrs treatment with IFN-α A/D in 5% FCS containing media (n=3).
HSC were maintained in 5% FCS containing media for 24hrs at increasing doses of IFN-α A/D (n=3). Control was also maintained in 5% FCS containing media with no IFN-α A/D. Cells were then lysed and protein analyzed for α-SMA. No difference as compared to control was found.

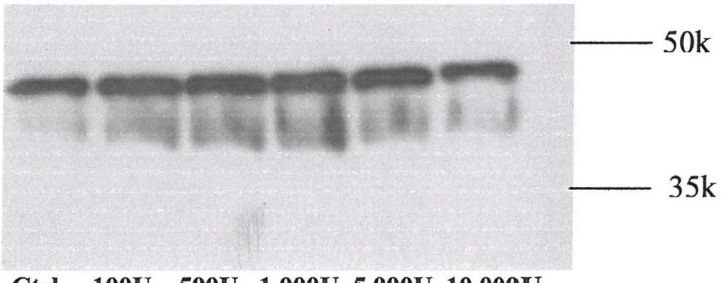

Figure 4-18 Western blot for α-SMA after 24hrs treatment with IFN-α A/D in serum free media (n=2).
HSC were maintained in FCS free media for 24hrs at increasing doses of IFN-α A/D (n=2). Control was also maintained in 5% FCS containing media with no IFN-α A/D. Cells were then lysed and protein analyzed for α-SMA. No difference as compared to control was found.

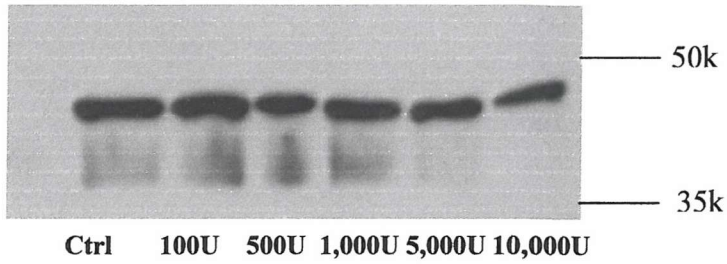

Due to a shortage of cells, further data contains three concentrations 100U/ml, 1000U/ml and 10,000U/ml. When treating the cells for 72hrs the IFN-α A/D was added on day 0 and was not renewed following this. Under these conditions, a decrease in the expression of α-SMA protein was evident in both HSCs (Figure 4-19) and PSCs (Figure 4-20).

Figure 4-19 Western blot for α-SMA response in HSC to 72hrs IFN-α A/D in 5% serum media (n=3).
HSC were maintained in 5% FCS containing media for 72hrs at three doses of IFN-α A/D (n=3). Control was also maintained in 5% FCS containing media with no IFN-α A/D. Cells were then lysed and protein analyzed for α-SMA. A decrease of α-SMA was clear in response to the IFN-α.

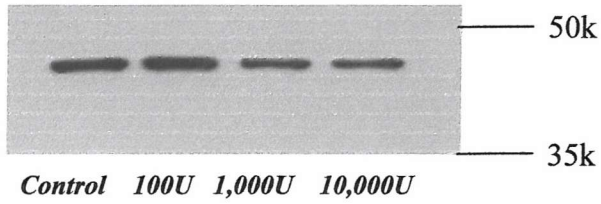

Figure 4-20 Western blot for α-SMA response in PSC to 72hrs IFN-α A/D in 5% serum media (n=1).
PSC were maintained in 5% FCS containing media for 72hrs at three doses of IFN-α A/D (n=1). Control was also maintained in 5% FCS containing media with no IFN-α A/D. Cells were then lysed and protein analyzed for α-SMA. A decrease of α-SMA was again found in response to the IFN-α.

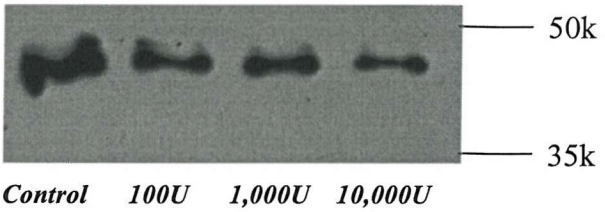

4.4.1.1 α-SMA expression in IFN-α treated freshly isolated HSCs

As previous work had given IFN-α prophylactically the response of a freshly isolated populations of HSCs, i.e. before activation on plastic, were studied. The Affymetrix data previously presented demonstrated that the IFN-α receptors were present. Furthermore, the IFN-α regulated genes were more highly expressed in the freshly isolated HSCs. It is possible that IFN-α exerts its effects in the liver through the prevention of activation of the HSC. If these cells were maintained in the quiescent state, then in patients with this treatment a decrease in α-SMA would be expected in addition to the decrease in fibrosis.

To examine whether IFN-α was able to prevent the initial activation of α-SMA in the quiescent cell and therefore its activation, freshly isolated cells were plated out in 5% FCS containing media with IFN-α. These cells were grown for 7 days to allow the activation of the HSCs and the synthesis of α-SMA. Primary cells treated as above, for 7 days in IFN-α had the treatment renewed every other day. In contrast to expectations, the IFN-α upregulated expression of the α-SMA (Figure 4-21), which also provides a disparity with previous results found in the activated cells.

Figure 4-21 Figure showing the effect of IFN-α on freshly isolated HSC on day 7. *Freshly isolated HSC were placed immediately in 5%FCS containing media, with varying doses of IFN-α. The control also had 5% FCS with no IFN-α. The media and IFN-α was replaced every two days. At day 7 the cells were removed, the protein extracted and analyzed for α-SMA (n=2).*

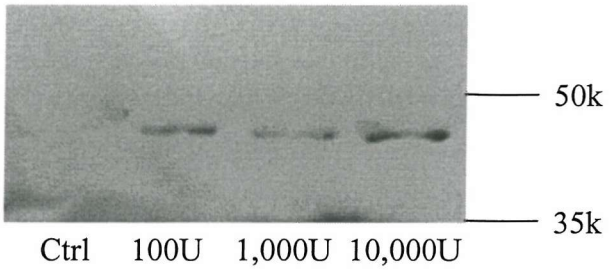

4.4.2 Expression of the Gelatinases

Cells treated for 24hrs with IFN-α A/D were also analyzed for their production of MMP-2 (Gelatinase A) and MMP-9 (Gelatinase B). To analyze these MMPs by zymography it was necessary to grow the cells in DMEM without FCS (due to background levels of gelatinases), but with the addition of 0.1% BSA. As a positive control, media from HSCs treated with 10g/ml Con A was also examined (Figure 4-22) - Con A activates Gelatinase A.

Figure 4-22 The Con A treated HSC, the positive control used on each of the gels shown below.

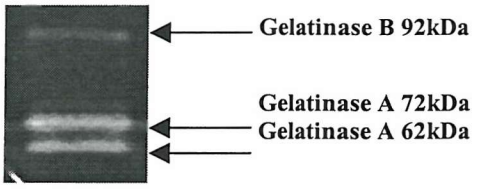

There was no dose response to IFN-α after 24hrs, and also no overall change in Gelatinase A (Figure 4-23). To further verify this a zymography gel was run loading double the standard protein amount (Figure 4-24) and also half the standard loading (Figure 4-25). In doing so, the former would show more clearly any changes in Gelatinase B levels and the latter, any changes in Gelatinase A levels. No change was found in either gel.

Figure 4-23 Zymogram showing the effect of a dose response (U/ml) to IFN-α A/D for 24hrs on Gelatinase A in HSC (n=3).

Serum was removed from HSC grown in serum free media for 24hrs with varying doses of IFN-α. No difference could be seen as compared to control (no IFN-α) (n=3).

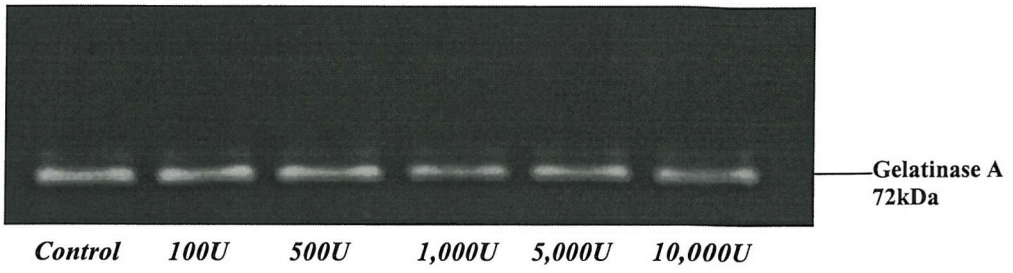

Figure 4-24 Zymogram showing the effect of IFN-α A/D (U/ml) on Gelatinase A in HSC (double loading)

Serum was removed from HSC grown in serum free media for 24hrs with varying doses of IFN-α. Double the amount of conditioned media was loaded to allow for analysis of Gelatinase B. No difference could be seen as compared to control (no IFN-α) (n=1).

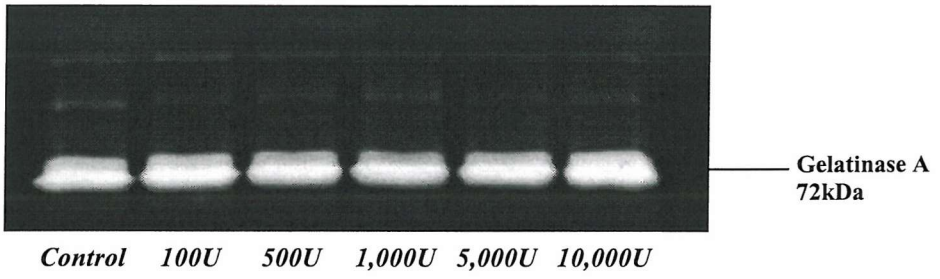

Figure 4-25 Zymogram showing the effect of IFN-α A/D (U/ml) on Gelatinase A in HSC (half loading)

Serum was removed from HSC grown in serum free media for 24hrs with varying doses of IFN-α. Half the standard amount of conditioned media was loaded to allow for analysis of small changes in Gelatinase A. No difference could be seen as compared to control (no IFN-α) (n=1).

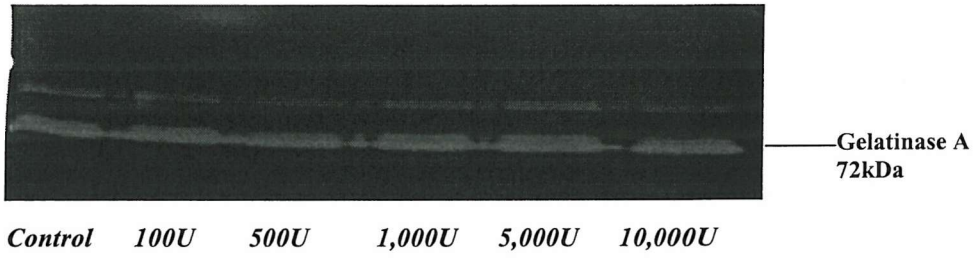

Expression of Gelatinase A and B was also examined after 72hrs. Previous studies in the group have shown that cells can be maintained in FCS free media for 72hrs. However, cells left in this media for later timepoints start to develop a high rate of apoptosis. The serum was collected from the last 24hrs of incubation.

After 72hrs, the expression of Gelatinase A in the HSC population still had no appreciable change in Gelatinase A or Gelatinase B (Figure 4-26). Additionally, no change was observed in either of the Gelatinases within the PSC populations (Figure 4-27).

Figure 4-26 Zymography showing expression of Gelatinase A and B in HSC after 72hrs IFN-α A/D (n=3).
Serum was removed from HSC grown in serum free media for 72hrs with varying doses of IFN-α. Once again, no difference could be seen as compared to control (no IFN-α) (n=3).

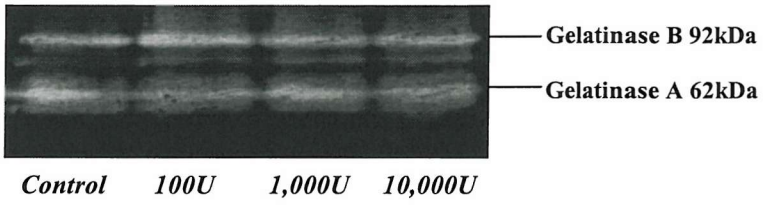

Figure 4-27 Zymography showing expression of Gelatinase A and B in PSC after 72hrs IFN-α A/D (n=3).
Serum was removed from PSC grown in serum free media for 24hrs with varying doses of IFN-α. No difference could be seen as compared to control (no IFN-α) (n=3).

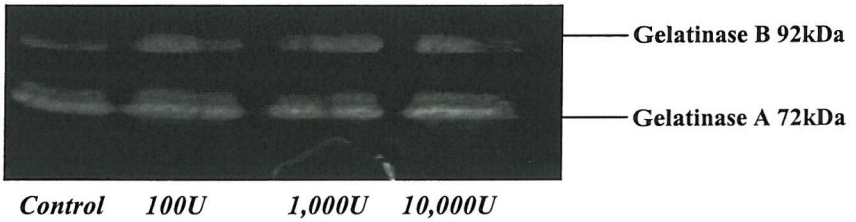

4.4.3 Effect of IFN-α A/D on secretion of Collagen

4.4.3.1 Total Collagen secretion

Total secreted collagen was assessed at 24hrs and 48hrs using a ^{3}H proline assay. In this assay it was also necessary to treat the cells in serum free conditions. IFN-α A/D was added in addition to the ^{3}H proline in serum free media containing 0.01% BSA and 25μg/ml Ascorbic Acid.

As can be seen in both Figure 4-28and Figure 4-29 no change was found in collagen secretion at either 24hrs or 48hrs within the HSCs. However the PSCs did show some reduction in collagen secretion at both timepoints, but this did not appear to be dose related. Furthermore, as this was only one population no absolute conclusion can be drawn from this result. Whilst the figures seem to be lower than control, studying further populations may indeed bring the average closer to the control group (Figure 4-30).

Figure 4-28 Graph showing the total secretion of collagen after 24hrs treatment with IFN-α A/D in HSC.
HSC were grown in serum free media for 24hrs with varying doses of IFN-α. Data is represented as a percentage change against control (untreated) cells. No change was found in total collagen production in the HSCs, n=3.

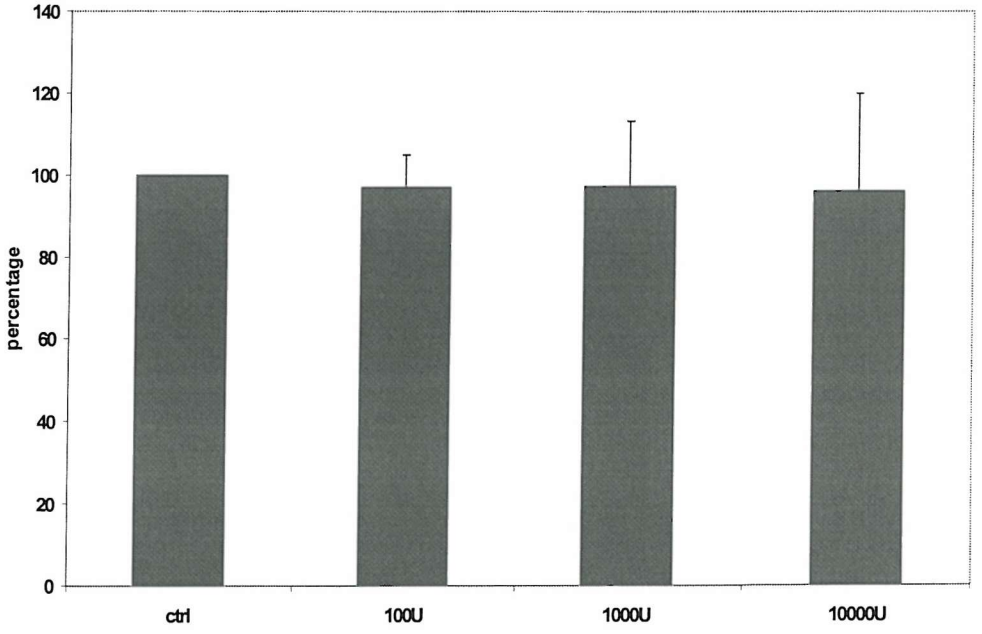

Figure 4-29 Graph showing the total secretion of collagen after 48hrs treatment with IFN-α A/D in HSC (n=3).

HSC were grown in serum free media for 48hrs with varying doses of IFN-α. Data is represented as a percentage change against control (untreated) cells. No change was found in total collagen production in the HSCs (n=3).

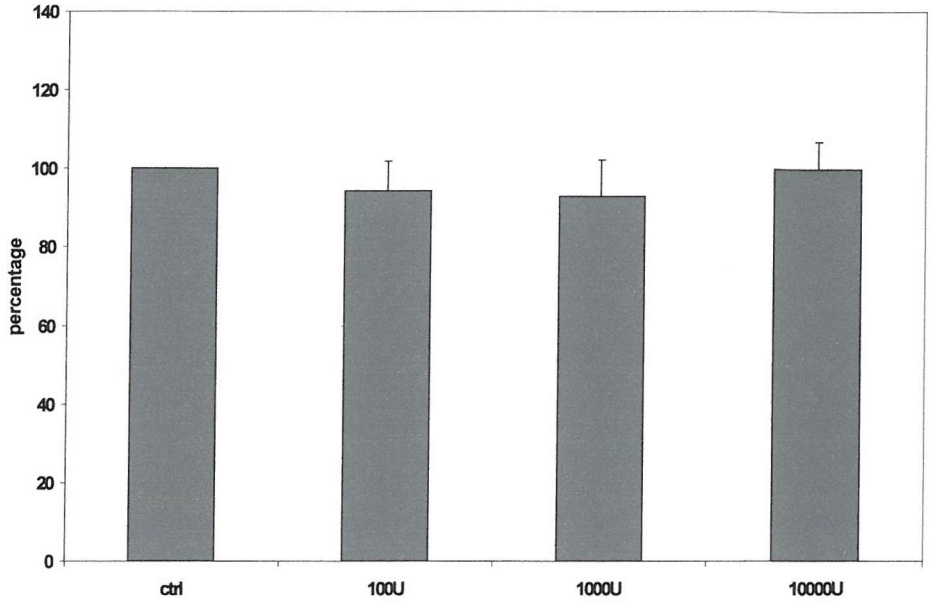

Figure 4-30 Graph showing total collagen secretion after 24hrs (dark grey) and 48hrs (light purple) with IFN-α A/D (n=1).

PSC were grown in serum free media for 24hrs and 48hrs with varying doses of IFN-α. Data is represented as a percentage change against control (untreated) cells. The PSCs show some reduction in collagen secretion at both timepoints (n=1).

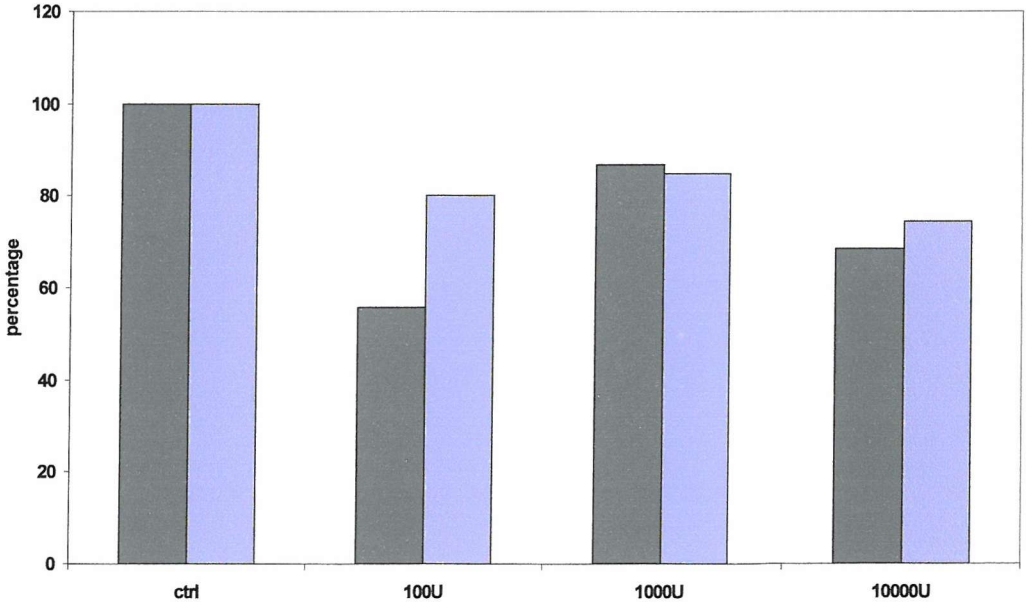

4.4.3.2 Effect of Interferon alpha on collagen mRNA expression.

Collagen expression was additionally analyzed using TaqMan® Realtime Quantitative PCR. The mRNA was extracted from cells treated with IFN-α A/D in 5% serum containing media for 24hrs and 72hrs. RT-PCR was performed and then the cDNA was used for the Realtime Quantitative PCR reaction using an Applied Biosystems 7700 machine. The collagen probe and primers were designed by Applied Biosystems according to their guidelines. L37a ribosomal protein was used as a house-keeping gene, as it had been demonstrated by Dr. E. Murray, Roche Discovery to be uneffected by HSC activation.

As shown in Figure 4-31 and Figure 4-32 no significant change was found in the mRNA levels of collagen of IFN-α A/D treated HSCs at either 24hrs or 72hrs. An increase is found at 24hrs with 1,000U and 10,000U of IFN-α A/D, however, this as previously stated is not significant.

PSCs were also treated identically to the HSCs, for 24hrs and 72hrs. It appears that collagen increases following IFN-α A/D treatment in the PSC. However, as before only one population was used, and only at 72hrs with 1,000U and 10,000U IFN-α A/D does the collagen increase substantially.

Figure 4-31 Graph showing the response of collagen in HSC to 24hrs of IFN-α
HSC were incubated in 5% FCS containing media for 24hrs in the presence of three doses of IFN-α. Relative expression was determined by normalizing data first to the housekeeping gene ribosomal protein L37a and secondly to the control group. Data is then logarithmically assessed. No significant difference was found between groups (n=3).

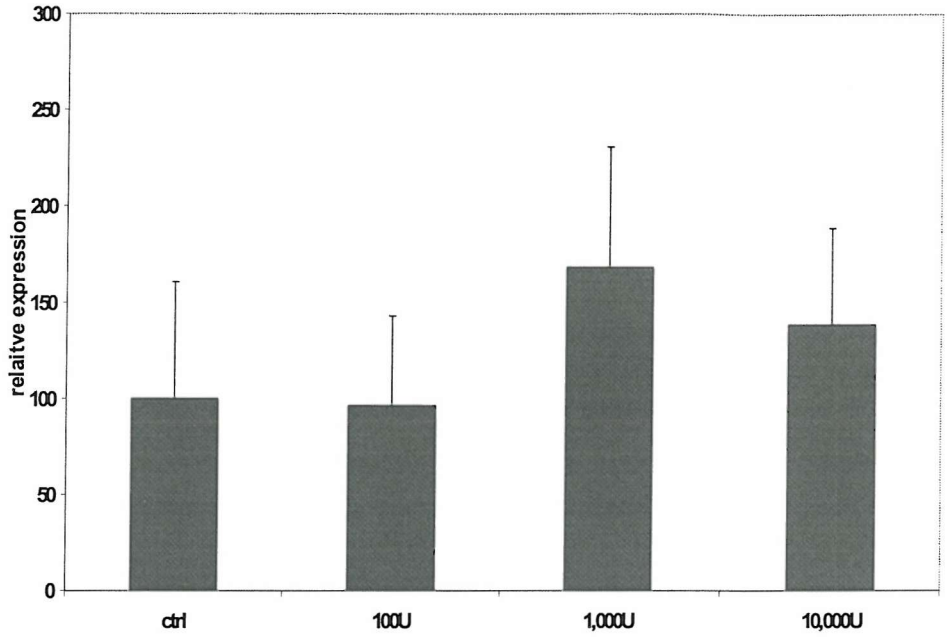

Figure 4-32 Graph showing the response of collagen to 72hrs of IFN-α
HSC were incubated in 5% FCS containing media for 72hrs in the presence of three doses of IFN-α. Relative expression was determined by normalizing data first to the housekeeping gene ribosomal protein L37a and secondly to the control group. Data is then logarithmically assessed. No significant difference was found between groups (n=3).

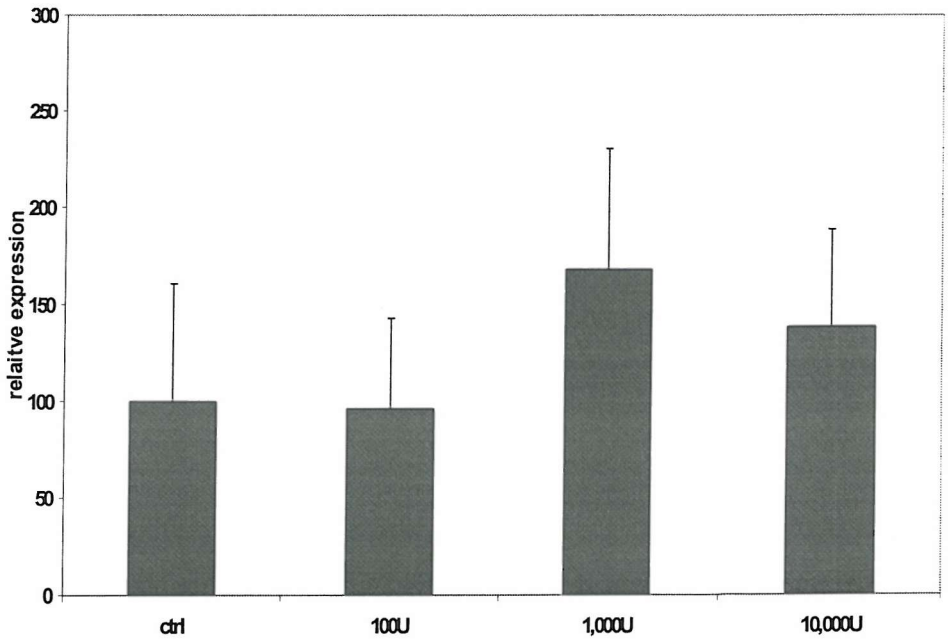

Figure 4-33 Graph showing the response of collagen to 24hrs and 72hrs of treatment with IFN-α by PSC.

PSC were treated with IFN-α for 24hrs and 72hrs in 5% FCS containing media at three doses of IFN-α. Relative expression was ascertained as previously stated with the HSC. An increase can be seen with the 72hrs treatment, but no significance was found (n=1) for both time points.

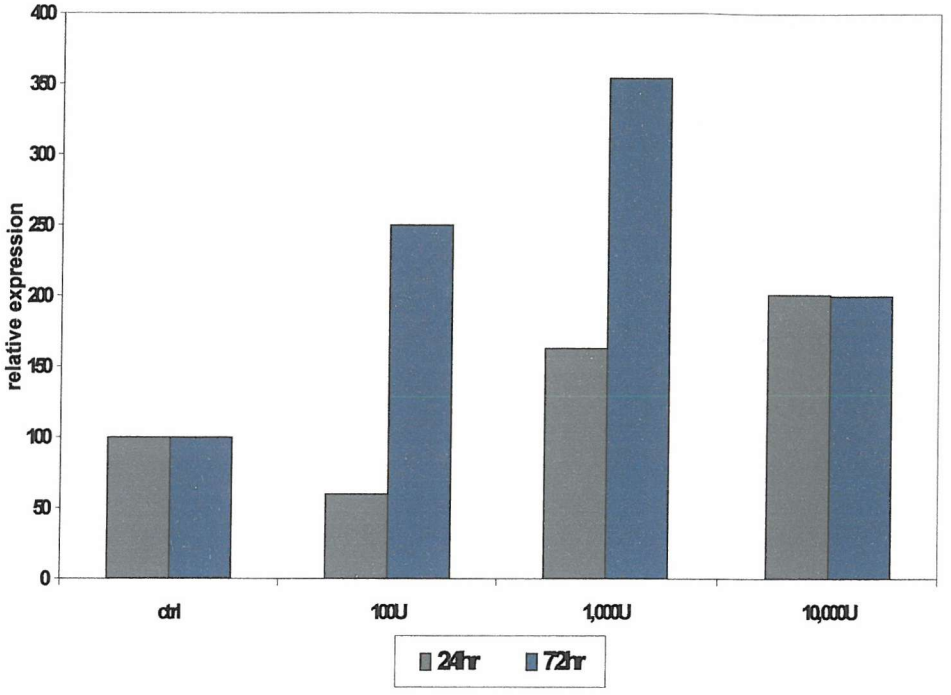

4.4.4 Effect of Interferon alpha on TIMP-1 expression

TIMP-1 expression was also studied in HSC and PSC treated for 24hrs and 72hrs with IFN-α A/D treatment in 5% serum containing media. TIMP-1 mRNA expression was analyzed using TaqMan® Realtime Quantitative PCR. The cDNA was created as above, and the probe and primers were designed as previously explained. L37a ribosomal protein was used as a housekeeping gene.

Whilst the increase, as shown in Figure 4-34, was consistent this increase was still insignificant in TIMP-1 mRNA levels in the HSC following 24hrs IFN-α A/D treatment. However, at 72hrs a larger increase was found in 1,000U and 10,000U IFN-α A/D treated groups, although still not statistically significant $p=0.4$ and $p=0.1$ respectively (Figure 4-35). This trend was correlated with the PSC populations treated for 24hrs and 72hrs, with a particularly big increase found at 72hrs at each dose (Figure 4-36).

Figure 4-34 Graph showing the response of TIMP-1 in HSCs following 24hrs IFN-α A/D treatment.

HSC were treated for 24hrs in 5% FCS containing media with three doses of IFN-α. Relative expression was determined as previously stated by normalizing to L37a and to control before logarithmically assessing the data. A consistent trend was found but no significant difference was demonstrated between groups (n=3).

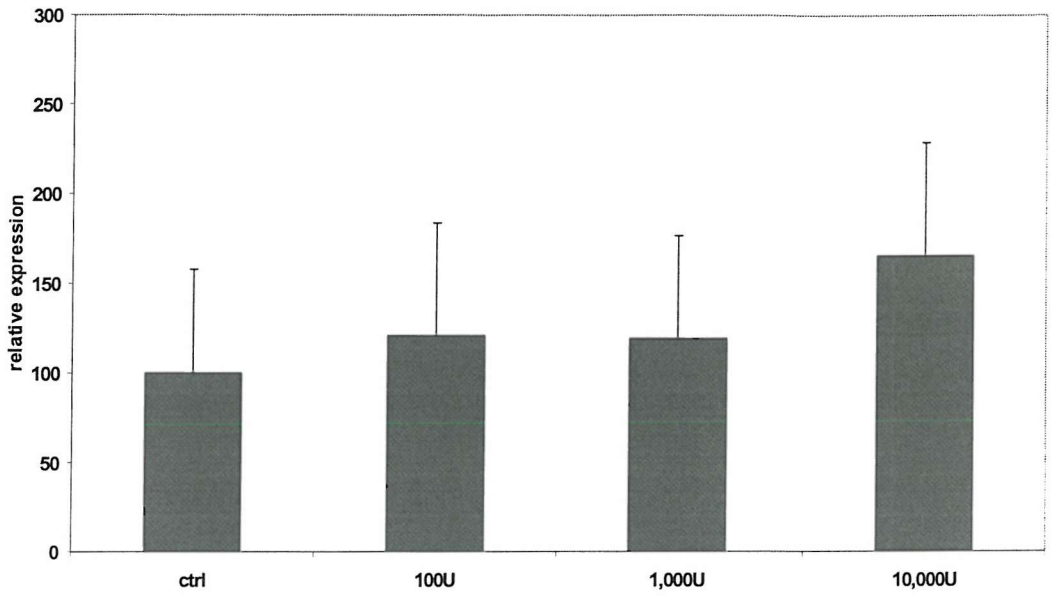

Figure 4-35 Graph showing the response of TIMP-1 in HSCs following 72hrs IFN-α A/D treatment.

HSC were treated for 72hrs in 5% FCS containing media with three doses of IFN-α. Relative expression was determined as previously stated by normalizing to L37a and to control before logarithmically assessing the data. Once again no significant difference was found between groups despite the apparent increase at 1,000U and 10,000U (n=3).

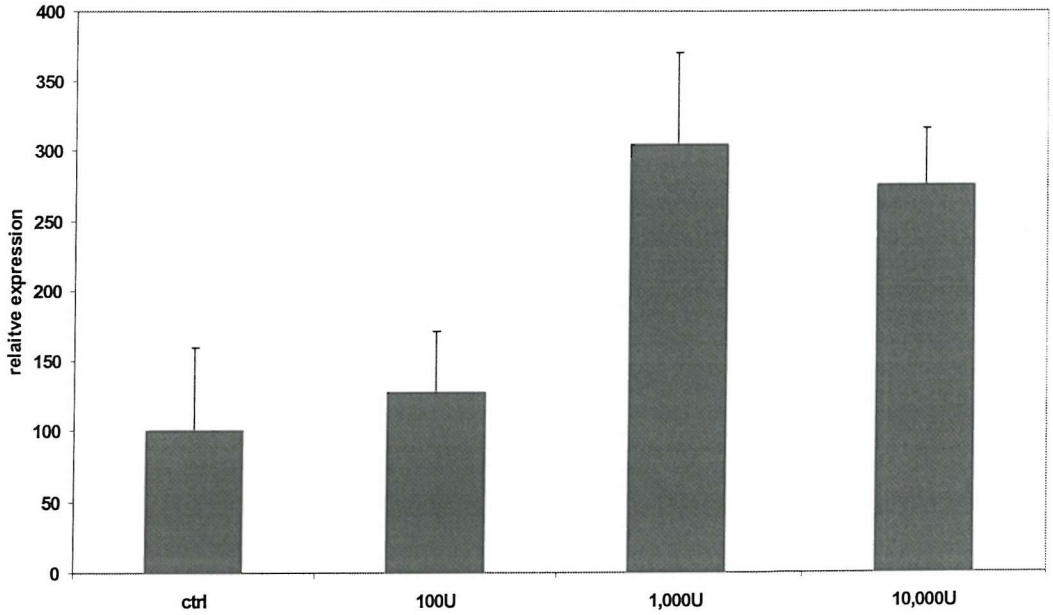

Figure 4-36 Graph showing the response of TIMP-1 following 24hrs and 72hrs IFN-α A/D treatment in PSC.

PSC were treated with IFN-α for 24hrs and 72hrs in 5% FCS containing media at three doses of IFN-α. Relative expression was ascertained as previously stated with the HSC. An increase can be seen with the 72hrs treatment, but no significance was found (n=1) for both time points.

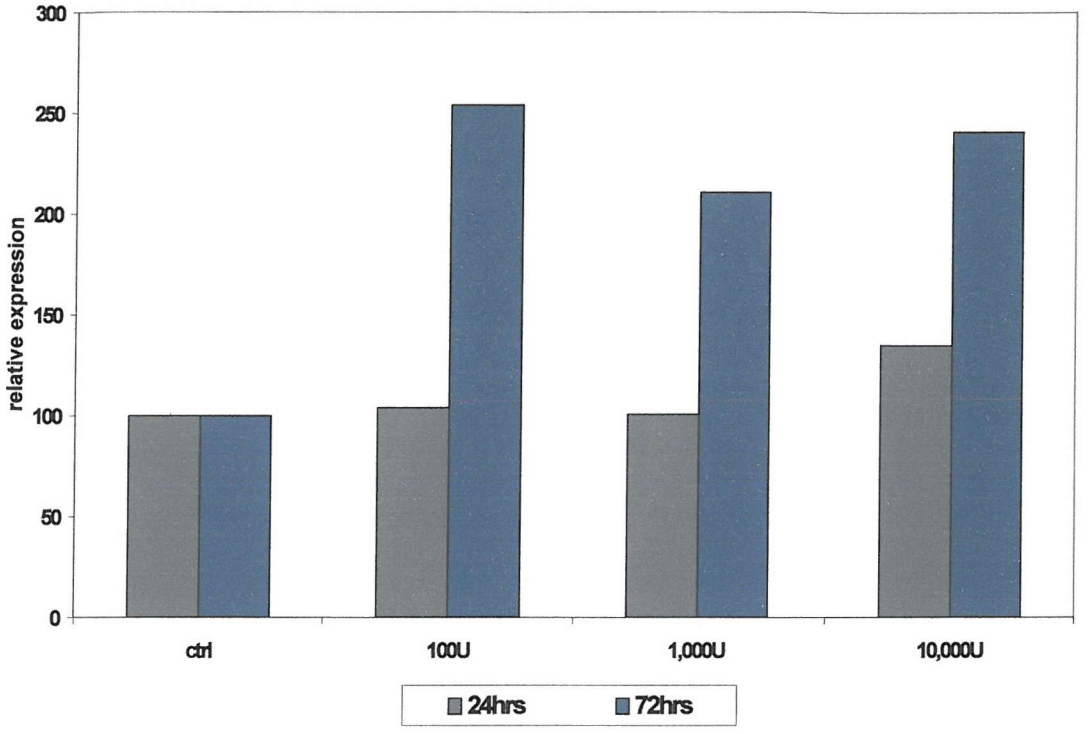

4.5 CONCLUSION

Clinical studies treating HCV patients with IFN-α have resulted in a decrease in fibrosis caused by the viral infection (Duchatelle 1998). IFN-α is given to these patients as an antiviral, but recent evidence suggests that IFN-α itself may have antifibrotic properties (Everson 1999) .

Previous groups have studied the effects of IFN-α both in vitro and *in vivo*, however the results from these studies have been contradictory and the IFN-α used has been a human protein. Because IFN-α is species specific the validity of results generated by studies using human recombinant IFN-α in rodent models must be questioned. As the HSC has been to be shown pivotal in the initiation and perpetuation of fibrosis within the liver, I aimed to analyze the effect of IFN-α on the HSC using an IFN-α known to be active on rodent cells. In addition, I also treated PSC with IFN-α to compare their response to that of the HSC.

Primarily, the Affymetrix data was undertaken to establish a database of genes up- and downregulated in the freshly isolated and activated HSC. The initial work presented here conforms with previous studies of HSC activation both from our group and others. Therefore, the Affymetrix data was first used verify the presence of the IFN-α receptors in the freshly isolated and activated HSC. This data confirmed their presence in the HSC and showed that these were unaffected by HSC activation. Furthermore, IFN-α regulated genes were assessed to study their regulation between the freshly isolated and activated HSC. This showed that the IFN-α regulated genes were upregulated in the quiescent cells as compared to the activated HSC, but were present in both states. Further confirmation was that an IFN-α regulated protein, 2'5'-oligoadenylate synthetase, was upregulated by IFN-α treatment of the HSC.

Having established that the HSC were responsive to IFN-α, the work then turned to study how any anti-fibrotic effect might be realised by dosing IFN-α on HSC. Apoptosis was then studied using staining with Acridine Orange. This dye, which allows the recognition of cell nuclei demonstrating an apoptotic morphology, showed that there was no increase or decrease in apoptosis in response to the presence of IFN-α in either the HSC or the PSC. The proliferation of the cells was then analyzed using ^{3}H Thymidine. In this case a decrease in proliferation was found at the higher two doses used, 5,000U and 10,000U, of which only 10,000U in HSC was found to be statistically significant. However, it was also noted that the lower two doses, 100U and 1,000U both showed an slight increase in proliferation in both HSC and PSC. To confirm this result an assay based on the colour change of a formazan product within the cell was used. Due to spurious results with the positive and negative controls this assay was not found to be suitable for work with HSCs, a conclusion which was later confirmed (Molecular Probes 2002). A picogreen assay was used to quantify changes in the amount of DNA to additionally confirm alterations in cell number. This assay showed a dose response to IFN-α in the HSCs and an overall reduction in DNA quantity in the HSCs and PSCs treated with IFN-α. As an additional confirmation of the antiproliferative action of IFN-α, the activation of ERK1 and ERK2 was studied. It was found that IFN-α treatment reduced the levels of these proteins following cell activation in 16% FCS containing media.

Protein markers known to increase in the activated HSC were also analyzed following treatment with IFN-α, at two timepoints 24hrs and 72hrs. The presence of α-SMA was analyzed by western blotting. No effect was found at 24hrs but at 72hrs a reduction in protein expression was observed. In contrast, freshly isolated HSC treated with IFN-α demonstrated an increase in their expression of α-SMA, thus suggesting

that the freshly isolated and activated HSC is differentially regulated by IFN-α. The expression of MMP-2 was analyzed using zymography; this also showed no effect due to treatment with IFN-α at either timepoint.

The secretion of collagen by the cells was analyzed with an assay measuring the ^{3}H proline incorporation in collagen. By this method no effect on collagen secretion was observed in HSC however a decrease in the PSCs collagen secretion was observed after 48hrs. This data was only generated using a single population of PSC and so it is difficult to conclude on the significance of this data. Collagen mRNA was additionally analyzed as collagen mRNA is known to be pre- and post-transcriptionally controlled (Stefanovic 1997; Stefanovic 2000). The mRNA levels showed no significant increase, although the most evident increase was found at 24hrs in1,000U and 10,000U IFN-α and not at 72hrs as would be expected. Larger increases were seen in the PSC populations but again only one population was studied.

TIMP-1 mRNA was also analyzed, and this again showed an increase in IFN-α treated groups at 72hrs but not at 24hrs, the rises in expression observed were not statistically significant. This increase was confirmed within the PSC population.

In conclusion, IFN-α has shown an antiproliferative effect, but this requires a high dose to obtain statistical significance. Of the activation markers studied, α-SMA has shown a decrease after 72hrs, but none of the other markers have shown a significant change. The mRNA levels of both collagen and TIMP-1 have shown an increase at certain timepoints and doses, which seems incongruous with the antifibrotic effect expected from IFN-α. However, these effects were not statistically significant and may not be biologically relevant. Taken with the data on the expression of MMPs this suggests that in the in vitro model of activated HSC, IFN-α does not regulate matrix secretions or turnover although the proliferation of the HSC may be reduced. Clearly,

if proliferation decreases then there will be a reduction in the overall expression of collagen, MMP-2 and TIMP-1 which may be anti-fibrotic. In wound healing terms it may be advantagous for the IFN-α mediated response to restrict activation of the wound healing myofibroblast population. Furthermore, in a situation of chronic inflammation it could be argued that a down regulatory effect of IFN-α would be beneficial by tending to limit tissue fibrosis.

5 THE EFFECT OF INTERFERON ALPHA A/D *IN VIVO*

5.1 INTRODUCTION

As discussed earlier, there have been several studies of IFN-α treatment of liver fibrosis in rat models *in vivo*. However, with the exception of one study, IFN-α was given from the start of liver injury and therefore measured the effects of IFN-α in preventing the development of fibrosis. These studies used three methods for causing liver injury, carbon tetrachloride (CCl_4), bile duct ligation (BDL) and Dimethylnitrosamine (DMN). Of the three studies which used BDL, one found IFN-α to have no effect whilst the other two studies both found a decrease in collagen content and improvement in liver function test parameters as compared to the untreated groups. However, the results from these studies were conflicting; the IFN-α was given from initiation of fibrosis and the IFN-α used was the human protein which would be expected to be ineffective in a rodent model.

The *in vivo* CCl_4 induced liver injury study found a decrease in collagen content and additionally liver function tests were shown to improve. However, this group concurrently ran an BDL induced liver injury study which demonstrated no improvement in any of the parameters studied. Finally, in the DMN induced liver injury study IFN-α treatment was shown to cause a reduction in serum ALT levels, which suggest a reduction in hepatocellular damage, and collagen content was also reduced. In this study two forms of IFN-α were used and there was a notable difference between the two types. Specifically, natural purified human leukocyte IFN-

α was far more effective than recombinant IFN-α 2b. This might be expected as the purified form would contain many different IFN-α proteins, and in addition might contain other IFN types, e.g. IFN-γ which is antifibrotic. However, the results are critical in that current evidence would suggest that human IFN may not be truly efficient in rat models.

To further elucidate the efficacy of IFN-α treatment in the fibrotic liver, a CCl_4 induced liver injury *in vivo* model was completed. However, whilst the majority of former studies had shown an improvement after giving IFN-α from the onset of liver injury, this does not representative of current patient treatment. At present, patients with liver fibrosis associated with chronic viral hepatitis are treated with IFN-α after the fibrosis is established. It is not possible to give therapeutic drugs at the onset of disease. In humans this would be analogous to giving a 18 year old man IFN-α three times per week whilst allowing him to start drinking 10 units of alcohol per day. Therefore, we induced liver fibrosis, as previously shown in Muriel 1996 before IFN-α therapy was administered.

Furthermore, as with the in vitro work, the IFN-α used was an IFN-α tested for efficacy on rats, as compared to previous studies where IFN-α drugs used on patients was used in the *in vivo* studies.

5.2 *IN VIVO* CARBON TETRACHLORIDE STUDIES

Thirty rats were given CCl_4 for 8 weeks, twice weekly. For the first two weeks CCl_4 was given at 0.05ml per 100g body weight, following which CCl_4 was given at 0.1ml per 100g body weight for the remainder of the studies. At 6 weeks the rats were divided into four groups (7/8 rats per group), the first of which continued to receive CCl_4 alone. The remaining three groups were all given IFN-α subcutaneously in addition to CCl_4, three doses were used: 75,000U/day, 150,000U/day and 500,000U/day for the remaining two weeks.

The rats were given free access to food and water, and CCl_4 dosing was titrated by twice weekly weighing of the animals. All procedures were carried out within Home Office guidelines and with appropriate Home Office Licence in place PPL:30/1414.

All the following data represents n=7 in each group, with the exception of 150,000U IFN-α where n=6.

5.3 PHYSIOLOGICAL MEASUREMENTS

5.3.1 Weight

Rats were grouped initially through their weight at the start of the study. The groups were chosen with the aim of minimising the initial difference in start weight. Therefore the rats were grouped to ensure that the mean weight of each group was within 10g of any other. Throughout the study, the weights were monitored on a twice weekly basis. An initial drop in weight occurred with the start of the carbon tetrachloride treatment, but at week two the weight of the rats started to increase again, and continued to do so throughout the

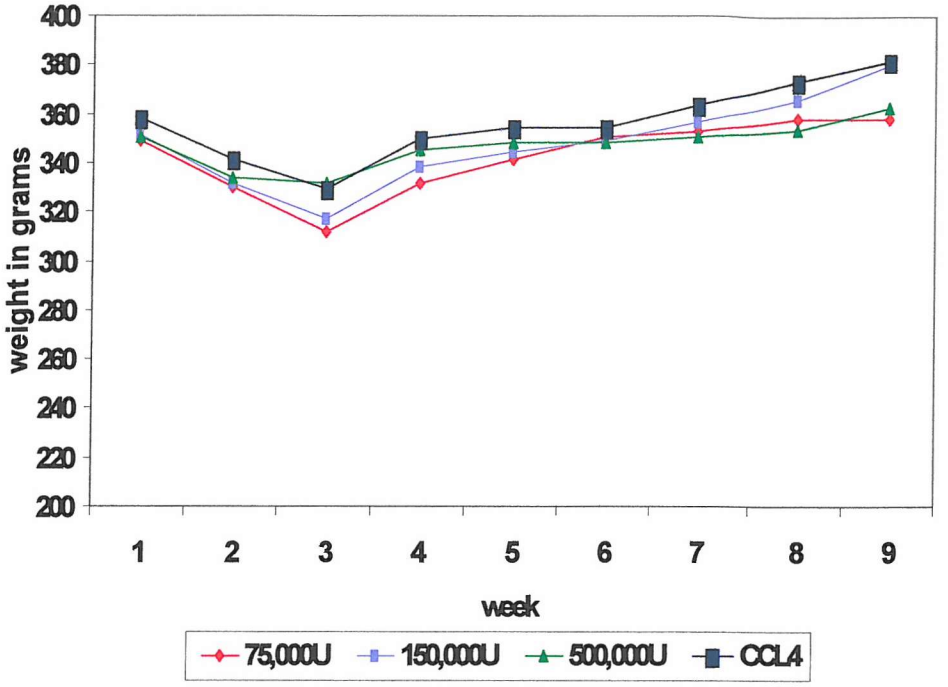

Figure 5-1 Graph of weight gain throughout the 8 weeks of the study.
Each group was weighed at the start of the week, and the mean weight plotted. The initial weight loss was expected due to the start of the CCL_4 injections.

rest of the study. No significant difference in weight gain was found between the groups, either before or during IFN-α A/D treatment (Figure 5-1).

5.3.2 Liver function tests

At the end of the 8 week treatment period, rats were euthanised and relevant tissue harvested. Following harvesting the rats at week 8, heart puncture was performed to remove a sample of serum. Liver function tests of ALT and AST were analyzed, as these are commonly used as markers of liver fibrosis. ALT and AST are released into the blood from the damaged hepatocytes, however AST can also be an indicator of muscle and heart cell damage. Neither AST or ALT levels demonstrated a statistically significant difference when the IFN-α A/D treated groups were compared with the control group (CCl_4 only group) as shown in Figure 5-2 and Figure 5-3.

Figure 5-2 Graph showing the levels of ALT between groups.
ALT levels were assessed between the four groups, control and the three dosed groups. Whilst the ALT levels were marginally higher in the IFN-α A/D treated groups as compared with CCL_4 only, this was not statistically significant.

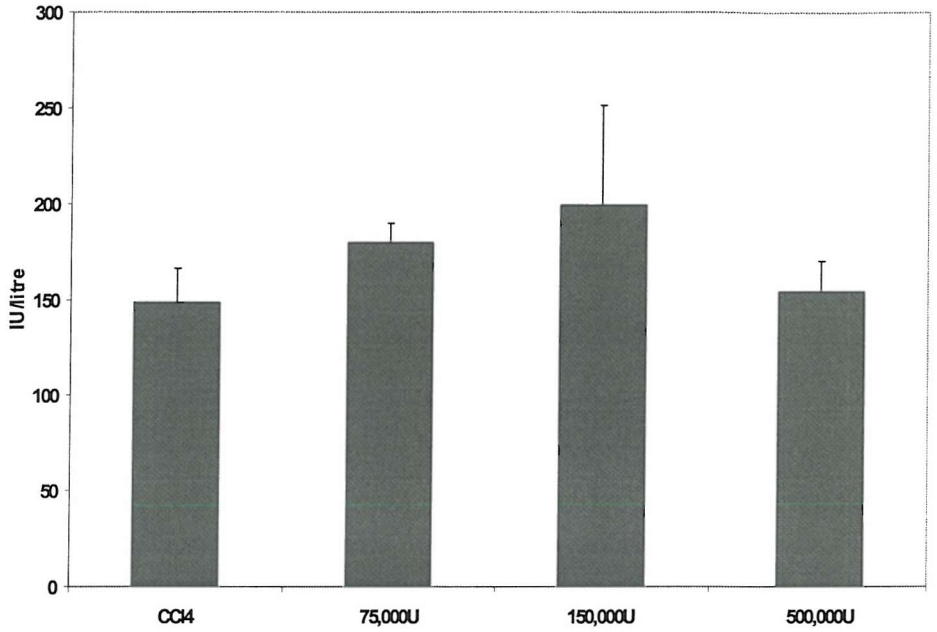

Figure 5-3 Graph showing the levels of AST between groups.
AST levels were also compared between CCL_4 only and the three IFN-α A/D treated groups. AST levels were also higher in the IFN-α A/D treated groups as compared with CCL4 only, however, again this was not statistically significant.

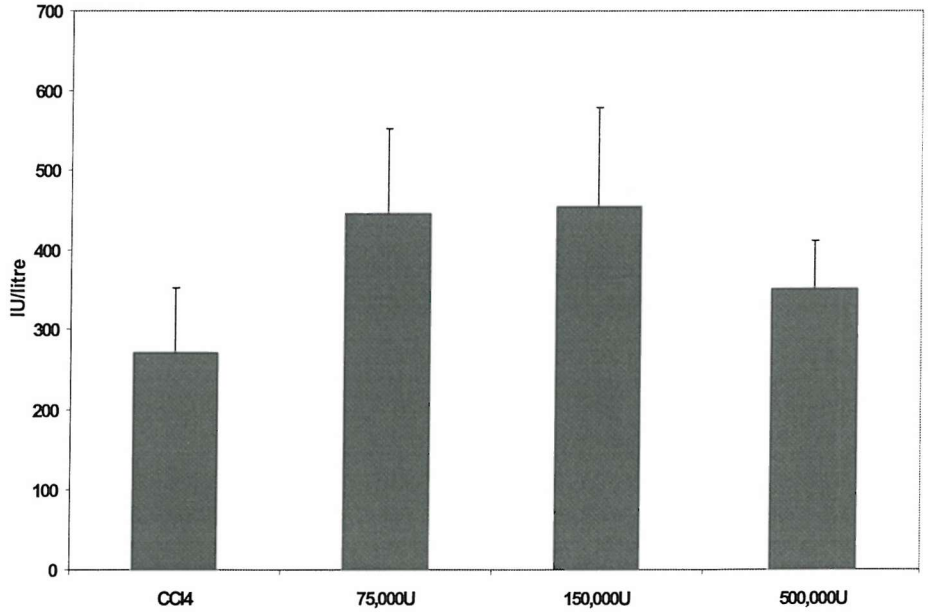

5.3.3 Ascites

At harvesting, ascites was also measured by draining from the peritoneal cavity, and measured using 5ml syringes. Commonly, with an increase in fibrosis, an increase in ascites would be also expected. In this analysis, both the 75,000U group and the 500,000U group had substantially less ascites than the CCl_4 only group, whereas the 150,000U group showed no decrease (Figure 5-4). However, in this group one animal had 11ml ascites skewing the group average. If this animal is excluded the group average is 0.9ml, analogous with the other two IFN-α A/D treated groups (0.82ml, 75,000U and 0.71ml, 500,000U). It should be noted that this animal also had a substantially enlarged spleen when compared to the rest of the group (5.3.6).

Figure 5-4 Graph showing the levels of ascites between groups.
Ascites levels were lower in the IFN-α A/D treated groups as compared with CCL4 only. However, as shown the average for the 150,000U group is in fact higher due to one animal which had 11mls ascites, thus skewing the data. Average for 150,000U without that animal was 0.9ml. None of the data was statistically significant.

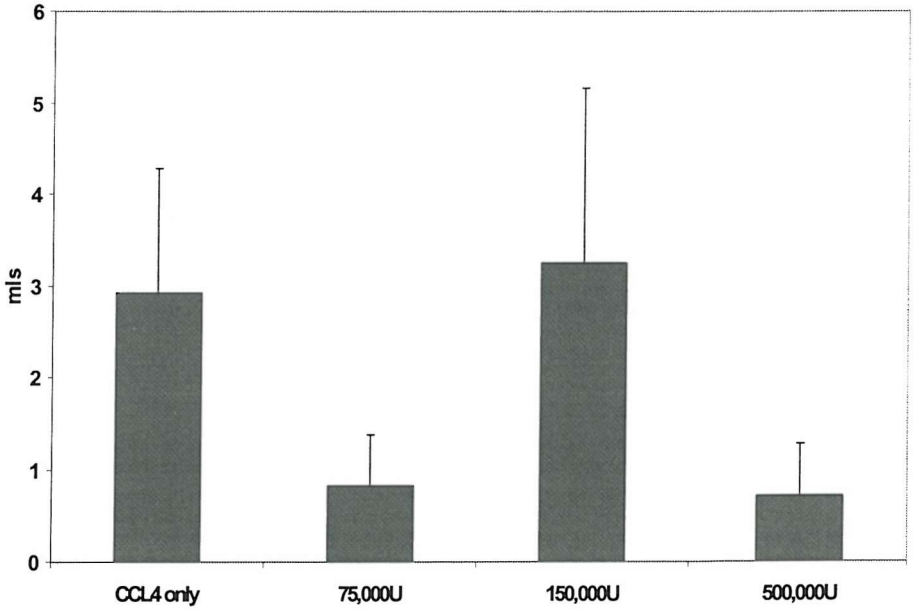

5.3.4 Clinical score

During the final week of the study it was noticed that the health of the rats appeared to be declining. To assess a large group of animals satisfactorily a clinical score was devised to enable monitoring of individuals in addition to the four groups within the study. This score was based on the clinical symptoms listed by the Home Office as indicators of ill-health within rodents (Table 5-1). The presence of each symptom scored 1 point, with the exception of ascites which was allocated 2 points due to its clinical importance in liver fibrosis. A second score was also devised to assess animal health based on ascites only (Table 5-2). This additionally allowed the two scores to be compared to see correlation between animal health based on all available markers and animal health based on ascites only, a marker strongly associated to liver fibrosis. The animals were scored for the remaining 4 days of the study, for each of the above methods of scoring. As shown in Figure 5-5 and Figure 5-6 the difference between groups using both scores was not substantial. There did appear to be a strong correlation between both methods. Nevertheless, the original aim was to complete a 10wk study CCl_4 induced liver fibrosis, with 4wks of IFN-α treatment but it became apparent that the rat's health was rapidly declining and therefore the trial was finished at 8wks.

Table 5-1 Table to show the symptoms scored for in the trial

SYMPTOM	*DESCRIPTION*
Ascites	*Swollen whole body with fluid which can clearly be seen or felt in the body mass*
Swollen stomach	*Onset of ascites, swelling in the stomach area only*
Spine outline visible	*The outline of the spine visible by looking at the rat*
"Staring" coat	*The coat sticking up and giving an ungroomed appearance*
Hunched posture	*The animal sits in a hunched posture while in cage, associated with pain*
Diarrhoea	*Diarrhoea observed around the animals rear*
Red eye	*A red outline to the eye*
Weight loss	*Weight loss*
Swollen testes	*Likely to be early ascites, found in this trial without swollen stomach or ascites*

Table 5-2 Table to show scoring based on ascites only

GRADE	DESCRIPTION
1	*No ascites*
2	*Negligible ascites*
3	*Moderate ascites – stomach as wide as hips*
4	*Ascites – stomach round "football tummy" or spine visible*
5	*Severe ascites – both "football tummy" and spine visible*

Figure 5-5 Graph showing the scores of each of the four groups on the penultimate day of the trial.
Using the general markers of health as described in Table 5.1, each animal was scored individually and the scores from each group averaged. No significant difference was found.

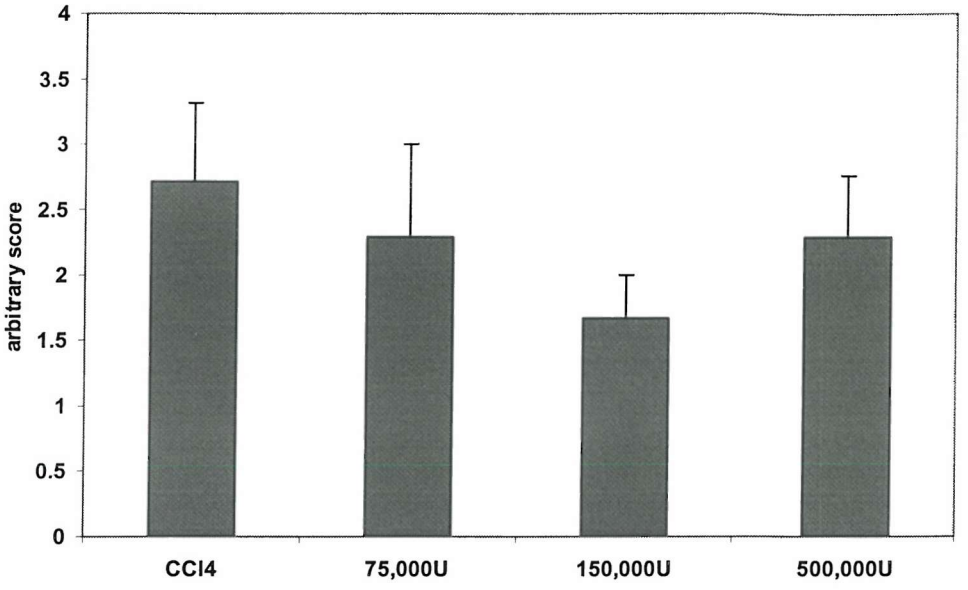

Figure 5-6 Graph showing the scores of each of the four groups on the penultimate day of the trial, based on ascites.
Using the ascites grading as described in Table 5.2, each animal was scored individually and the scores from each group averaged. No significant difference was found.

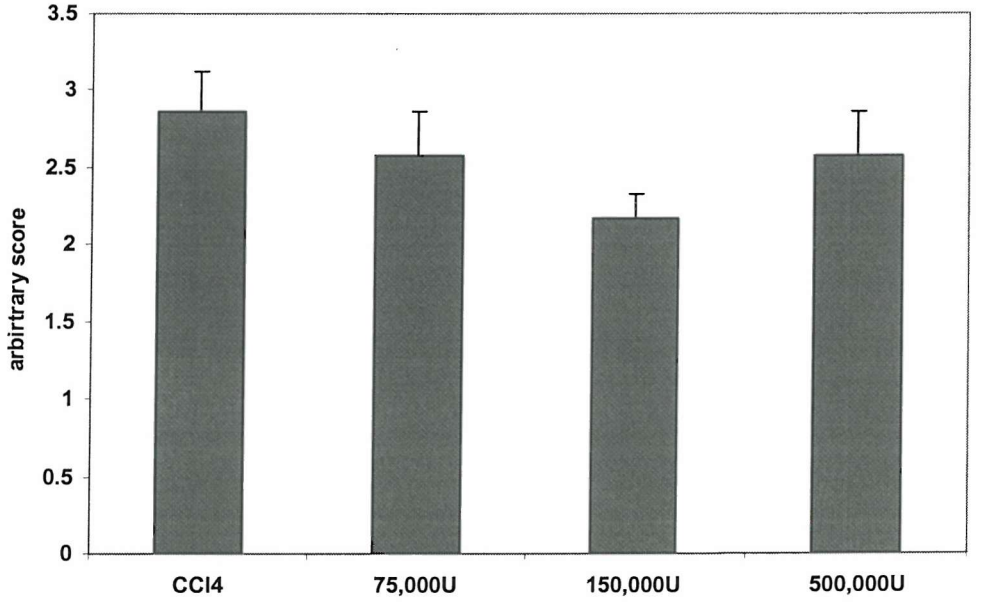

5.3.5 Portal hypertension

To provide an index to quantify portal vein hypertension the diameter of the portal vein was measured during dissection. No significant change was found between the different groups although the IFN-α A/D treated groups were on average higher than the CCL_4 only group.

Figure 5-7 Graph showing the average diameter of the portal vein.
Portal vein diameter was measured during dissection. No significant difference was found between the groups.

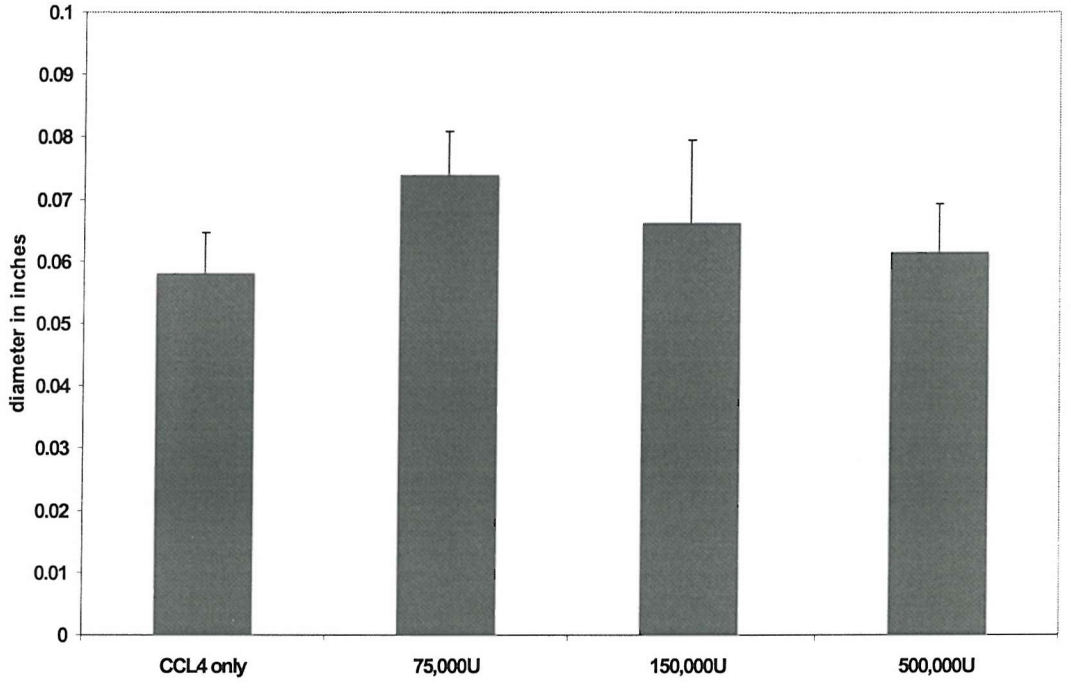

5.3.6 Weight of the Spleen

Portal hypertension can result in enlargement of the spleen. This occurs because the splenic vein enters directly into the portal vein and therefore becomes congested as portal pressure increases. To act as a surrogate marker of portal hypertension the weight of the spleen determined. After calculation of mean spleen weight no significant change was found between the groups. The largest error bars being within

the 150,000U group where one animal had an enlarged spleen, twice the size of the rest of the group.

Figure 5-8 Graph showing the average weight of the spleen.
Wet weight of the spleen was measured immediately following dissection to help assess any portal hypertension

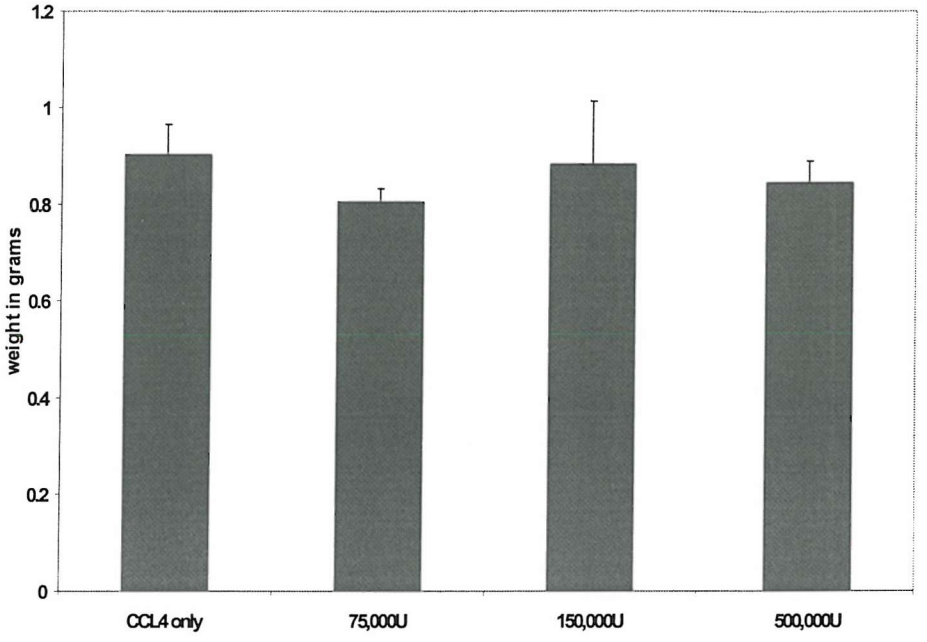

5.3.7 Western blotting for albumin.

Ascites forms because of restriction in portal blood flow, increased portal pressure and changes in Starling's forces across the capillary beds. Albumin may be reduced in liver fibrosis and forms the major component of the capillary oncotic pressure. To further determine the mechanism underlying the difference found in ascites between the treated and untreated groups, serum albumin levels were assessed. Downregulation was found in three out of seven animals that had no IFN-α treatment as compared to the treated groups. This suggests that maintenance of albumin levels did not account for the reduction of ascites.

Figure 5-9 Western blot of the 500,000U IFN-α group and the CCl_4 only group.
Two of the animals in the CCl_4 only group show a clear reduction in the level of albumin when compared to the 5000,000U IFN-α A/D group. However, as can be seen there is otherwise no difference between the two groups in the levels of albumin.

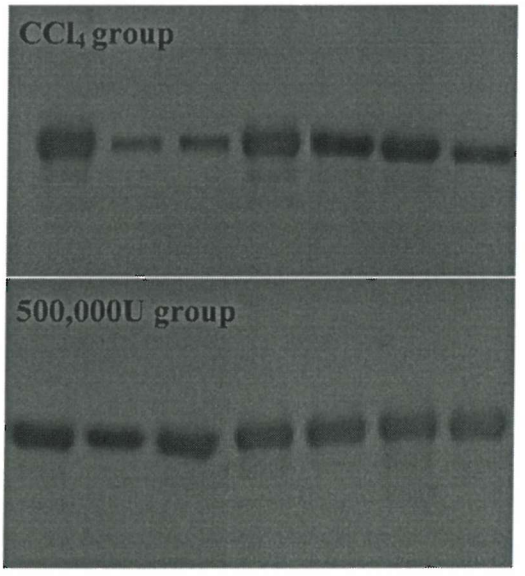

5.3.8 Weight of the liver

Liver weight was also recorded, and shows an average increase in liver weight in response to treatment with IFN-α A/D. However, the error bars within the groups are large and therefore no significance was found (Figure 5-10).

Figure 5-10 Graph showing the weight of the liver (wet weight) in each group.
The wet weight of the liver was also recorded following dissection. There is negligible difference in liver weights between the four groups.

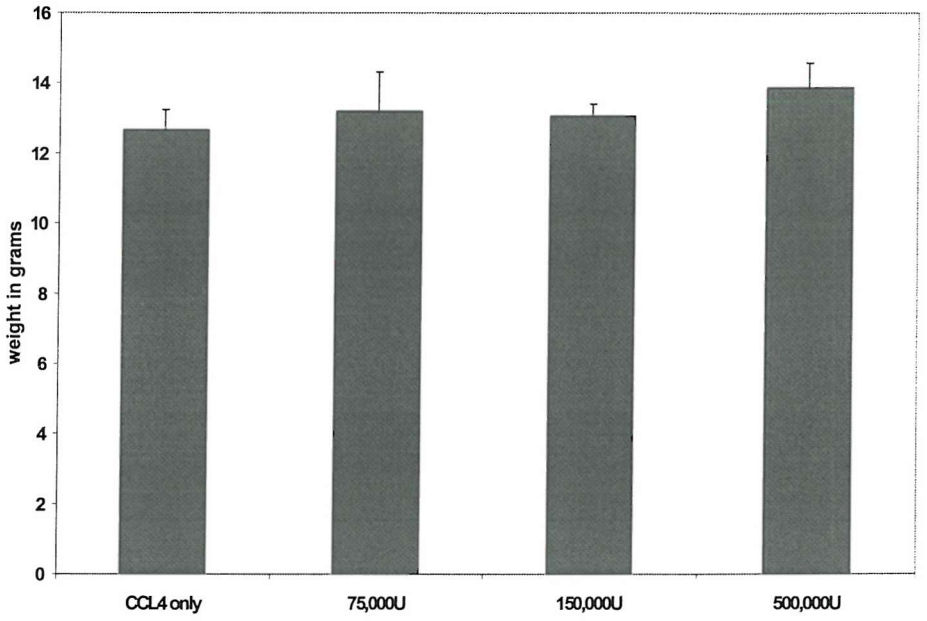

5.4 ANALYSIS OF THE FIBROSIS IN THE LIVER

For the initial analysis of fibrosis within the liver, a lobe was removed, divided and placed in 10% buffered paraformaldehyde solution and embedded in paraffin. Sections were then cut, and stained in picrosirius red solution. All histological scoring were performed blind, identities of the animals and the treatment they had received was unknown to the pathologist who scored the sections.

Sections were scored using a method developed by Kerry Thompson 1997 PhD.

Table 5-3 Scoring system for liver fibrosis sections stained with sirius red.

Score	Criteria required in the section
0	No sign of fibrosis
1	Thin bands of fibrosis
2	Thin bands of fibrosis, joining hepatic veins
3	Thick bands of fibrosis, hepatic veins joining and forming nodules

Figure 5-11 Slides of Sirius red stained sections showing scores 1 to 4.
These are representative sections demonstrating the scores as outlined in Table 5-3.

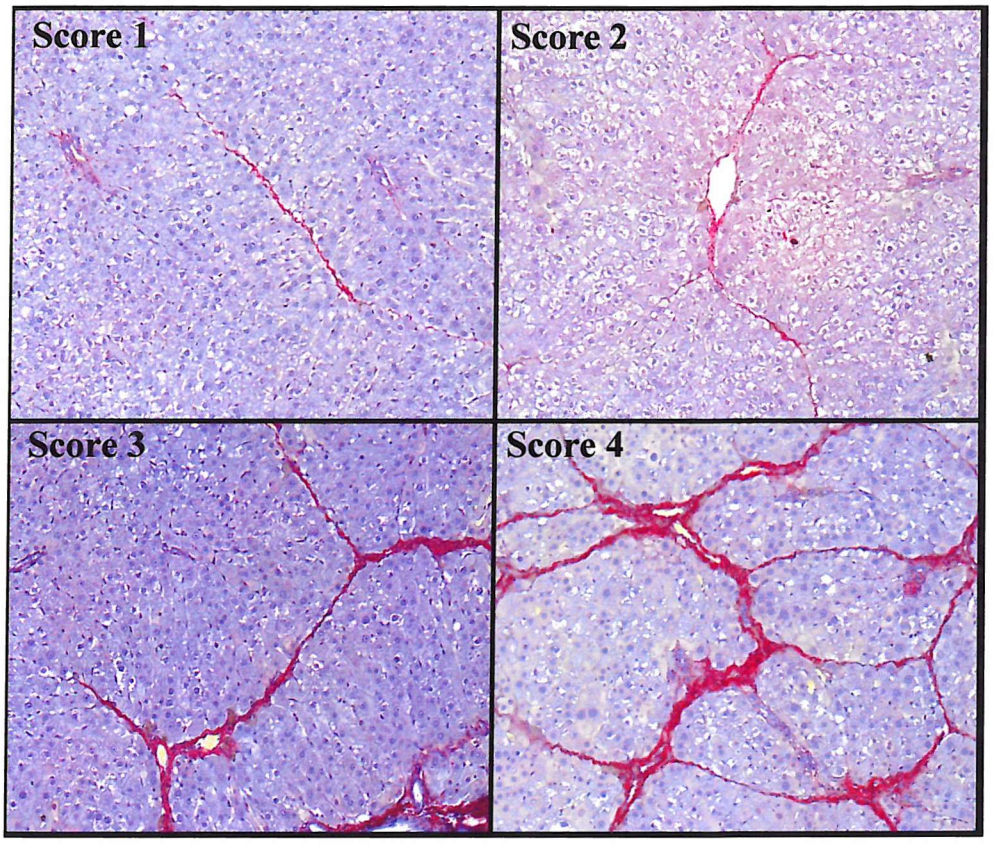

In both the lower doses of the IFN-α A/D treatment, 75,000U and 150,000U, no difference in the level of fibrosis could be found. However, at 500,000U IFN-α A/D there was a decrease in fibrosis, confirmed statistically with the student's T-test ($p=0.011$).

Figure 5-12 Graph showing the mean fibrosis score for the four groups of rats studied.

In each group n=7, except for 150,000U where n=6. Only at 500,000U IFN-α A/D was any statistically significant difference using the student's T-test (p=0.011) as shown with the asterisk.

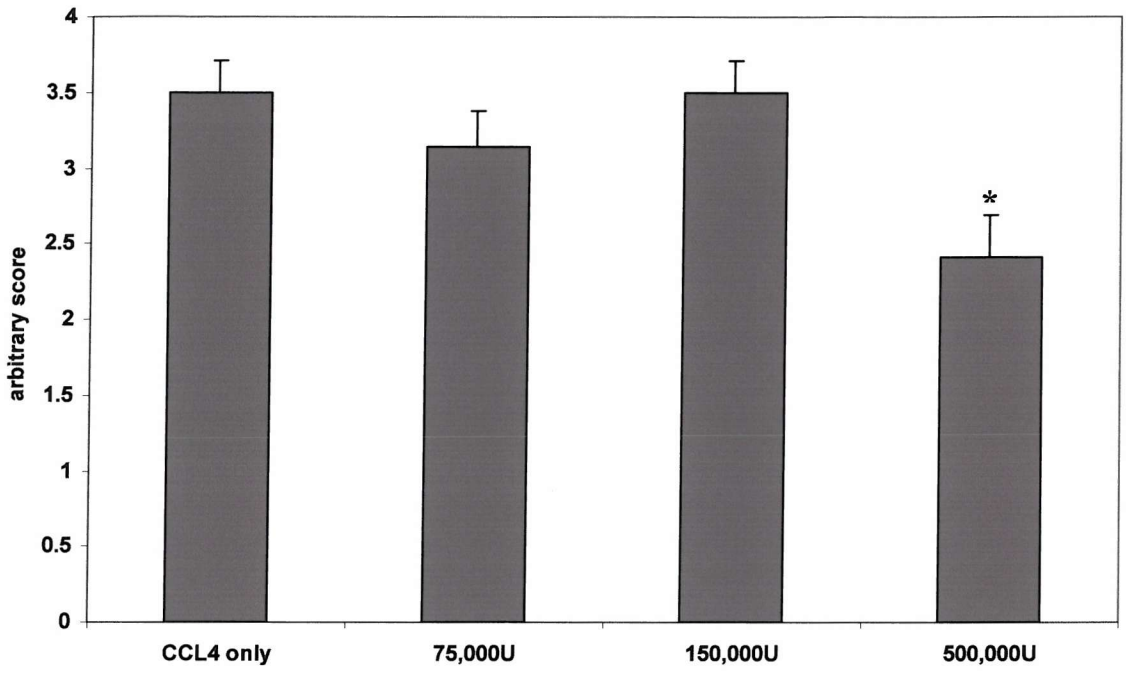

Figure 5-13 Typical sections from the CCl_4 only group (left) and the 500,000U IFN-α A/D (right)

These sections were chosen as they represent the average of each of the groups. Therefore, samples within each group were above and below these shown.

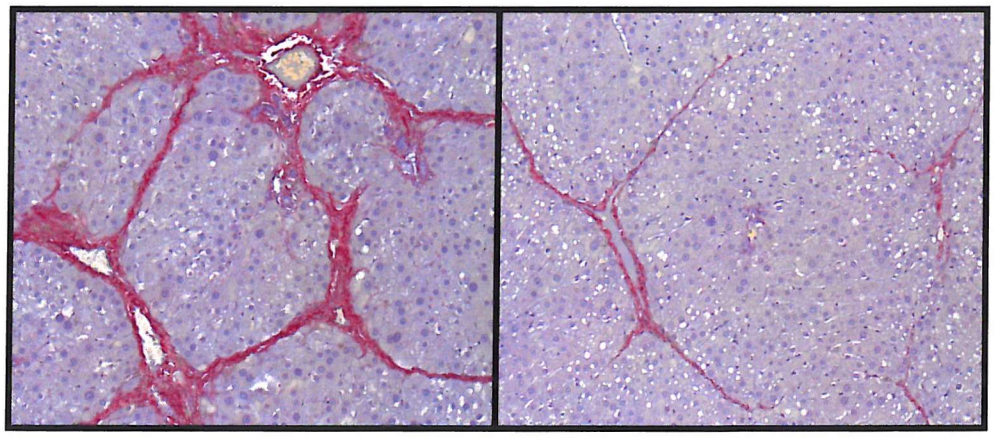

5.5 α-SMA CONTENT

5.5.1 Histological staining

Staining for α-SMA was also carried out as a marker for the activated stellate cells. This was first analyzed using a scoring method developed by Dr. H. Sadler and Dr. C. Constandinou. Scoring was ascertained according to the criteria below:

Percentage of α-SMA positive broad bands within the section

Percentage of α-SMA positive cells within the broad bands

Percentage of α-SMA positive fine bands within the section

Percentage of α-SMA positive sinusoidal staining within the section

Each criterion was scored using the same scoring system:

Score	Percentage positive staining
1	0-25%
2	25-50%
3	50-75%
4	75-100%

Using this method, a decrease was found with the IFN-α groups, but this was not statistically significant (Figure 5-14). To confirm this result, α-SMA positive cells were counted in 20 random x40 magnification views. This method of counting confirmed the previous results (Figure 5-15). In both sets of data within each of the IFN-α treated groups one or two rats had particularly high scores as compared to the rest of their group. This then produced large error bars, however in the IFN-α untreated group the scores were very similar and thus gave smaller error bars. This is more clearly seen in the scatter graphs of the data, Figure 5-16 and Figure 5-17.

Therefore within a group of treated animals, most had a pronounced improvement with only one or two with none. In contrast, those animals not treated had closely comparable disease progression. This effect is also seen within human studies, where within a treatment group some patients respond well and others show no effect as compared to untreated patients whose progression of the disease remain very similar.

Figure 5-14 Graph showing the mean score for α-SMA staining throughout the model.
A decrease in α-SMA staining was found, but this was not statistically significant.

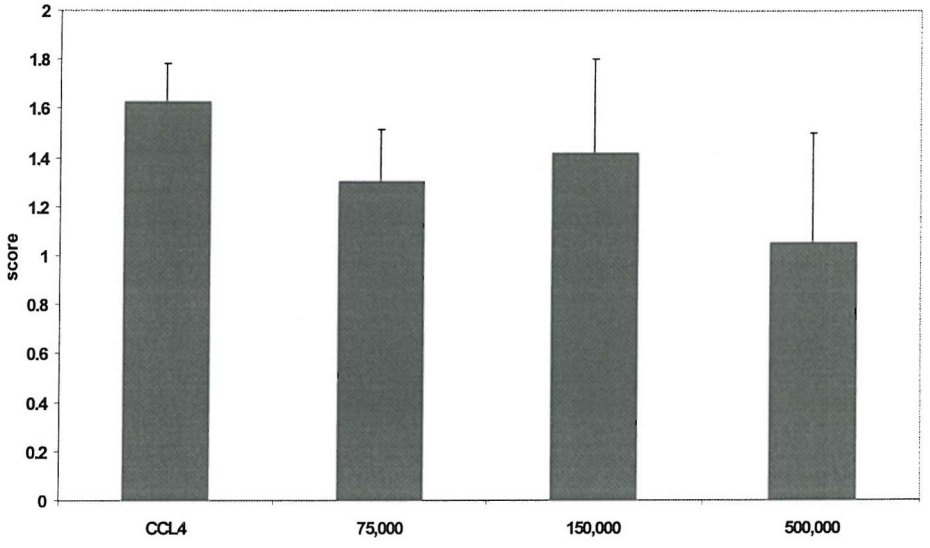

Figure 5-15 Graph showing the average cell count per x40 view.
As found before, there was a trend of a decrease in the number of α-SMA positive cells, but was not statistically significant.

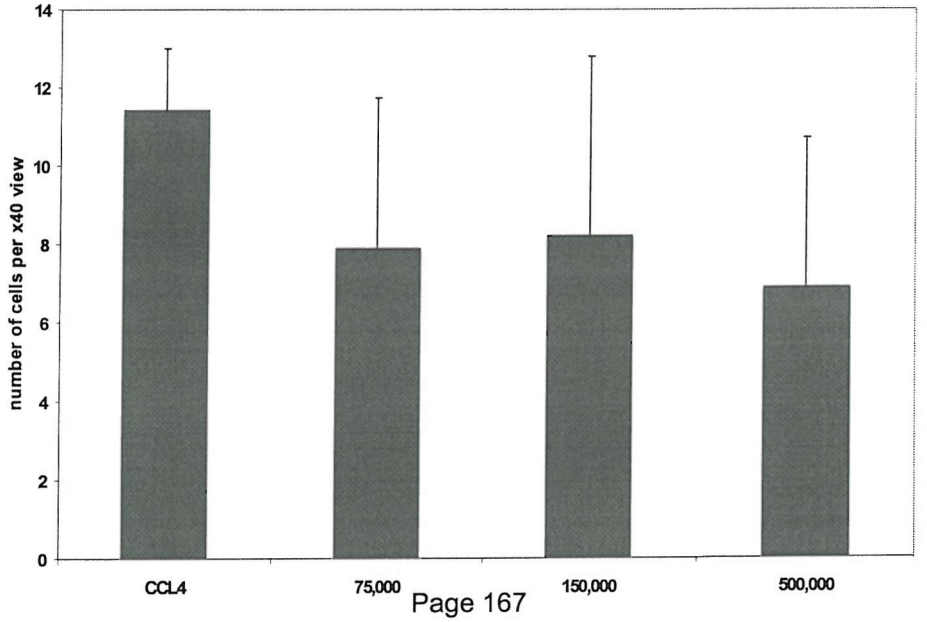

Figure 5-16 Scatter graph showing the distribution of scores for α-SMA staining throughout the groups.

This scatter graph demonstrates the variation within each group, and shows clearly the increasing group deviance with the increasing dose of IFN-α (data fromFigure 5-14).

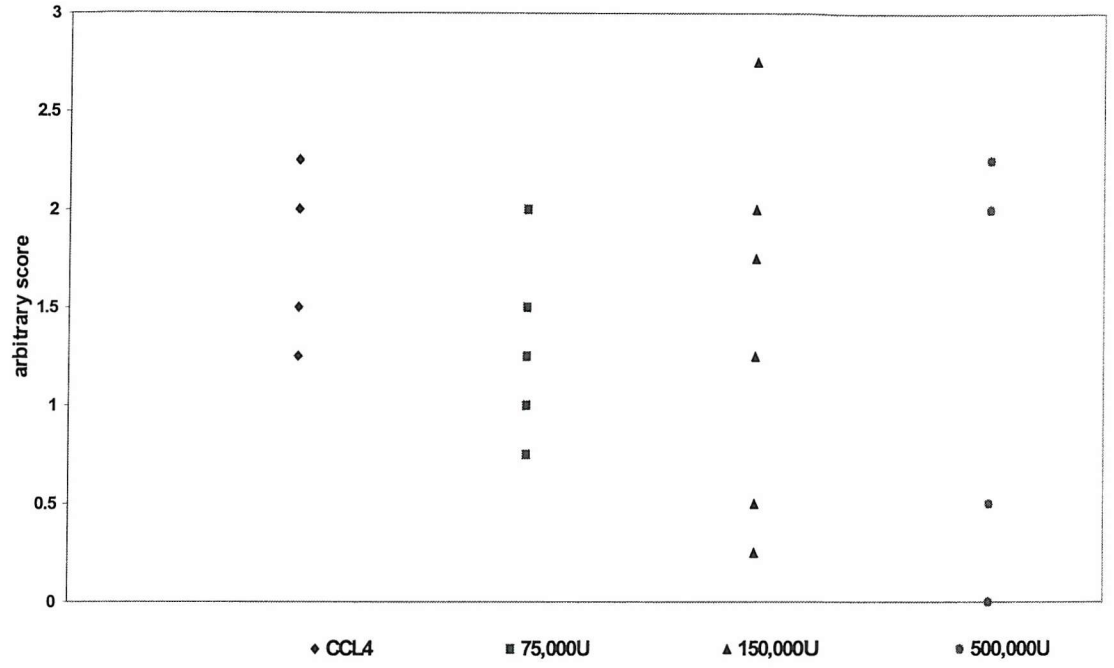

Figure 5-17 Scatter graph showing the distribution within the α-SMA positive cell count data throughout the groups.

This scatter graph also demonstrates the variation within each group, and again shows the increasing group deviance with the increasing dose of IFN-α (data fromFigure 5-15).

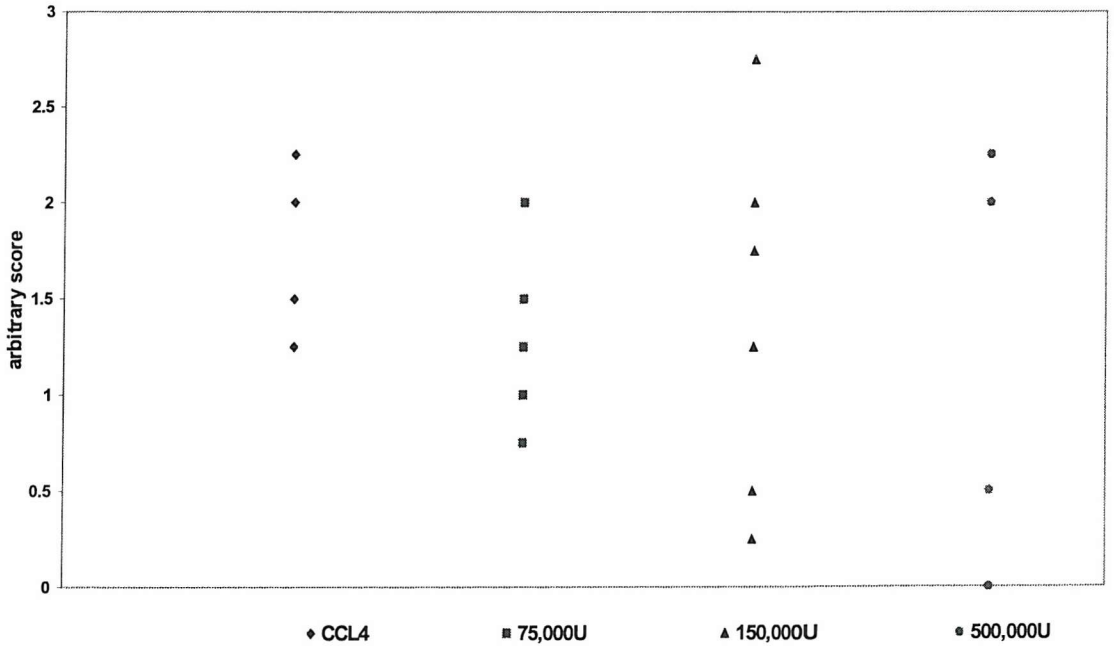

5.5.2 Western blotting for α-SMA

To further elucidate any regulation by IFN-α of α-SMA, the α-SMA protein was analysed by western blotting. Each animal from the four treatment groups was analysed. Once again, whilst a reduction in α-SMA can be seen in the IFN-α treated groups, the reduction is not dramatic and α-SMA is not lost entirely. The 500,000U group does show a clear reduction in five of seven IFN-α treated livers as compared to the CCl_4 only group. A decrease in α-SMA is also seen within the 75,000U group, but remarkably there appears to be little decrease in the 150,000U group. All the western blots were loaded equally for protein and the same batch of antibodies used. However, the variation within a group of animals is clearly seen here.

Figure 5-18 Western blot for α-SMA, showing all four groups.
Protein extracted from liver homogenates of each rat were used to in western blotting for α-SMA. Each group is shown together. The 500,000U group shows a clear reduction in α-SMA as compared to the control group. Some reduction can also be seen in the 75,000U group, but there is little difference in the 150,000U group.

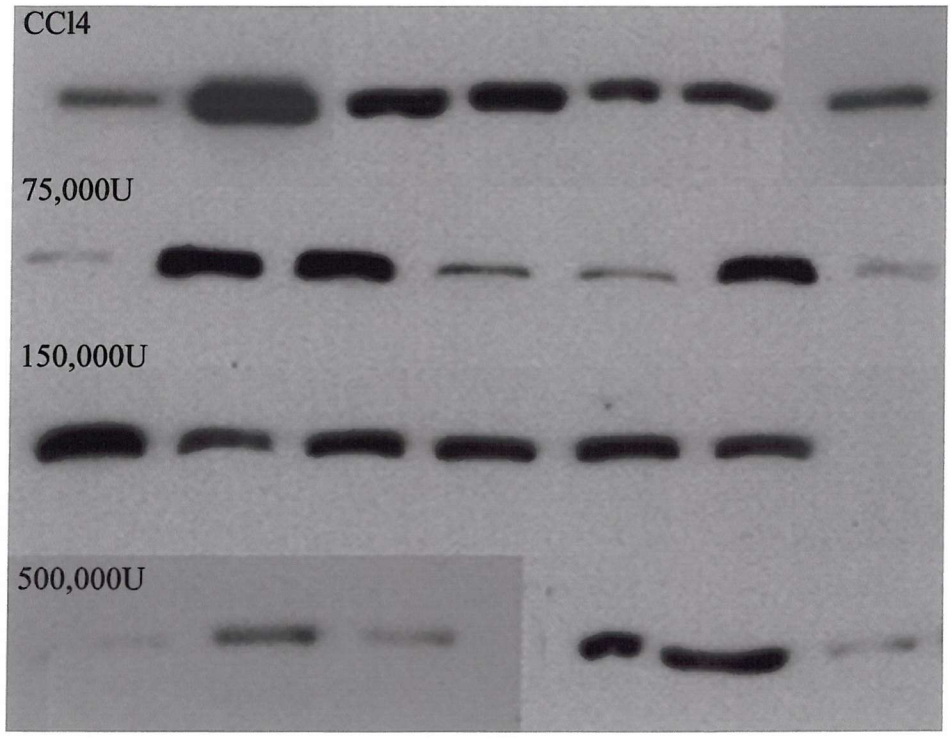

5.6 COLLAGEN CONTENT OF THE LIVER

5.6.1 Hydroxyproline assay

To assess the amount of collagen within the liver, a hydroxyproline assay was used. This assay measures hydroxyproline, which constitutes approximately 15% of the amino acids within collagen. Therefore, hydroxyproline content can be used as a surrogate measurement for collagen.

Liver was used from each animal in the group, and the final content averaged. A standard curve was also run, and the equation from this was used to allow an accurate reading of the collagen amount.

No difference was found in the lower dosed groups, 75,000U and 150,000U, but at 500,000U significance was almost achieved at p=0.057. These results do however correspond with the Sirius red staining data (5.4). Sirius red, as already mentioned, stains for the cationic groups in the collagen.

Figure 5-19 Graph showing the quantity of hydroxyproline found in each group.

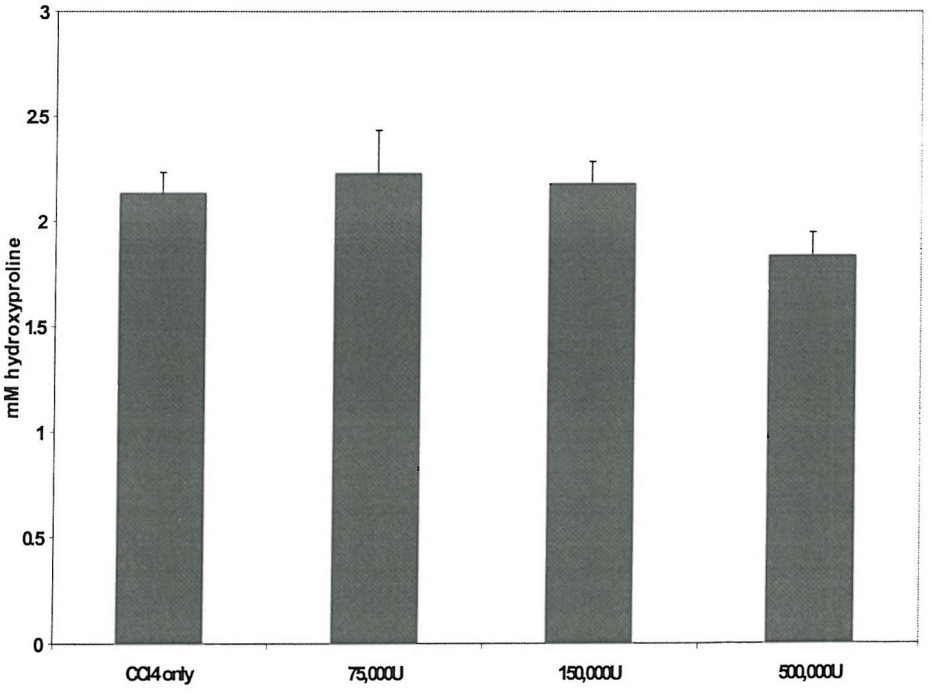

5.6.2 Collagen mRNA

Collagen was also assessed using TaqMan® Realtime Quantitative PCR. As previously described (2.7) the primers and probes were used according instructions supplied by Applied Biosystems. Frozen liver was homogenised in cold (4°C) GIT lysate to lyse the cells. The mRNA was extracted and a portion was run on an integrity gel to check for any degradation of the RNA. RT-PCR was performed at previously stated to yield cDNA. The cDNA was then used in the TaqMan® Realtime Quantitative PCR reaction.

As shown in Figure 5-20 there appears to be a drop in collagen mRNA levels is demonstrated with two lowest levels IFN-α treatment, 75,000U and 150,000U, whereas at 500,000U an increase is found. On closer analysis of the data, two rats within this group were found to have higher levels of collagen mRNA than the remainder of the group. This has then distorted the data presented below. Nonetheless, the only statistically significant result was from the 150,000U group ($p=0.005949$).

Figure 5-20 Graph showing the effects of IFN-α A/D therapy on collagen mRNA levels in the whole liver.
cDNA from each animal was analyzed for collagen and each group averaged. Due to the large error bars statistical significance was only founding the 150,000U group. However, the 500,000U group, whilst lower than control, demonstrated an increase compared to the lower dosage groups.

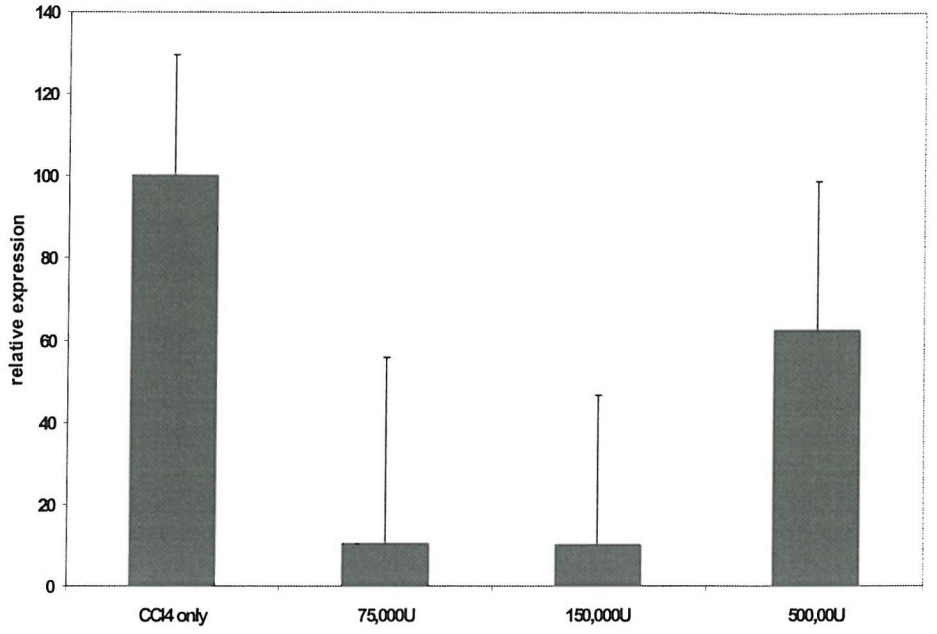

5.7 MMPS IN THE LIVER

5.7.1 Zymography

The MMPs Gelatinase A and Gelatinase B (MMP-2 and MMP-9) were studied using zymography of harvested liver homogenates. Frozen liver samples were homogenized in protein lysis buffer. The samples were then run on an SDS-PAGE gel and stained with Coomassie Blue to check that the protein was not degraded. The protein was measured using the BCA assay, and the samples were loaded equally onto the zymography gel.

As shown in Figure 5-21 there is a clear downregulation of the gelatinases in the IFN-α treated groups, most clearly seen in the 500,000U IFN-α A/D group. Both the pre-

and active forms of MMP-2 decrease as the IFN-α increases. The active form of MMP-2 is undetectable in the 500,000U group. A greater difference is found with MMP-9, where this is found in half the lanes of both the CCl_4 only and 75,000U IFN-α groups. However, it is not found at all within the 150,000U group and in only one lane of the 500,000U group.

Figure 5-21 Zymography gels showing all four groups from the model.
At the top is the CCl_4 only group below which are representative gels from each treatment group defined according to the dose of IFN-α. The CCl_4 only group has more MMP-2, both pre- and active forms, than is found in the IFN-α treated groups. This is most clearly seen in the 500,000U treated group. There is also a decrease in MMP-9 in each of the IFN-α treated groups, and in the 500,000U treated group only one lane contains MMP-9.

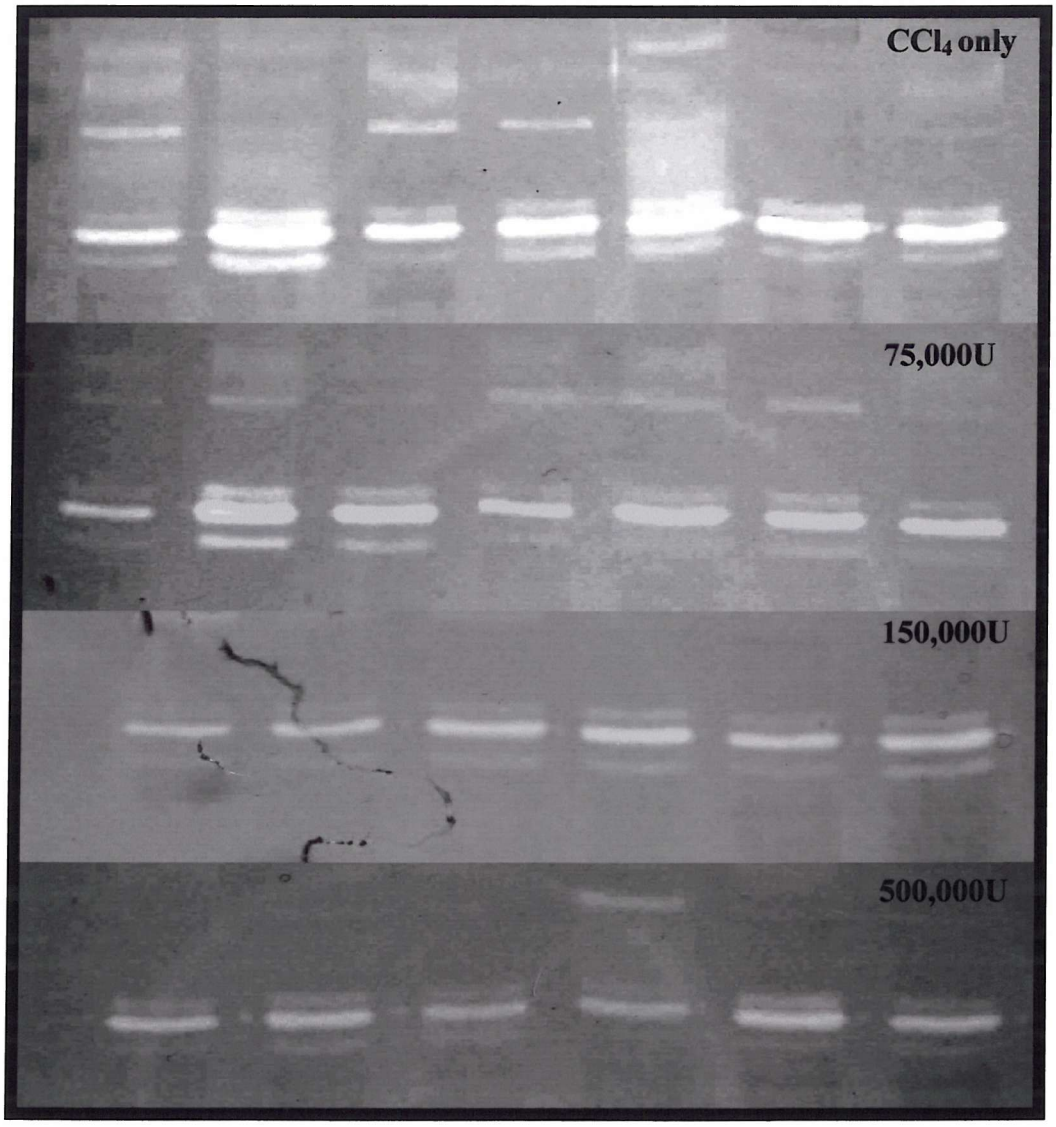

5.7.2 Collagenolytic assay

To further examine the MMPs following IFN-α A/D treatment a collagenolytic assay was used. The ^{3}H Proline labelled collagen is added to the whole liver protein lysate and incubated, allowing the MMPs within the lysate to degrade the collagen. ^{3}H labelled Proline is measured as it is released from collagen. This assay uses whole collagen, and therefore is able to assess the activity of the interstitial collagenases which degrade whole collagen combined with gelatinase activity (which can only degrade collagen once the triple helix has been disrupted). As can be seen there was a negligible increase in collagenolytic activity in the IFN-α treated groups. Once again, significance was not achieved.

Figure 5-22 Graph showing the collagenolytic activity found within the whole liver protein lysates.
As ^{3}H Proline is released from the degraded collagen, a higher cpm relates to an increase in collagenolytic activity thus demonstrating an increase in the level of MMPs. Little difference was found between the four groups, although the IFN-α treated groups all showed a trend marginally above that of CCl_4 only group.

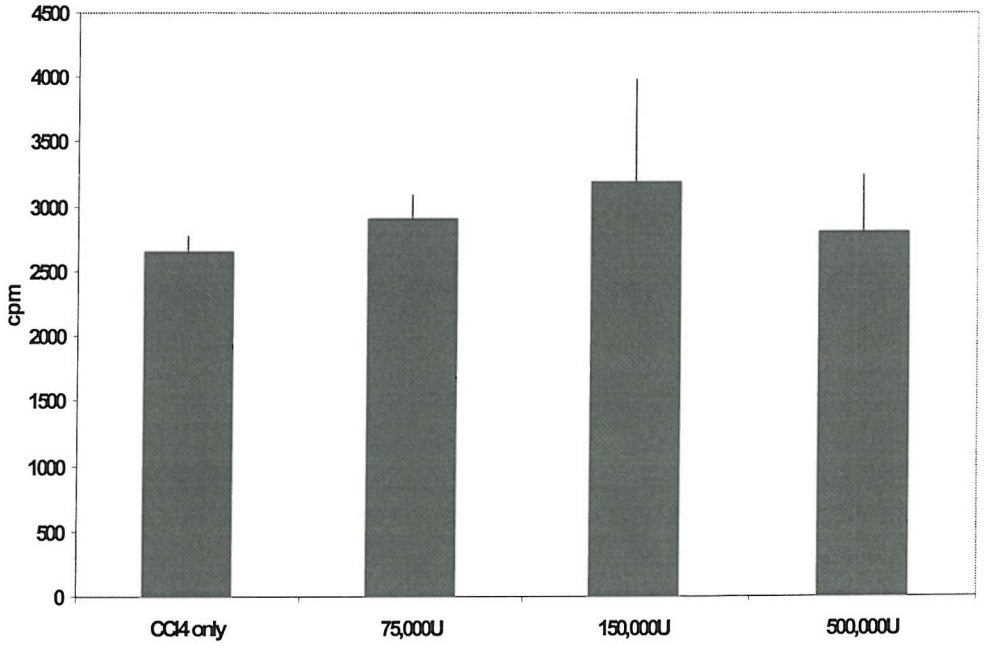

5.7.3 MMP-13 mRNA determination

MMP-13, the major rodent collagenase, was also studied at the mRNA level using TaqMan® Realtime Quantitative PCR. The cDNA was extracted as previously described in 5.6.2.

As shown in (Figure 5-23) IFN-α appears to downregulate MMP-13 mRNA. Both the 75,000U and 150,000U groups were statistically significant, p=0.003476 and p=0.000711 respectively. However, as found in the collagen TaqMan data, there is an increase in the 500,000U group with levels becoming more analogous to the levels found in the CCl_4 only group. As found previously in the mRNA levels of collagen (5.6.2) when the data was examined closely the same two animals were found to distort this data, once again having higher levels of MMP-13 than the remainder of the group.

Figure 5-23 Graph showing the response of MMP-13 to IFN-α treatment.
cDNA from each animal was analyzed for MMP-13 and each group averaged. Statistical significance was found in both 75,000U and 150,000U IFN-α, p=0.003476 and p=0.000711 respectively. However, the 500,000U group, whilst lower than control, demonstrated an increase compared to these groups. This data is highly comparable to that of the collagen mRNA levels.

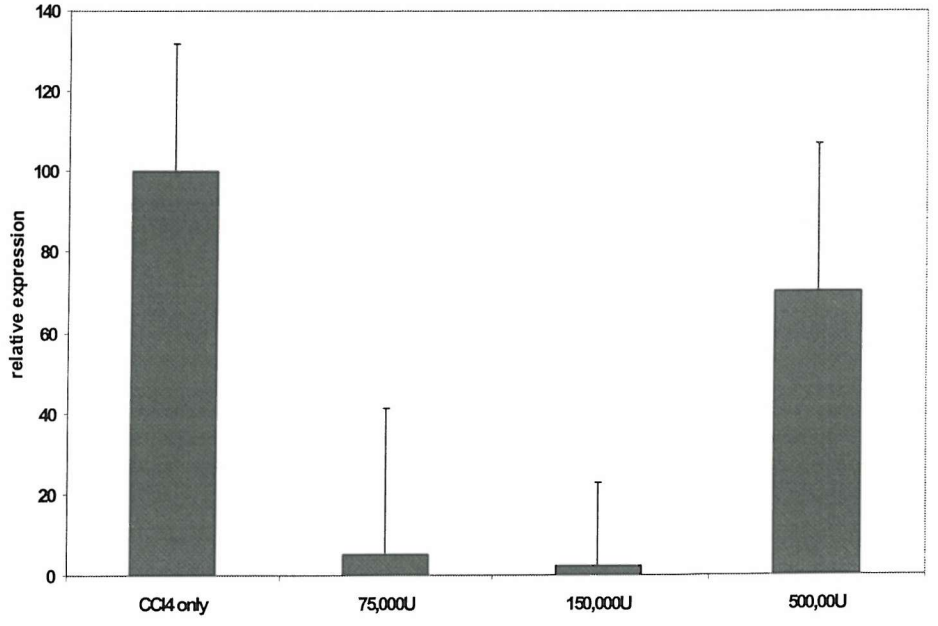

5.8 TIMP-1 mRNA

TIMP-1 mRNA was additionally examined in the whole liver with the TaqMan® Realtime Quantitative PCR using the probes and primers as described in 2.7. TIMP-1 shows a dose dependant decrease in expression, however the levels of expression between four groups was close and no statistical significance was found.

Figure 5-24 Graph showing the expression of TIMP-1 mRNA following IFN-α treatment.
cDNA from each animal was analyzed for TIMP-1 and each group averaged. Once again, due to the large error bars no statistical significance was found, but trend was clear demonstrating a decrease in TIMP-1 with an increase in the dose of IFN-α.

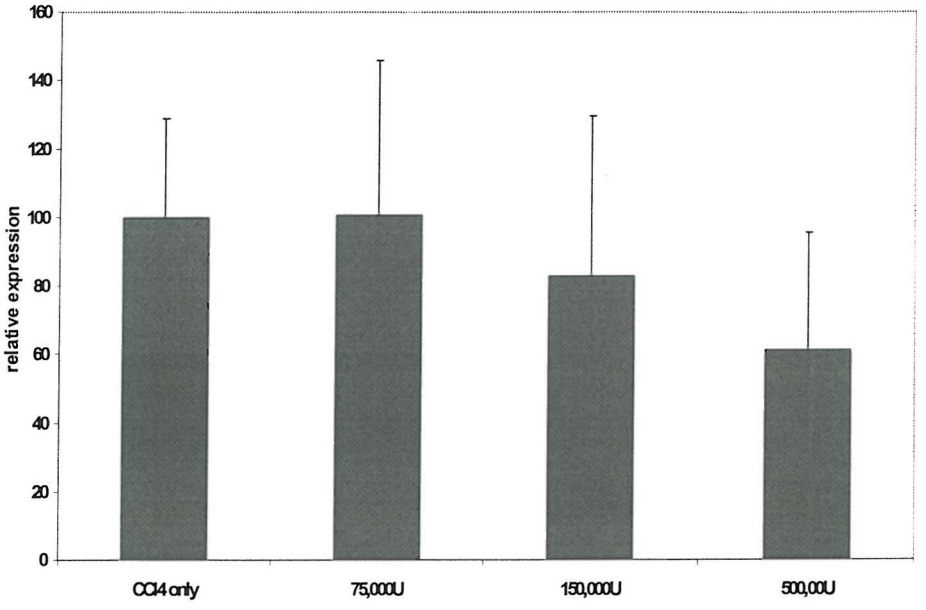

5.9 EXPRESSION OF AN IFN-α REGULATED PROTEIN IN THE WHOLE LIVER

As previously shown, following IFN-α treatment, the IFN-α regulated protein 2'5'-oligoadenylate synthetase is upregulated in response to IFN-α treatment. Therefore, 2'5'-oligoadenylate synthetase was also examined in the whole liver to assess whether in the diseased situation a response to IFN-α is still found.

As shown in Figure 5-25, no change is found in 2'5'-oligoadenylate synthetase expression between the groups.

Figure 5-25 Graph showing the response of the IFN-α regulated protein 2'5'-oligoadenylate synthetase to IFN-α treatment in the whole liver.
No change in mRNA levels was found.

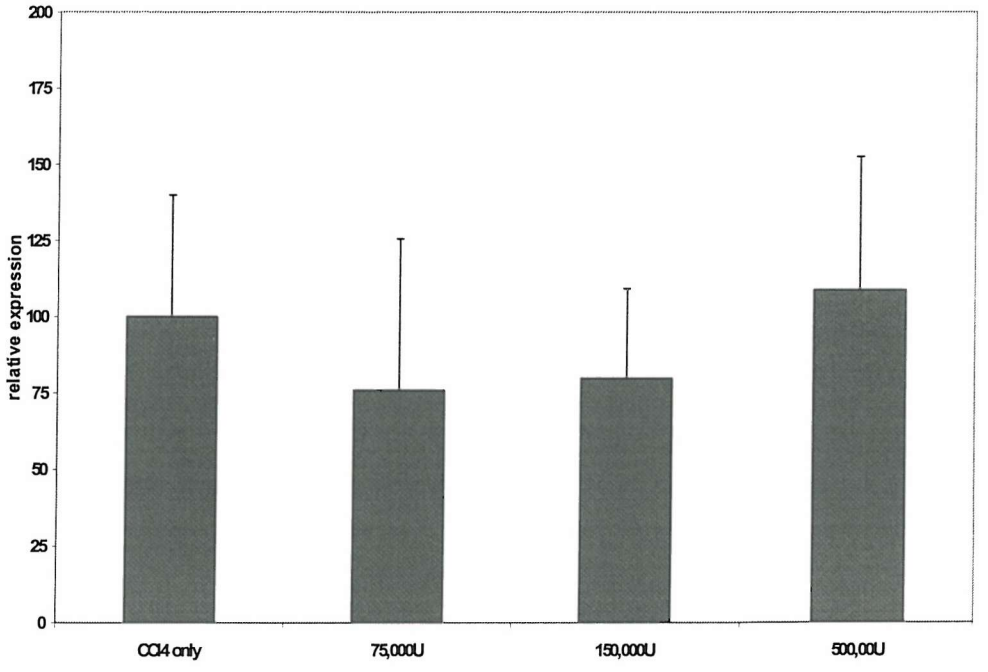

5.10 INFLAMMATION WITHIN THE LIVER

Inflammation was studied in representative sections for each harvested liver using histological stains for different components of the inflammatory system. These were used to give a score to allow an overall picture of the level and nature of the inflammatory response to be represented. Sections were stained with Haematoxylin & Eosin (H & E), CD3 antibody and Dignam PAS. Staining with H & E allowed a score for general inflammation, whereas the CD3 stain gave a T-cell specific score (95% of T-cells are CD3 positive). The Dignam PAS stain allowed for a macrophage specific score to be given. As with previous scoring, the scoring was done blind by a pathologist external to the group.

No difference was found between groups in either total inflammation (Figure 5-26) or in the scoring for macrophages (Figure 5-27). However, the T-cell data showed an increase as compared to control in the 150,000U and 500,000U IFN-α treated groups (Figure 5-28) which was found to be statistically significant in the 500,000U group ($p=0.02$).

Figure 5-26 Graph showing the scoring from each group using the H&E stain.

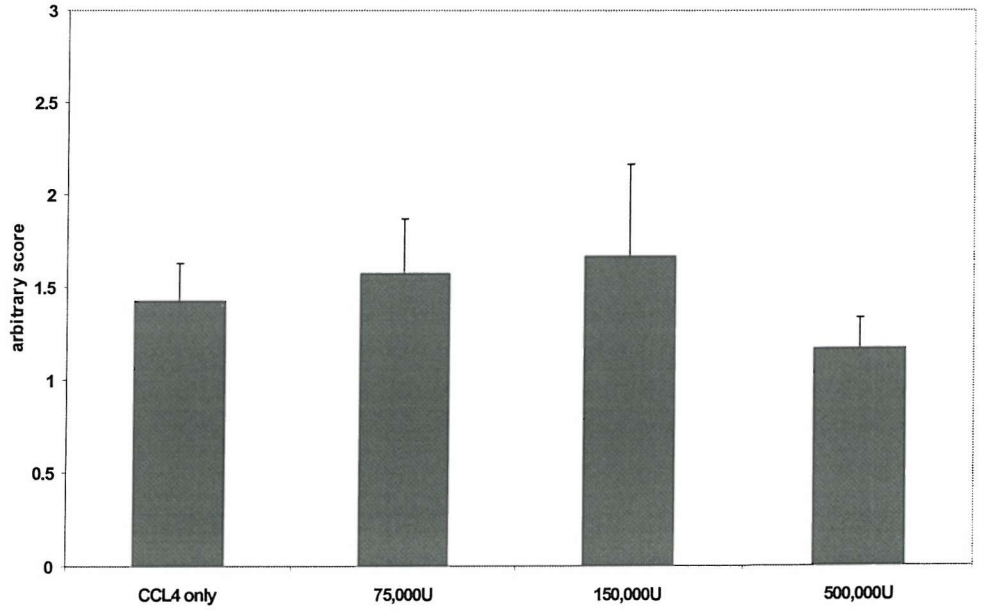

Figure 5-27 Graph showing the scoring of macrophages using Dignam PAS stain.
Slides from each animal were scored blind by a pathologist. The Dignam PAS stain was used to assess the levels of macrophages within the sections. No difference was found between the groups.

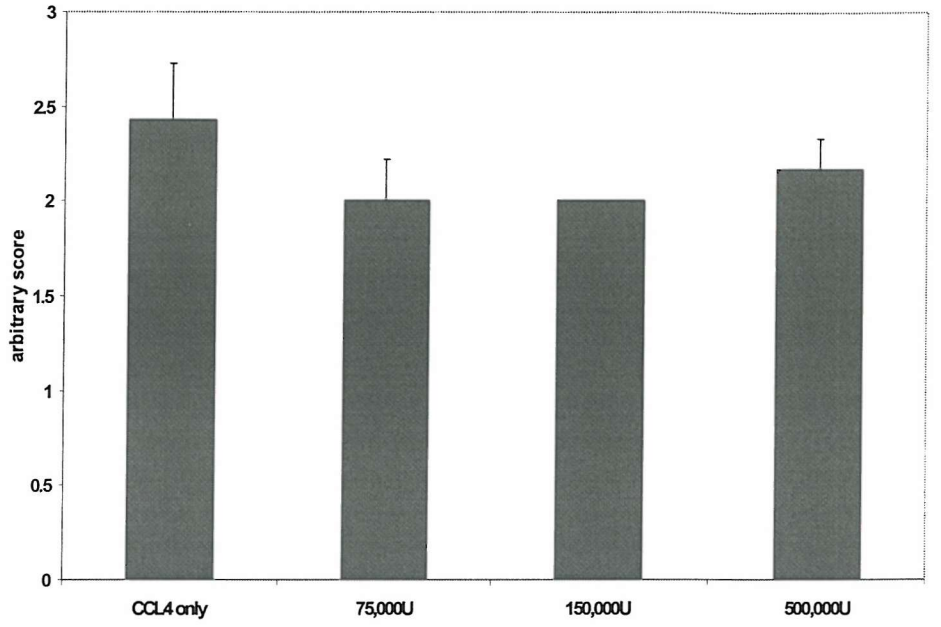

Figure 5-28 Graph showing the scoring of T-cells using CD3 stain.
Slides from each animal were scored blind by a pathologist. The CD3 stain was used to assess the levels of T-cells within the sections. An increase was demonstrated in 150,000U and 500,000U IFN-α which was found to be statistically significant in the 500,000U IFN-α group.

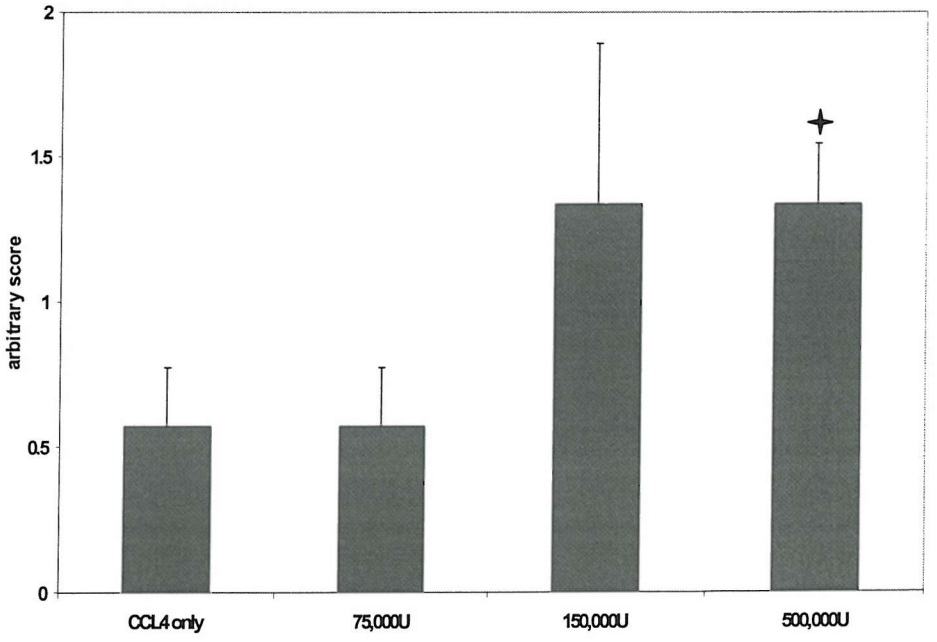

5.11 PCNA STAINING

Staining for Proliferating Cell Nuclear Antigen (PCNA) was also used to examine whether any antiproliferative effects of IFN-α could be shown in the whole liver. Initially PCNA was stained concurrently with α-SMA to enable co-localization of the two markers and identify proliferating HSC. However, due to the chromogens used on these antibodies it remained impossible to identify the co-localized proteins when overlayed (Figure 5-29). Fluorescence tagged antibodies were not used because the intention was to count proliferating cells and the fading of fluorescent markers was felt to preclude their use in this technique.

Therefore, the liver sections were stained for PCNA alone, and all cells positive for PCNA were counted (Figure 5-30). Whilst most cells counted as PCNA positive were hepatocytes, the data was divided into hepatocytes and HSC. In the total cell count an increase in PCNA positive cells was found in the IFN-α treated group, thus suggesting that IFN-α treatment increases cellular proliferation in the liver (Figure 5-31-A). However, when this data is segregated into hepatocytes only (Figure 5-31-C) and HSC only (Figure 5-31-B) it can be seen that IFN-α decreases HSC proliferation but an increase remains within the hepatocytes. Due to the bias in the number of hepatocytes counted versus HSC, it is the increase in hepatocyte proliferation which is demonstrated in the total cell count. The other IFN-α treated groups were not examined.

This suggests that in vitro IFN-α is able to decrease proliferation if the HSC, and furthermore, supports work demonstrating that IFN-α may protect hepatocyte function within the cirrhotic liver (Muriel 1994; Muriel 1995; Lu 2002).

Figure 5-29 Picture showing co-staining of the liver sections with PCNA and α-SMA.
The HSCs are clearly seen with the red staining in their cytoplasm. In this section a line of CCl_4 induced fibrosis can be seen using the α-SMA stain of the HSCs. There is one HSC which may be positive for PCNA (brown nuclear staining) in addition to α-SMA (shown with the arrow) but this is not clearly distinguished.

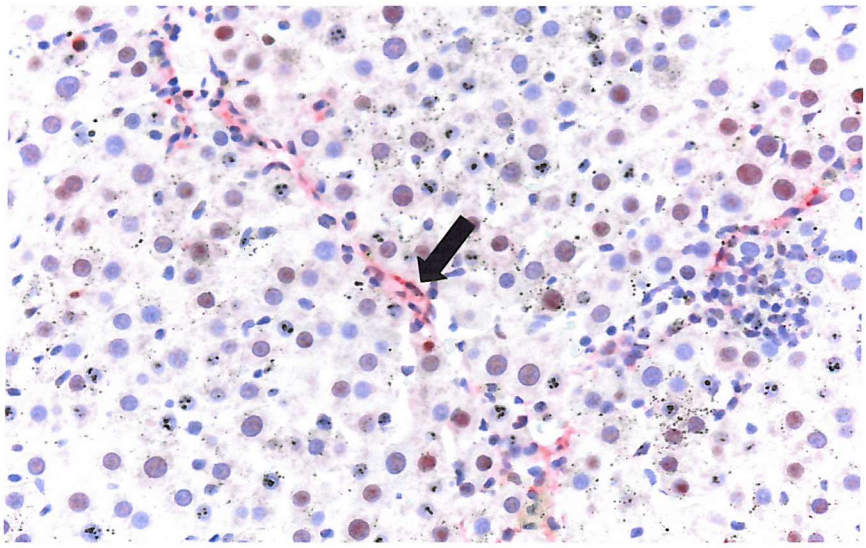

Figure 5-30 Picture showing the PCNA stain alone in the liver section.
As can be seen the brown PCNA stain was much clearer alone, and counting PCNA positive cells was much easier (hepatocyte positive for PCNA shown by arrow).

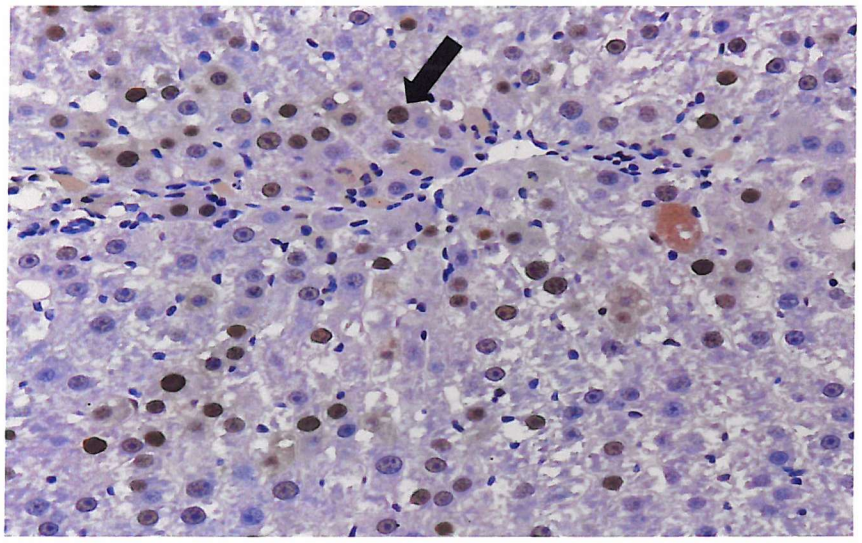

Figure 5-31 PCNA staining in the liver sections.

All cells positive for PCNA were counted in the CCl_4 only and 500,000U IFN-α groups. As shown in Figure 5-31-A an increase in PCNA positive cells was found in the 500,000U group. However, when the data was represented according to cell type positive for PCNA, it is clear that the proliferation is found primarily in the hepatocyte population and not the HSC.

A) Graph to show total number of PCNA positive cells in the sections

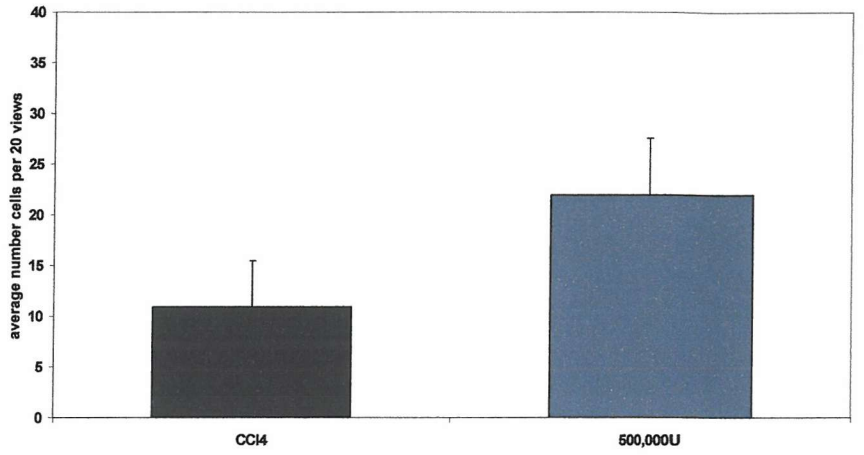

B) Graph to show the total number of HSC only in the sections

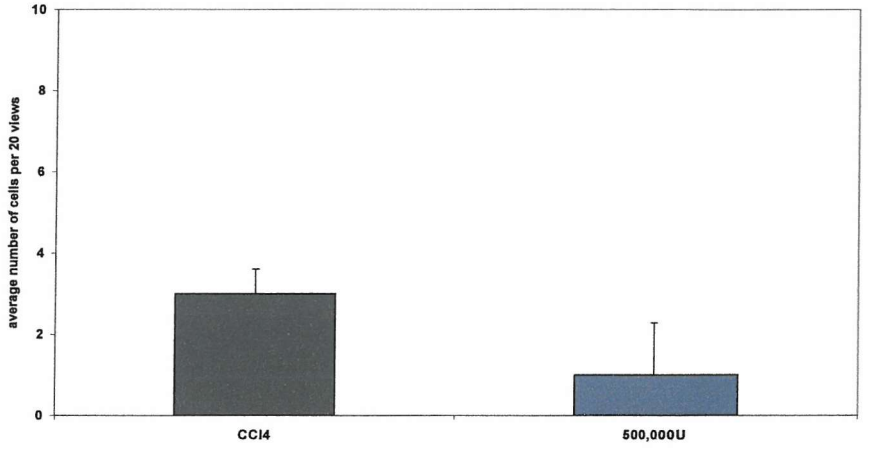

C) Graph to show the total number of hepatocytes PCNA positive in the sections

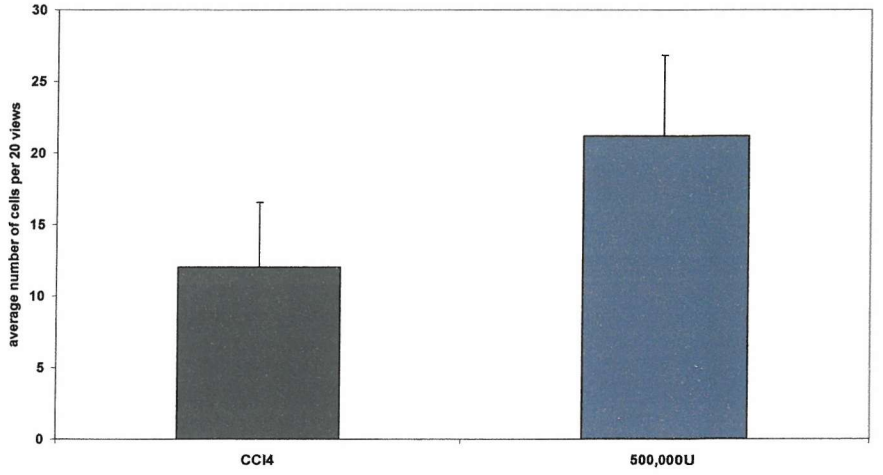

CONCLUSION

Previous studies have studied the effects of IFN-α *in vivo* using rat models of liver fibrosis. However, these studies have used human IFN-α and in addition they have administered IFN-α from the outset of induced liver injury. The results have been conflicting from these studies, and despite clinical observations that IFN-α is antifibrotic, these studies have not been able to elucidate the mechanism by which IFN-α is able to reduce fibrosis.

Therefore, I used a rat model that induced fibrosis by injection of carbon tetrachloride for 6wks. At this timepoint, the injections were continued and in addition, IFN-α was given therapeutically to specific cohorts. Consistently a decrease in several parameters was observed suggesting a decrease in fibrosis in the IFN-α treated groups. However, little of the data was statistically significant. A statistically significant reduction in fibrosis was found through scoring sections stained for collagen in the 500,000U group. However, whilst a reduction was found using the hydroxyproline assay, significance was not achieved. Furthermore, collagen 1 alpha 1 mRNA levels also verified a reduction but statistical significance was only achieved in the 150,000U group. Curiously, the collagen mRNA levels demonstrated an increase in the 500,000U group compared to the lower IFN-α treated groups which was found to be due to two animals that had particularly high levels.

The data studying α-SMA was not so conclusive. Scoring the sections and counting α-SMA positive cells per slide showed a reduction that was not significant in either case. However, western blotting for α-SMA did show a clear decrease in α-SMA protein levels in the IFN-α treated groups. Taken together these results do suggest a decrease in activated HSC number in the treated liver.

The liver function tests ALT and AST showed demonstrated no difference between the groups. Similarly, through the clinical scoring system devised, no significant difference was found between cohorts. However, it was observed that the CCl_4 only cohort had much ascites, an observation that was confirmed at the end of the trial. The ascites levels were found to be dramatically reduced in the IFN-α treated groups, although due to the wide variation in the groups was not statistically significant.

The reduction in ascites observed probably reflected a reduction in portal pressure following a reduction in fibrosis. The method used to measure portal pressure were indirect and relatively inaccurate. In addition I determined whether IFN-α treatment may have regulated hepatic function and increased albumin secretion in the treated groups. Western blotting for albumin showed that there was a decrease in two animals from the CCl_4 only group, but was not sufficient evidence to propose that IFN-α may be protecting hepatocyte function and thereby reducing ascites.

MMP activity was additionally studied using zymography, a collagenolytic assay and mRNA levels of MMP-13 (rat collagenase). Comparison of the groups using zymography showed that as the dose of IFN-α increased there was a decrease in Gelatinase A (MMP-2). As HSC are major producers of MMP-2, this might corroborate with the drop in HSC reflected by the α-SMA measurements. However, more apparent was the decrease in Gelatinase B (MMP-9) which is only found in one animal in the 500,000U group. This animal is one of the two which skewed the data of both collagen and MMP-13 mRNA levels. A significant decrease was found in the mRNA levels of MMP-13 of both the 75,000U and 150,000U groups. However, no change was found in collagenolytic activity between the groups.

TIMP-1 mRNA was also found to decrease in a dose dependant fashion, however, once again, statistical significance was not found. The expression of 2'5'-

oligoadenylate synthetase showed some increase in the IFN-α treated groups, but not significantly.

To assess whether IFN-α was affecting inflammation within the liver, sections were stained to score for T-cells, macrophages and H&E to allow an overview of all inflammatory cells. This data showed an increase in T-cell numbers with IFN-α treatment (statistically significant at 500,000U), but no change occurred with the macrophages or other inflammatory monocytes.

Finally, based on the in vitro work where a reduction in proliferation was found, the sections were stained for PCNA and cell counting used to gather data on any effect on proliferation. The total cell count was found to increase with IFN-α treatment, however, when the two cells, hepatocytes and HSC were analyzed separately it was established that IFN-α decreased PCNA positive HSC, but increased PCNA positive hepatocytes. This suggests that in vitro IFN-α is able to decrease proliferation of the HSC, and furthermore, supports work demonstrating that IFN-α may protect hepatocyte function within the cirrhotic liver (Muriel 1994; Muriel 1995; Lu 2002).

Alpha smooth muscle actin, TIMP-1, MMP-2, MMP-9 and collagen are all products of the activated HSC. Taken together the data suggests that either directly or indirectly via a modification of the immune/inflammatory response IFN-α has downregulated HSC function and proliferation resulting in a reduction of overall fibrosis. Hepatic stellate cells may also be affected by modification of the inflammatory response. The data presented here suggests that no such modification occurs with respect to overall proteins and inflammation. However, the change observed in T-cell populations sustained in the treated liver is intriguing and may have impacted on HSC phenotype and function.

6 DISCUSSION

Initially, to compare the homology between the PSC and the HSC it was necessary to develop a reliable method for extracting PSCs. With sufficient numbers of PSC, the expression of markers of activation could be studied. Both PSC and HSC were then analyzed for their response to IFN-α, this included studying apoptosis, proliferation and activation. To further the understanding of IFN-α in the treatment of liver fibrosis, a rat model was used which induced fibrosis in the animals, following which IFN-α was given therapeutically.

The activated HSC has been shown to produce all components required in alteration of the extracellular matrix of the injured liver. The HSC produces all matrix proteins, MMPs and TIMPs. Due to the implications of this, much work on liver fibrosis has centred on the regulation of the HSC. The PSC, like the HSC, has been implicated in the development of pancreatic fibrosis (Bachem 1998).

This work shows homology between the PSC and HSC, as the PSC also activates following injury, a process which can be mimicked *in vitro* by culture on uncoated plastic in the presence of serum. Pancreatic stellate cells were shown to demonstrate immunoreactivity for desmin and α-SMA both markers of myofibroblasts, and also markers of the activated HSC. Synthesis of the common fibrotic markers was also found to be akin to the HSC. In addition, I have shown that the activated phenotype of the PSC, by the parameters measured (TIMP-1 and α-SMA), is also reversible when surrounding matrix is altered, in a manner identical to that observed in the HSC (Gaca 2000). When cultured on matrigel, a basement membrane-like gel, apparent deactivation of the cells occurs as defined by the change in cell phenotype and the decrease in expression of TIMP-1 and α-SMA. Whilst cell numbers were very low in

these studies, they underline the importance of cell matrix in regulating PSC activation and contribute new information to the field. They also show the plasticity of the activated PSC phenotype which might be exploited for development of antifibrotics. Together with the previous data on the HSC this demonstrates more evidence to the generic nature of the fibrotic process throughout myofibroblastic cells, such as the mesangial cell and related cells such as lung fibroblasts (Powell 1999). Collagen, the major matrix protein secreted by these cell types, is crucial in the formation of a scar, the healing mechanism which these cells cause. However, recent evidence has shown that differences do exist between fibroblasts derived from different tissues (Parsonage 2003). Only by continuing to extract these PSC populations can these *in vitro* models relevant to the field of fibrosis provide further data on antifibrotic agents and differences between fibroblastic cells be examined.

To confirm that the HSCs were responsive to the IFN-α treatment in tissue culture models, 2'5'-oligoadenylate synthetase mRNA levels were measured. This showed a moderate increase in the HSCs both at 24hrs and 72hrs. A concentration response was present although it was disappointing that a statistically significant result was not obtained. The PSC population demonstrated a dramatic dose response in terms of 2'5'-oligoadenylate synthetase mRNA levels after IFN-α stimulation. Taken together with the affymetrix data on HSC receptor expression and the HSC response to IFN-α, it seems likely that HSC express functional receptors for IFN-α in both quiescent and activated phenotypes and are responsive to IFN-α. As demonstrated in 4.4.1.1 freshly isolated cells (quiescent) exhibit apparent increased activation in the presence of IFN-α. Thus, whilst both phenotypes, quiescent and activated, are able to respond to IFN-α, their response is dissimilar.

Treatment of HCV infected patients with IFN-α has been shown to be associated with a reduction in fibrosis that appears to be independent of the antiviral action (Sakaida 1999) (Everson 1999). To investigate whether IFN-α ameliorates fibrosis through induction of HSC apoptosis IFN-α treated cells were examined following examination of nuclear morphology using staining with Acridine Orange. Both HSC and PSC were studied for evidence of nuclear blebbing and condensation. These studies demonstrated that IFN-α does not effect the rate of apoptosis, either to increase or decrease it. Much evidence exists to demonstrate the pro-apoptotic effect of IFN-α in specific cell types, but the evidence is largely limited to cancer cell lines (Sangfelt 1997; Roth 1998; Caraglia 1999; Thyrell 2002). Evidence for a pro-apoptotic effect for IFN-α has also been observed for cells of the immune system such as macrophages and T-cells (Dao 1994; Adler 1995; Kirou 2000). Recently however, one group assessed apoptosis *in vitro* with HSC (Saile 2003). They found that IFN-α inhibited apoptosis in both quiescent (day 2 freshly isolated HSC) and activated (day 7 freshly isolated HSC). An identical range of IFN-α doses were used. Therefore, although the apoptosis studies presented in this thesis do not correlate with much of the previous work in other cell types, it may support the work by Saile 2003. Clearly, no inhibition was seen in my work, but my experiments used 5% FCS containing media and HSC used were passage 1-3 due to restrictions on numbers of available cells. The HSC used by Saile 2003 were all freshly isolated, quiescent HSC were used at day 2 and activated HSC were used at day 7 and in addition the HSC were maintained in 0.3% serum containing medium. Therefore, the HSC were less activated and most importantly maintained in the presence of fewer external growth factors.

Further work was undertaken to examine the effects of IFN-α on HSC and PSC proliferation. Previously IFN-α induced inhibition of proliferation has been reported

in human cells (Mallat A 1995), but a comparative study in rat HSCs found that IFN-α had no effect on proliferation (Shen 2002). Therefore, I studied the effect of IFN-α in rat HSCs and PSCs. Proliferation was analysed using primarily the ^{3}H Thymidine proliferation assay. Both HSC and PSC were treated with IFN-α where it was observed to have an anti-proliferative effect as found by Mallat (Mallat A 1995). Whilst my studies broadly agree with those of Mallat the discrepancy between our data and that of Shen et al data is curious. Mallat used human HSC, but the IFN-α used was also human IFN-α. Shen (Shen 2002) used rat HSC isolated in a similar manner to the HSC used in our group, and in addition used the same recombinant IFN-α protein from the same manufacturer as used in my work. The HSC used by Shen were cultured in 10% serum containing media, therefore a higher concentration of growth factors, including pro-proliferative factors, would have been present compared to the 5% FCS used in my work. However, Mallat 1995 also used 10% serum containing media, although this serum contained 50% fetal calf serum and 50% human serum. In my studies, whilst there is an antiproliferative effect, proliferation was only reduced by little under 30%, it is not completely inhibited. With a greater number of proliferative factors any effect of IFN-α may not have been seen, and conceivably a 50:50 mix of growth factors from two species may have different potency with respect to growth promoting effects.

To reinforce the data observed using the ^{3}H Thymidine proliferation assays, a proliferation assay based on a different principle was used, i.e. a tetrazolium dye conversion based assay. This assay did initially show a good correlation with cell number per well but did not confirm previous data in experimental manipulation. The usefulness of this assay was brought into question as the assays did not give reproducible data for positive and negative controls. Positive controls were used, as in

the previous proliferation assay, of cells grown in 16% FCS containing media and negative controls were used with cells grown in 0.01% BSA containing FCS free media. It was observed that the cells in the negative controls as compared to the 16% FCS treated control had increased proliferation. Further analyses were done to determine if the effect was related to the media alone, as background absorbance had to be taken into account. However, this was not the case, and further investigation found that this assay does not work in the presence of a cellular enzyme glutathione S-transferase (GST) which is found in the HSC (Whalen 1999). GST is also able to reduce the tetrazolium salt and therefore may produce spurious results (Molecular Probes 2002). Finally whilst the MTS assay provides a surrogate marker of proliferation the assay actually measures mitochondrial activity and can only be considered to measure cell numbers in certain well defined conditions. For these reasons this assay was not further used.

Therefore the antiproliferative effect of IFN-α was confirmed using a Picogreen assay to determine overall cell numbers by quantifying DNA. Total DNA was found to be reduced in the IFN-α treated cells after 72hrs treatment, which suggests a trend towards a reduction in proliferation which supports the data from the ^{3}H Thymidine proliferation assay.

In addition further evidence of the antiproliferative effect of IFN-α was observed by determining the levels of ERK1 and ERK2 in IFN-α treated HSC. Previously we have shown that onset of proliferation in HSC stimulated by serum is accompanied by rapid activation (less than 20mins) of the MAPKs, ERK1 and ERK2 (Gaca 2002). In addition, IFN-α has been shown to downregulate ERK1 and ERK2 and additively reduce the antiproliferative effect of ERK inhibitors (Romerio 2000; Romerio 2002). Therefore, ERK1 and ERK2 were studied in the HSC and PSC by removing the cells

from cell cycle with 0.05% FCS containing media for 24hrs following which they were activated in 16% FCS containing media. Hepatic stellate cells treated with IFN-α had less phosphorylated, active forms of ERK1 and ERK2 following activation, evident at 30mins and 1hr. This work corresponded with that found previously in both our group with respect to ERK expression by proliferating HSC and that of Romerio 2002 in T-cell population (Romerio 2002).

The effect of IFN-α on HSC activation was elucidated in several experiments analysing markers of activation. Markers of activation, α-SMA, Gelatinase A and B, collagen protein and TIMP-1 were studied in both HSC and PSC. After 24hrs of IFN-α treatment, no effect on the regulation of any proteins was observed. Following 72hrs of IFN-α treatment a reduction in α-SMA was found in HSC, but neither Gelatinase A or B were affected. Collagen was also studied, but once again, no change in total collagen production was found after 24hrs or 48hrs IFN-α treatment. As with the zymography, the collagen assays required treatment of the HSC in serum free media. This in itself limits cell growth, and is commonly used to quiesce cells. Therefore, data from these assays might not be comparable with the conditions used for the analysis of α-SMA expression where cells were concurrently serum exposed. As can be noted, in the collagen assay undertaken with PSC there was a decrease in total collagen production at 24 and 48hrs of IFN-α treatment, although this was only observed in one population. However, no decrease was found in any of the HSC preparations studied. The data in HSC with respect to collagen expression was confirmed with analysis of the mRNA levels, which also showed no change although the increase apparently observed in the PSC population studied was unexpected in the context of the other results. At 24hrs no change was found in TIMP-1 expression of

HSC exposed to IFN-α, but at 72hrs an increase was found, although not statistically significant.

Therefore, IFN-α has been shown to inhibit α-SMA synthesis after 72hrs treatment corresponding with the work of Mallat 1995. No other activation markers studied in either PSC or HSC show any increase or decrease, except for a decrease in collagen in PSCs after 48hrs which, as it derives from a single study, is inconclusive. The work of Mallat 1995 found a decrease in collagen synthesis and mRNA expression, however, the cells were treated for 6 days with IFN as compared to the 2 days in my studies. As the collagen assay is carried out without the presence of serum, it was not possible to study this length of treatment in this work due to reduced cell viability in these conditions. However, the possibility remains that longer incubation with IFN-α may decrease collagen levels.

Collagen is subjected to a series of regulatory steps including: mRNA expression, mRNA stability, post-transcriptional regulation, secretion, modification and cross-linking (Stefanovic 1995; Krupsky 1997; Stefanovic 1997). It was therefore important that our studies included mRNA levels in addition to secreted protein to define the level at which IFN-α was regulating collagen. Despite this relatively thorough approach, no difference in collagen mRNA expression was demonstrated over the times studied. Intriguingly the *in vivo* data also suggests that IFN-α was not directly regulating collagen. The HSC have been established as the major source of collagen in the fibrotic liver, thus the in vivo data is compatible with the tissue culture model.

Given the current results, IFN-α has demonstrated little ability to reduce the synthesis of any proteins associated with activation in the stellate cell – only α-SMA expression has been decreased. However, it has shown a reproducible effect on cell proliferation. Therefore, IFN-α may be halting the cells during their cell cycle. In doing so, it could

reduce proliferation and additionally by halting the cells in their cycle may also effect apoptosis. If IFN-α halted the HSC proliferation in vivo, this might explain its antifibrotic effect, or at least have the effect of checking and resetting the fibrotic stage in a treated liver during a progressive process.

There is now a substantial body of evidence showing that IFN-α may be able to prevent cells from leaving the G1/G0 resting state. To date this work has only used malignant cell lines and T cells. Erickson (1999) showed that IFN-α inhibited IL-2 activation of T lymphocytes from G1 to S-phase. They found inhibition of the G1 cyclin D3, the cyclin dependant kinase 6 (Cdk6), and also of the pocket proteins p130, pRb and p107 (Erickson 1999). Similar findings have been found in Daudi cells, a malignant cell line from Burkitt's lymophoma. Kumar and Atlas 1992 showed that IFN-α treatment *in vitro* on the Daudi cells could induce the underphosphorylated form of retinoblastoma protein (pRB) (Kumar 1992). The underphosphorylated form is found in the G1/0 phase of the cell cycle and phosphorylation of this protein has been shown to commit the cell to entering S-phase (Buchkovich 1989). Therefore, based on my current data IFN-α may be holding the cells in the G1/G0 phase. This effect may or may not be reversible once the IFN-α has been removed.

One criticism of the *in vitro* data in both HSC and PSC is the small numbers of independent studies performed. Most data refers to three populations at most which is the minimum for any statistical interpretation, and thus any conclusion drawn from this data is susceptible to a Type I or Type II error. However, in mitigation, all of my data were replicated in preparations of HSC and PSC isolated de novo from separate organs. The cell preparations were time consuming and not always successful. I suggest that my findings were therefore more relevant to human disease than could be obtained using stellate cell lines which are easily obtained 'off the shelf' and can be

easily expandable to high numbers for large replicate studies. Stellate cell lines are available and used by several groups, but these are high generation passage cells and data derived from them might be of questionable significance to human pathophysiology. A further criticism is that *in vitro* work has limited value in interpreting cell changes in the diseased organ. This is a generic problem in interpreting culture-based data and not confined to my studies. Whilst treatment of HSC with a particular growth factor or cytokine may cause an effect *in vitro*, the environment in vivo is far more complex with multiple stimuli from cells in the surrounding parenchyma which may enhance or erase this effect. In appreciation of that, where possible *in vitro* data was performed in the presence of 5% FCS containing media as opposed to serum free media. However, since any response of HSC *in vitro* may be inhibited or enhanced by the specific milieu it can be difficult to extrapolate the *in vitro* response to the in vivo situation. However, in mitigation for my approach, the tissue culture plastic model of stellate cell activation is very widely used in the field. However, there is increasing awareness of limitations of this model. For example, it is becoming apparent that the culture matrix for stellate cells can profoundly influence their response to soluble growth factors – indeed, some pioneering studies of matrix-dependent effects have been published by members of the Southampton Liver Group (Gaca 2003). The matrix in the liver undergoes substantial remodelling during fibrogenesis and this is likely to modulate HSC phenotype and responses. Therefore, although the plastic culture model is currently accepted, more complex models – e.g. using liver slices, co-cultures - certainly need to be pursued and developed.

The *in vivo* study examined the effects of IFN-α on the progression of already established fibrosis and therefore better mimicked the clinical situation where IFN-α is

started in the context of an established disease. Using histological assessment of fibrosis by sirius red staining a statistically significant difference was found between the control group, and the highest dose of IFN-α, 500,000U. Given that the IFN-α treatment was only given for 2 weeks rather than the planned 4 weeks the results are quite dramatic.

This trend was also found in the sections examined for α-SMA also given a histological score and in addition individual cells counted in a series of random views. However, this was not statistically significant and the error bars were large in the IFN-α treated groups. Therefore, the IFN-α has had some effect on decreasing the overall numbers of HSCs present in the fibrotic liver, and has been able to ameliorate the fibrotic process to some extent.

No difference was found in AST and ALT levels, which is disappointing given that any improvement in the fibrosis would imply a decrease in AST and ALT levels. A transient increase of serum aminotransferase is seen in HCV patients given therapeutic IFN-α (Hoofnagle 1997), however it is also likely that insufficient time was given for any significant improvement. Health of the individual animals was monitored closely for the final five days of the trial due to the observed decline in the health of the IFN-α A/D treated animals. Due to the large numbers of animals, individual animals were monitored using a scoring system. This enabled the health and comfort of the animals to be properly ascertained, and resulted in the trial finishing two weeks earlier than planned, due to IFN-α morbidity. This also is supported by clinical knowledge where it is advised that patients with decompensated cirrhosis should not receive IFN-α therapeutically as this may result in death (NICE 2000). This clinical picture probably results from the cytotoxic lymphocytes mediated killing of infected hepatocytes (Ramadori 1990). Obviously the pattern of disease in a CCl_4 model is different.

However, IFN-α does have systemic effects including: fever, malaise, tachycardia, chills, headache, arthralgias, and myalgias. Therefore it is possible that the apparent ill-health of the animals resulted from the systemic side-effects of the IFN-α treatment. Nevertheless, their parameters of liver fibrosis were found to be improved.

One of the foremost results found in the *in vivo* study was the reduction in ascites in IFN-α treated groups. Ascites develops due to an increase in portal pressure from the fibrotic liver and a decrease in albumin levels due to hepatocytic damage thereby reducing effective hepatocyte function. As fibrosis within the liver increases, this causes portal pressure to rise in order that blood flow is maintained through the liver. However, as the rise in the intrahepatic portal pressure that occurs as fibrosis develops, blood is forced to find other routes and so collateral blood vessels form. In addition fluid is forced into the body cavity but this is at too high a rate to be drained. Furthermore, the decrease in albumin alters the osmotic balance and less fluid is drawn from the body cavity into the bloodstream than is usual. Together these processes cause ascites, the accumulation of fluid within the body cavity.

The diameter of the portal vein was measured to provide a means of assessing portal hypertension, however no difference was found between the groups. Spleen wet weight was also examined at the study's conclusion, but again no difference was found between the groups. Enlargement of the spleen can occur due to the increased portal pressure. Finally, the level of serum albumin in the 500,000U IFN-α group and the CCl_4 only group was assessed by western blotting. This found a decrease in two of the CCl_4 only animals, but was not sufficient to explain the dramatic decrease in ascites difference found in the IFN-α treated animals.

IFN-α has been shown to have contractile properties, and it was postulated that IFN-α may be causing contraction of the HSC thus reducing portal pressure and ascites in

IFN-α treated animals. Work was undertaken by Dr. D. Rockey's group assessing the contractile properties of IFN-α treated HSC using a collagen lattice contraction assay. Hepatic stellate cells were treated with IFN-α for 24hrs and 3 days in 5% FCS containing media. However, no change in their contraction was demonstrated (Dr. D. Rockey M.D., personal communication).

Fort 1998 measured portal pressure using a Philips CM 130 multichannel recorder which uses a catheter inserted into the superior mesenteric and splenic veins ((Fort 1998)). However, no difference was found between IFN-α treated and untreated. Previous work has shown that IFN-α may maintain both hepatocyte and HSC function but this focussed on oxidative damage (Lu 2002). Perhaps through as yet unknown mechanisms IFN-α is able to reduce ascites. However, our working hypothesis is that IFN-α reduced portal pressure via the reduction in fibrosis observed in the liver.

Collagen in the liver was assessed by measuring hydroxyproline content, staining for Sirius red and analysis of collagen mRNA by TaqMan® Realtime Quantitative PCR. Both the Sirius red staining and the hydroxyproline assay found a decrease in collagen in the IFN-α treated groups. This was statistically significant in the former but was not statistically significant in the latter. The mRNA levels were only significant in the 150,000U whilst in the highest dosed group the level of collagen mRNA unexpectedly rose. This was also demonstrated in the mRNA levels of MMP-13 (with the addition of the 75,000U also reaching statistical significance in this case), and on further investigation was found to represent two animals which have higher levels than the rest of the group. When the data regarding these animals was followed through, one was found to have the highest expression of α-SMA in the western blots, and the other was the only animal to have MMP-9 in the zymography within the 500,000U group.

A decrease in collagen was found in all of the previous studies of *in vivo* liver fibrosis models, analysing both hydroxyproline and collagen mRNA (Muriel 1996; Fort 1998; Bueno 2000; Vendemiale 2001). Although, one study found that only one IFN-α, a leukocyte-IFN-α, reduced collagen whereas the other, a human recombinant IFN-α 2b had no effect (as analysed by hydroxyproline). Whilst my data correlates well with this work, the reduction found here better reflects the data presented in Fort 1998, Bueno 2000 and Vendemiale 2001 as compared to Muriel 1996 who found that IFN-α reduced collagen to normal levels (Fort 1998; Bueno 2000; Vendemiale 2001). Of interest, Fort 1998 found that IFN-α only reduced collagen in liver fibrosis induced by CCl_4 whereas in BDL induced fibrosis hydroxyproline was reduced but not procollagen mRNA. This is an intriguing result and suggests that enhanced matrix degradation may be important in mediating the effect of IFN-α within the liver. Furthermore, Vendemiale (Vendemiale 2001) found that only one IFN-α reduced collagen, a leukocyte IFN-α, whereas the other, a human recombinant IFN-α2b had no effect (as analyzed by hydroxyproline).

Within my data, an increase in collagen was found, but only within the mRNA levels, as opposed to the other two techniques which examined protein levels. Therefore, this difference may also reflect on the levels of MMPs within the liver. The MMPs were studied using a collagenolytic assay, zymography and TaqMan® Realtime Quantitative PCR to analyse mRNA levels of MMP-13, the major rat collagenase. The collagenolytic assay demonstrated no change between the groups, however a clear change was found in the zymography where both MMP-2 and MMP-9 were shown to decrease substantially with the increasing doses of IFN-α. In addition, the mRNA levels of MMP-13 also decreased. These findings suggest that IFN-α does not inhibit

liver fibrosis by increasing matrix degradation, at least on the basis of the MMPs examined.

Only one group had analysed MMP levels *in vivo* (Bueno 2000). Zymography was used to analyse the gelatinases from whole liver extracts and non-parenchymal cell (NPC) extracts. In this study, MMP levels increased with IFN-α treatment. This increase was found to be minimal in the whole liver, but very strong in the NPC extracts. It was proposed that this MMP activity came from the Kupffer cells. However, the model used was a BDL induced liver fibrosis in a different strain of rats (Wistar). Carbon tetrachloride is known to cause an inflammatory reaction in addition to the fibrosis, and it is possible that the difference in the disease dynamics have caused this disparity between my MMP findings and theirs. BDL induced liver fibrosis is known to produce very little inflammation, whilst the inflammatory reaction of CCl_4 is more analogous to that of alcoholic induced liver fibrosis. Tissue inhibitor of matrix metalloproteinase 1 showed an apparent decrease with IFN-α treatment which although not statistically significant, once more conflicted with previous work. Again, from the same study (Bueno 2000) TIMP-1 as assessed by RT-PCR was found not to change with IFN-α treatment of the BDL induced liver fibrosis. Reverse transcription PCR is not particularly accurate when used as a quantitative method of analysis, and in addition the decrease of TIMP-1 levels in my data was not found to be statistically significant. Nevertheless, my data is suggestive that IFN-α might decrease fibrosis, by decreasing collagen, TIMP-1 and MMP-2. Each one of these is a marker of HSC activation and together suggest that IFN-α decreases in HSC activation or proliferation or both.

Finally, levels of the IFN-α induced protein 2'5' oligoadenylate synthetase were analysed in liver. This had not been done by any previous groups in an *in vivo* study.

Disappointingly the mRNA levels did not change with IFN-α treatment, with the exception of a small non-significant increase found in the 500,000U IFN-α group. With more time, further IFN-α induced proteins would have been analysed, and previous work has shown differential regulation of the IFN-α induced proteins.

IFN-α is an innate cytokine, with inflammatory properties. Given therapeutically it is able to cause flu-like symptoms (Czerwionka-Szaflarska 2000; Hadziyannis 2000). Inflammation is known to play a key role in the pathogenesis of liver fibrosis. Therefore it was important to assess whether any difference in inflammation could be found in the treated livers as compared with the control livers. Inflammation was analysed using histological staining, and scored by an expert pathologist who was blinded to the sample identity. Kupffer cells have been shown to be crucial in the perpetuation of liver fibrosis induced through both CCl_4 and alcohol (Adachi 1994; Rivera 2001). Curiously, in this work, no difference was found in the analysis of overall inflammation or in macrophages. Unexpectedly, a statistically significant increase was found in the T-cell scores in the 500,000U group. As previously described, a predominance of either Th1 or Th2 cells can affect the level of fibrosis achieved (Shi 1997). This is also found in human liver disease; viral persistence in Hepatitis C is associated with a prevalence of the Th2 subset whereas a Th1 subset is found in primary biliary cirrhosis, an autoimmune disease (Kobayashi 1998; Nagano 1999). Nevertheless, the marker used in this work does not differentiate between the subsets, CD3 is a generic lymphocyte marker. Lymphocytes are known to secrete many profibrogenic cytokines, such as IL-1β, IL-4 and TGFβ, which increase HSC collagen production, and TNFα, a survival factor for activated HSC (Tiggleman 1995) (Saile 1999). In addition, *in vitro* evidence has shown the ability of the activated

lymphocyte to kill hepatocytes (Ramadori 1990). Therefore the increase in T-cells seems incongruous with the decrease in fibrosis observed.

Counting of PCNA-positive proliferating cells also showed that IFN-α increased the number of PCNA positive cells. When this data is scrutinized, the increase in PCNA positive cells is in the hepatocyte population. However, the number of HSC positive for PCNA decreased in the 500,000U IFN-α treated group. This suggests that IFN-α is aiding hepatocyte proliferation and thereby liver regeneration. The reduced HSC proliferation in the liver supported the similar results observed in *in vitro* IFN-α treated HSC.

When comparing the *in vivo* studies, one important observation is that none of the previous studies used a species-specific cytokine, all used human IFN-α. It is well known that IFN-α is a species-specific cytokine (personal communication, Roche) (Medscape 2000). All of my work *in vitro* and *in vivo* has also used a recombinant human IFN-α, however, this has been assessed for its activity on rodent cells. Furthermore, all but one of these groups gave IFN-α with the onset of liver injury whereas in my studies fibrosis was established before IFN-α therapy was administered, thus more closely resembling the clinical situation where individuals present with developed liver fibrosis.

Due to the ill health of the animals in the study only two weeks of IFN-α therapy was given whereas previous studies have treated for four weeks. This in itself may be the reason why little of this data was found to be statistically significant. Both Fort (Fort 1998) and Bueno (Bueno 2000) had a 25% mortality and 20% and 30% mortality in their studies. Whilst illustrating the high doses involved and the side-effects of IFN-α therapy this is not acceptable under Home Office guidelines and thus this study was finished at an earlier date than hoped. However, the *in vivo* data potentially correlates

with clinical observations, where cirrhotic patients receiving IFN-α would be expected to quickly decline in health.

Previous *in vivo* data in this area used three different models of liver fibrosis, BDL, CCl_4, and DMN. The latter two models are both hepatotoxic although CCl_4 is catalysed to CCl_3* radical while DMN disrupts DNA structure, nevertheless both typically initiate a centrilobular fibrosis associated with an inflammatory response. BDL causes a portal fibrosis after 7 days with proliferation of bile ducts and little inflammation. As shown by Fort (Fort 1998) the model of fibrosis used (CCl_4 and BDL) did produce a difference in the efficacy of IFN-α, where IFN-α only showed a reduction in fibrosis parameters in the CCl_4 model. However, Bueno (Bueno 2000) used the same type of IFN-α (IFN-α2a) and did find amelioration of fibrosis in the BDL model. Therefore, based on previous work the capability of IFN-α does not seem to reflect on the level of inflammation or initial start point of fibrosis.

Once again, this data is vulnerable to Type I and Type II statistical errors due to the low numbers of replicate animals at certain time points and dosages, particularly at the longer dosing times when morbidity was apparent in the rats. Animal models are extremely time and money consuming, and there are clear practical limits on how many rats can be injected singlehandedly. For this reason a larger trial was not possible for this work. Compared to studies with cell cultures, large error values are frequently found in data acquired from both *in vivo* models and patient trials due to the greater complexity. This emphasises the importance of large cohort numbers to minimise these effects. However, in my rat model many of the effects of IFN were clearly negative or of small magnitude, and therefore addition of more animals into the cohorts – within reasonable limits – would not likely have affected this outcome.

Conclusion

In summary, based on the proliferation data the efficacy of IFN-α *in vivo* may be through its ability to reduce proliferation of HSC. The *in vitro* data supports previous evidence that IFN-α has antiproliferative abilities in HSC and can downregulate α-SMA, but no evidence for the downregulation of collagen was found. In addition IFN-α was not found to regulate TIMP-1 or MMP-2 and MMP-9 *in vitro*. These results have also been demonstrated in the PSC and whilst limited in numbers may suggest a universal antiproliferative role of IFN-α in myofibroblast-like cells.

The *in vivo* data does support data found previously in other studies that IFN-α is able to reduce fibrosis and collagen within the liver, although decreases were smaller than in previous work. *In vivo,* α-SMA levels decreased with IFN-α treatment as did MMP-2 and MMP-9 levels, conflicting with previous work. However, little or no regulation of MMP-13, collagenases, TIMP-1 and 2'5' oligoadenylate synthetase was found.

Therefore, the precise mechanism of the antifibrotic role of IFN-α remains to be ascertained. However, based on my data IFN-α has an antiproliferative effect with the ability to downregulate certain markers of activation within the HSC. This downregulation is small and as such is only found following long-term treatment. Nevertheless, with a decrease in HSC proliferation and some markers of activation a decrease in fibrosis is found, thus correlating with clinical observations. Certain areas are missing from this work, and this may give more information as to the mechanism by which this consistent decrease in fibrosis is found. One cytokine, shown to have strong pro-fibrotic effects is TGF-β. During this work, TGF-β levels were not determined following IFN-α treatment either *in vitro* or *in vivo*. Previous work has shown the actions of IFN-α to antagonize that of TGF-β, however, preliminary work in our laboratory has demonstrated an increase in total TGF-β levels following

treatment with IFN-α (see 9.1). Furthermore, PAI-1 an inhibitor of plasmin (crucial to MMP activation) is also increased in the activated HSC, and has been shown previously to decrease with *in vivo* IFN-α treatment. Preliminary work has shown an increase *in vitro* (see 9.2) in my study. These two areas would remain the obvious extension to this work. Furthermore, the antifibrotic effect observed with IFN-α therapy in liver fibrosis may be due to the regulation of another cell-type within the liver. Previous work has already shown that IFN-α is able to increase the levels of the antioxidant enzyme superoxide dismutase and decrease levels of lipid peroxidation in the hepatocyte undergoing oxidative stress (Lu 2002). The hepatocytes consist of 80% of the liver cells, and are the principle target of any toxic agents in the liver. Therefore it must be considered that any protective regulation of the hepatocyte by IFN-α may provide a substantial antifibrotic effect. Further work should then include study of this cell type.

7 APPENDIX 1 – SOLUTIONS USED IN THE METHODS

Cell culture reagents

PSG:	penicillin 10 mU/ml streptomycin 10 μg/ml gentamycin 32 μg/ml (in sterile water)
DMEM:	
Standard 16% cell media:	100mls DMEM 20mls FCS 5mls PSG

RNA isolation reagents

DEPC treated water:	1ml DEPC 1 litre distilled water left overnight then autoclaved
4 M GIT:	DEPC water 4M GIT 26 mM sodium acetate to adjust to pH5
GIT lysis buffer:	10ml 4M GIT 100μl β-mercaptoethanol

RNA electrophoresis reagents

10X MOPS:	DEPC water 10 mM EDTA 0.2 M MOPS 50 mM sodium acetate to adjust to pH 7
RNA loading buffer (ESB):	0.5% bromophenol blue DEPC water 7% formaldehyde 50% formamide 7% glycerol 1% MOPS

Northern blotting reagents

Pre/Hybridization buffer:	0.5% blocking reagent (Boehringer-Mannhein) 5 ml 50X Denhardt's reagent 25 ml formamide 1 ml 10mg/ml herring sperm DNA 2.5 ml 20X sodium orthophosphate - EDTA 0.5g SDS 12.5 ml 20X SSC make up to 50 ml with DEPC water
50X Denhardt's solution:	DEPC water 1% Ficoll 1% PVP
10X SSC	DEPC water 1.5M sodium chloride 150 mM sodium citrate adjust to pH7
20X SSC:	DEPC water 3M sodium chloride 300 mM sodium citrate adjust to pH7
Stringency buffer 0.2% SDS/ 0.2% SSC:	2 g SDS 10 ml 20X SSC make up to 1 litre with DEPC water

Whole liver protein extraction

Homogenisation buffer (whole liver):	50mM Tris HCl (pH 7.6) 0.25% Triton X-100 0.15M sodium chloride 10mM calcium chloride 0.1mM Phenylmethylsulfonylfluoride 10µM Leupeptin 10µM Pepstatin A 0.1mM Iodoacetamide 25µg/ml Aprotonin

Protein Assay

Working reagent	20mls Copper II Sulfate Pentahydrate 4% 400µl Bicinchoninic Acid

SDS- PAGE reagents

10% resolving gel:	5 ml 40% acrylamide 100 µl 10% APS 8 ml distilled water 0.2 ml 10% SDS 10 µl TEMED 5 ml 1.5M Tris pH 8.8
5X running buffer:	0.2 M glycine 1 mM SDS 0.25 mM Trizma base
sample buffer:	0.2mls 0.5% bromophenol blue 4 ml distilled water 0.8 ml glycerol 1.5 ml 10% SDS 0.5 M tris-HCl pH 6.8

Western blotting reagents

Transfer buffer	27 mM glycine 20 % methanol 50 mM tris

Immunodetection reagent

TTBS	500 mM sodium chloride 100 mM Trizma base pH 7.5 0.1% Tween-20

Zymography reagents

8% resolving gel:	4 ml 40% acrylamide 100 µl 10% APS 9 ml distilled water 1 ml 20 µg/ml gelatin 0.2 ml 10% SDS 10 µl TEMED 5 ml 1.5M Tris pH 8.8
5 % Triton X-100:	500 mls distilled water 12.5 mls Triton X-100
Gelatinase incubation buffer	5 mM calcium chloride 50 mM Tris pH8
Coomassie blue stain	10% acetic acid (v/v) 0.5% Coomassie blue (w/v) 45% distilled water (v/v) 45% methanol (v/v)
Destain	10% acetic acid (v/v) 80% distilled water (v/v)

	10% methanol (v/v)
Collagen assay reagents:	
Collagenase buffer	780 µl NEM solution 1820 µl Tris/ $CaCl_2$ buffer
Collagenase plus buffer	980 µl collagenase (2450 U) 780 µl NEM 980 µl Tris/ $CaCl_2$ buffer
N-Ethylmaleride (NEM) solution:	50 mM NEM in water
Tris/ $CaCl_2$ buffer:	0.3M $CaCl_2$ 0.2M Tris pH 7.5
Immunostaining reagents:	
Tris buffered saline	8g sodium chloride 0.605g Tris 380µl HCl 1litres distilled water make up in 100mls, pH to 7.65, then add remaining 90mls
Mayers Haemalum	1g Haematoxylin 1 litre Distilled water 50g Potassium/ammonium alum 1g Citric acid 50g chloral hydrate 0.2g sodium hydrate
Harris Haematoxylin	2.5g Haematoxlyin 25ml absolute alcohol 50g Potassium chloride 500ml distilled water 0.5g Sodium iodate 20ml glacial acetic acid
Eosin	5g Eosin yellowish 1g Calcium chloride 500ml distilled water
Picro Sirius Red	100ml saturated aqueous picric acid 0.1g Sirius Red
Culture blocking solution	100ml DMEM 20mls FCS 1g Bovine serum albumin

Hydroxyproline Assay reagents

Chloramine T stock buffer (100mls):	5.69g sodium acetate 3.76g tri-sodium citrate 0.504g citric acid 38.2mls dI water 61.8mls isopropanol (can be stored at 4°C)
Chloramine T reagent:	0.7g chloramines T 40mls stock buffer 10mls dI water
Citrate buffer:	14.7g tri-sodium citrate 9.2g Citric acid 500mls dI H_2O Immediately prior to use dilute 1:5 with citrate buffer: isopropanol.
Ehrlich's reagent:	20g dimethyyaminobenzaldehyde 33ml Concentrated HCl Immediately before use dilute in 8 volumes isopropanol, i.e. 267mls

8 APPENDIX II – IN VITRO TRANSCRIPTION METHODS

Improved Method for Generating Microarray Probes using Sub-microgram Amounts of Total RNA.

E.J. Murray, Roche Discovery, Welwyn Garden City, Hertfordshire, AL7 1AA

Materials

1) First round double stranded cDNA synthesis on initial cellular total RNA
We use a custom designed cDNA kit from Life Technologies which is now available for general purchase (cat no.11917-010). The kit contains;
1. Superscript II Reverse Transcriptase (200U/ uL)
2. First strand synthesis buffer (5X)
3. 10 mM dNTPs : pH 7.2
4. T7-T24 Primer(100 pmole/uL)
5'GGC CAG TGA ATT GTA ATA CGA CTC ACT ATA GGG AGG CGG-(T)24 3' (61 mer)
5. 25 mM $MgCl_2$:
6. 100 mM DTT:
7. RNase Out (Life Tech, Cat. No.10777-019)
8. Second strand buffer (5X)
9. 10 mM dNTPs
10. E.coli DNA ligase (10 U/uL)
11. E.Coli DNA polymerase I (10 U/uL)
12. E.coli RNase H (2 U/uL)
13. T4 DNA polymerase (5 U/uL)
14. A cooling bath maintained at 16°C
15. RNase free distilled water : Add 1-2 drops diethylpyrocarbonate / L glass distilled deionised water and autoclave to sterilise. This also removes excess DEPC which breaks down to ethanol, CO_2 and water.

2) Clean up of first round cDNA products
1. Phase Lock Gel™ (PLG) Light (5-3 PRIME p1-188233)
2. 2 mL Eppendorf tubes
3. Phenol:Chloroform:Isoamylalcohol (PCI) : Melt up to 100g ultrapure phenol and saturate with 10 mM Tris-HCl, pH 7.4. Remove the Tris upper aqueous layer and add 24 mL chloroform to a 25 mL aliquot phenol. Add 1 mL isoamyl alcohol and mix. Store at 4° C under 10 mM Tris-HCl, pH 7.4 in a dark glass bottle. Also available from Life Technologies (cat no. 15593-031)
4. 5M ammonium acetate: made with RNase free water and autoclaved
5. 80% ethanol : Made with RNase free water.

3) First round *in vitro* transcription of cDNA (no biotin modification)
We use the Ambion T7 Megascript kit (cat no. 1334) which contains
1. 75 mM ATP
2. 75 mM GTP
3. 75 mM CTP
4. 75 mM UTP
5. T7 polymerase buffer (10X)
6. T7 polymerase enzyme mix

4) Clean up of in vitro transcribed RNA
We use the Qiagen RNeasy mini kit (cat no. 74104) which contains
1. RNase free water : see above
2. Buffer RLT: lysis buffer
3. 100% ethanol
4. RNeasy mini spin columns
5. Buffer RPE: elution buffer
6. 0.5 M ammonium acetate
7. Pellet paint (Novagen, cat no. 69049)
8. 80% ethanol

5) Second round double stranded cDNA synthesis (on *in vitro* transcribed RNA)
We use a custom designed cDNA kit from Life Technologies which is now available for general purchase (cat no.11917-010). The kit contains
1. Superscript II Reverse Transcriptase (200U/ uL)
2. 10 X First strand buffer
3. 10 mM dNTPs mix
4. Random 9-mer : made in-house
5. 25 mM $MgCl_2$
6. 0.1 M DTT
7. RNase Out (Life Tech, Cat. No.10777-019)
8. T7-T24 Primer (100 pmole/ul): see section 2.1
9. 5x second strand buffer
10. 10 mM dNTPs
11. E.coli DNA polymerase I (10U/uL)
12. E.coli RNase H (2 U/uL)
13. T4 DNA polymerase (5 U/uL)

6) Second round cDNA clean up
1. Phase Lock GelTM(PLG) Light, 2 mL (5-3 PRIME p1-188233)
2. Phenol:Chloroform:Isoamylalcohol (PCI) (25:24:1)
3. Pellet paint (Novagen, cat no.69049)
4. QIA quick PCR purification kit (QIAGEN, Cat. No.28104)
5. 5 M ammonium acetate
6. 100% ethanol

7) Second round in vitro transcription of cDNA (biotinylated RNA)
We use the Ambion T7 Megascript kit (cat no. 1334) which contains
1. 75 mM ATP
2. 75 mM GTP

3. 75 mM CTP
4. 75 mM UTP
5. T7 polymerase buffer (10X)
6. T7 polymerase enzyme mix
7. 10 mM biotin-11-CTP (ENZO 42818) **(NOTE 2)**
8. 10 mM biotin-16-UTP (ENZO 42814)

Methods

1) First strand cDNA synthesis on initial cellular total RNA

1. Dispense 6 uL total cellular RNA in RNase free distilled water to a clean sterilised 1.5 mL Eppendorf tube. Add 1 uL 10 mM dNTP mix and 1 uL T(24)T7 primer .
2. Incubate each sample at 65 °C for 5 minutes. Cool on ice for at least 1 minute.
3. Make a reaction cocktail of the following buffers by adding in the indicated order;

5XRT buffer	4 uL
25 mM $MgCl_2$	4 uL
0.1M DTT	2 uL
RNase Out	1 uL

4, Add 11 uL reaction cocktail to Eppendorf containing the RNA/primer tube, mixing gently, and collect by a brief spin. Incubate at 42 °C for 2 min.

5. Add 1 ul (200 U) SuperScript II reverse transcriptase to each tube at 42 °C, mix, and incubate at 42 °C for a further 60 minutes.
6. Spin first-strand cDNA reactions briefly and cool on ice.
7. Make a reaction cocktail of the following buffers by adding in the indicated order ;

DEPC-water	91 uL
5X second strand buffer	30 uL
dNTP mix (10 mM)	3 uL
E.Coli DNA ligase(10 U/ul)	1 uL
E.Coli DNA polymerase (10 U/ul)	4 uL
RNase H (2 U/ul)	1uL

8. Add 130 uL reaction cocktail to first strand cDNA reaction on ice. Mix well, spin briefly and incubate at 16 °C for 2 hours.
9. Add 2 ul T4 DNA polymerase (5 U/uL) at 16 °C, and incubate at 16 °C for a further 5 minutes.
10. Place reactions at room temperature and immediately proceed to section 3.2

2) Clean up of first round cDNA products

1. Add an equal volume (152 uL) phenol-chloroform-IAA to the cDNA sample and vortex.
2. Pellet a Phase Lock Gel by brief centrifugation.
3. Pipette the entire cDNA-phenol/chloroform mixture to the PLG tube, and centrifuge at full speed for 2 min in a microcentrifuge.

4. Transfer upper aqueous phase to a new 1.5 ml tube.

5. Add 0.6 volume of 5 M ammonium acetate and 0.5 uL Pellet Paint. Mix briefly.

6. Precipitate the double stranded cDNA by adding 2.5 volume 100 % ethanol and mix by finger flicking. Microcentrifuge at full speed at 4 °C for 15 minutes.

7. The pellet should be clearly visible as a tight dark pink pellet Rinse carefully with approximately 100 uL 80 % ethanol.
8. Air dry and dissolve in 8 uL RNase free water.

3) First round *in vitro* transcription of cDNA (no biotin modification)

1. Make a reaction cocktail of the following components in the indicated order ;

75 mM ATP	2 uL
75 mM GTP	2 uL
75 mM CTP	2 uL
75 mM UTP	2 uL
10x T7 polymerase buffer	2 uL
T7 enzyme mix	2 uL

2. Add 14 uL reaction cocktail to 6 uL cDNA
3. Incubate at 37 °C for 5 hours

4) Clean up of in vitro transcribed RNA

1. Bring volume of the IVT reaction up to 100 uL with RNase free water.

2. Add 350 uL Buffer RLT to the sample, and mix thoroughly.
3. Add 250 uL of 100 % ethanol to the lysate, and mix well by pipetting. Do not centrifuge.
4. Apply sample (700 uL) to a RNeasy mini spin column fitted to a collection tube, as supplied by the kit. Centrifuge for 15 seconds in a microcentrifuge set at 11000 rpm.
5. Transfer the RNeasy column into a new 2 mL collection tube. Add 500 uL Buffer RPE and centrifuge for15 seconds at 11000 rpm. Discard the flow-through and reuse the collection tube.
6. Pipette 500 uL Buffer RPE onto the RNeasy column, and centrifuge for 2 minutes at maximum speed to dry the RNeasy membrane.
7. Transfer the RNeasy column into a new 1.5 mL collection tube, and pipette 30 uL RNase-free water directly onto the RNeasy membrane. Centrifuge for 1 min at 11000 rpm to elute. Repeat the elution step with another 30 uL RNase free water.
8. Add 0.6 volume 5M ammonium acetate and 0.5 uL pellet paint, and gently mix by flicking.
9. Precipitate by adding 2.5 volume 100% ethanol and centrifuge in a microcentrifuge at 15,000 rpm at 4 °C for 15 minutes.
10. The pellet should be easily visible. Rinse 80% ethanol and air dry.
11. Redissolve in 6 uL RNase-free water and proceed to the second round cDNA synthesis.

5) Second round double stranded cDNA synthesis (on *in vitro* transcribed RNA)

1. Add 1 uL 10 mM dNTP mix and 1 uL random 9-mer (1 ug/uL) to reaction tube containing 6 uL IVT products.
2. Incubate each sample at 65 °C for 5 min, then place on ice for at least 1 min.
3. Make a reaction cocktail of the following buffers in the indicated order ;

5XRT buffer	4 uL
25 mM $MgCl_2$	4 uL
0.1M DTT	2 uL
RNase Out	1 uL

5. Add 11 uL reaction cocktail to each RNA/primer mixture, mix gently, and collect by a brief spin.
6. Incubate at 25 °C for 2 minutes.
7. Add 1 uL (200 Units) of SuperScript II reverse transcriptase to each tube, mix, and incubate at 25 °C for 10 minutes.
8. Incubate at 42 °C for 1 hour
9. Add 1 uL RNase H and incubate at 37 °C for 20 minutes.

10. Incubate at 95 °C for 2minutes and chill on ice. Spin reactions briefly.
11. Add 1 uL T24-T7 primer and incubate at 65 °C for 5 minutes then at 42 °C for 10 minutes. Spin briefly and place them on ice.
12.Make the following reaction cocktail of the following buffers in the indicated order:

DEPC-water	91 uL
5X second strand buffer	30 uL
dNTP mix(10 mM)	3 uL
E.Coli DNA polymerase (10 U/ul)	4 uL
RNase H (2 U/ul)	1 uL

13. Mix well, spin briefly and incubate at 16 °C for 2 hours.

14. Add 2 uL T4 DNA polymerase.
15. Incubate at 16 °C for 5 minutes and proceed purification step.

6) Second round cDNA clean up

1. Add an equal volume (152 uL) phenol-chloroform-IAA to the cDNA sample and vortex.
2. Pellet a Phase Lock Gel by brief centrifugation.
3. Pipette the entire cDNA-phenol/chloroform mixture to the PLG tube, and centrifuge at full speed for 2 minutes in a microcentrifuge.

4. Transfer upper aqueous phase to a new 1.5 mL tube.
5. Add 0.6 volume of 5 M ammonium acetate and 0.5 uL Pellet Paint. Mix briefly.

6. Precipitate the double stranded cDNA by adding 2.5 volume 100 % ethanol and mix by finger flicking. Microcentrifuge at full speed at 4 °C for 15 minutes.

7. The pellet should be clearly visible as a tight dark pink pellet. Rinse carefully with approximately 100 uL 80 % ethanol.

8. Air dry and dissolve in 20 uL RNase free water.
9. Add 100 uL PB buffer (supplied in QIA quick kit) and add to a QIA quick spin column in a provided 2-mL collection tube.
10. To bind DNA, apply the sample to the QIA quick column and centrifuge for 30~60 s at >=13,000rpm on an Eppendorf microcentrifuge.
11. Repeat step 10 one or two more times.
12. Discard the flow-through. Place the QIA quick column back into the same tube.
13. To wash, add 0.75 mL Buffer PE (supplied in QIA quick kit) to the QIA quick column and centrifuge for 30~60 seconds at >=13,000 rpm in Eppendorf microcentrifuge.
14. Discard flow-through and place the QIAquick column back in the same tube. Centrifuge the column for an additional 1 minute at maximum speed to dry the filter.
15. Place QIA quick column in a clean 1.5-mL microtube.
16. To elute DNA add 50 uL BufferEB to the centre of the QIA quick membrane and centrifuge the column for 1 minute at >=13,000 rpm.
17. Repeat step 16.
18. Add 0.6 volume (60 uL) ammonium acetate and 0.5 uL Pellet Paint and mix well.
19. Add 2.5 volume (375 ul) ethanol and mix well. Pellet the purified cDNA in a microcentrifuge at full speed at 4 °C for 15 minutes.
20. Rinse the pellet carefully twice with 500 uL 70 % ethanol and with 50 ul 100% ethanol once.
21. Air-dry the pellet and dissolve in 1.5 uL DEPC-water.

3.7 Second round in vitro transcription of cDNA (biotinylated RNA)

1. Make a reaction cocktail of the following components in the indicated order ;

75 mM ATP	2 uL
75 mM GTP	2 uL
75 mM CTP	1.5 uL
75 mM UTP	1.5 uL
10 mM Bio-11 CTP	3.5 uL
10 mM Bio-16 UTP	3.5 uL
10x T7 polymerase buffer	2 uL
T7 enzyme mix	2 uL

2. Add 14 uL reaction cocktail to 1.5 uL cDNA
3. Incubate at 37 °C for 5 hours .
4. Clean up biotinylated RNA products as described in section 3.4

9 APPENDIX III

9.1 TGF-β EXPRESSION

TGF-β was assessed using an elisa developed by Dr. E. Williams and Dr. F Shek to measure total TGF-β. Previously IFN-α has been found to antagonize TGF-β, a mechanism which would cause a reduction in perpetuation of the fibrotic state in the HSC. We found no change in the active TGF-β, but an increase in the total TGF-β. This work was done by Dr. F.Shek.

Figure 9-1 Graph showing the effect of IFN-α on active TGF-β.

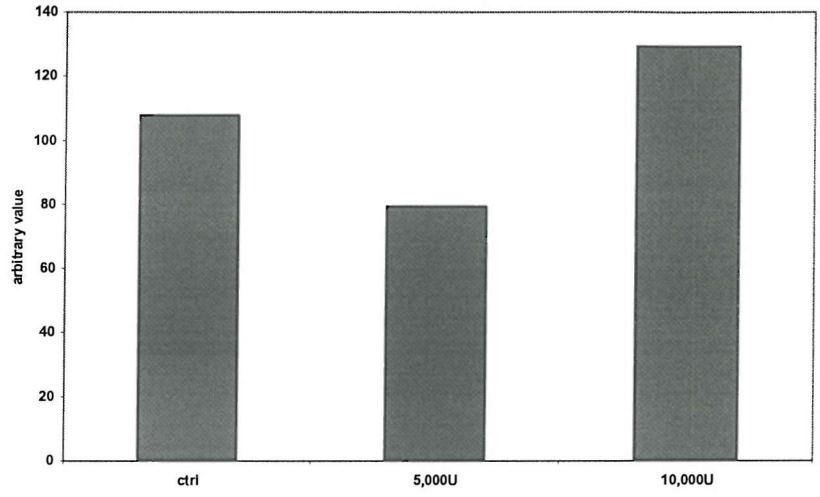

Figure 9-2 Graph showing the effect of IFN-α on total TGF-β.

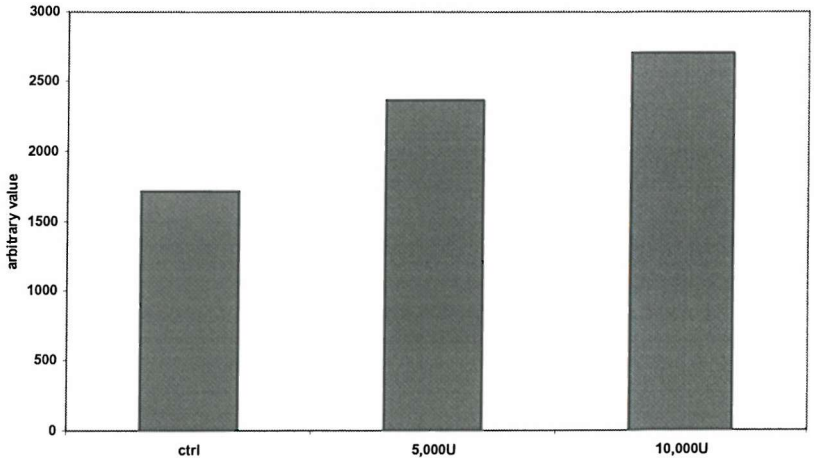

9.2 PAI-1 EXPRESSION

The expression of PAI-1 was also assessed within the IFN-α treated groups. PAI-1 inhibits the conversion of plasminogen to plasmin. Plasmin regulates two areas of fibrosis. Firstly it is required for the activation of some MMPs, i.e. MMP-1, MMP-3, MMP-9, and secondly it activates latent TGF-β. Bueno (2000) had observed a decrease in the expression of PAI-1 in the whole liver homogenates and the non-parenchymal cell lysates from fibrotic rat livers treated with IFN-α (Bueno 2000). Therefore, I examined the expression of PAI-1 with Western blotting. Treatment with IFN-α for 72hrs showed a clear upregulation in the HSC and also in the PSC.

Figure 9-3 Western blot showing PAI-1 expression in the activated HSC after 72hrs.

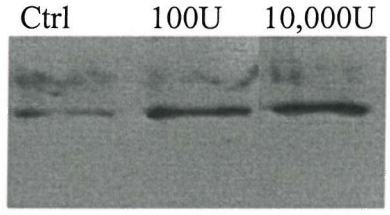

Figure 9-4 Western blot showing PAI-1 expression in the activated PSC after 72hrs.

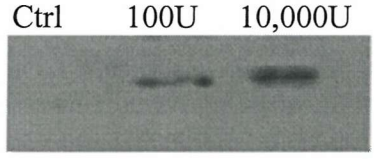

10 REFERENCES

Adachi, Y., Bradford, B.U., Gao, W., Bojes, H.K., Thurman, R.G., (1994). "Inactivation of Kupffer cells prevents early alcohol-induced liver injury." Hepatology 20(2): 453-460.

Adler, B., H. Adler, et al. (1995). "Interferon-alpha primes macrophages for lipopolysaccharide-induced apoptosis." Biochem Biophys Res Commun 215(3): 921-7.

Alberts, B., Bray, D., Lewis, J., Raff, M., Roberts, K., Watson, J. (1989). Molecular Biology of the Cell. New York and London, Garland Publishing.

Alcolado, R., M. J. Arthur, et al. (1997). "Pathogenesis of liver fibrosis." Clin Sci (Lond) 92(2): 103-12.

Apte, M. V., P. S. Haber, et al. (1998). "Periacinar stellate shaped cells in rat pancreas: identification, isolation, and culture." Gut 43(1): 128-33.

Apte, M. V., P. S. Haber, et al. (1999). "Pancreatic stellate cells are activated by proinflammatory cytokines: implications for pancreatic fibrogenesis." Gut 44(4): 534-41.

Bachem, M. G., D. Meyer, et al. (1993). "The response of rat liver perisinusoidal lipocytes to polypeptide growth regulator changes with their transdifferentiation into myofibroblast-like cells in culture." J Hepatol 18(1): 40-52.

Bachem, M. G., E. Schneider, et al. (1998). "Identification, culture, and characterization of pancreatic stellate cells in rats and humans." Gastroenterology 115(2): 421-32.

Baker, A. H., A. B. Zaltsman, et al. (1998). "Divergent effects of tissue inhibitor of metalloproteinase-1, -2, or -3 overexpression on rat vascular smooth muscle cell

invasion, proliferation, and death in vitro. TIMP-3 promotes apoptosis." J Clin Invest 101(6): 1478-87.

Balachandran, S., Kim, CN., Yeh, WC., Mak, TW., Bhalla, K., Barber, GN. (1998). "Activation of the dsRNA-dependent protein kinase, PKR, induces apoptosis through FADD-mediated death signalling." EMBO J 17: 6888-6902.

Bedossa, P. and V. Paradis (1995). "Transforming growth factor-beta (TGF-beta): a key-role in liver fibrogenesis." J Hepatol 22(2): 37-42.

Bedossa, P., T. Poynard, et al. (1993). "Transforming growth factor beta 1: in situ expression in the liver of patients with chronic hepatitis C treated with alpha interferon." Gut 34(2): S146-7.

Beeson, P. B. (1985). "Retrospective commentary on the bacterial endocarditis study." Rev Infect Dis 7(4): 574-6.

Benyon, R. C. and M. J. Arthur (1998). "Mechanisms of hepatic fibrosis." J Pediatr Gastroenterol Nutr 27(1): 75-85.

Benyon, R. C. and M. J. Arthur (2001). "Extracellular matrix degradation and the role of hepatic stellate cells." Semin Liver Dis 21(3): 373-84.

Benyon, R. C., C. J. Hovell, et al. (1999). "Progelatinase A is produced and activated by rat hepatic stellate cells and promotes their proliferation." Hepatology 30(4): 977-86.

Benyon, R. C., J. P. Iredale, et al. (1996). "Expression of tissue inhibitor of metalloproteinases 1 and 2 is increased in fibrotic human liver." Gastroenterology 110(3): 821-31.

Bergman, L. L., R. (1963). "Two improved and simplified methods for the spectrophotometric determination of hydroxyroline." Analytical Chemistry 35: 1961-1965.

Biron, C. A., G. Sonnenfeld, et al. (1984). "Interferon induces natural killer cell blastogenesis in vivo." J Leukoc Biol 35(1): 31-7.

Breitkopf, K., Lahme, B., Tag, C.G., Gressner, A.M., (2001). "Expression and matrix deposition of latent transforming growth factor beta binding proteins in normal and fibrotic rat liver and transdifferentiating hepatic stellate cells in culture." Journal of Hepatology 33(2): 387-396.

Buchkovich, K., L. A. Duffy, et al. (1989). "The retinoblastoma protein is phosphorylated during specific phases of the cell cycle." Cell 58(6): 1097-105.

Bueno, M. R., A. Daneri, et al. (2000). "Cholestasis-induced fibrosis is reduced by interferon alpha-2a and is associated with elevated liver metalloprotease activity." J Hepatol 33(6): 915-25.

Butler, G. S., M. J. Butler, et al. (1998). "The TIMP2 membrane type 1 metalloproteinase "receptor" regulates the concentration and efficient activation of progelatinase A. A kinetic study." J Biol Chem 273(2): 871-80.

Caraglia, M., A. Abbruzzese, et al. (1999). "Interferon-alpha induces apoptosis in human KB cells through a stress- dependent mitogen activated protein kinase pathway that is antagonized by epidermal growth factor." Cell Death Differ 6(8): 773-80.

Castillo, T., Koop, D.R., Kamimura, S., Triadafilopoulos, G., Tsukamoto, H. (1992). "Role of cytochrome P-450 2E1 in ethanol-, carbon tetrachloride- and iron-dependent microsomal lipid peroxidation." Hepatology 16(4): 992-996.

Chen, A., Davis, B.H., (2000). "The DNA Binding Protein BTEB Mediates Acetaldehyde-Induced, Jun N-Terminal Kinase-Dependent I(I) Collagen Gene Expression in Rat Hepatic Stellate Cells." Molecular and Cellular Biology 20: 2818-2826.

Choubey, D., Lengyel, P. (1995). "Binding of an interferon-inducible protein (p202) to the retinoblastoma protein." J Biol Chem 270: 6134-6140.

Clark, S. A., H. B. Angus, et al. (1988). "Defenestration of hepatic sinusoids as a cause of hyperlipoproteinaemia in alcoholics." Lancet 2(8622): 1225-7.

Corpechot, C., V. Barbu, et al. (2002). "Hypoxia-induced VEGF and collagen I expressions are associated with angiogenesis and fibrogenesis in experimental cirrhosis." Hepatology 35(5): 1010-21. t&artType=abs&id=ajhep0351010&target=.

Czaja, M. J., F. R. Weiner, et al. (1989). "In vitro and in vivo association of transforming growth factor-beta 1 with hepatic fibrosis." J Cell Biol 108(6): 2477-82.

Czerwionka-Szaflarska, M., A. Chrobot, et al. (2000). "Studies of the effectiveness of interferon alpha treatment for chronic hepatitis C in children." Med Sci Monit 6(5): 964-70.

Dao, T., T. Ariyasu, et al. (1994). "Natural human interferon-alpha augments apoptosis in activated T cell line." Cell Immunol 155(2): 304-11.

Der, S. D., A. Zhou, et al. (1998). "Identification of genes differentially regulated by interferon alpha, beta, or gamma using oligonucleotide arrays." Proc Natl Acad Sci U S A 95(26): 15623-8.

Dever, T. E., Feng, L., Wek, R.C., Cigan, A.M., Donahue, T.F., Hinnebusch, A.G. (1992). "Phosphorylation of initiation factor 2 alpha by protein kinase GCN 2 mediates gene-specific translational control of GCN 4 in yeast." Cell 68: 585-596.

Domanski, P., M. Witte, et al. (1995). "Cloning and expression of a long form of the beta subunit of the interferon alpha beta receptor that is required for signaling." J Biol Chem 270(37): 21606-11.

Duchatelle, V., P. Marcellin, et al. (1998). "Changes in liver fibrosis at the end of alpha interferon therapy and 6 to 18 months later in patients with chronic hepatitis C: quantitative assessment by a morphometric method." J Hepatol 29(1): 20-8.

Duncan, M. R. and B. Berman (1989). "Differential regulation of glycosaminoglycan, fibronectin, and collagenase production in cultured human dermal fibroblasts by interferon-alpha, -beta, and -gamma." Arch Dermatol Res 281(1): 11-8.

Edwards, D. R., Rocheleau, H., Sharma, R.R., Wills, A.J., Cowie, A., Hassell, J.A., Heath, J.K. (1992). "Involvement of AP1 and PEA3 binding sites in the regulation of murine tissue inhibitor of metalloproteinases-1 (TIMP-1) transcription." Biochim. Biophys Acta 1171: 41-55.

Edwards, D. R., G. Murphy, et al. (1987). "Transforming growth factor beta modulates the expression of collagenase and metalloproteinase inhibitor." Embo J 6(7): 1899-904.

Elias, J. A., S. A. Jimenez, et al. (1987). "Recombinant gamma, alpha, and beta interferon regulation of human lung fibroblast proliferation." Am Rev Respir Dis 135(1): 62-5.

Erickson, S., O. Sangfelt, et al. (1999). "Interferon-alpha inhibits proliferation in human T lymphocytes by abrogation of interleukin 2-induced changes in cell cycle-regulatory proteins." Cell Growth Differ 10(8): 575-82.

Erusalimsky, J. D., D. Gilmore, et al. (1987). "The induction of class I HLA by interferon-alpha is independent of the cell cycle, but the expression is enhanced by a G1/S block." Eur J Immunol 17(5): 623-8.

Everson, G. T., D. M. Jensen, et al. (1999). "Efficacy of interferon treatment for patients with chronic hepatitis C: comparison of response in cirrhotics, fibrotics, or nonfibrotics." Hepatology 30(1): 271-6.

Ferbas, J. J., J. F. Toso, et al. (1994). "CD4+ blood dendritic cells are potent producers of IFN-alpha in response to in vitro HIV-1 infection." J Immunol 152(9): 4649-62.

Fibbi, G., M. Pucci, et al. (1999). "Functions of the fibrinolytic system in human Ito cells and its control by basic fibroblast and platelet-derived growth factor." Hepatology 29(3): 868-78.

Fort, J., C. Pilette, et al. (1998). "Effects of long-term administration of interferon alpha in two models of liver fibrosis in rats." J Hepatol 29(2): 263-70.

Foster, G. R., O. Rodrigues, et al. (1996). "Different relative activities of human cell-derived interferon-alpha subtypes: IFN-alpha 8 has very high antiviral potency." J Interferon Cytokine Res 16(12): 1027-33.

Fraser, R., S. A. Clark, et al. (1988). "Nicotine decreases the porosity of the rat liver sieve: a possible mechanism for hypercholesterolaemia." Br J Exp Pathol 69(3): 345-50.

Friedman, S. L. (1999). "Stellate cell activation in alcoholic fibrosis--an overview." Alcohol Clin Exp Res 23(5): 904-10.

Friedman, S. L. (2000). "Molecular regulation of hepatic fibrosis, an intergrated cellular response to tissue injury." J Biol. Chem 275(4): 2247-2250.

Friedman, S. L. and M. J. Arthur (1989). "Activation of cultured rat hepatic lipocytes by Kupffer cell conditioned medium. Direct enhancement of matrix synthesis and stimulation of cell proliferation via induction of platelet-derived growth factor receptors." J Clin Invest 84(6): 1780-5.

Friedman, S. L., F. J. Roll, et al. (1989). "Maintenance of differentiated phenotype of cultured rat hepatic lipocytes by basement membrane matrix." J Biol Chem 264(18): 10756-62.

Friedman, S. L., S. Wei, et al. (1993). "Retinol release by activated rat hepatic lipocytes: regulation by Kupffer cell-conditioned medium and PDGF." Am J Physiol 264(5 Pt 1): G947-52.

Gaca, M. D., Zhou, X., Issa, R., Kiriella, K., Iredale, J.P., Benyon, R.C., (2003). "Basement membrane-like matrix inhibits proliferation and collagen synthesis by activated rat hepatic stellate cells: evidence for matrix-dependent deactivation of stellate cells." Matrix Biology 22(3): 229-239.

Gaca, M. D., X. Zhou, et al. (2002). "Regulation of hepatic stellate cell proliferation and collagen synthesis by proteinase-activated receptors." J Hepatol 36(3): 362-9.

Gaca, M. D. A., Zhou, X., Kishanee, K., Issa, R., Iredale, J.P., Benyon, R.C. (2000). "Extracellular matrix regulates hepatic stellate cell phenotype and survival." Journal of Hepatology 32: 83.

Garcia-Sastre, A. (2002). "Mechanisms of inhibition of the host interferon alpha/beta-mediated antiviral responses by viruses." Microbes Infect 4(6): 647-55.

Gard, A. L., F. P. White, et al. (1985). "Extra-neural glial fibrillary acidic protein (GFAP) immunoreactivity in perisinusoidal stellate cells of rat liver." J Neuroimmunol 8(4-6): 359-75.

Geerts, A., Lazou. J.M., De Bleser. P., Wisse, E., (1991). "Tissue distribution, quantitation and proliferation kinetics of fat-storing cells in carbon tetrachloride-injured rat liver." Hepatology 13(6): 1193-1202.

Geerts, A. (2001). "History, Heterogenity, Developmental Biology, and functions of Quiescent Hepatic Stellate Cells." Seminars in Liver Disease 21(3): 311-335.

Ghahary, A., E. E. Tredget, et al. (2001). "Induction of collagenase mRNA expression in dermal fibroblasts by IFN- alpha 2b and determination of the IFN-alpha 2b

responsive element on 5'- flanking regions of collagenase promoter." J Interferon Cytokine Res 21(8): 611-20.

Ghosh A, S. S., Sen G (2000). "Cell growth regulatory and anti-viral effects of the P69 isozyme of 2-5 (A) synthetase." Virology 266: 319-328.

Gil, J. and M. Esteban (2000). "The interferon-induced protein kinase (PKR), triggers apoptosis through FADD-mediated activation of caspase 8 in a manner independent of Fas and TNF-alpha receptors." Oncogene 19(32): 3665-74.

Gisslinger, H., R. Kurzrock, et al. (2001). "Autocrine cell suicide in a Burkitt lymphoma cell line (Daudi) induced by interferon alpha: involvement of tumor necrosis factor as ligand for the CD95 receptor." Blood 97(9): 2791-7.

Goldberg, G. I., Strongin, A., Collier, I.E., Genrich, L.T., Marmer, B.L. (1992). "Interaction of 92-kDa Type-IV collagenase with the tissue inhibitor of metalloproteinases prevenst dimerization, complex formation with interstitial collagenase, and activation of the proenzyme with stromelysin." J. Biol. Chem 267: 4583-4591.

Gressner, A. M. (1995). "Cytokines and cellular crosstalk involved in the activation of fat- storing cells." J Hepatol 22(2): 28-36.

Guerret, S., A. Desmouliere, et al. (1999). "Long-term administration of interferon-alpha in non-responder patients with chronic hepatitis C: follow-up of liver fibrosis over 5 years." J Viral Hepat 6(2): 125-33.

Guo J, S. G. (1998). "The interferon-induced protein, P56, binds to the P48 subunit of the translation initiation factor eIF-3 and inhibits translation." Eur. Cytokine Network 9: 325.

Haber, P. S., G. W. Keogh, et al. (1999). "Activation of pancreatic stellate cells in human and experimental pancreatic fibrosis." Am J Pathol 155(4): 1087-95.

Hadziyannis, S. J. (2000). "Why and how to treat chronic hepatitis C." Can J Gastroenterol 14 Suppl B: 45B-48B.

Hahn, E., G. Wick, et al. (1980). "Distribution of basement membrane proteins in normal and fibrotic human liver: collagen type IV, laminin, and fibronectin." Gut 21(1): 63-71.

Harada, H., M. Matsumoto, et al. (1996). "Regulation of IFN-alpha/beta genes: evidence for a dual function of the transcription factor complex ISGF3 in the production and action of IFN- alpha/beta." Genes Cells 1(11): 995-1005.

Hartmann, R., P. L. Norby, et al. (1998). "Activation of 2'-5' oligoadenylate synthetase by single-stranded and double-stranded RNA aptamers." J Biol Chem 273(6): 3236-46.

Harvey, W. H., O. S. Harb, et al. (1994). "Interferon-alpha-2b downregulation of oncogenes H-ras, c-raf-2, c-kit, c-myc, c-myb and c-fos in ESKOL, a hairy cell leukemic line, results in temporal perturbation of signal transduction cascade." Leuk Res 18(8): 577-85.

He, C. S., S. M. Wilhelm, et al. (1989). "Tissue cooperation in a proteolytic cascade activating human interstitial collagenase." Proc Natl Acad Sci U S A 86(8): 2632-6.

Hellerbrand, C., Jobin, C., Licato, L. L., Sartor, R. B., Brenner, D.A. (1998). "Cytokines induce NF-kB in activated but not in quiescent rat hepatic stellate cells." American Journal of Physiology 275: G269-278.

Henriet, P., G. G. Rousseau, et al. (1992). "Cloning and sequencing of mouse collagenase cDNA. Divergence of mouse and rat collagenases from the other mammalian collagenases." FEBS Lett 310(2): 175-8.

Hirai, N., Y. Kato, et al. (1986). "Natural killer (NK) cell activity and its in vitro response to interferon-alpha(Le) in chronic liver diseases and hepatocellular carcinoma." Liver 6(4): 212-20.

Hoofnagle, J., H, and Di Bisceglie A,D (1997). "The treatment of Chronic Viral Hepatitis." The New England Journal of Medicine(January 30 1997): 347-356.

Ikejiri, N. (1990). "The vitamin A-storing cells in the human and rat pancreas." Kurume Med J 37: 7-81.

Iredale, J. P. (1997). "Tissue inhibitors of metalloproteinases in liver fibrosis." Int J Biochem Cell Biol 29(1): 43-54.

Iredale, J. P., R. C. Benyon, et al. (1996). "Tissue inhibitor of metalloproteinase-1 messenger RNA expression is enhanced relative to interstitial collagenase messenger RNA in experimental liver injury and fibrosis." Hepatology 24(1): 176-84.

Iredale, J. P., R. C. Benyon, et al. (1998). "Mechanisms of spontaneous resolution of rat liver fibrosis. Hepatic stellate cell apoptosis and reduced hepatic expression of metalloproteinase inhibitors." J Clin Invest 102(3): 538-49.

Isaacs, A. and J. Lindenmann (1957). "Virus Interference. I. The Interferon." Proc Roy Soc (London) 147: 258-267.

Issa, R., Zhou, X., Trim, N., Millward-Sadler, H., Krane, S., Benyon, C., Iredale, J., (2003). "Mutation in collagen-1 that confers resistance to the action of collagenase results in failure of recovery from CCl4-induced liver fibrosis, persistence of activated hepatic stellate cells, and diminished hepatocyte regeneration." FASEB J. 17(1): 47-49.

Issa, R., E. Williams, et al. (2001). "Apoptosis of hepatic stellate cells: involvement in resolution of biliary fibrosis and regulation by soluble growth factors." Gut 48(4): 548-57.

Ito, T., Nemoto, M. (1952). "Uber die kupfferschen Sternzellen und die "Fettspeicherungszellen" in der Blutkapillarenwand der menschlichen Leber." Okajima Folia Anat Jpn 24: 243-258.

Jaster, R., G. Sparmann, et al. (2002). "Extracellular signal regulated kinases are key mediators of mitogenic signals in rat pancreatic stellate cells." Gut 51(4): 579-84.

Jewett, A. and B. Bonavida (1995). "Interferon-alpha activates cytotoxic function but inhibits interleukin- 2-mediated proliferation and tumor necrosis factor-alpha secretion by immature human natural killer cells." J Clin Immunol 15(1): 35-44.

Kadowaki, N., S. Antonenko, et al. (2000). "Natural interferon alpha/beta-producing cells link innate and adaptive immunity." J Exp Med 192(2): 219-26.

Kaplowitz, e. M. D. N. (1992). Liver and Biliary Diseases. London, Williams and Wilkins.

Kaplowitz N, T. H. (1996). "Oxidative stress in liver disease." Progression in Liver Disease 14: 131-160.

Kaser, A., S. Nagata, et al. (1999). "Interferon alpha augments activation-induced T cell death by upregulation of Fas (CD95/APO-1) and Fas ligand expression." Cytokine 11(10): 736-43.

Kaser A, N. S., Tilg H (1999). "Interferon alpha augments activation-induced T cell death by upregulation of Fas (CD95/APO-1) and Fas ligand expression." Cytokine 11(10): 736-43.

Kawada, N. (1997). "The hepatic perisinusoidal stellate cell." Histol Histopathol 12(4): 1069-80.

Kennedy, R. H., Bockmann, D.E., Uscang, L., Choux, R., Grimaud, J.A., Sarles, H. (1987). "Pancreatic extracellular matrix alterations in chronic pancreatitis." Pancreas 2: 61-72.

Kimura, T., Y. Kadokawa, et al. (1996). "Essential and non-redundant roles of p48 (ISGF3 gamma) and IRF-1 in both type I and type II interferon responses, as revealed by gene targeting studies." Genes Cells 1(1): 115-24.

Kirou, K. A., R. K. Vakkalanka, et al. (2000). "Induction of Fas ligand-mediated apoptosis by interferon-alpha." Clin Immunol 95(3): 218-26.

Kitamura, Y., Ninomiya, H., (2003). "Smad expression of hepatic stellate cells in liver cirrhosis in vivo and hepatic stellate cell line in vitro." Pathology International 53(1): 18-26.

Knauper, V., Will, H., Lopez-Otin, C., et al. (1996). "Cellular mechanisms for human procollagenase-3 (MMP-13) activation - evidence that MT1-MMP (MMP-14) and gelatinase A (MMP-2) are able to generate activate enzyme." J Biol. Chem 271: 17124-17131.

Knittel, T., Mehde, M., Grundman, A., Saile, B., Scharf, J.G., Ramadori, G. (2000). "Expression of matrix metalloproteinases and their inhibitors during hepatic tissue repair in the rat." Histochem Cell Biol. 113: 443-453.

Knittel, T., C. Dinter, et al. (1999). "Expression and regulation of cell adhesion molecules by hepatic stellate cells (HSC) of rat liver: involvement of HSC in recruitment of inflammatory cells during hepatic tissue repair." Am J Pathol 154(1): 153-67.

Knittel, T., M. Mehde, et al. (1999). "Expression patterns of matrix metalloproteinases and their inhibitors in parenchymal and non-parenchymal cells of rat liver: regulation by TNF-alpha and TGF-beta1." J Hepatol 30(1): 48-60.

Knittel, T. and G. Ramadori (1995). "Molecular Biology." Current Opinion in Gastroenterology 11: 258-266.

Kobayashi, K., Ishii, M., Igarashi, T., Satoh, T., Miyazaki, Y., Yajima, Y., Ukai, K., Suzuki, and K. H., A., Ueno, Y., Miura, T., Toyota, T., (1998). "Profiles of cytokines produced by CD4-positive T lymphocytes stimulated by anti-CD3 antibody in patients with chronic hepatitis C." Journal of Gastroenterology 33(4): 500-507.

Krupsky, M., P. P. Kuang, et al. (1997). "Regulation of type I collagen mRNA by amino acid deprivation in human lung fibroblasts." J Biol Chem 272(21): 13864-8.

Kumar, R. and I. Atlas (1992). "Interferon alpha induces the expression of retinoblastoma gene product in human Burkitt lymphoma Daudi cells: role in growth regulation." Proc Natl Acad Sci U S A 89(14): 6599-603.

LaBrecque, D. (1994). "Liver regeneration: a picture emerges from the puzzle." Am J Gastroenterol 89(8 Suppl): S86-96.

Lang, A., Schoonhoven, R., Tuvia, S., Brenner, D.A., Rippe, R.A. (2000). "Nuclear factor KB in proliferation, activation, and apoptosis in rat hepatic stellate cells." Journal of Hepatology 33: 49-58.

Leco, K. J., R. Khokha, et al. (1994). "Tissue inhibitor of metalloproteinases-3 (TIMP-3) is an extracellular matrix-associated protein with a distinctive pattern of expression in mouse cells and tissues." J Biol Chem 269(12): 9352-60.

Lee, S. B., D. Rodriguez, et al. (1997). "The apoptosis pathway triggered by the interferon-induced protein kinase PKR requires the third basic domain, initiates upstream of Bcl- 2, and involves ICE-like proteases." Virology 231(1): 81-8.

Levy MT, M. G., Abbott CA et al (1999). "Fibroblast activation protein: a cell surface dipeptidyl peptidase and gelatinase expressed by stellate cells at the tissue remodelling interface in human cirrhosis." Hepatology 29: 1768-1778.

Li, H., K. Nishio, et al. (1995). "Cell cycle-dependent localization of tissue inhibitor of metalloproteinases-1 immunoreactivity in cultured human gingival fibroblasts." Nagoya J Med Sci 58(3-4): 133-42.

Liu, X., J. Zhang, et al. (2000). "[Effects of platelet-derived growth factor on the proliferation of hepatic stellate cells and their expressions of genes of collagens and platelet-derived growth factor]." Zhonghua Bing Li Xue Za Zhi 29(1): 27-9.

Lu, G., I. Shimizu, et al. (2002). "Interferon-alpha enhances biological defense activities against oxidative stress in cultured rat hepatocytes and hepatic stellate cells." J Med Invest 49(3-4): 172-81.

Maeyer-Guignard, E. D. M. a. J. D. (1994). Interferons. The Cytokine Handbook, Academic Press Ltd: 265-283.

Maher, J. J. and R. F. McGuire (1990). "Extracellular matrix gene expression increases preferentially in rat lipocytes and sinusoidal endothelial cells during hepatic fibrosis in vivo." J Clin Invest 86(5): 1641-8.

Mallat A, P. A., Blazejewski S, Rosenbaum J, Dhumeaux D, Mavier P (1995). "Interferon Alfa and Gamma inhibit proliferation and collagen synthesis of human Ito cells in culture." Hepatology 21(4): 1003-1010.

Marra, F., Valente, A.J., Pinzani, M., Abboud, H.E., (1993). "Cultured human liver fat-storing cells produce monocyte chemotactic protein-1. Regulation by proinflammatory cytokines." J.Clin. Invest 92(4): 1674-1680.

Marra, F., Arrighi, M.C., Fazi, M., Caligiuri, A., Pinzani, M., Romanelli, R.G., Efsen, E., Laffi, G., Gentilini, P. (1999). "Extracellular signal-regulated kinase activation differentially regulates platelet-derived growth factor's actions in hepatic stellate cells, and is induced by in vivo liver injury in the rat." Hepatology 30(4): 951-958.

Martinelli, G., N. Testoni, et al. (2000). "Quantification of BCR-ABL transcripts in CML patients in cytogenetic remission after interferon-alpha-based therapy." Bone Marrow Transplant 25(7): 729-36.

Matsuoka, M., K. Tani, et al. (1998). "Interferon-alpha-induced G1 phase arrest through up-regulated expression of CDK inhibitors, p19Ink4D and p21Cip1 in mouse macrophages." Oncogene 16(16): 2075-86.

McCrudden, R. and J. P. Iredale (2000). "Liver fibrosis, the hepatic stellate cell and tissue inhibitors of metalloproteinases." Histol Histopathol 15(4): 1159-68.

McGuire, R. F., D. M. Bissell, et al. (1992). "Role of extracellular matrix in regulating fenestrations of sinusoidal endothelial cells isolated from normal rat liver." Hepatology 15(6): 989-97.

Medscape (2000). Interferon alpha 2a, Recomb. Injection. Phamrmacology and Chemistry. Medcape online. 2000.

Medscape (2000). Phamrmacology and Chemistry. (Interferon alfa-2a, Recomb. Injection). Medscape online, AHFS DI™. 2000.

Milani, S., H. Herbst, et al. (1991). "Transforming growth factors beta 1 and beta 2 are differentially expressed in fibrotic liver disease." Am J Pathol 139(6): 1221-9.

Min W, G. S., Lengyel P (1996). "The interferon-inducible p202 protein as a modulator of transcription: inhibition of NF-kappa B, c-FOS and c-JUN activities." Mol Cell Biol 16: 359-368.

Mitsuda, A., T. Suou, et al. (2000). "Changes in serum tissue inhibitor of matrix metalloproteinase-1 after interferon alpha treatment in chronic hepatitis C." J Hepatol 32(4): 666-72.

Molecular Probes, I. (2002). Molecular Probes Handbook. 2002.

Montoya, M., G. Schiavoni, et al. (2002). "Type I interferons produced by dendritic cells promote their phenotypic and functional activation." Blood 99(9): 3263-71.

Morrison, S. J., P. M. White, et al. (1999). "Prospective identification, isolation by flow cytometry, and in vivo self-renewal of multipotent mammalian neural crest stem cells." Cell 96(5): 737-49.

Muench, R. (1992). "Etioogy and natural history of chronic pancreatitis." Digestive Disorders 10(6): 335-344.

Muriel, P. (1995). "Interferon-alpha preserves erythrocyte and hepatocyte ATPase activities from liver damage induced by prolonged bile duct ligation in the rat." J Appl Toxicol 15(6): 449-53.

Muriel, P. (1996). "Alpha-interferon prevents liver collagen deposition and damage induced by prolonged bile duct obstruction in the rat." J Hepatol 24(5): 614-21.

Muriel, P., J. Bolanos, et al. (1994). "Effect of alpha-interferon on erythrocyte and hepatocyte plasma membranes derived from cirrhotic rats." Pharmacology 48(1): 63-8.

Murphy, F. R., R. Issa, et al. (2002). "Inhibition of Apoptosis of Activated Hepatic Stellate Cells by Tissue Inhibitor of Metalloproteinase-1 Is Mediated via Effects on Matrix Metalloproteinase Inhibition. Implications for Reversibility of Liver Fibrosis." J Biol Chem 277(13): 11069-76.

Murphy, G., Docherty, A.J.P. (1992). "The matrix metalloproteinases and their inhibitors." Amer J Respir Cell Molec Biol 7: 120-125.

Murphy, G., Stanton, H., Cowell, S. et al. (1999). "Mechanisms for pro matrix metalloproteinase activation." APMIS 107: 38-44.

Nagano, T., Yamamoto, K., Matsumoto, S., Okamoto, R., Tagashira, M., Ibuki, N., Matsumura, S., and K. Yabushita, Okano, N., Tsuji, T., (1999). "Cytokine profile in the liver of primary biliary cirrhosis." Journal of Clinical Immunology 19(6): 422-427.

Nagano, Y. and Y. Kojima (1954). "Pouvoir immunisant du virus vaccinal inactive par des rayons ultraviolets." C.R. Soc. Biol. 48: 1700-1702.

Nagase, H., Y. Itoh, et al. (1994). "Interaction of alpha 2-macroglobulin with matrix metalloproteinases and its use for identification of their active forms." Ann N Y Acad Sci 732: 294-302.

Neuberger, J. (1994). "Cirrhosis and hepatocellular carcinoma." European Journal of Gastroenterology and Hepatology 6: 1119-1121.

Nguyen, K. B., T. P. Salazar-Mather, et al. (2002). "Coordinated and distinct roles for IFN-alpha beta, IL-12, and IL-15 regulation of NK cell responses to viral infection." J Immunol 169(8): 4279-87.

NICE (2000). Technical Appraisal. No.14, National Institute for Clinical Excellence.

Nieto, N., S. L. Friedman, et al. (2002). "Stimulation and proliferation of primary rat hepatic stellate cells by cytochrome P450 2E1-derived reactive oxygen species." Hepatology 35(1): 62-73.

Niki, T., De Blesser, P.J., Zu, G. et al (1996). "Comparison of the glial fibrillary acidic protein and desmin staining in normal and CCL4-induced fibrotic rat livers." Hepatology 23: 1538-1545.

Niki, T., M. Pekny, et al. (1999). "Class VI intermediate filament protein nestin is induced during activation of rat hepatic stellate cells." Hepatology 29(2): 520-7.

Novick, D., B. Cohen, et al. (1994). "The human interferon alpha/beta receptor: characterization and molecular cloning." Cell 77(3): 391-400.

Oakley, F., Trim, N., Constandinou, C.M., Ye, W., Gray, A.M., Frantz, G., Hillan, K., Kendall, T., Benyon, R.C., Mann, D.A., Iredale, J.P., (2003). "Hepatocytes express nerve growth factor during liver injury: evidence for paracrine regulation of hepatic stellate cell apoptosis." American Journal of Pathology. 163(5): 1849-1858.

Oberg, K. (1992). "The action of interferon alpha on human carcinoid tumours." Semin Cancer Biol 3(1): 35-41.

Parsonage, G., Falciani, F., Burman, A., Filer, A., Ross, E., Bofill, M., Martin, S., Salmon, M., Buckley, C.D., (2003). "Global gene expression profiles in fibroblasts from synovial, skin and lymphoid tissue reveals distinct cytokine and chemokine expression patterns." Thrombosis and Haemostasis 90: 688-697.

Petricoin, E. F., 3rd, S. Ito, et al. (1997). "Antiproliferative action of interferon-alpha requires components of T- cell-receptor signalling." Nature 390(6660): 629-32.

Pinzani, M., Carloni, V., Marra, F., Riccardi, D., Laffi, G., Gentilini, P., (1994). "Biosynthesis of platelet-activating factor and its 1O-acyl analogue by liver fat-storing cells." Gastroenterology 106(5): 1301-1311.

Pinzani, M., F. Marra, et al. (1998). "Signal transduction in hepatic stellate cells." Liver 18(1): 2-13.

Powell, D. W., R. C. Mifflin, et al. (1999). "Myofibroblasts. I. Paracrine cells important in health and disease." Am J Physiol 277(1 Pt 1): C1-9.

Ramadori, G., Veit, T., Schwogler, S., et al (1990). "Expression of the gene of the alpha-smooth muscle actin isoform in rat liver and in rat fat-storing (ITO) cells." Virchows Arch [B] 59: 349-357.

Ramadori, G., Moebius, U., Dienes, H.P., Meuer, S., Meyer zum Buschenfelde, K.H., (1990). "Lymphocytes from hepatic inflammatory infiltrate kill rat hepatocytes in primary culture. Comparison with peripheral blood lymphocytes." Virchows Arch B Cell Pathol Incl Mol Pathol 59(5): 263-270.

Ramadori, G. (1991). "The stellate cell (Ito-cell, fat-storing cell, lipocyte, perisinusoidal cell) of the liver. New insights into pathophysiology of an intriguing cell." Virchows Arch B Cell Pathol Incl Mol Pathol 61(3): 147-58.

Ratziu, V., Lalazar, A., Wong, L., Dang, Q., Collins, C., Shaulian, E., Jensen, S., Friedman, S.L., (1998). "Zf9, a Kruppel-like transcription factor up-regulated *in vivo* during early hepatic fibrosis." Proceedings of the National Acadamy of Science USA 95: 9500-9505.

Riela, A., Zinsmeister, A.R., Melton, L.J., et al (1990). "Trends in the incidence and clinical characteristics of chronic panreatitis." Pancreas 5: 727.

Rippe, R. A., Almounajed, G., Brenner, D.A., (1995). "Sp1 binding activity increases in activated Ito cells." Hepatology 22: 241-251.

Rivera, C. A., Bradford, B.U., Hunt, K.J., Adachi, Y., Schrum, L.W., Koop, D.R., Burchardt, E.R., Rippe, R.A., Thurman, R.G., (2001). "Attenuation of CCl(4)-induced hepatic fibrosis by GdCl(3) treatment or dietary glycine." American Journal of Physiological Gastrointestinal Liver Physiology. 281(1): G200-207.

Roberts, G. P. and J. Brunt (1985). "Identification of an epidermal cell-adhesion glycoprotein." Biochem J 232(1): 67-70.

Roche (2002). Dispase II (neutral protease, grade II), Roche.

Rockey, D. C. (1995). "Characterization of endothelin receptors mediating rat hepatic stellate cell contraction." Biochem Biophys Res Commun 207(2): 725-31.

Rockey, D. C. and S. L. Friedman (1992). "Cytoskeleton of liver perisinusoidal cells (lipocytes) in normal and pathological conditions." Cell Motil Cytoskeleton 22(4): 227-34.

Rogoff, T. M. and P. E. Lipsky (1981). "Role of the Kupffer cells in local and systemic immune responses." Gastroenterology 80(4): 854-60.

Romerio, F., A. Riva, et al. (2000). "Interferon-alpha2b reduces phosphorylation and activity of MEK and ERK through a Ras/Raf-independent mechanism." Br J Cancer 83(4): 532-8.

Romerio, F. and D. Zella (2002). "MEK and ERK inhibitors enhance the anti-proliferative effect of interferon-alpha2b." Faseb J 16(12): 1680-2.

Roth, S., W. Gong, et al. (1998). "Expression of different isoforms of TGF-beta and the latent TGF-beta binding protein (LTBP) by rat Kupffer cells." J Hepatol 29(6): 915-22.

Roth, S., K. Michel, et al. (1998). "(Latent) transforming growth factor beta in liver parenchymal cells, its injury-dependent release, and paracrine effects on rat hepatic stellate cells." Hepatology 27(4): 1003-12.

Roth, W., B. Wagenknecht, et al. (1998). "Interferon-alpha enhances CD95L-induced apoptosis of human malignant glioma cells." J Neuroimmunol 87(1-2): 121-9.

Saile, B., C. Eisenbach, et al. (2003). "Antiapoptotic effect of interferon-alpha on hepatic stellate cells (HSC): a novel pathway of IFN-alpha signal transduction via Janus kinase 2 (JAK2) and caspase-8." Eur J Cell Biol 82(1): 31-41.

Saile, B., T. Knittel, et al. (1997). "CD95/CD95L-mediated apoptosis of the hepatic stellate cell. A mechanism terminating uncontrolled hepatic stellate cell proliferation during hepatic tissue repair." Am J Pathol 151(5): 1265-72.

Saile, B., N. Matthes, et al. (1999). "Transforming growth factor beta and tumor necrosis factor alpha inhibit both apoptosis and proliferation of activated rat hepatic stellate cells." Hepatology 30(1): 196-202.

Saito, J. M., Bostick, M.K., Campe, C.B., Xu, J., Maher, J.J., (2003). "Infiltrating neutrophils in bile duct-ligated livers do not promote hepatic fibrosis." Hepatology Research 25(2): 180-191.

Sakaida, I., A. Nagatomi, et al. (1999). "Quantitative analysis of liver fibrosis and stellate cell changes in patients with chronic hepatitis C after interferon therapy." Am J Gastroenterol 94(2): 489-96.

Samid, D., E. H. Chang, et al. (1984). "Biochemical correlates of phenotypic reversion in interferon-treated mouse cells transformed by a human oncogene." Biochem Biophys Res Commun 119(1): 21-8.

Samuel, C. E. (1998). "Protein-nucleic acid interactions and cellular responses to Interferon." Methods: A Comparison to methods in enzymology 15: 161-165.

Sangfelt, O., S. Erickson, et al. (1997). "Induction of apoptosis and inhibition of cell growth are independent responses to interferon-alpha in hematopoietic cell lines." Cell Growth Differ 8(3): 343-52.

Sangfelt, O., S. Erickson, et al. (1999). "Molecular mechanisms underlying interferon-alpha-induced G0/G1 arrest: CKI-mediated regulation of G1 Cdk-complexes and activation of pocket proteins." Oncogene 18(18): 2798-810.

Sarles, H. (1992). "Chronic pancreatitis and diabetes." Baillieres Clin Endocrinol Metab 6(4): 745-75.

Sarles, H., J. P. Bernard, et al. (1990). "Pathogenesis of chronic pancreatitis." Gut 31(6): 629-32.

Sarner, M. (1995). "Pancreatic Inflammatory Disease." Gut 37: 455-456.

Sato, H., Kinoshita, T., Takino, T., Nakayama, K., Seiki, M. (1996). "Activation of a recombinant membrane type 1-matrix metalloproteinase (MT1-MMP) by furin and its interaction with tissue inhibitor of metalloproteinases (TIMP)-2." FEBS Lett. 393: 101-104.

Schafer, S., O. Zerbe, et al. (1987). "The synthesis of proteoglycans in fat-storing cells of rat liver." Hepatology 7(4): 680-7.

Schnabl, B., Y. O. Kweon, et al. (2001). "The role of Smad3 in mediating mouse hepatic stellate cell activation." Hepatology 34(1): 89-100. t&artType=abs&id=ajhep0340089&target=.

Schuetz, E. G., D. Li, et al. (1988). "Regulation of gene expression in adult rat hepatocytes cultured on a basement membrane matrix." J Cell Physiol 134(3): 309-23.

Schuppan, D. (1990). "Structure of the extracellular matrix in normal and fibrotic liver: collagens and glycoproteins." Semin Liver Dis 10(1): 1-10.

Sen, G. C. (2000). "Novel functions of Interferon-induced proteins." seminars in Cancer Biology 10: 93-101.

Serejo, F., A. Costa, et al. (2001). "Alpha-interferon improves liver fibrosis in chronic hepatitis C: clinical significance of the serum N-terminal propeptide of procollagen type III." Dig Dis Sci 46(8): 1684-9.

Seyer, J. M., E. T. Hutcheson, et al. (1977). "Collagen polymorphism in normal and cirrhotic human liver." J Clin Invest 59(2): 241-8.

Shek, F. W., R. C. Benyon, et al. (2002). "Expression of transforming growth factor-beta 1 by pancreatic stellate cells and its implications for matrix secretion and turnover in chronic pancreatitis." Am J Pathol 160(5): 1787-98.

Shen, H., M. Zhang, et al. (2002). "Different effects of rat interferon alpha, beta and gamma on rat hepatic stellate cell proliferation and activation." BMC Cell Biol 3(1): 9.

Shi, Z., Wakil, A., E., Rockey, D., C., (1997). "Strain-specific differences in mouse hepatic wound healing are mediated by divergent T helper cytokine responses." Proceedings of the National Acadamy of Science of the USA 94: 10663-10668.

Shirachi, M., M. Sata, et al. (1998). "Liver-associated natural killer activity in cirrhotic rats." Microbiol Immunol 42(2): 117-24.

Smart, D. E., Vincent, K.J., Arthur, M.J.P., Eickelberg, O., Castellazzi, M., and J. Mann, Mann, D., (2001). "JunD Regulates Transcription of the Tissue Inhibitor of Metalloproteinases-1 and Interleukin-6 Genes in Activated Hepatic Stellate Cells." The Journal of Biological Chemistry 276: 24414-24421.

Smedsrod, B., P. J. De Bleser, et al. (1994). "Cell biology of liver endothelial and Kupffer cells." Gut 35(11): 1509-16.

Sobesky, R., P. Mathurin, et al. (1999). "Modeling the impact of interferon alfa treatment on liver fibrosis progression in chronic hepatitis C: a dynamic view. The Multivirc Group." Gastroenterology 116(2): 378-86.

Sprenger, H., Kaufmann, A., Garn, H., Lahme, B., Gemsa, D., Gressner, A.M., (1997). "Induction of neutrophil-attracting chemokines in transforming rat hepatic stellate cells." Gastroenterology 113: 277-285.

Stark, G. R., Kerr, I.M., Williams, B.R.G., Silvermann, R.H., Schrieber, R.D. (1998). "How Cells Respond to Interferons." Annu. Rev. Biochem 67: 227-264.

Stefanovic, B., C. Hellerbrand, et al. (1995). "Post-transcriptional regulation of collagen alpha 1(I) mRNA in hepatic stellate cells." Nucleic Acids Symp Ser 33: 212-4.

Stefanovic, B., C. Hellerbrand, et al. (1997). "Posttranscriptional regulation of collagen alpha1(I) mRNA in hepatic stellate cells." Mol Cell Biol 17(9): 5201-9.

Stefanovic, B., J. Lindquist, et al. (2000). "The 5' stem-loop regulates expression of collagen alpha1(I) mRNA in mouse fibroblasts cultured in a three-dimensional matrix." Nucleic Acids Res 28(2): 641-7.

Sugihara, A., Tsujimura,T., Fujita, Y., Nakata, Y., Terada, N., (1999). "Evaluation of role of mast cells in the development of liver fibrosis using mast cell-deficient rats and mice." Journal of Hepatology 30(5): 859-867.

Suzuki K, E. J., Morodomi T, Salvesen G, Nagase H (1990). "Mechanism of activation of tissue procollagenase by matrix metalloproteinase 3 (stromelysin)." Biochemistry 29: 10261-10270.

Svegliati-Baroni, G., Ridolfi, F., Caradonna, Z., Alvaro, D., Marzioni, M., Saccomanno, S., Candelaresi, C., Trozzi, L., Macarri, G., Benedetti, A., Folli, F.,

(2003). "Regulation of ERK/JNK/p70S6K in two rat models of liver injury and fibrosis." Journal of Hepatology 39: 528-537.

Sympson, C. J., Talhouk, R.S., Alexander, C.M., Chin, J.R., Clift, S.M., Bissell, M.J., Werb, Z., (1994). "Targeted expression of stromelysin-1 in mammary gland provides evidence for a role of proteinases in branching morphogenesis and the requirement for an intact

basement membrane for tissue-specific gene expression." Journal of Cell Biology 125(3): 681-693.

Teschke, R., Vierke, W., Goldermann, L., (1983). "Carbon tetrachloride (CCl4) levels and serum activities of liver enzymes following acute CCl4 intoxication." Toxicol Lett. 17(1-2): 175-180.

Thomas, N. S., A. R. Pizzey, et al. (1998). "p130, p107, and pRb are differentially regulated in proliferating cells and during cell cycle arrest by alpha-interferon." J Biol Chem 273(37): 23659-67.

Thyrell, L., S. Erickson, et al. (2002). "Mechanisms of Interferon-alpha induced apoptosis in malignant cells." Oncogene 21(8): 1251-62.

Tiggleman, A. M., Boers, W., Linthorst, C., Sala, M., Chamuleau, R.A., (1995). "Collagen synthesis by human liver (myo)fibroblasts in culture - evidence for regulatory role of IL-1beta, IL-4, TGF-beta and IFN-gamma." Journal of Hepatology 23: 307-317.

Toth, C. A. and P. Thomas (1992). "Liver endocytosis and Kupffer cells." Hepatology 16(1): 255-66.

Tougaard, L. (1973). "The degree of mineralization in bone tissue. The phosphorus-hydroxyproline ratio determined on small amounts of bone tissue." Scand J Clin Lab Invest 32(4): 351-5.

Tredget, E. E., R. Wang, et al. (2000). "Transforming growth factor-beta mRNA and protein in hypertrophic scar tissues and fibroblasts: antagonism by IFN-alpha and IFN-gamma in vitro and in vivo." J Interferon Cytokine Res 20(2): 143-51.

Tsushima, H., S. Kawata, et al. (1999). "Reduced plasma transforming growth factor-beta1 levels in patients with chronic hepatitis C after interferon-alpha therapy: association with regression of hepatic fibrosis." J Hepatol 30(1): 1-7.

Vendemiale, G., I. Grattagliano, et al. (2001). "Increased oxidative stress in dimethylnitrosamine-induced liver fibrosis in the rat: effect of N-acetylcysteine and interferon-alpha." Toxicol Appl Pharmacol 175(2): 130-9.

Wake, K. (1971). ""Sternzellen" in the liver: perisinusoidal cells with special reference to storage of vitamin A." American Journal Anatomy 132: 429-462.

Wake, K. (1980). "Perisinusoidal stellate cells (fat-storing cells, interstitial cells, lipocytes), their related structure in and around the liver sinusoids, and vitamin A-storing cells in extrahepatic organs." Int Rev Cytol 66: 303-53.

Watanabe, T., M. Niioka, et al. (2000). "Gene expression of interstitial collagenase in both progressive and recovery phase of rat liver fibrosis induced by carbon tetrachloride." J Hepatol 33(2): 224-35.

Watari N, H. Y., Mabuchi Y (1982). "Morphological studies on a vitamin A-storing cell and its complex with macrophage observed in mouse pancreatic tissues following excess vitamin A administration." Okajimas Folia Anat Jpn 58: 837-858.

Whalen, R., D. C. Rockey, et al. (1999). "Activation of rat hepatic stellate cells leads to loss of glutathione S- transferases and their enzymatic activity against products of oxidative stress." Hepatology 30(4): 927-33.

Wickenhauser, C., B. Schmitz, et al. (2000). "Interferon alpha2b directly induces fibroblast proliferation and transforming growth factor beta secretion of macrophages." Br J Haematol 109(2): 296-304.

Will H, A. S., Butler GS, Smith B, Murphy G (1996). "The soluble catalytic domain of membrane type 1 matrix metalloproteinase cleaves the propeptide of progelatinase A and initiates autoproteolytic activation - regulation by TIMP-2 and TIMP-3." J Biol Vhem 271: 17119-17123.

Williams, B. (1999). "PKR, a sentinal kinase for cellular stress." Oncogene 18: 6112-6120.

Wisse, E. (1970). "An electron micorscope study of the fenestred endothelial linign of rat liver sinusoids." J. Ultrastructural Res. 31: 125-150.

Wisse, E., R. B. De Zanger, et al. (1985). "The liver sieve: considerations concerning the structure and function of endothelial fenestrae, the sinusoidal wall and the space of Disse." Hepatology 5(4): 683-92.

Worthington Biochemical Corporation (2003). Cell Isolation Theory, Worthington Biochmical Corporation. 2003.

Wright, M. C., R. Issa, et al. (2001). "Gliotoxin stimulates the apoptosis of human and rat hepatic stellate cells and enhances the resolution of liver fibrosis in rats." Gastroenterology 121(3): 685-98.

Yagura, M., S. Murai, et al. (2000). "Changes of liver fibrosis in chronic hepatitis C patients with no response to interferon-alpha therapy: including quantitative assessment by a morphometric method." J Gastroenterol 35(2): 105-11.

Yanai, Y., O. Sanou, et al. (2001). "Analysis of the antiviral activities of natural IFN-alpha preparations and their subtype compositions." J Interferon Cytokine Res 21(10): 835-41.

Yokoi, Y., K. Matsuzaki, et al. (1986). "[Desmin filaments in cultured Ito cells]." Nippon Shokakibyo Gakkai Zasshi 83(6): 1230.

Yoshiji, H., S. Kuriyama, et al. (2000). "Tissue inhibitor of metalloproteinases-1 promotes liver fibrosis development in a transgenic mouse model." Hepatology 32(6): 1248-54.

Zafarullah, M., S. Su, et al. (1996). "Tissue inhibitor of metalloproteinase-2 (TIMP-2) mRNA is constitutively expressed in bovine, human normal, and osteoarthritic articular chondrocytes." J Cell Biochem 60(2): 211-7.

Zhou, A., Paranjape, J., Brown, T.L., Nie, H., Naik, S., Dong, B., Chang, A., Trapp, B., Fairchild, R., Colmenares, C., Silverman, R.H. (1997). "Interferon action and apoptosis are defective in mice devoid of 2',5'-oligoadenylate-dependent RNase L." EMBO J 16(3): 6355-6363.